Sparse recovery from Fourier measurements using compactly supported shearlets

vorgelegt von

Master of Science

Jackie Ken Yip Ma

geboren in Hamburg

Von der Fakultät II - Mathematik und Naturwissenschaften

der Technischen Universität Berlin

zur Erlangung des akademischen Grades

Doktor der Naturwissenschaften

– Dr. rer. nat. –

genehmigte Dissertation

Promotionsausschuss

Vorsitzender: Prof. Dr. Stefan Felsner

Gutachterin: Prof. Dr. Gitta Kutyniok

Gutachter: Prof. Dr. Akram Aldroubi

Gutachter: Prof. Dr. Anders Hansen

Tag der wissenschaftlichen Aussprache: 5. August 2016

Berlin 2016

Zusammenfassung

In dieser Arbeit studieren wir das Abtasten und die Rekonstruktion von Signalen, die eine dünnbesetzte Struktur besitzen. Wir werden dabei verschiedene Modelle betrachten. Zuerst studieren wir das Abtast- und Rekonstruktionsproblem mittels *Generalized Sampling.* Generalized Sampling ist eine lineare Rekonstruktionsmethode, die es erlaubt zwei beliebige *Frames* zu benutzen, einen für das Abtasten und den anderen für die Rekonstruktion. Ein wesentlicher Fokus wird in dieser Arbeit auf *Shearlets* liegen, welches ein Repräsentationssystem ist, das die sogenannte *Optimal Sparse Approximation Rate* fuer *cartoon-ähnliche* Funktionen erfüllt. Für das Abtastystem werden wir häufig die Fourierbasis betrachten, da diese auch in der Magnetresonanztomografie (MRT) verwendet wird. Unabhängig von dem Abtast- und Rekonstruktionsproblem mit Hilfe von Shearlets werden wir die fundamentale Eigenschaft der linearen Unabhängigkeit von Shearlets untersuchen und eine neue Konstruktion für Shearlets auf beschränkten Gebieten geben.

Des Weiteren studieren wir die Rekonstrution von dünn besetzten Signalen durch ℓ^1-Minimierung was fundamental ist im Gebiet des *Compressed Sensing*s – eine Theorie, die die Akquisition und Rekonstruktion von dünnbesetzten Signalen durch lösen eines Optimierungsproblems anhand von einer unvollständigen Menge an Messungen studiert. Dabei werden wir zwei verschiedene Situationen studieren: Zunächst untersuchen wir das unendlich dimensionale Problem mit Hilfe von multiskalen Abtaststrategien und lokalisierten Rekonstruktionssystemen, welche wiederum mit einer natürlichen Multiskalenstruktur versehen sind, wie zum Beispiel die Shearletsysteme. Insbesondere werden wir eine Verallgemeinerung der Shearlets betrachten, nämlich das der *α-Moleküle.* Wir zeigen, dass eine stabile Rekonstruktion von Fouriermessungen für solche Systeme möglich ist, dabei werden wir insbesondere die *Balancing Property* untersuchen, die im Wesentlichen das Abtastschema unter Berücksichtigung der Struktur des Rekonstruktionssystems bestimmt und zeigen, wie man diese für Systeme wie *α-Shearlets* nachweisen kann.

Anschließend studieren wir *nicht-konvexes Compresses Sensing* in dem wir über ℓ^p-quasinormen für $p \in (0, 1)$ minimieren. Wir zeigen die Stabilität der Lösungen die man durch eine derartige Minimierung über *Primal Frame Coefficients* oder über *Dual Frame Coefficients* erhält. Für Letzteres führen wir ein neues Konzept ein, das der sogenannten *Frames mit identifizierbaren dualen Frames.* Die Resultate hierzu werden in größerer Allgemeinheit bewiesen und sind anwendbar auf alle Abtastmatrizen, die die sogenannte *Restricted Isometry Property* erfüllen. In einigen zusätzlichen numerischen Experimenten vergleichen wir dann Rekonstruktionen, die durch ℓ^p-quasinormen erhalten wurden, mit Rekonstruktionen die durch klassisches Compressed Sensing, erhalten worden sind, d.h.

durch Minimierung über die ℓ^1-Norm. Diese Experimente sind dann für Shearletrekonstruktionen anhand von Fouriermessungen durchgeführt worden.

Wir werden außerdem einen neuen Algorithmus vorstellen der auf der Multiskalenstruktur der *sparsifizierenden Transformen* beruht, wie zum Beispiel die Shearlet- oder Wavelettransformation. Insbesondere wird diese Stuktur mit *reweighted ℓ^1-minimization* kombiniert. Wir testen den Algorithmus an diversen Bildern, in dem von einigen Fouriermessungen der jeweiligen Bilder, Shearletrekonstruktionen berechnen werden.

Darüberhinaus werden wir in dieser Arbeit Shearlets auf reale Daten anwenden. Als erstes rekonstruieren wir medizinische Daten anhand von Fouriermessungen, die von einem MRT-Gerät aufgenommen worden sind. Insbesondere rekonstruieren wir ein 3D Volumen anhand eines radial abgetasteten *k-Raums*. Anschließend betrachten wir ein *Inpainting Problem* aus der Elektronenmikroskopie.

Abstract

The main topic of this thesis is to study the sampling and reconstruction problem of signals that have a sparse structure. We thereby consider different models. First, we study the sampling and reconstruction problem using *generalized sampling* which is a linear reconstruction method that allows to use two arbitrary frames one as a sampling system and another one as a reconstruction system. The particular focus is then on using *shearlets* as a reconstruction system, since they provide the optimal sparse approximation rate for *cartoon-like functions*, which are compactly supported functions that are smooth up to a piecewise smooth discontinuity curve. As for the sampling process we often focus on the Fourier system, as these have a direct application to *magnetic resonance imaging.* In the context of shearlets, we also study the fundamental property of linear independence and present a novel construction of shearlets on bounded domains in this thesis.

Further, we study the recovery of sparse signals by using ℓ^1-minimization which is at the heart of *compressed sensing* – a theory that studies the acquisition and recovery of sparse signals via an optimization problem from an incomplete amount of acquired data. This will be done in two ways: First, we investigate the infinite dimensional problem using *multilevel sampling schemes* as well as localized systems that carry an intrinsic multiscale structure such as shearlets. In fact, we will consider the more general case of α-molecules and show how recovery guarantees can be obtained for such systems in combination with Fourier samples. One focus will be on the *balancing property* which essentially determines the samples that must be acquired for successful recovery. It relates the sampling procedure to the sparsity structure of the system and we will show how it can be verified for certain type of systems such as α-shearlets.

Next, we consider non-convex priors such as the ℓ^p-quasi norms for $p \in (0, 1)$. We show theoretical stability of solutions that are obtained from ℓ^p-minimization when minimizing over dual coefficients as well as over primal coefficients. For the latter case we introduce a new concept called *identifiability of duals* which guarantees the sparsity equivalence between the primal and the dual system. The theoretical results are presented in full generality and apply to all sampling matrices that fulfill the *restricted isometry property* RIP. In some numerical experiments we will then compare the different solutions that are obtained by ℓ^1-minimization and ℓ^p-minimization, respectively, for the case of Fourier samples and shearlet reconstructions.

We then also introduce a novel algorithm that is based on the multilevel structure of sparsifying transforms such as shearlets or wavelets. In particular, this structure is combined with the idea of *reweighted ℓ^1-minimization.* This algorithm is intensively tested and compared to other methods. Again the focus will be on Fourier measurements in these

experiments.

Finally, we apply shearlet based recovery to real data. First, we recover medical images from Fourier measurements as they appear in the applications. In fact, we will recover a 3D volume from radially subsampled k-space data. Furthermore, we also consider an inpainting problem appearing in electron microscopy.

Acknowledgements

I want to thank my advisor Gitta Kutyniok for her constant help and support during my PhD. It has been my great pleasure to be her PhD student, thereby learning and profiting from her experience. Furthermore, I want to thank Ben Adcock, Akram Aldroubi, Anders Hansen, Christoph Kolbitsch, Gitta Kutyniok, Maximilian März, Philipp Petersen and Zineb Saghi for collaborations and/or fruitful discussions.

I also want to thank all my colleagues in Berlin for the wonderful memories that we share, especially I want to thank Philipp Petersen for being a great friend and collaborator.

Finally, I want to thank Akram Aldroubi and Anders Hansen for being part of the refereeing committee of this thesis.

Jackie Ma

May 17, 2016

Contents

II Applications

Appendix

Part I

Theory

Introduction

In this thesis we present several new results for different models that are prominently used in applied mathematics for *sampling and reconstruction problems*. By a sampling and reconstruction problem we understand the recovery of a certain object of interest from an incomplete amount of samples. Such sampling and reconstruction problems appear in many different practical areas such as *signal transmission*, *medical imaging*, and *image inpainting*.

The latter two are of particular interest and serve as leading motivations of our theoretical results when it comes to applications. Indeed, the theoretical foundations and results that are presented in this thesis will be supplemented with applications to special image reconstruction tasks considered in *magnetic resonance imaging* (MRI) and *electron microscopy* (EM). In particular, we will use real experimental MR data in Chapter 6 to recover a spatial volume from its k-space measurements. Further, in Chapter 7 we will recover certain objects from its pixel data acquired in *scan transmission electron microscopy* to verify some of the theoretical concepts of this thesis.

Representation systems

We model the sampling and reconstruction problem in a (separable) Hilbert space $(\mathcal{H}, \langle \cdot, \cdot \rangle)$ with a particular focus on L^2 – the space of square integrable functions. Modelling the problem in a Hilbert space has the advantage that we can rely on many powerful results from functional analysis and especially harmonic analysis in the scenario where $\mathcal{H}$ is L^2. Also this assumption is general enough so that the results that we obtain can be applied to many problems such as the medical data reconstruction in MRI where essentially Fourier coefficients of the signal are acquired.

Furthermore, the model assumption of working in a Hilbert space has the advantage that every signal $f \in \mathcal{H}$ that we wish to recover has a representation of the form

$$f = \sum_{\lambda \in \Lambda} \langle f, \psi_\lambda \rangle \psi_\lambda \tag{0.1}$$

for some orthonormal basis $(\psi_\lambda)_{\lambda \in \Lambda}$ of $\mathcal{H}$. However, one should not expect that (0.1) is the only possible representation formula of f and indeed, this is not case. Let us generally call any $(\psi_\lambda)_{\lambda \in \Lambda} \subseteq \mathcal{H}$ a *representation system* for $\mathcal{H}$ if for any $f \in \mathcal{H}$ there exists at least one sequence of scalars $(c_\lambda)_{\lambda \in \Lambda} \in \ell^2(\Lambda)$ such that

$$f = \sum_{\lambda \in \Lambda} c_\lambda \psi_\lambda. \tag{0.2}$$

Clearly, any orthonormal basis $(\psi_\lambda)_{\lambda\in\Lambda}$ of $\mathcal{H}$ is a representation system.

Another different type of representation system in a Hilbert space is given by the concept of *frames.* [(i)] We call a sequence of elements $(\psi_\lambda)_{\lambda\in\Lambda}$ of $\mathcal{H}$ a *frame* for $\mathcal{H}$ if there exist two constants $0 < A \leq B < \infty$ such that for all $f \in \mathcal{H}$

$$A\|f\|^2 \leq \sum_{\lambda\in\Lambda} |\langle f, \psi_\lambda\rangle|^2 \leq B\|f\|^2 \tag{0.3}$$

holds. Equation (0.3) guarantees that the so-called *frame operator*

$$\begin{aligned} S : \mathcal{H} &\longrightarrow \mathcal{H}, \\ f &\mapsto \sum_{\lambda\in\Lambda} \langle f, \psi_\lambda\rangle \psi_\lambda, \end{aligned}$$

which is indeed a linear bounded operator as per definition, possesses a linear bounded inverse operator S^{-1}. Note that

$$\langle Sf, f\rangle = \sum_{\lambda\in\Lambda} |\langle f, \psi_\lambda\rangle|^2.$$

Therefore a frame is indeed a representation system since

$$f = SS^{-1}f = \sum_{\lambda\in\Lambda} \langle S^{-1}f, \psi_\lambda\rangle \psi_\lambda.$$

Now, given an orthonormal basis it is easy to construct a frame that itself is not an orthonormal basis, in particular every Hilbert space contains infinitely many frames. Thus, in general, one might pursuit to find a frame that suits the problem at hand better than others.

For example, if $\mathcal{H}$ is the Hilbert space L^2 and we were interested in the approximation of functions that have certain characteristic properties, such as smoothness properties, then one might be better off with a representation system that itself consists of smooth functions and share similar properties as the function that one tries to approximate. This idea leads to the following general philosophy: First one specifies the class of functions that one is interested in. Then the second step is to develop a notion of *optimal approximation* for this class functions. The next crucial step is then to construct an actual representation system that achieves the optimal approximation rate.

One particular instance that fits perfectly into this philosophy are *shearlet frames* that have been introduced in [GKL06, LLKW05] as an optimal approximating system for so-called *cartoon-like functions* which are a simplified mathematical model for natural images.

Shearlet frames will play a great role in the upcoming content of this thesis, thus, in Chapter 1 we will give a compact introduction into shearlets as well as present a novel construction of *shearlets systems on bounded domains* such as $[0, 1]^2$.

[(i)] In Appendix A.1 - we provide some basic definitions and properties of frame theory.

Sampling and reconstruction model

In the previous section we mentioned the flexibility of choosing a representation system in order to represent the initial object of interest efficiently. Now we want to specify how this can be used for certain types of sampling and reconstruction models but first, we fix the model for the sampling procedure.

Suppose we are given some linear functionals $m_k : \mathcal{H} \longrightarrow \mathbb{C}, k \in \mathbb{N}$ that are ought to measure an object of interest $f \in \mathcal{H}$. More precisely, given the set of measurements

$$\{m_k(f) \,:\, k = 1, 2, \ldots\}, \tag{0.4}$$

how can we retrieve f? Note that the model assumption (0.4) covers the case where Fourier measurements are acquired. Moreover, how can the information be used that f can be nicely approximated by a specific representation system? In other words, given the measurements (0.4) and an a priori chosen representation system $(\psi_\lambda)_{\lambda\in\Lambda}$, we want to find coefficients $(\widetilde{c}_\lambda)_{\lambda\in\Lambda} \in \ell^2(\Lambda)$ such that

$$\sum_{\lambda\in\Lambda} \widetilde{c}_\lambda \psi_\lambda \approx f.$$

At this point it becomes very evident why it could be of great advantage to choose the representation system accordingly. In fact, if we know something about the coefficients in the expansion above – such as *sparsity*, i.e. only very few coefficients in the representation are non-zero – then possibly less (non-zeros) coefficients need to be computed so that the error in the approximation is small. Indeed, if the first exact coefficients of a representation can be computed, then the error of the approximation would decay as the tail of this coefficient sequence. (ii)

Sampling and reconstruction problems of this kind can mathematically be formalised by the concept of *generalized sampling* which was developed by Adcock et al. in [AH12a, AH12b, AHP13]. Generalized sampling is a reconstruction method that allows one to study the existence and error behaviour of reconstructions given a fixed number of measurements of the above form (0.4) and an arbitrary reconstruction system of choice. In particular, generalized sampling provides certain characteristic quantities that, if properly understood, can tell us precisely how many measurements are needed to be acquired - in an asymptotic sense - in order to recover a fixed number of coefficients that one wants to recover. For that purpose it is again a great advantage to have some a priori knowledge about the representation system or in particular the coefficients that are needed in the representation (0.2) of it.

We will introduce the method of generalized sampling and its main characteristics in Chapter 2 in more detail and study its capabilities of recovering functions from their Fourier measurements, i.e. in (0.4) we have $m_k(f) = (\mathcal{F}f)(\xi_k)$ for appropriately chosen frequencies $\xi_k \in \mathbb{R}^2, k = 1, 2, \ldots$. We thereby focus of reconstructions using a shearlet frame. In this context, we will also draw a comparison with a similar analysis that have been done for wavelet systems. (iii)

(ii) Provided the *synthesis operator* $T : \ell^2(\Lambda) \longrightarrow \mathcal{H}, (c_\lambda)_{\lambda\in\Lambda} \mapsto \sum_{\lambda\in\Lambda} c_\lambda\psi_\lambda$ is bounded.

(iii) Some basic definition and properties of wavelets will be presented in Appendix B.

Sparse recovery via optimization

In the above reconstruction scheme we already mentioned *sparsity* as a possible desired ingredient in the model. Note that the sparsity of an element depends on the representation system and is measured by its number of non-zero coefficients in that particular representation system, cf. (0.2).

The additional information of having a sparse signal that one wants to reconstruct allows one to reconstruct the (sparse) object from significantly less number of measurements than one might first expect. For instance, in the event of Fourier measurements, i.e. $m_k(f) = (\mathcal{F}f)(k), k \in \mathbb{Z}$, it is known that every L^1-function f on the torus $\mathbb{T}$ [(iv)] can be represented in terms of complex exponentials by

$$f = \sum_{k\in\mathbb{Z}} m_k(f)e^{-2\pi i(\cdot)\xi}, \quad \text{almost everywhere}$$

provided the sequence of measurements $(m_k(f))_{k\in\mathbb{Z}}$ is in $\ell^1(\mathbb{Z})$. This means that the measurements can immediately be used for the reconstruction. However, if we were to subsample the data in that way as well as reconstruct it by this reconstruction procedure, then one might observe that the truncated Fourier series

$$\sum_{k=-N}^{N} m_k(f)e^{-2\pi i(\cdot)\xi}$$

converges considerably slow and thus results in a far from optimal reconstruction. Note that it is in particular this example for which a novel method called *compressed sensing* has led to astonishing new recovery results. However, the recovery guarantees in compressed sensing usually come at the cost of a reconstruction formula. In particular, in compressed sensing the reconstruction is not obtained by a closed form solution, such as the truncated Fourier series in the previous example, but rather via solving a convex optimization problem of the form

$$\min_g \sum_{\lambda\in\Lambda} |\langle g, \psi_\lambda\rangle| \quad \text{subject to} \quad m_k(g) = m_k(f), \tag{0.5}$$

where $(\psi_\lambda)_{\lambda\in\Lambda}$ denotes the sparsifying system, for example a shearlet system. Note that minimizing the sum of absolute values in (0.5) tends to impose a sparsity constraint of the reconstruction are sought. In Chapter 3 we will give a more detailed introduction into compressed sensing and analyse it for the scenario where again Fourier measurements are acquired and shearlet reconstructions.

In Chapter 4 we then consider a different type of minimization problem namely we will study solutions that are obtained from the non-convex optimization problem

$$\min_g \sum_{\lambda\in\Lambda} |\langle g, \psi_\lambda\rangle|^p \quad \text{subject to} \quad m_k(g) = m_k(f), \quad 0 < p < 1 \tag{0.6}$$

and arbitrary sparsifying systems $(\psi_\lambda)_{\lambda\in\Lambda}$. Further, in a sequence of numerical examples we will explain what can potentially be gained by considering the minimization (0.6) for any p smaller than one.

[(iv)] That is the unit sphere with opposite sites identified.

Basics and notations

In this thesis we will assume the reader to have some basic knowledge in Fourier analysis, frame theory and wavelet analysis. At the end of the thesis we have also included some basic definitions and results that are helpful.

Furthermore, the following notations are used in this thesis unless it is stated otherwise:

$\#$:	Cardinality of a set.
$\lvert\cdot\rvert$:	Absolute value of scalars of $\mathbb{C}$.
$\lVert\cdot\rVert$:	Norm of the Hilbert space $\mathcal{H}$.
$a \lesssim b$:	a is less than equal to b up to a constant with a and b being positive scalars.
$C^N(\mathbb{R}^d)$:	Space of N-times differentiable functions on $\mathbb{R}^d$ with $d \in \mathbb{N}$.
$\mathcal{F}, \widehat{f}$:	Fourier transform of a function $f \in L^1(\mathbb{R}^d) \cap L^2(\mathbb{R}^d)$, i.e. $$(\mathcal{F}f)(\xi) = \widehat{f}(\xi) = \int_{\mathbb{R}^d} f(x) e^{-2\pi\langle x,\xi\rangle}\, dx.$$ The Fourier transform can be extended to L^2-functions and we will use the same notation for this case.
$\langle\cdot,\cdot\rangle$:	Standard inner product of either L^2, ℓ^2, or $\mathbb{C}^N$.
j:	Scaling number which is always assumed to be an integer in $\mathbb{N} \cup \{0\}$ In particular, we will often write $j \geq 0$ which always means $j \in \mathbb{N} \cup \{0\}$,
Λ:	Countable index set which will often be left out as it is clear in most cases. For example we shall write $(c_\lambda)_\lambda$ instead of $(c_\lambda)_{\lambda\in\Lambda}$ everywhere where it cannot cause any confusion. We will do the same with sums, i.e. we write $\sum_\lambda$ instead of $\sum_{\lambda\in\Lambda}$.
$\ell^p(\Lambda)$:	Sequence space equipped with norm $$\lVert(c_\lambda)_{\lambda\in\Lambda}\rVert_p = \left(\sum_{\lambda\in\Lambda} \lvert c_\lambda\rvert^p\right)^{1/p}, \quad 1 \leq p < \infty.$$ We will write ℓ^p on many occasions.
$L^p(\Omega)$:	Lebesgue space with norm $$\lVert f\rVert_p = \left(\int_\Omega \lvert f(x)\rvert^p\, dx\right)^{1/p}, \quad 1 \leq p < \infty.$$ If $\Omega = \mathbb{R}^d$, then we will simply write L^p whenever it cannot cause any confusion.
$\mathbb{N}_0$:	Extended set of positive integers, i.e. $\mathbb{N}_0 = \mathbb{N} \cup \{0\}$.
supp:	Support of a vector in $\mathbb{C}^d$ or an everywhere defined function.

All other variables and notations are introduced in the respective sections.

Chapter 1

Shearlets

We already mentioned shearlets in the introduction as a powerful representation system that is in fact optimal for a certain class of images. In this chapter we present an overview of shearlet systems and their approximation properties to make this statement more precise. We start with a recap of the most common constructions of shearlet systems, namely *band-limited* shearlet systems and *compactly supported* shearlet systems. Then we discuss the class of *cartoon-like functions* for which shearlets yield an optimal sparse approximation rate. We will then also discuss how such systems can be implemented and the last section of this chapter is devoted to a novel construction of shearlet systems on *bounded domains*.

1.1 Classical shearlet frames

Shearlets were first introduced by K. Guo, G. Kutyniok, D. Labate, W.-Q Lim and G. Weiss in [GKL06, LLKW05] and are representation systems for $L^2(\mathbb{R}^d)$ that are based on *anisotropic scaling*, *shearing*, and *translations*. Anisotropic scaling and in particular shearing are concepts that only make sense in dimension two or greater. We will restrict our presentation to the case $d = 2$. However, constructions for higher dimensions are known in the literature [KLL12].

The anisotropic scaling that is used for a shearlet system is obtained by using *parabolic scaling matrices*

$$A_{2^j} = \begin{pmatrix} 2^j & 0 \\ 0 & 2^{j/2} \end{pmatrix}, \qquad \widetilde{A}_{2^j} = \begin{pmatrix} 2^{j/2} & 0 \\ 0 & 2^j \end{pmatrix},$$

with *scaling parameter* $j \in \mathbb{N}_0$. The shear action can also be achieved by a matrix; we denote by

$$S_k = \begin{pmatrix} 1 & k \\ 0 & 1 \end{pmatrix}$$

the *shearing matrices* with *shearing parameter* $k \in \mathbb{Z}$.

Using the anisotropic scaling matrix, the shearing matrix and the standard integer shifting operation of functions in $L^2(\mathbb{R}^2)$ one can define the *cone adapted discrete shearlet system* as follows.

Definition 1.1 ([KKL12]). *Let* $\phi, \psi, \widetilde{\psi} \in L^2(\mathbb{R}^2)$ *be the* generating functions *and* $c = (c_1, c_2) \in \mathbb{R}^+ \times \mathbb{R}^+$. *Then the* (cone adapted discrete) shearlet system *is defined as*

$$\mathcal{SH}(\phi, \psi, \widetilde{\psi}, c) = \Phi(\phi, c_1) \cup \Psi(\psi, c) \cup \widetilde{\Psi}(\widetilde{\psi}, c),$$

where

$$\Phi(\phi, c_1) = \{\phi(\cdot - c_1 m) \,:\, m \in \mathbb{Z}^2\},$$
$$\Psi(\psi, c) = \left\{\psi_{j,k,m} = 2^{3j/4}\psi\left((S_k A_{2^j}) \cdot - cm\right) \,:\, j \geq 0, |k| \leq 2^{j/2}, m \in \mathbb{Z}^2\right\},$$
$$\widetilde{\Psi}(\widetilde{\psi}, c) = \left\{\widetilde{\psi}_{j,k,m} = 2^{3j/4}\widetilde{\psi}\left((S_k^T \widetilde{A}_{2^j}) \cdot - \widetilde{c}m\right) \,:\, j \geq 0, |k| \leq 2^{j/2}, m \in \mathbb{Z}^2\right\},$$

and the multiplication of c *and* $\widetilde{c} = (c_2, c_1)$ *with the translation parameter* m *should be understood entry wise.*

The first question we want to address is under which assumptions does this shearlet system form a frame for $L^2(\mathbb{R}^2)$. The possibility of reaching this property certainly depends on the choice of generators. In general, the type of generators are divided into two different types namely *band-limited* ones and those that are compactly supported. The first known shearlet system that achieves the frame property is build on band-limited generators. Moreover, for these types of shearlet systems one can even obtain a *Parseval frame* for $L^2(\mathbb{R}^2)$.

Band-limited shearlets

The following example of a band-limited shearlet Parseval frame can be found in [GL09, GKL06] and is called *classical shearlet.*

Let ψ_1 be in $L^2(\mathbb{R})$ satisfying the following so-called *Calderón condition*

$$\sum_{j \in \mathbb{Z}} |\widehat{\psi}_1(2^{-j}\xi_1)| = 1 \quad \text{for every } \xi_1 \in \mathbb{R},$$

with $\widehat{\psi}_1 \in \mathbb{C}^\infty(\mathbb{R})$ and supp $\widehat{\psi}_1 \subseteq [-1/2, -1/16] \cup [1/16, 1/2]$. Furthermore, let ψ_2 be in $L^2(\mathbb{R})$ such that

$$\sum_{l=-1}^{1} \widehat{\psi}_2(\xi_2 + l) = 1 \quad \text{for every } \xi_2 \in [-1, 1]$$

with $\widehat{\psi}_2 \in C^\infty(\mathbb{R})$ and supp $\widehat{\psi}_2 \subseteq [-1, 1]$. The classical shearlet is then defined as

$$\widehat{\psi}(\xi_1, \xi_2) = \widehat{\psi}_1(\xi_1)\widehat{\psi}_2(\xi_2\xi_1).$$

The system

$$\{\psi_{j,k,m} \,:\, j, k \in \mathbb{Z}, m \in \mathbb{Z}^2\}$$

then forms a Parseval frame for $L^2(\mathbb{R}^2)$. As outline in [GKL06] a modified cone-adapted shearlet system that forms a Parseval frame for $L^2(\mathbb{R}^2)$ can be constructed by projecting and tilting the shearlet elements that live inside one a priori fixed cone as well as choosing an appropriate generator for ϕ.

This second type of shearlet generators are constructed to be compactly support. With the implied perfect localization in time, cone-adapted shearlet systems can be constructed. In this thesis we will only focus on compactly supported shearlet frames.

Compactly supported shearlets

Compactly supported shearlets have perfect spatial localization which is useful for example in edge classification [KP15], image separation [KL12b], construction of optimal boundary adapted systems [GKMP15], etc. For the latter see also Section 1.4.

The first explicit construction of a compactly supported shearlets system was presented by Kittipoom et al. in [KKL12]. Beyond the explicit construction the authors have proved the following general result.

Theorem 1.2 ([KKL12]). *Let $\phi, \psi \in L^2(\mathbb{R}^2)$ such that*

$$|\widehat{\phi}(\xi_1, \xi_2)| \leq C_1 \min\{1, |\xi_1|^{-r}\} \min\{1, |\xi_2|^{-r}\}$$

and

$$|\widehat{\psi}(\xi_1, \xi_2)| \leq C_2 \min\{1, |\xi_1|^{\alpha}\} \min\{1, |\xi_1|^{-r}\} \min\{1, |\xi_2|^{-r}\},$$

for some constants $C_1, C_2 > 0$ and $\alpha > r > 3$. Further let $\widetilde{\psi}(x_1, x_2) = \psi(x_2, x_1)$ and assume there exists a positive constant $A > 0$ such that

$$|\widehat{\phi}(\xi)|^2 + \sum_{j \geq 0} \sum_{|k| \leq \lceil 2^{j/2} \rceil} |\widehat{\psi}(S_k^T (A_j)^{-1} \xi)|^2 + \sum_{j \geq 0} \sum_{|k| \leq \lceil 2^{j/2} \rceil} |\widehat{\widetilde{\psi}}(S_k (\widetilde{A}_j)^{-1} \xi)|^2 > A$$

holds almost everywhere. Then there exists $c = (c_1, c_2) \in \mathbb{R}^+ \times \mathbb{R}^+$ such that the cone-adapted shearlet system $\mathcal{SH}(\phi, \psi, \widetilde{\psi}, c)$ forms a frame for $L^2(\mathbb{R}^2)$.

Remark 1.3. *The frame bounds of the shearlet system depend on the degree of frequency decay as well as the sampling parameter c.*

We next turn to the approximation properties of shearlets which are really at the heart of shearlet theory. More precisely, we discuss the *sparse approximation rate* for *cartoon-like functions*.

1.2 Approximation properties

The great benefit of shearlets over more conventional multiscale representation systems such as wavelets are the optimal sparse approximation rate of *cartoon-like functions*.

Cartoon-like functions

The idea of a model for natural images that is based on C^2 functions up to some C^2 edge stems from the early works by Donoho [Don99, Don01], see also [CD02] and the references therein. This class functions was then later coined *class of cartoon-like functions* and its definition in one of the latest forms is as follows.

Definition 1.4. *Let $\nu > 0$ and $f : \mathbb{R}^2 \longrightarrow \mathbb{C}$ a function of the form*

$$f = g + h\chi_B,$$

where $B \subset [0,1]^2$ is a set whose boundary is a closed C^2 curve with curvature bounded by ν and $g, h \in C^2(\mathbb{R}^2)$ are compactly supported in $[0,1]^2$ with $\|g\|_{C^2}, \|h\|_{C^2} \leq 1$. Then we call f a cartoon-like function*. The set of cartoon-like functions is called* class of cartoon-like functions *and is denoted by $\mathcal{E}^2(\nu)$.*

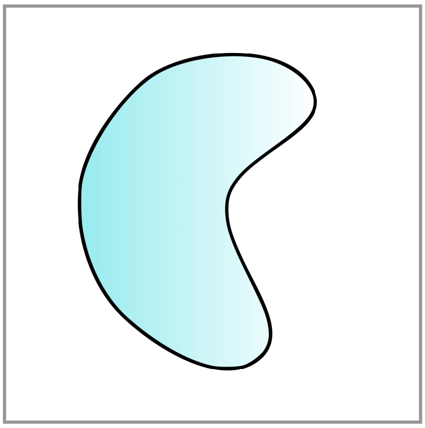

Figure 1.1: Cartoon-like function

Donoho considered this class of functions in [Don01] in order to study the intrinsic sparsity of images as well as the optimality of dictionies for this model. We briefly discuss the optimality of dictionaries for such functions since shearlets are indeed one of such dictionaries.

Optimal sparse approximation rate

Following the discussion in [Don01] one needs additional assumptions in order to exclude pathological examples of optimal dictionaries. Donoho has chosen to use a *polynomial constraint on the search depth* which has the following meaning. In order to find the first N terms of the approximation of a function f by a countable dictionary $(\psi_\lambda)_{\lambda\in\mathbb{N}}$ one is only allowed to search in the first $\pi(N)$ elements of the dictionary, where π is an a-priori chosen polynomial independent of f. As explained in [Don01] this assumption can be translated into the decay of *tail coefficients*. More precisely, suppose $(\psi_\lambda)_{\lambda\in\mathbb{N}}$ is a tight frame and one looks for a good N-term approximation, then seeing the first $\pi(N)$ coefficients $(\langle f, \psi_\lambda\rangle)_{\lambda\in\mathbb{N}}$ is sufficient provided $\sum_{\lambda>\pi(N)} |\langle f, \psi_\lambda\rangle|$ has sufficient algebraic decay. Therefore, in the context of frames the design of optimal dictionaries for certain classes of functions is often based on an analysis of the frame coefficients $(\langle f, \psi_\lambda \rangle)_{\lambda \in \mathbb{N}}$.

In the same paper [Don01] Donoho proved that there is no depth-search limited dictionary whose best N-term approximation f_N of a cartoon-like function f can have a error $\|f - f_N\|^2$ that decays faster than N^{-2}. More precisely, an example of a dictionary reaching this rate was also presented, hence, we have

$$\|f - f_N\| \asymp N^{-2}.$$

Thus the following definition of an optimally sparse approximating frame for cartoon-like functions have been established.

Definition 1.5. *Let $(\psi_\lambda)_{\lambda \in \mathbb{N}}$ be a frame for $L^2(\mathbb{R}^d)$, where $d = 2, 3$. Then $(\psi_\lambda)_{\lambda \in \mathbb{N}}$ provides* optimally sparse approximation of cartoon-like images $f \in \mathcal{E}^2(\mathbb{R}^d)$*, if the associated N-term approximation f_N satisfies*

$$\|f - f_N\|_{L^2}^2 \lesssim N^{-2/(d-1)} \qquad \text{as } N \to \infty,$$

and

$$|c_n^*| \lesssim n^{-(d+1)/(2d-1)} \qquad \text{as } n \to \infty,$$

where log*-factors will be ignored.*

One very prominent system that reaches this optimal rate is the *curvelet system* introduced by Candès and Donoho in [CD02]. This system is a band-limited directional multiscale system that is based on rotation instead of shearing.

The following theorem whose proof can be found in [KL11] provides a sufficient condition for compactly supported shearlet frames to fulfill the optimally sparse approximation rate of cartoon-like functions.

Theorem 1.6 ([KL11])**.** *Let $\mathcal{SH}(\phi, \psi, \widetilde{\psi}, c)$ be a compactly supported shearlet frame with*

i) $|\widehat{\psi}(\xi)| \leq C \min\{1, |\xi_1|^\alpha\} \min\{1, |\xi_1|^{-r}\} \min\{1, |\xi_2|^{-r}\}$,

ii) $\left|\frac{\partial}{\partial \xi_2} \widehat{\psi}(\xi)\right| \leq |h(\xi_1)| \left(1 + \frac{\xi_2}{\xi_1}\right)^{-r}$,

where $\alpha > 5, r \geq 4, h \in L^1(\mathbb{R}), C > 0$ is some constant. Further assume $\widetilde{\psi}$ fulfills i) and ii) with switched roles of ξ_1 and ξ_2. Then for any fixed $\nu > 0$ and $f \in \mathcal{E}^2(\nu)$ we have

$$\|f - f_N\|_2^2 \leq C'(\log N)^3 N^{-2}, \qquad \text{as } N \longrightarrow \infty,$$

where f_N is the best N-term approximation obtained using the N largest shearlets coefficients of f in magnitude allowing polynomial depth search and C' is some constant independent of N.

Remark 1.7. *It is known that standard wavelet orthonormal bases only obtain a rate of order N^{-1}, see [KL12a]. Moreover, both rates for shearlets and wavelets are sharp.*

Speaking of wavelet orthonormal bases one might wonder about the existence of shearlet orthonormal bases. However, as for today there is no construction of an orthonormal shearlet basis known. Surely, an orthonormal basis has a lot more structure than a general frame, such as *linear independence.* We will next discuss this property for compactly supported shearlet systems.

1.3 Linear independence

As we already mentioned in the beginning of the introduction of this thesis, every Hilbert space possesses an orthonormal basis. Moreover, every orthonormal basis is linearly independent. Another representation system that is more general than an orthonormal basis, yet still linearly independent is a *Riesz basis*.

Definition 1.8. *A complete sequence $(\psi_\lambda)_{\lambda\in\Lambda} \subseteq \mathcal{H}$ is called a* Riesz basis *if there exists constants $0 < A, B < \infty$ such that for all $(c_\lambda)_{\lambda\in\Lambda}$ it holds*

$$A \sum_{\lambda\in\Lambda} |c_\lambda|^2 \leq \left\| \sum_{\lambda\in\Lambda} c_\lambda \psi_\lambda \right\|^2 \leq B \sum_{\lambda\in\Lambda} |c_\lambda|^2.$$

Remark 1.9. *The Riesz basis property has been studied for shearlets in [FM15].*

A frame can be linearly independent but does not necessarily have to be. As there are different types of linear independence in the infinite dimensional setting we first give a definition to clarify the terminology.

Definition 1.10. *Let $(\psi_\lambda)_{\lambda\in\Lambda}$ be a sequence of elements in a Banach space $\mathcal{X}$.*

*i) If $\sum_{\lambda\in\Lambda} c_\lambda \psi_\lambda = 0$ implies $c_\lambda = 0$ for every $\lambda \in \Lambda$, then we call $(\psi_\lambda)_{\lambda\in\Lambda}$ ω-*independent.

ii) If for any finite set $\Lambda_0 \subset \Lambda$ we have $\sum_{\lambda\in\Lambda_0} c_\lambda \psi_\lambda = 0$ if and only if $c_\lambda = 0$ for all $\lambda \in \Lambda_0$, then we call $(\psi_\lambda)_{\lambda\in\Lambda}$ linearly independent.

We wil now turn to study the linear independence of compactly supported shearlets. This has been studied by the author of this thesis and his collaborator in [MP15]. Furthermore, parts of this section follows [MP15] closely.

The linear independence of compactly supported shearlets is examined for the case when the generators are separable, i.e.

$$\phi(x_1, x_2) := \phi^1(x_1)\phi^1(x_2), \quad \psi(x_1, x_2) := \psi^1(x_1)\phi^1(x_2), \quad \widetilde{\psi}(x_1, x_2) := \psi(x_2, x_1) \quad (1.1)$$

where ϕ^1 is assumed to be a continuous compactly supported scaling function and ψ^1 is a corresponding (compactly supported) wavelet, cf. Appendix B.1 or [Dau92, HW96, Mal09] for definitions of such functions.

Clearly one can not expect that all type of shearlet systems as in Definition 1.1 are linearly independent. Furthermore, a shearlet system contains a part of an oversampled wavelet system whose linear independence has been studied on its own over decades [CL02, BS10, BS06]. However, one can prove the linear independence for the following set of *admissible, compactly supported, separable shearlet systems.*

Definition 1.11. *Let ϕ, ψ be as in (1.1) and let $c = (c_1, c_2) \in \mathbb{Q}^+ \times \mathbb{Q}^+$ with $c_i = a_i/b_i$, where $a_i, b_i \in \mathbb{N}$ and b_i is odd for $i = 1, 2$. Further, let the wavelet system*

$$\left\{\phi^1(\cdot - c_i m), \psi^1(2^j \cdot - c_i m) \,:\, j \geq 0, m \in \mathbb{Z}\right\}$$

be linearly independent for $i = 1, 2$. Then the system $\mathcal{SH}(\phi, \psi, \widetilde{\psi}, c)$ is called admissible, compactly supported, separable shearlet system.

These type of shearlet systems are a special case of the shearlet systems defined in Definition 1.1. In fact, in Definition 1.11 the choice of generators and sampling constants are specified.

The following theorem holds true.

Theorem 1.12 ([MP15]). *Every admissible compactly supported separable shearlet system is linearly independent.*

One approach that can be used to examine the linear independence of systems evolved in harmonic analysis, such wavelets and shearlets, is to study the localization properties [Grö03, BS06]. The proof of Theorem 1.12 is vastly different in that its arguments are almost solely based on the support properties such as the shape of the supports. The proof of Theorem 1.12 is consists of several steps that we shall outline below. The proofs of the partial results are moved to Appendix C.6 and can also be found in [MP15].

Idea behind the proof of Theorem 1.12

The idea behind the proof of Theorem 1.12 is the following. On the one hand one wants to chunk the full shearlet system into several smaller systems that have distinct properties such as the shape of their supports so that across these buckets the functions are linearly independent. On the other hand each of the subsets itself must be linearly independent as well. We will now explain how this can be achieved.

The shearlet system contains an oversampled wavelet system, so we first study and characterise the linear independence of these functions. The following lemma essentially follows from the multiresoluton analysis of the scaling function.

Lemma 1.13 ([MP15]). *Let ϕ^1 be a continuous compactly supported scaling function with $\operatorname{supp} \phi^1 = [0, s]$ for some $s > 0$, $(V_j)_{j\in\mathbb{Z}}$ an associated multiresolution analysis (cf. Definition B.1), and let ψ^1 be a corresponding wavelet. Moreover, let $(W_j)_{j\in\mathbb{Z}}$ denote the wavelet spaces and let $j_0, J \in \mathbb{N}\cup\{0\}$ with $j_0 < J$. If $f \in L^2(\mathbb{R})$ has compact support and*

$$0 \neq f \in \bigoplus_{j_0\leq j\leq J} W_j,$$

then f is continuous and

$$\min(\operatorname{supp} f) \in 2^{-(J+1)}\mathbb{Z}.$$

In particular

$$\min(\operatorname{supp} f(\cdot - \omega)) \in 2^{-(J+1)}\mathbb{Z} + \omega, \qquad \text{for all } \omega \in \mathbb{R}.$$

Proof. See Appendix C.1 or [MP15]. □

Furthermore, it is clear that functions with staggered supports are linear independent, which is the statement of the next lemma.

Lemma 1.14 ([MP15]). *Let $N \in \mathbb{N}$ and $f_1, \dots, f_N \in L^2(\mathbb{R})$ be continuous compactly supported functions and $a_i = \min(\operatorname{supp} f_i) \in \mathbb{R}$ for $i = 1, \dots, N$. If $a_i \neq a_j$ for all $1 \leq i, j \leq N$ with $i \neq j$, then the functions $f_1, \dots, f_N$ are linearly independent. Furthermore, if $\alpha = (\alpha_i)_{i=1}^N \in \mathbb{C} \setminus \{0\}$, then $\min(\operatorname{supp} \sum \alpha_i f_i) \in \{a_i \ : \ i = 1 \dots N\}$.*

Proof. See Appendix C.2 or [MP15]. □

Lemma 1.13 allows the characterization of the left corner of functions that can be covered by finitely many wavelet functions. This characterization together with the auxiliary result Lemma 1.14 one can prove that certain oversampled wavelets are indeed linearly independent.

Proposition 1.15 ([MP15]). *Let $(V_j)_{j\in\mathbb{Z}}$ be an MRA with continuous compactly supported scaling function and let ψ^1 be a corresponding continuous compactly supported wavelet. Moreover, let $i = 1,\ldots,n$, $J \in \mathbb{N}_0$, $(t_i)_i \in (0,1)$ such that $t_i - t_j \notin 2^{-J-1}\mathbb{Z}$, for all $i \neq j$. Furthermore for $j = 0,...,J$ let $L_j^i \subset \mathbb{Z}$ be of finite cardinality. Then the union of*

$$\Omega_n^i := \left\{ \{\psi^1(2^j(\cdot - t_i) + l\}_{l\in L_j^i} \right\}_{j=0}^{J}, \quad 1 \le i \le n$$

is linearly independent.

Proof. See Appendix C.3 or [MP15]. □

Note that the statement of Proposition 1.15 is a result concerning 1D functions. However, due to the separability assumption of the generators (1.1) the result becomes of great use as the linear independence of the 2D shearlets can be traced back to their 1D wavelet parts. In particular, every shearlet is an oversampled wavelet multiplied with an oversampled scaling function by the separability assumption of the generators. Thus, all shearlets in one fixed cone can be grouped into a set of functions such that the linear independence is determined by the linear independence of the 1D scaling functions. This yields the next theorem.

Theorem 1.16 ([MP15]). *Let $\mathcal{SH}(\phi,\psi,\widetilde{\psi},c) = \Phi(\phi,c_1)\cup\Psi(\psi,c)\cup\tilde{\Psi}(\tilde{\psi},c)$ be an admissible compactly supported separable shearlet system. Then the two cones $\Psi(\psi,c)$ as well as $\tilde{\Psi}(\tilde{\psi},c)$ are linearly independent.*

Proof. See Appendix C.4 or [MP15]. □

The next step is to decompose the shearlet system into parts with and without shearing. To this end, let

$$\Gamma_1 := \{\psi_{j,k,m}, \text{ with } k \neq 0\ \}, \quad \Gamma_2 := \{\tilde{\psi}_{j,k,m}, \text{ with } k \neq 0\ \}$$

and

$$\Gamma_3 := \{\psi_{j,k,m}, \text{ with } k = 0\ \} \cup \{\tilde{\psi}_{j,k,m}, \text{ with } k = 0\ \} \cup \Phi(\phi,c_1). \tag{1.2}$$

The linear independence of the two function systems Γ_1 and Γ_2 follow from Theorem 1.16. The linear independence of Γ_3 is shown separately.

Lemma 1.17 ([MP15]). *Let $\mathcal{SH}(\phi,\psi,\tilde{\psi},c) = \Phi(\phi,c_1)\cup\Psi(\psi,c)\cup\tilde{\Psi}(\tilde{\psi},c)$ be an admissible compactly supported separable shearlet system. Then, Γ_3 is linearly independent.*

Proof. See Appendix C.5 or [MP15]. □

Summarizing, Theorem 1.16 and Lemma 1.17 show that any finite subset of functions from Γ_1, Γ_2, and Γ_3 is linearly independent. Theorem 1.12 then follows by showing that $\operatorname{span}\Gamma_1 \cap \operatorname{span}\Gamma_2 = \{0\}$, $\operatorname{span}\Gamma_1 \cap \operatorname{span}\Gamma_3 = \{0\}$, and $\operatorname{span}(\Gamma_1 \cup \Gamma_3) \cap \operatorname{span}\Gamma_2 = \{0\}$ by examining the distinct different support structures of functions that are build from linear combinations of functions from Γ_1, Γ_2, and Γ_3, see Figure 1.2.

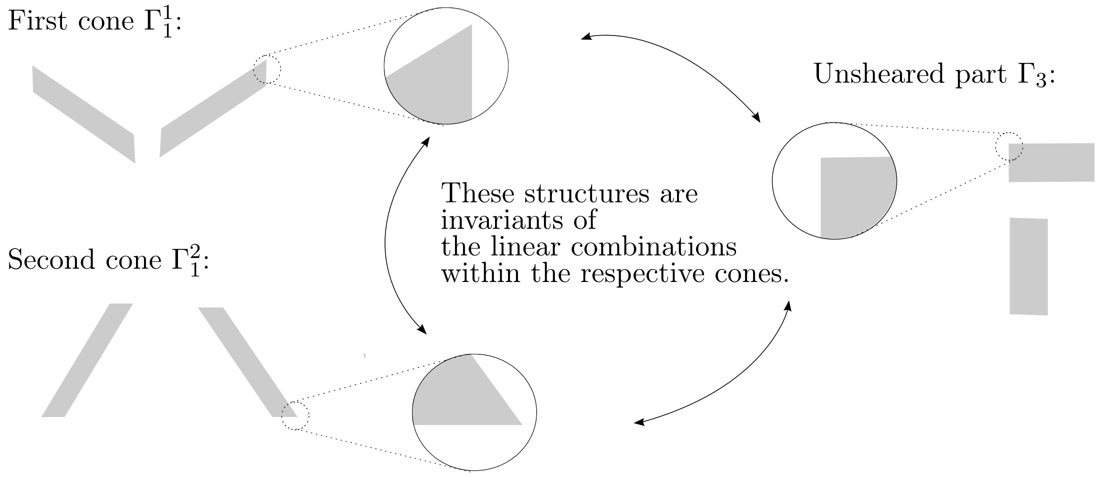

Figure 1.2: [MP15]: Display of the supports of two shearlet elements from Γ_1, Γ_2 and Γ_3.

1.4 Shearlets on bounded domains

In many cases the signal of interest is supported on a finite domain. For example images usually admit a finite region that is interesting for the user. Depending on the specific application this causes more or less problems. For example, if one were to reconstruct a brain image in magnetic resonance imaging, then the surrounding of the brain is usually constant as there are (almost) no corresponding frequencies measured. However, in other cases, for example bone scanning in *computed tomography*, the object is very frequently supported at the boundaries which then causes artifacts.

One way to get around this issue could be to scan a region that is wide enough so that artifacts of the boundary do not disturb the region of interest. However, if a boundary adapted system is already available, then such an additional waste of resources is not necessary.

In order to satisfy such needs, different attempts to construct a systems on bounded domains has been made, e.g. [KL11], [CDD00], [GKMP15]. In this section we therefore present the boundary shearlet system introduced by the author and his collaborators in [GKMP15]. Furthermore, parts of this section follow the presentation in [GKMP15] closely.

Construction

Since compactly supported shearlet systems on $\mathbb{R}^2$ are already known one can adapt each of these shearlet system onto a bounded domain Ω which we will assume to be $[0,1]^2$ in the following. Now for a shearlet system on the bounded domain Ω we will keep all shearlets whose support are completely contained in Ω. Further, in order to handle the boundary appropriately we will include boundary elements from a boundary wavelet system. More precisely, let $\mathcal{SH}(\phi, \psi, \widetilde{\psi}, c)$ be a compactly supported shearlet system and let q be such that $\operatorname{supp} \psi_{j,k,0}, \operatorname{supp} \widetilde{\psi}_{j,k,0} \subseteq B_{\frac{q}{2}2^{-j/2}}(0)$ for all $j \geq 0, |k| \leq 2^{j/2}$, where $B_r(0) := \{x \in \mathbb{R}^2 : |x_1|, |x_2| \leq r\}$. Then we define

$$\Gamma_r := \{x \in \Omega : d(x, \partial\Omega) < q2^{-r}\},$$

which is an inner tubular region that characterizes the used boundary wavelets. Before we give the precise definition of the boundary shearlet system we fix the notation that we will use for the boundary wavelets.

2D Wavelets on $[0,1]^2$

2D boundary adapted wavelets can be constructed in a straight forward manner by tensor products of 1D boundary adapted wavelets introduced in [CDV93], see also Section B.2 for some basic constructions and properties. For this, let ϕ^1 be a 1D compactly supported Daubechies scaling function. Further, let ψ^1 be the corresponding wavelet to ϕ^1 with p vanishing moments, and let $(\phi^{\text{int}}_{j,m})_{j,m}$ and $(\psi^{\text{int}}_{j,m})_{j,m}$ be the scaling functions and wavelets as described in Section B.2 of the appendix, respectively.

If $J \in \mathbb{N}$ denotes the smallest number such that $2^J \geq 2p$, then the 2D scaling functions can be obtained by

$$\omega_{J,(m_1,m_2),0} := \phi^{\text{int}}_{J,m_1} \otimes \phi^{\text{int}}_{J,m_2}, \quad 0 \leq m_1, m_2 \leq 2^J - 1.$$

The corresponding 2D wavelet functions are defined by the tensor products given by

$$\omega_{j,(m_1,m_2),\upsilon} := \begin{cases} \phi^{\text{int}}_{j,m_1} \otimes \psi^{\text{int}}_{j,m_2}, & j \geq J, \upsilon = 1, \\ \psi^{\text{int}}_{j,m_1} \otimes \psi^{\text{int}}_{j,m_2}, & j \geq J, \upsilon = 2, \\ \psi^{\text{int}}_{j,m_1} \otimes \phi^{\text{int}}_{j,m_2}, & j \geq J, \upsilon = 3, \end{cases}$$

for $0 \leq m_1, m_2 \leq 2^j - 1$ with $j \geq J$. Then we define the 2D boundary wavelet system as follows.

Definition 1.18. *Let ϕ^1 be a 1D compactly supported Daubechies scaling function, and let ψ^1 be the corresponding wavelet to ϕ^1. Further, assume the interior wavelets $\omega^1 = \psi^1 \otimes \phi^1$, $\omega^2 = \psi^1 \otimes \psi^1$, and $\omega^3 = \phi^1 \otimes \psi^1$ satisfy*

$$|\widehat{\omega^\upsilon}(\xi)| \lesssim \frac{\min\{1, |\xi_i|^\alpha\}}{\max\{1, |\xi_1|^\beta\} \max\{1, |\xi_2|^\beta\}} \tag{1.3}$$

for some $\beta > \alpha + 1 > 1$. Then

$$\mathcal{W}(\phi^1) := \{\omega_{j,m,\varepsilon} \,:\, (j, m, \upsilon) \in \Delta\}$$

is called boundary wavelet system associated with ϕ^1*, with indexing set given by*

$$\Delta := \left\{(J,(m_1,m_2),0) : 0 \leq m_1, m_2 \leq 2^J - 1\right\} \\ \cup \left\{(j,m,\upsilon) : j \geq J, 0 \leq m_1, m_2 \leq 2^j - 1, \upsilon \in \{1,2,3\}\right\}.$$

Then boundary shearlet system can now be defined as follows.

Definition 1.19 ([GKMP15])**.** *Let $\mathcal{SH}(\phi,\psi,\tilde{\psi},c)$ be a shearlet frame and $\tau > 0$ as well as $t > 0$. Further, let $\mathcal{W}(\phi^1)$ be a boundary wavelet system and set*

$$\mathcal{W}_{t,\tau}(\phi^1) : = \{\omega_{j,m,\upsilon} \in \mathcal{W}(\phi^1) : (j,m,\upsilon) \in \Delta_{t,\tau}\},$$

where

$$\Delta_{t,\tau} : = \{(j,m,\upsilon) \in \Delta : \operatorname{supp}\, \omega_{j,m,\upsilon} \cap \Gamma_{\tau(j-t)} \neq \emptyset\}.$$

Further, let

$$\Lambda = \{(j,k,m,\varepsilon) : \varepsilon \in \{0,1\}, \psi_{j,k,m,\varepsilon} \in \mathcal{SH}(\phi,\psi,\widetilde{\psi},c)\}$$

be the index set of all shearlets and

$$\psi_{j,k,m,\varepsilon} := \begin{cases} \psi_{j,k,m} & \textit{if } \varepsilon = 1, \\ \phi_m & \textit{if } \varepsilon = 0, \\ \widetilde{\psi}_{j,k,m} & \textit{if } \varepsilon = -1, \end{cases}$$

Then with

$$\Lambda_0 := \{(j,k,m,\varepsilon) \in \Lambda : \operatorname{supp}\, \psi_{j,k,m,\varepsilon} \subseteq \Omega\}$$

denoting the index set of all shearlets whose support is fully contained in Ω we define the boundary shearlet system with offsets t and τ *as*

$$\mathcal{BSH}_{t,\tau}(\phi^1;\phi,\psi,\widetilde{\psi},c) := \{\psi_{j,k,m,\varepsilon} : (j,k,m,\varepsilon) \in \Lambda_0\} \cup \mathcal{W}_{t,\tau}(\phi^1).$$

Further, we write $\Lambda_0^c := \Lambda \setminus \Lambda_0$ and $\Delta_{\tau,t}^c := \Delta \setminus \Delta_{t,\tau}$.

This definition of a boundary shearlet system mimics precisely the program we just intuitively described before. The reader should also notice that as $j \to \infty$, the size of the tubular region shrinks accordingly. This is in particular needed in order to keep a strong cross localization of the Gramian of the system which will also secure the frame property, see Theorem 1.20.

The crucial question that first arises for this novel construction of a shearlet system is whether they still share the same characterizing properties of the compactly supported shearlet system on $\mathbb{R}^2$, that is the frame property and the optimal sparse approximation of cartoon-like functions. In the next two section we will address these two issues.

Frame property

The frame property follows from a careful analysis of the decay of the cross Gramian between the the wavelet system and the shearlet system. The following theorem holds.

Theorem 1.20 ([GKMP15]). *Let $\mathcal{W}(\phi^1)$ boundary wavelet system and and α, β be as in (1.3). Further, let $\mathcal{SH}(\phi, \psi, \widetilde{\psi}, c)$ be a compactly supported shearlet frame with frame bounds A and B and suppose assume the generator ψ satisfies*

$$|\widehat{\psi}(\xi_1, \xi_2)| \leq C \frac{1}{\max\{1, |\xi_1|^{\beta'}\} \max\{1, |\xi_2|^{\beta'}\}}, \quad \text{for a.e. } (\xi_1, \xi_2) \in \mathbb{R}^2,$$

for some $\beta' > 1 + \alpha$. Additionally, let $\tau > 0$ and $\mu > 0$ such that $((1-\mu)/\tau - 2)\alpha > \frac{5}{2}$. Then there exists a constant C (dependent on $\phi^1, \phi, \psi, \widetilde{\psi}, c, \tau, \mu$) such that for all $t > 0$:

$$\sum_{(j_s,k,m_s,\varepsilon)\in\Lambda_0^c} \sum_{(j_w,m_w)\in\Delta_{\tau,t}^c} |\langle \omega_{j_w,m_w,\upsilon}, \psi_{j_s,k,m_s,\varepsilon}\rangle_{L^2(\Omega)}|^2 \leq C \cdot 2^{-2(1-\mu)\alpha t}.$$

Furthermore, if $t > 0$ such that

$$A' := \frac{A - C 2^{-2(1-\mu)\alpha t + 1}}{2B} > 0, \tag{1.4}$$

then the boundary shearlet system $\mathcal{BSH}_{t,\tau}(\phi^1; \phi, \psi, \widetilde{\psi}, c)$ yields a frame for $L^2(\Omega)$. Furthermore, a lower and an upper frame bound are given by A' and $B + 1$, respectively.

For the proof of Theorem 1.20 we will use the following auxiliary lemma.

Lemma 1.21 ([GKMP15]). *Let $\psi \in L^2(\mathbb{R}^2)$ be such that there exists $C > 0$ with*

$$|\widehat{\psi}(\xi_1, \xi_2)| \leq C \frac{\min\{1, |\xi_1|^\alpha\}}{\max\{1, |\xi_1|^\beta\} \max\{1, |\xi_2|^\beta\}}, \quad \text{for a.e. } (\xi_1, \xi_2) \in \mathbb{R}^2,$$

where $\beta/2 > \alpha > 1$. Then, for $\varepsilon = -1, 1$,

$$\sum_{|k| \leq 2^{j/2}} |(\psi_{j,k,m,\varepsilon})^\wedge(\xi_1, \xi_2)| \leq 2^{-3/4j} C' \frac{1}{\max\{1, |2^{-j}\xi_1|^{\beta/2}\}} \frac{1}{\max\{1, |2^{-j}\xi_2|^{\beta/2}\}},$$

for a.e. $(\xi_1, \xi_2) \in \mathbb{R}^2$ and a constant C'.

Proof. We only present the proof for the case $\varepsilon = -1$. The other case can be shown analogously. We divide the proof in two cases.

Case I: Assume $|\xi_1| \geq |\xi_2|/2$. Then

$$\begin{aligned} \max\{1, |\xi_1|^\beta\} \max\{1, |\xi_2|^\beta\} &\geq \max\{1, |\xi_1|^{\frac{\beta}{2}}\} \max\{1, |\xi_1|^{\frac{\beta}{2}}\} \\ &\geq 2^{-\frac{\beta}{2}} \max\{1, |\xi_1|^{\frac{\beta}{2}}\} \max\{1, |\xi_2|^{\frac{\beta}{2}}\}. \end{aligned}$$

Using this estimate, as well as the fact that

$$\sum_{|k| \leq 2^{j/2}} \frac{\min\{1, |2^{-j}\xi_1|^\alpha\}}{\max\{1, |k 2^{-j}\xi_1 + 2^{-j/2}\xi_2|^\beta\}} \leq \sup_{(\xi_1,\xi_2)\in\mathbb{R}^2} \sum_{k\in\mathbb{Z}} \frac{\min\{1, |\xi_1|^\alpha\}}{\max\{1, |k\xi_1 + \xi_2|^\beta\}} < C',$$

for some constant C' we obtain

$$\begin{aligned}
&\sum_{|k|\le 2^{j/2}} |(\psi_{j,k,m,\varepsilon})^\wedge(\xi_1,\xi_2)| \\
&\qquad \le C2^{-3/4j}\frac{1}{\max\{1,|2^{-j}\xi_1|^\beta\}} \sup_{(\xi_1,\xi_2)\in\mathbb{R}^2} \sum_{|k|\le 2^{j/2}} \frac{\min\{1,|2^{-j}\xi_1|^\alpha\}}{\max\{1,|k2^{-j}\xi_1+2^{-j/2}\xi_2|^\beta\}} \\
&\qquad \le C''2^{-3/4j}\frac{1}{\max\{1,|2^{-j}\xi_1|^\beta\}} \\
&\qquad \le C''2^{-3/4j}\frac{1}{\max\{1,|2^{-j}\xi_1|^{\beta/2}\}\max\{1,|2^{-j}\xi_2|^{\beta/2}\}}.
\end{aligned}$$

On the other hand, if **Case II:** $0 < |\xi_1| \le |\xi_2|/2$, then

$$\begin{aligned}
\max\{1,|k2^{-j}\xi_1+2^{-j/2}\xi_2|^\beta\} &\ge \max\{1,(|2^{-j/2}\xi_2|-|k2^{-j}\xi_1|)^\beta\} \\
&\ge \max\{1,(|2^{-j/2}\xi_2|-|2^{-j/2}\xi_1|)^\beta\} \\
&\ge \max\{1,(|2^{-j/2}\xi_2/2|)^\beta\} \\
&\ge 2^{-\beta}\max\{1,(|2^{-j/2}\xi_2|)^\beta\},
\end{aligned}$$

and hence

$$\begin{aligned}
&\sum_{|k|\le 2^{j/2}} |(\psi_{j,k,m,\varepsilon})^\wedge(\xi_1,\xi_2)| \\
&\qquad \le C2^{-3/4j}\frac{1}{\max\{1,|2^{-j}\xi_1|^\beta\}} \sum_{|k|\le 2^{j/2}} \frac{|2^{-j}\xi_1|^\alpha}{\max\{1,|k2^{-j}\xi_1+2^{-j/2}\xi_2|^\beta\}} \\
&\qquad \le C'2^{-3/4j}\frac{1}{\max\{1,|2^{-j}\xi_1|^\beta\}} \sum_{|k|\le 2^{j/2}} \frac{|2^{-j}\xi_1|^\alpha}{\max\{1,|2^{-j/2}\xi_2|^\beta\}} \\
&\qquad \le C'2^{-3/4j}\frac{1}{\max\{1,|2^{-j}\xi_1|^\beta\}} \frac{|2^{-j/2}\xi_1|^\alpha}{\max\{1,|2^{-j/2}\xi_2|^\beta\}} \\
&\qquad \le C''2^{-3/4j}\frac{1}{\max\{1,|2^{-j}\xi_1|^\beta\}} \frac{|2^{-j/2}\xi_2|^\alpha}{\max\{1,|2^{-j/2}\xi_2|^\beta\}} \\
&\qquad \le C''2^{-3/4j}\frac{1}{\max\{1,|2^{-j}\xi_1|^\beta\}} \frac{1}{\max\{1,|2^{-j/2}\xi_2|^{\beta-\alpha}\}}.
\end{aligned}$$

The lemma is proven. □

We continue with a proof of Theorem 1.20.

Proof of Theorem 1.20. First, observe that for a fixed scale j_s and fixed shearing parameter k the number of shearlet translates $(\psi_{j_s,k,m,\varepsilon})_m$ that have a nontrivial intersection with the support of one fixed wavelet $\omega_{j_w,m_w,v}$ is bounded by a constant independent of j_w, m_w, j_s and k.

Second, we observe that the support of an arbitrary wavelet $\omega_{j_w,m_w,v} \in \mathcal{W}(\phi^1)$ has at least a distance of size $q2^{\tau(t-j_w)}$ to the boundary. Further, the support of a shearlet

$\psi_{j_s,k,m_s,\varepsilon}$ with index $(j_s,k,m_s,\varepsilon) \in \Lambda_0^c$ is not fully contained in Ω and has at most a support length of size $q2^{-j_s/2}$. Hence, for all $(j_s,k,m_s,\varepsilon) \in \Lambda_0^c$ and $j_w < 1/(2\tau)j_s + t$, each $\omega_{j_w,m_w,\upsilon} \in \mathcal{W}(\phi^1) \setminus \mathcal{W}_{t,\tau}(\phi^1)$ satisfies

$$\operatorname{supp} \omega_{j_w,m_w,\upsilon} \cap \operatorname{supp} \psi_{j_s,k,m_s,\varepsilon} = \emptyset.$$

Hence, we assume in the sequel $j_w > 1/(2\tau)j_s + t$. Furthermore, assume without loss of generality that $\upsilon = 1$. For $\upsilon = 2, 3$, the following computations can be made in a similar manner with ξ_1 and ξ_2 interchanged. Also note that, by the same argument as above, for $\upsilon = 0$ we have

$$\langle \omega_{J_0,m',0}, \psi_{j,k,m,\varepsilon} \rangle_{L^2(\mathbb{R}^2)} = 0.$$

Since the total number of wavelet translates for a fixed level j_w is of order 2^{2j_w} a use of the previous observations as well as Parseval's identity shows that there exists a constant $C > 0$ independent of τ and t such that

$$\begin{aligned}
&\sum_{(j',m') \in \Delta_{\tau,t}^c} \sum_{(j,k,m,\varepsilon) \in \Lambda_0^c} |\langle \omega_{j',m',1}, \psi_{j,k,m,\varepsilon} \rangle_{L^2(\Omega)}|^2 \\
&\qquad \le C \sum_{j_w=0}^{\infty} \sum_{j_s=0}^{(2\tau)(j_w-t)} \sum_{|k| \le 2^{j_s/2}} 2^{2j_w} \max_{m_s,m_w} |\langle \widehat{\omega_{j_w,m,1}}, \widehat{\psi_{j_s,k,m_s,\varepsilon}} \rangle_{L^2(\Omega)}|^2. \qquad (1.5)
\end{aligned}$$

Using the frequency decay of the corresponding shearlet and wavelet atoms as well as applying Lemma 1.21 yields by the simples substitution $\xi \mapsto 2^{j_s}\xi$ that

$$\begin{aligned}
&\sum_{j_s=0}^{(2\tau)(j_w-t)} \sum_{|k| \le 2^{j_s/2}} 2^{2j_w} \max_{m_w,m_s} |\langle \widehat{\omega_{j_w,m_w,1}}, \widehat{\psi_{j_s,k,m_s,\varepsilon}} \rangle_{L^2(\Omega)}|^2 \\
&\qquad \lesssim \sum_{j_s=0}^{(2\tau)(j_w-t)} 2^{-3/2j_s} \Bigg(\int_{\mathbb{R}^2} \frac{\min\{1, |2^{-j_w}\xi_1|^\alpha\}}{\max\{1, |2^{-j_w}\xi_1|^\beta\} \max\{1, |2^{-j_w}\xi_2|^\beta\}} \\
&\qquad\qquad \cdot \frac{1}{\max\{1, |2^{-j_s}\xi_1|^{\beta'}\} \max\{1, |2^{-j_s}\xi_2|^{\beta'}\}} \, d\xi \Bigg)^2 \\
&\qquad \lesssim \sum_{j_s=0}^{(2\tau)(j_w-t)} 2^{5/2j_s} \Bigg(\int_{\mathbb{R}^2} \frac{\min\{1, |2^{j_s-j_w}\xi_1|^\alpha\}}{\max\{1, |2^{j_s-j_w}\xi_1|^\beta\} \max\{1, |2^{j_s-j_w}\xi_2|^\beta\}} \\
&\qquad\qquad \cdot \frac{1}{\max\{1, |\xi_1|^{\beta'}\} \max\{1, |\xi_2|^{\beta'}\}} \, d\xi \Bigg)^2. \\
&\qquad \lesssim \sum_{j_s=0}^{\infty} 2^{5/2j_s} \left(\int_{\mathbb{R}^2} \frac{\min\{1, |2^{j_s-j_w}\xi_1|^\alpha\}}{\max\{1, |\xi_1|^{\beta'}\} \max\{1, |\xi_2|^{\beta'}\}} \, d\xi \right)^2 \\
&\qquad \lesssim \sum_{j_s=0}^{\infty} 2^{5/2j_s + 2\alpha(j_s-j_w)} \left(\int_{\mathbb{R}^2} \frac{|\xi_1|^\alpha}{\max\{1, |\xi_1|^{\beta'}\} \max\{1, |\xi_2|^{\beta'}\}} \, d\xi \right)^2.
\end{aligned}$$

By assumption we have $\beta' - \alpha > 1$, thus the integral above is finite and we can conclude

$$\sum_{j_s=0}^{(2\tau)(j_w-t)} \sum_{|k|\leq 2^{j_s/2}} 2^{2j_w} \max_{m_w,m_s} |\langle \widehat{\omega_{j_w,m_w},1}, \widehat{\psi_{j_s,k,m_s,\varepsilon}} \rangle_{L^2(\Omega)}|^2 \lesssim \sum_{j_s=0}^{(2\tau)(j_w-t)} 2^{5/2j_s+2\alpha(j_s-j_w)}. \tag{1.6}$$

By rewriting the the right hand side of (1.6) into

$$2^{-2\alpha\mu j_w} \sum_{j_s=0}^{(2\tau)(j_w-t)} 2^{5/2j_s+2\alpha(j_s-(1-\mu)j_w)}. \tag{1.7}$$

and using $j_w > 1/(2\tau)j_s + t$, we get the following bound

$$\sum_{j_s=0}^{\infty} 2^{5/2j_s+2\alpha(j_s-(1-\mu)j_w)} \lesssim 2^{-2\alpha(1-\mu)t} \sum_{j_s}^{\infty} 2^{5/2j_s+2\alpha(j_s-(1-\mu)(1/(2\tau)j_s)}.$$

By assumption the latter sum is finite. Finally, note that

$$\sum_{j_s=0}^{\infty} 2^{5/2j_s+2\alpha(j_s-(1-\mu)j_w)} \lesssim 2^{-2\alpha(1-\mu)t}. \tag{1.8}$$

Combining the estimates (1.5)-(1.8) implies the first claim of the theorem

$$\sum_{(j_s,k,m,\varepsilon)\in\Lambda_0^c} \sum_{(j_w,m')\in\Delta_{\tau,t}^c} |\langle \omega_{j_w,m',\upsilon}, \psi_{j_s,k,m,\varepsilon} \rangle_{L^2(\Omega)}|^2 \lesssim \sum_{j_w=0}^{\infty} 2^{-2\alpha\mu j_w} 2^{-2\alpha(1-\mu)t} \lesssim 2^{-2\alpha(1-\mu)t}.$$

We next turn to prove the frame property. First, observe that

$$L^2(\Omega) = \operatorname{span}(\mathcal{W}(\phi^1) \setminus \mathcal{W}_{t,\tau}(\phi^1)) \oplus \operatorname{span}(\mathcal{W}_{t,\tau}(\phi^1)) =: W_1 \oplus W_2.$$

Define $f_1 := P_{W_1} f$ and $f_2 := P_{W_2} f$, where P_{W_i} denotes the orthogonal projection onto the spaces Ξ_i, $i = 1, 2$.

By the frame property of the full shearlet system restricted to $L^2(\Omega)$ we have for any $f \in L^2(\Omega)$

$$\|f\|_{L^2(\Omega)}^2 \leq \frac{1}{A} \sum_{(j,k,m,\varepsilon)\in\Lambda} |\langle f, \psi_{j,k,m,\varepsilon} \rangle_{L^2(\Omega)}|^2,$$

where A is the lower frame bound of the shearlet frame. Splitting the right hand side appropriately, yields

$$\begin{aligned} \|f\|_{L^2(\Omega)}^2 \leq \frac{1}{A} \Bigg(&\sum_{(j,k,m,\varepsilon)\in\Lambda_0} |\langle f, \psi_{j,k,m,\varepsilon} \rangle_{L^2(\Omega)}|^2 + 2 \sum_{(j,k,m,\varepsilon)\in\Lambda_0^c} |\langle f_1, \psi_{j,k,m,\varepsilon} \rangle_{L^2(\Omega)}|^2 \\ &+ 2 \sum_{(j,k,m,\varepsilon)\in\Lambda_0^c} |\langle f_2, \psi_{j,k,m,\varepsilon} \rangle_{L^2(\Omega)}|^2 \Bigg) =: T_1 + T_2 + T_3. \end{aligned} \tag{1.9}$$

By construction of the boundary shearlet system we only need to further consider T_2 and T_3. We continue by estimating T_2 first. Using Parseval's identity and the Cauchy Schwarz inequality we get

$$\begin{aligned}
&\sum_{(j,k,m,\varepsilon)\in\Lambda_0^c} |\langle f_1, \psi_{j,k,m,\varepsilon}\rangle_{L^2(\Omega)}|^2 \\
&= \sum_{(j,k,m,\varepsilon)\in\Lambda_0^c} \left| \sum_{(j',m',\upsilon)\in\Delta_{t,\tau}^c} \langle f_1, \omega_{j',m',\upsilon}\rangle_{L^2(\Omega)} \langle \omega_{j',m',\upsilon}, \psi_{j,k,m,\varepsilon}\rangle_{L^2(\Omega)} \right|^2 \\
&\leq \sum_{(j,k,m,\varepsilon)\in\Lambda_0^c} \left(\sum_{(j',m',\upsilon)\in\Delta_{\tau,t}^c} |\langle f_1, \omega_{j',m',\upsilon}\rangle_{L^2(\Omega)}|^2 \sum_{(j',m',\upsilon)\in\Delta_{\tau,t}^c} |\langle \omega_{j',m',\upsilon} \psi_{j,k,m,\varepsilon}\rangle_{L^2(\Omega)}|^2 \right) \\
&\leq \|f_1\|_{L^2(\Omega)}^2 \sum_{(j,k,m,\varepsilon)\in\Lambda_0^c} \sum_{(j',m',\upsilon)\in\Delta_{\tau,t}^c} |\langle \omega_{j',m',\upsilon}, \psi_{j,k,m,\varepsilon}\rangle_{L^2(\Omega)}|^2.
\end{aligned}$$

Hence, from the first claim of the theorem we can conclude

$$\sum_{(j,k,m,\varepsilon)\in\Lambda_0^c} |\langle f_1, \psi_{j,k,m,\varepsilon}\rangle_{L^2(\Omega)}|^2 \leq C\|f_1\|_{L^2(\Omega)}^2 2^{-(2\alpha(1-\mu))t} \tag{1.10}$$

for some constant $C > 0$. For T_3 we can apply the frame inequality of the shearlet frame directly so that

$$\sum_{(j,k,m,\varepsilon)\in\Lambda_0^c} |\langle f_2, \psi_{j,k,m,\varepsilon}\rangle_{L^2(\Omega)}|^2 \leq B\|f_2\|_{L^2(\Omega)}^2.$$

Further, since $f_2 \in W_2$ we have

$$\|f_2\|_{L^2(\Omega)}^2 = \sum_{(j,m,\upsilon)\in\Delta_{\tau,t}} |\langle f_2, \omega_{j,m,\upsilon}\rangle_{L^2(\Omega)}|^2 = \sum_{(j,m,\upsilon)\in\Delta_{\tau,t}} |\langle f, \omega_{j,m,\upsilon}\rangle_{L^2(\Omega)}|^2. \tag{1.11}$$

Applying (1.10) and (1.11) to (1.9) yields that A' is a lower frame bound for the boundary shearlet system. Note that t was chosen such that $A' > 0$. The existence of an upper frame bound for the boundary shearlet system follows by extending both subsystems to the full systems and apply the frame inequality for the shearlet frame and Plancherel for the wavelet ONB. Hence, an upper frame bound for the boundary shearlet system $\mathcal{BSH}_{t,\tau}(\phi^1; \phi, \psi, \widetilde{\psi}, c)$ is given by $B + 1$. □

Having established the frame property we next discuss the sparse approximation rate of cartoon-like functions.

Cartoon-like functions on bounded domains

As we mentioned several times one of the characteristic properties of shearlet systems on $\mathbb{R}^2$ is their optimal sparse approximation ability of cartoon-like function. To obtain a similar result for the boundary shearlet system we first want to specify the model of cartoon-like functions on bounded domains. This is done in the following definition.

Definition 1.22 ([GKMP15]). *Let $\nu > 0$, $D \subset \mathbb{R}^2$, and $f = f_1 + \chi_D f_2$ with $f_i \in C^2(\mathbb{R}^2)$ and* supp $f_i \subset [-c_{supp}, c_{supp}]^2$ *for some $c_{supp} > 0$ and $i = 1, 2$ such that $f(2c_{supp} \cdot -(1/2, 1/2)) \in \mathcal{E}^2$. Further, let $\#(\partial D \cap \partial\Omega) \leq M$ for some $M \in \mathbb{N}$ and let ∂D and $\partial\Omega$ only intersect transversely. Then we call $P_\Omega f$ a* cartoon-like function on Ω, *and denote the set of* cartoon-like functions on Ω *by $\mathcal{E}^2(\nu, \Omega)$.*

Note that in Definition 1.22 it is now allowed to have a discontinuity curve of the cartoon that intersect the boundary, cf. Figure 1.1 and Figure 1.3.

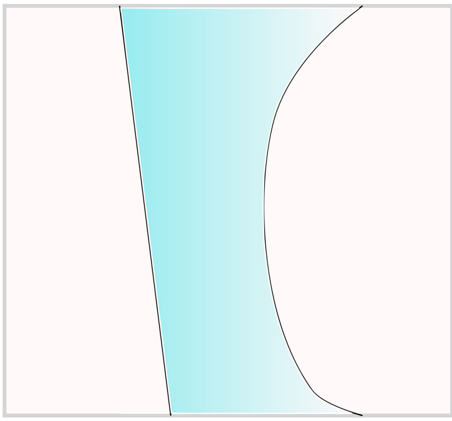

Figure 1.3: Cartoon-like functions on a bounded domain.

Optimal sparse approximation rate

Let $\mathcal{BSH}_{t,\tau}(\phi^1; \phi, \psi, \widetilde{\psi}, c) =: (\varphi_n)_n$ be a boundary shearlet frame for $L^2(\Omega)$. Further, let $f \in \mathcal{E}^2(\nu, \Omega)$, and let $(\theta_n(f))_{n\in\mathbb{N}}$ be the non-increasing rearrangement of the analysis coefficients $(|\langle \varphi_n, f \rangle_{L^2(\Omega)}|^2)_{n\in\mathbb{N}}$. Then, by the frame inequality, we have

$$\|f - f_N\|_2^2 \lesssim \sum_{n \geq N} \theta_n(f) \quad \text{for all } N \in \mathbb{N}.$$

The following theorem can be seen as an analogue of Theorem 1.6 for shearlets on bounded domains and the new class of boundary adapted cartoon-likefunctions. Indeed the theorem below shows that the optimal sparse approximation rate as presented in Definition 1.5 for the non-boundary adapted scenario is still valid in this case. However, what does not seem to be clear at first glance is whether the rate is still optimal. But this can be seen by the following argument: If the optimal rate was faster than N^{-2}, then any system on $[0, 1]^2$ that reaches this faster rate can be extended to a system on $\mathbb{R}^2$ that would have a faster rate for the classical cartoon-like functions as in Definition 1.5.

Theorem 1.23 ([GKMP15]). *Let $\phi, \psi, \widetilde{\psi}$ fulfill the assumptions of Theorem 1.6, and let $\mathcal{W}(\phi^1)$ be a boundary wavelet system as in Definition 1.18. Further let $t > 0$, $\tau > 1/3$, and let $\mathcal{BSH}_{t,\tau}(\phi^1; \phi, \psi, \widetilde{\psi}, c) =: (\varphi_n)_{n\in\mathbb{N}}$ be a boundary shearlet frame for $L^2(\Omega)$. Then $\mathcal{BSH}_{t,\tau}(\phi^1; \phi, \psi, \widetilde{\psi}, c)$ yields almost optimally sparse approximation for cartoon-like functions on Ω, i.e., for all $f \in \mathcal{E}^2(\nu, \Omega)$,*

$$\|f - f_N\|_{L^2(\Omega)}^2 \lesssim N^{-2} \log(N)^3 \quad \textit{for } N \to \infty,$$

where $f_N = \sum_{n\in I_n} \langle f, \varphi_n \rangle_{L^2(\Omega)} \varphi_n^d$ *with* I_n *containing the* N *largest coefficients* $\langle f, \varphi_n \rangle_{L^2(\Omega)}$ *in modulus and* $(\varphi_n^d)_{n\in\mathbb{N}}$ *is the canonical dual frame of* $(\varphi_n)_{n\in\mathbb{N}}$.

Proof. See Appendix C.7 or [GKMP15]. □

We end this section with two comments. First, the construction shown in this thesis which can also be found in [GKMP15] is a first construction of shearlet systems on bounded domains that has been further developed in [Pet16] to other domains of Ω than $[0,1]^2$, as well as more general boundary systems. Indeed in [Pet16] the author has extended the work of [GKMP15] to biorthogonal Riesz bases. Second, beyond the frame property as well as the optimal sparse approximation it was also shown in [GKMP15] that this novel boundary shearlet system can also characterise the Sobolev spaces $H^s(\Omega)$. We refer to the paper [GKMP15] and the thesis [Pet16] for more interest on this matter.

Chapter 2

Generalized sampling

In the previous chapter we have discussed shearlet frames and their optimal sparse approximation rate of cartoon-like functions. Since the class of cartoon-like functions model natural images, in a simplified realm, shearlet systems are of great interest as a reconstruction system. In this chapter we will make this idea more precise and discuss in more detail the shearlet reconstructions from Fourier measurements.

The reconstruction method that we discuss in this chapter is *generalized sampling (GS)* which was first introduced by Adcock et al. in a series of papers [AH12a, AH12b, AHP13]. This reconstruction method is build upon *consistent reconstructions* which was introduced in [UA94, Eld03, EW05] and allows one to study the reconstruction of objects in a general Hilbert space where the system that is used to model the samples and the system that is used for the reconstruction can be arbitrary frames. However, the theory of consistent reconstructions requires the number of measurements and the number of elements used for the reconstruction to be the same. This requirement is relaxed in GS and leads to superior results [AHP13]. More precisely, it is key in GS to let the number of measurements and the number of reconstruction elements to vary independently of each other. This idea can also be expressed in terms of discretizations. Indeed, the reconstruction problem is an infinite dimensional problem that involves the need of working with bi-infinite matrices $U = (u_{i,j})_{i,j\in\mathbb{N}}$. One way to discretize the problem is to apply an (even) finite section method and consider $U^{[N,N]} = (u_{i,j})_{i,j=1,\ldots,N}$. However, as it was argued in [AH12a] this can lead to several difficulties concerning the stability and convergence of the discretized problem. Generalized sampling proposes to use an uneven finite section method by considering $U^{[M,N]} = (u_{i,j})_{i=1,\ldots,M,j=1,\ldots,N}$.

2.1 Reconstruction method

We first fix some notation that we use throughout this section. For a *sampling system* $\{s_1, s_2, \ldots\} \subset \mathcal{H}$ - whose elements we call *sampling vectors* - we define the corresponding sampling space $\mathcal{S} \subset \mathcal{H}$ as the closure of its span, i.e.

$$\mathcal{S} = \overline{\operatorname{span}}\{s_k \,:\, k \in \mathbb{N}\}.$$

The finite dimensional analogue of the sampling space $\mathcal{S}$ is denoted by

$$\mathcal{S}_M = \operatorname{span}\{s_1, \ldots, s_M\},$$

where $M \in \mathbb{N}$ indicates the number of sampling vectors and hence the number of measurement. We now assume that the measurements $(m_f(k))_{k\in\mathbb{N}}$ of an object $f \in \mathcal{H}$ with respect to a fixed sampling system $\{s_1, s_2, \ldots\}$ can be modeled as linear measurements of the form

$$m_f(k) := \langle f, s_k \rangle, \quad k \in \mathbb{N}. \tag{2.1}$$

Analogously for a *reconstruction system* $\{r_1, r_2, \ldots\} \subset \mathcal{H}$ we define the reconstruction space $\mathcal{R} \subset \mathcal{H}$ as the closed span of the *reconstruction elements*, that is

$$\mathcal{R} = \overline{\operatorname{span}}\{r_k \,:\, k \in \mathbb{N}\}$$

and, likewise, its finite dimensional version is denoted as

$$\mathcal{R}_N = \operatorname{span}\{r_1, \ldots, r_N\}, \quad N \in \mathbb{N}.$$

Using the above notation a reconstruction method shall be the following.

Definition 2.1. *For a sampling system $\{s_k \,:\, k \in \mathbb{N}\}$ and a reconstruction space $\mathcal{R}_N$ a mapping*

$$F_{N,M} : \mathcal{H} \longrightarrow \mathcal{R}_N$$

is called reconstruction method*, if, for every $f \in \mathcal{H}$, the signal $F_{N,M}(f)$ depends only on $m(f)_1, \ldots, m(f)_M$, where the samples $m(f)_j$ are defined in* (2.1)*.*

Remark 2.2. *Note that a reconstruction method does not need to be linear.*

In order to avoid pathological examples, we will require the following subspace condition

$$\mathcal{R} \cap \mathcal{S}^\perp = \{0\} \quad \text{and} \quad \mathcal{R} + \mathcal{S} \text{ is closed.} \tag{2.2}$$

Such an assumption is clearly plausible, otherwise there would be reconstructions, i.e. elements $f \in \mathcal{R} \setminus \{0\}$ whose measurements are all zero, since f is also an element of $\mathcal{S}^\perp$. Moreover, the subspace condition guarantees a well posedness of the finite dimensional reconstruction problem, cf. Theorem 2.3.

Since in practice we are not able to process an infinite amount of information we are mainly interested in the finite-dimensional reconstruction problem that reads as follows:

Given a finite number of measurements $\langle f, s_1 \rangle, \ldots, \langle f, s_M \rangle$ of some unknown $f \in \mathcal{H}$, we wish to determine a reconstruction $f_N \in \mathcal{R}_N$ such that $\|f - f_N\|$ is small and $f_N \to f$ as $N \to \infty$ fast.

The existence of a reconstruction to the above problem is guaranteed by the following theorem.

Theorem 2.3 ([AHP13])**.** *Let $\mathcal{S}_M$ and $\mathcal{R}_N$ be as above and $P_{\mathcal{S}_M}$ be the following finite rank operator:*

$$P_{\mathcal{S}_M} : \mathcal{H} \to \mathcal{S}_M,$$

$$f \mapsto \sum_{k=1}^{M} \langle f, s_k \rangle s_k.$$

If (2.2) *holds, then there exists an* $M \in \mathbb{N}$ *such that the system of equations*

$$\langle P_{\mathcal{S}_M} f_{N,M}, r_j \rangle = \langle P_{\mathcal{S}_M} f, r_j \rangle, \quad j = 1, \ldots, N \tag{2.3}$$

has a unique solution $f_{N,M} \in \mathcal{R}_N$. *Moreover, the smallest* $M \in \mathbb{N}$ *such that the system is uniquely solvable is the least number* $M \in \mathbb{N}$ *so that*

$$c_{N,M} := \inf_{\substack{f \in \mathcal{R}_N, \\ \|f\|=1}} \|P_{\mathcal{S}_M} f\| > 0. \tag{2.4}$$

Furthermore,

$$\|f - P_{\mathcal{R}_N} f\| \leq \|f - f_{N,M}\| \leq \frac{1}{c_{N,M}} \|f - P_{\mathcal{R}_N} f\|, \tag{2.5}$$

where $P_{\mathcal{R}_N} : \mathcal{H} \to \mathcal{R}_N$ *denotes the orthogonal projection onto* $\mathcal{R}_N$.

We close this section with two definitions.

Definition 2.4 ([AHP13])**.** *The solution* $f_{N,M}$ *in Theorem 2.3 is called* generalized sampling reconstruction.

Theorem 2.3 shows that it is sufficient to study the quantity $c_{N,M}$ in (2.4) in order to guarantee the existence of generalized sampling reconstructions. This quantity has already been studied in the literature, in particular, in context with sampling and reconstruction in arbitrary systems by Unser and Aldroubi in [UA94].

Definition 2.5 ([UA94, Tan00])**.** *The quantity* $c_{N,M}$ *in* (2.4) *is called the* infimum cosine angle *between the subspaces* $\mathcal{R}_N$ *and* $\mathcal{S}_M$.

Remark 2.6. *The infimum consine angle between two spaces is not symmetric.*

In order to quantify the quality of the reconstruction and compare it to other reconstruction methods, we will next recall two quality measures that have been proposed in [AHP13].

Quality measures

We consider two quality measures for general reconstruction methods. The first one is the *quasi-optimality constant.*

Definition 2.7 ([AHP13])**.** *For any fixed reconstruction method* $F_{N,M} : \mathcal{H} \longrightarrow \mathcal{R}_N$, *cf. Definition 2.1, let* $\mu = \mu(F_{N,M}) > 0$ *be the least number such that*

$$\|f - F_{N,M}(f)\| \leq \mu \|f - P_{\mathcal{R}_N}(f)\| \quad \text{for all } f \in \mathcal{H}.$$

Then we call μ *the* quasi-optimality constant *of* $F_{N,M}$. *If no such constant exists, then we write* $\mu = \infty$. *If* μ *is small, we say* $F_{N,M}$ *is* quasi-optimal.

The second measure quantifies the robustness against perturbations.

Definition 2.8 ([AHP13]). *Let $F_{N,M} : \mathcal{H} \longrightarrow \mathcal{R}_N$ be a reconstruction method, cf. Definition 2.1. The* (absolute) condition number $\kappa = \kappa(F_{N,M}) > 0$ *is defined as*

$$\kappa = \sup_{f \in \mathcal{H}} \lim_{\varepsilon \searrow 0} \sup_{\substack{g \in \mathcal{H}, \\ 0 < \|m(g)\|_{\ell^2} \leq \varepsilon}} \left(\frac{\|F_{N,M}(f+g) - F_{N,M}(f)\|}{\|m(g)\|_{\ell^2}} \right),$$

where $m(g) = (m(g)_1, \ldots, m(g)_M, 0, \ldots)$. If κ is small, then we say $F_{N,M}$ is well conditioned*, otherwise $F_{N,M}$ is called* ill-conditioned.

Using the quasi-optimality constant and the absolute condition number we associate to any reconstruction method a *reconstruction constant* which is defined as the maximum of both quantities and, hence, can be seen as a worst estimate.

Definition 2.9 ([AHP13, AHP14]). *Let $F_{N,M} : \mathcal{H} \longrightarrow \mathcal{R}_N$ be a reconstruction method. The* reconstruction constant *of $F_{N,M}$ is defined as*

$$C(F_{N,M}) = \max\{\mu(F_{N,M}), \kappa(F_{N,M})\},$$

where $\mu(F_{N,M})$ is the quasi-optimality constant and $\kappa(F_{N,M})$ is the (absolute) condition number.

In the event that the sampling system is an orthonormal basis for its span - which is the situation we are mainly interested in - the infimum cosine angle can be expressed via the reconstruction constant, in fact, by [AHP13]

$$\frac{1}{c_{N,M}} = \mu(G_{N,M}) = \kappa(G_{N,M}) = C(G_{N,M}),$$

where $G_{N,M}$ refers to the generalized sampling reconstruction method described by Theorem 2.3.

Now, in order to study the quality of the reconstruction in terms of the convergence $\|f - f_{N,M}\|$ it is crucial to have good control on the infimum cosine angle $c_{N,M}$. Moreover, it seems intuitively clear, that the number of measurements M must grow if one wants to increase N. We make this more precise in the next section.

2.2 Stable sampling rate

As we already pointed out it is of great importance to have an estimate for the asymptotic behaviour of $c_{N,M}$ with regard to increasing N. In particular, we want to study how M scales with increasing N and a fixed upper value for $c_{N,M}$ since this would tell us how many measurements M we need for recovering the signal in an N dimensional reconstruction space. The following quantity carries this information.

Definition 2.10. *For any fixed $N \in \mathbb{N}$ and $\theta > 1$ the* stable sampling rate $\Theta(N, \theta)$ *is defined as*

$$\Theta(N, \theta) = \min\left\{ M \in \mathbb{N} \,:\, c_{N,M} > \frac{1}{\theta} \right\}.$$

Linear stable sampling rate

One particular focus is on a linear behaviour of the stable sampling rate. We explain why this is the case. Suppose the stable sampling rate is linear in N, i.e., $\Theta(N,\theta) = \mathcal{O}(N)$ as $N \to \infty$. Furthermore, we assume that the reconstruction space provides some approximation behavior of the function of interest. More precisely, let $f \in \mathcal{H}$ be the object of interest and suppose there exist $C_f, D_f, \gamma_f > 0$ depending on f such that

$$C_f N^{-\gamma_f} \leq \|f - P_{\mathcal{R}_N} f\| \leq D_f N^{-\gamma_f}, \quad \text{for all } N \in \mathbb{N}. \tag{2.6}$$

Then the following result holds.

Theorem 2.11 ([AHP13]). *Suppose that the stable sampling rate $\Theta(N,\theta)$ is linear in N, i.e. $\Theta(N,\theta) = \mathcal{O}(N)$ as $N \to \infty$. Let $f \in \mathcal{H}$ be fixed and let*

$$F_M : (m(f)_1, \dots, m(f)_M) \mapsto F_M(f) \in \mathcal{R}_{\psi_f(M)},$$

be a reconstruction method, where $\psi_f : \mathbb{N} \longrightarrow \mathbb{N}$ with $\psi_f(M) \leq \lambda M$ for some $\lambda > 0$. Assume that (2.6) holds. Then, for any $\theta > 1$, there exist constants $d(\theta) \in (0,1)$ and $c(\theta, C_f, D_f) > 0$ such that

$$\|f - G_{d(\theta)M,M}(f)\| \leq c(\theta, C_f, D_f)\|f - F_M(f)\||, \quad \textit{for all } M \in \mathbb{N},$$

where $G_{N,M}$ denotes the generalized sampling reconstruction method.

Theorem 2.11 shows that generalized sampling cannot be outperformed in the event of a linear stable sampling rate.

Stable sampling rate for wavelets

The stable sampling rate for 1D wavelets was first considered in [AHP14]. The results were then extended to 2D by the author and his collaborators in [AHKM15]. For convenience we recall the related result here in a shortened form.

A straight forward generalization of dyadic 1D MRA wavelets can be obtained by considering the dyadic scaling matrix of the form

$$A = \begin{pmatrix} 2 & 0 \\ 0 & 2 \end{pmatrix}.$$

In this section we will restrict to this case only, however, the stable sampling rate can also be computed for more general scaling matrices and we refer the interested reader to the work [AHKM15] for such generalizations.

Reconstruction Space

Assume the function $f \in \mathcal{H} = L^2(\mathbb{R}^2)$ that we want to reconstruct is compactly supported in, say, $[0,a]^2$ for some positive integer a. Note that with a view to applications such as image reconstructions this is a reasonable assumption, since images typically have a finite field of view. Similarly, we assume that the scaling function and the wavelets that are used as generators for the wavelet reconstruction system to be compactly supported in $[0, a]^2$ as well. As wavelet bases arise from translated and scaled versions of the generators, see Appendix B, we can now restrict to the following set of functions

$$\Omega_1 := \{\phi_{0,m} \,:\, m =\in \mathbb{Z}^2, \text{supp } \phi_{0,m} \cap [0, a]^2 \neq \emptyset\}$$

and

$$\Omega_2 := \{\psi^p_{j,m} \,:\, j \in \mathbb{N} \cup \{0\},\; m \in \mathbb{Z}^2, \text{supp } \psi^p_{j,m} \cap [0, a]^2 \neq \emptyset, p = 1, 2, 3\}.$$

These functions will clearly be sufficient since the other scaling functions and wavelets that do not intersect the region of interest will have inner product with the object of interest equal to zero.

The reconstruction space $\mathcal{R}$ is now defined as the closed linear span of the functions in Ω_1 and Ω_2, i.e.

$$\mathcal{R} = \overline{\text{span}}\{\varphi \,:\, \varphi \in \Omega_1 \cup \Omega_2\}.$$

In order to define the finite dimensional reconstruction space we will first order the elements in $\Omega_1 \cup \Omega_2$. There are many different possibilities to order this set of functions and the results also may depend on this ordering. The ordering that we propose arise quite naturally from the wavelet structure. Indeed, we first group all elements corresponding to their scale together. This results in J buckets each of them consisting of functions that differ by their translation parameter. The translation parameter is in $\mathbb{Z}^2$ and can thus be ordered in a lexicographical manner. Finally we order all buckets along their scales. Using this ordering we define the finite dimensional reconstruction space $\mathcal{R}_N$ as follows:

$$\mathcal{R}_N = \text{span}\{\varphi_i \,:\, i = 1, \dots, N\}, \quad N \in \mathbb{N}.$$

In order to take full advantage of the multiresolution structure of wavelets and their approximation properties, it is very convenient to consider a finite dimensional reconstruction spaces that contains all elements up to a certain scale. In this case, one could follow the approach in [AHP14, AHKM15] and construct the reconstruction space via the space

$$V_0^{(a)} := \text{span}\{\phi_{0,m} \,:\, m \in \mathbb{Z}^2, \text{supp } \phi_{0,m} \cap [0, a]^2 \neq \emptyset\}$$

and the truncated wavelet spaces

$$W_j^{(a)} := \text{span}\{\psi^p_{j,m} \,:\, m \in \mathbb{Z}^2, \text{supp } \psi^p_{j,m} \cap [0, a]^2 \neq \emptyset, p = 1, 2, 3\}.$$

Indeed, the reconstruction space that contains all wavelet elements up to a certain scale J is then given by

$$\mathcal{R}_{N_J} = V_0^{(a)} \oplus W_0^{(a)} \oplus \ldots \oplus W_{J-1}^{(a)}.$$

For the finite dimensional reconstruction space $\mathcal{R}_{N_J}$ we have 2^{2J} many elements (asymptotically in J).

Sampling space

To define the sampling space consisting of elements of the Fourier basis, we first choose $T_1, T_2 > 0$ sufficiently large such that

$$\mathcal{R} \subset L^2([-T_1, T_2]^2).$$

The values T_1 and T_2 can be computed depending on the length of the support of the wavelets. Indeed, choosing $T_1 \geq a-1$ and $T_2 \geq 2a-1$ is sufficient. To allow an arbitrarily dense sampling, for each $\varepsilon \leq \frac{1}{T_1+T_2}$, we define the sampling vectors

$$s_l^{(\varepsilon)} = \varepsilon e^{2\pi i \varepsilon \langle l, \cdot \rangle} \cdot \chi_{\left[-\frac{T_1}{\varepsilon(T_1+T_2)}, \frac{T_2}{\varepsilon(T_1+T_2)}\right]^2}, \quad l \in \mathbb{Z}^2. \tag{2.7}$$

Based on these sampling vectors, we now define the sampling space $\mathcal{S}^{(\varepsilon)}$ by

$$\mathcal{S}^{(\varepsilon)} = \overline{\operatorname{span}} \left\{ s_l^{(\varepsilon)} \,:\, l \in \mathbb{Z}^2 \right\}.$$

The finite-dimensional subspaces $\mathcal{S}_M^{(\varepsilon)}$, $M = (M_1, M_2) \in \mathbb{N} \times \mathbb{N}$, are then given by

$$\mathcal{S}_M^{(\varepsilon)} = \operatorname{span} \left\{ s_l^{(\varepsilon)} \,:\, l = (l_1, l_2) \in \mathbb{Z}^2, -M_i \leq l_i \leq M_i, i = 1, 2 \right\}.$$

Note that the total number of reconstruction elements is then of order $M_1 \cdot M_2$.

Theorem 2.12 ([AHKM15])**.** *For the Fourier sampling space and the wavelet reconstruction space above the stable sampling rate is linear, i.e.* $\Theta(N_j, \theta) = \mathcal{O}(N_J)$ *as* $J \to \infty$, *where* N_J *denotes the number of generating reconstruction elements in* $\mathcal{R}_{N_J}$ *at scale* $J - 1 \in \mathbb{N}$.

Proof. This is Corollary 3.4 in [AHKM15]. □

Remark 2.13. *The stable sampling rate for general expanding matrices has also been determined in [AHKM15]. Furthermore, in this work the stable sampling rate has also been investigated for boundary wavelets with the result showing a linear stable sampling rate again.*

The importance and benefit of a linear stable sampling rate was already discussed previously. Therefore, wavelets are very well suited for the reconstruction from Fourier measurements in the context of generalized sampling. However, since other systems such as the shearlet system provide a better sparse approximation rate of cartoon-like functions, and thus provide a better algebraic decay in (2.6) it is natural to study the stable sampling rate for shearlets. This is what we will study in the next section.

2.3 Generalized sampling using shearlets

The main objective in this section is the study of the stable sampling rate for compactly supported shearlets assuming to have access to finitely many Fourier measurements of the signal of interest. In particular, we will assume the same measurements as in the previous wavelets case and only alter the reconstruction space by choosing shearlets instead of wavelets. This will be important as we want to make a comparison between both reconstructions.

Similar as in the previous section we first start with making the reconstruction space as well as the sampling space more precise. After having these spaces we will prove a stable sampling rate for this configuration. In Section 2.4 we will then compare the result to the stable sampling rate for wavelets. The results of this section are mainly based on the work [Ma15a] and follows the presentation of the results therein.

Shearlet reconstruction space

We will use the same notations for the shearlet system as we have already introduced in Chapter 1, in particular, $\phi, \psi, \widetilde{\psi}$ denote the generators and j refers to the scaling parameter, k the shearing parameter, and m denotes the translation parameter of a shearlet atom $\psi_{j,k,m}$. The sampling constant will from now on assumed to be $c = (c_1, c_2) = (1, 1)$. This is just to ease some notation and does not have any serious impact on any argument made. Mostly the constants will change for different values of c_1 and c_2.

The generators ϕ, ψ, and $\widetilde{\psi}$ that we want to use to build a proper reconstruction space will be assumed to be compactly supported in $[0, a]^2$ for some positive integer a. The reconstruction space is then build upon the translated, scaled and sheared elements that intersect a fixed region of interest which is also assumed to be $[0, a]^2$ for simplicity.

For the scaling functions we define the index set Ω to consist of all translates for which the elements intersect the region of interested, i.e. let

$$\Omega = \left\{m \in \mathbb{Z}^2 \,:\, \operatorname{supp} \phi_m \cap [0, a]^2 \neq \emptyset\right\} = \{(m_1, m_2) \in \mathbb{Z}^2 \,:\, -a \leq m_1, m_2 \leq a\}.$$

We now proceed by the same procedure for shearlets as we did for wavelets. This means we consider all shearlets whose support intersect the region of interest $[0, a]^2$. Depending on the scale $J - 1 \in \mathbb{N}_0$ we denote the index set Λ_J to be the set

$$\Lambda_J = \left\{(j, k, m) \in \mathbb{Z} \times \mathbb{Z} \times \mathbb{Z}^2 \,:\, 0 \leq j \leq J - 1, |k| \leq 2^{j/2}, m \in \Omega_{j,k}\right\},$$

where $\Omega_{j,k} = \{m \in \mathbb{Z}^2 \,:\, \operatorname{supp} \psi_{j,k,m} \cap [0, a]^2 \neq \emptyset\}$ is, due to the compact support of each $(\psi_{j,k,m})_m$, of finite cardinality. For $\widetilde{\psi}$ we similarly define

$$\widetilde{\Lambda}_J = \left\{(\widetilde{j}, \widetilde{k}, \widetilde{m}) \in \mathbb{Z} \times \mathbb{Z} \times \mathbb{Z}^2 \,:\, 0 \leq \widetilde{j} \leq J - 1, |\widetilde{k}| \leq 2^{j/2}, \widetilde{m} \in \widetilde{\Omega}_{\widetilde{j},\widetilde{k}}\right\}$$

with $\widetilde{\Omega}_{\widetilde{j},\widetilde{k}} = \{\widetilde{m} \in \mathbb{Z}^2 \,:\, \operatorname{supp} \widetilde{\psi}_{\widetilde{j},\widetilde{k},\widetilde{m}} \cap [0, a]^2 \neq \emptyset\}$ being of finite cardinality.

Note that the scale essentially determines the total number of shearlet elements that intersect the region of interest. In particular for any fixed scale j and any fixed shearing k with $|k| \leq 2^{j/2}$, the number of shearlet elements $(\psi_{j,k,m})_m$ that intersect the region of interest if of order $2^{3/2j}$. The total number of shearlet elements $(\psi_{j,k,m})_{k,m}$ that intersect the region of interest is of order 2^{2j}. The reconstruction space $\mathcal{R}$ is then defined as the closed span of all *feasible* shearlets, where the feasibility of a shearlet ψ_λ is determined by its belonging to Λ_J. This yields the following finite dimensional reconstruction space:

$$\mathcal{R}_{N_J} = \operatorname{span}\left\{ \{\phi_m \,:\, m \in \Omega\} \cup \{\psi_{j,k,m} \,:\, (j, k, m) \in \Lambda_J\} \cup \left\{\widetilde{\psi}_{\widetilde{j},\widetilde{k},\widetilde{m}} \,:\, (\widetilde{j}, \widetilde{k}, \widetilde{m}) \in \widetilde{\Lambda}_J\right\} \right\}. \tag{2.8}$$

This definition yields that for a fixed scale $J-1$ we, asymptotically, have $N_J = 2^{2J}$ many reconstruction elements in $\mathcal{R}_{N_J}$ as $J \to \infty$. Since we only have finitely many elements in the reconstruction space per scale, we can perform an ordering. This ordering can be performed quite naturally. In fact, first, the full system is chunked into its different scales $j = 0, 1, \ldots, J-1$ similar to the wavelet case. Then each subsystem can be chunked into the corresponding shearing parameters $k = -2^{j/2}, \ldots, 2^{j/2}$. The translation are then ordered in a lexicographical manner. Finally, the system will be ordered along scales and shears.

The attentive reader might have noticed that the ordering we just described does not result in a uniquely determined sequence of reconstruction elements, meaning there are several different orderings that obey the above construction. In particular, we have not mentioned how the selection should be performed across different cones. However, in our analysis and also in the numerical experiments, we will only use full shearlet systems determined by the scale meaning all shearlets across all cones up to a fixed scale, hence the reconstruction space is uniquely determined for such cases.

Assumptions on the generator

We like to stress that we assume the certain smoothness properties of the shearlet system that are needed in order to have a frame in the first place. These assumptions are fairly standard in shearlet theory. More precisely, we will assume the generators ϕ and ψ to have sufficient vanishing moments and decay in frequency, i.e. we assume there exist some constants $C_1, C_2 > 0$ such that

$$|\widehat{\phi}(\xi_1, \xi_2)| \leq C_1 \cdot \frac{1}{(1+|\xi_1|)^r} \frac{1}{(1+|\xi_2|)^r} \tag{2.9}$$

and

$$|\widehat{\psi}(\xi_1, \xi_2)| \leq C_2 \cdot \min\{1, |\xi_1|^\alpha\} \cdot \frac{1}{(1+|\xi_1|)^r} \frac{1}{(1+|\xi_2|)^r}, \tag{2.10}$$

where the *regularity parameters* $\alpha > 0$ and $r > 0$ are large enough so that the shearlet system forms a frame for $L^2(\mathbb{R}^2)$. The generator $\widetilde{\psi}(x_1, x_2) := \psi(x_2, x_1)$ for the second cone inherits the smoothness properties from ψ.

We next turn to the definition of the Fourier sampling space.

Fourier sampling space

The Fourier sampling space is defined in the same way as for the wavelet case and we merely recall here for notational purposes. Let T_1 and T_2 be such that

$$\mathcal{R} \subset L^2([-T_1, T_2]^2).$$

Now, let $\varepsilon \leq \frac{1}{T_1+T_2} < 1$ control the sampling density. The sampling vectors are then defined as standard complex exponentials restricted on the area $[T_1, T_2]^2$ with density ϵ and samples on the grid $\mathbb{Z}^2$, i.e.

$$s_\ell^{(\varepsilon)} := \varepsilon e^{2\pi i \varepsilon \langle \ell, \cdot \rangle} \cdot \chi_{\left[-\frac{T_1}{\varepsilon(T_1+T_2)}, \frac{T_2}{\varepsilon(T_1+T_2)}\right]^2}, \quad \ell \in \mathbb{Z}^2. \tag{2.11}$$

These sampling vectors are then used to define the sampling space

$$\mathcal{S}^{(\varepsilon)} := \overline{\operatorname{span}} \left\{ s_\ell^{(\varepsilon)} \,:\, \ell \in \mathbb{Z}^2 \right\}.$$

Of course a finite dimensional version of this space can be defined directly. However, similar as for the reconstruction, we are only interested in specific cases. Recall that for the reconstruction space we considered all shearlet elements up to a certain scale. For the sampling space we will consider all sampling vectors whose sampling point lies in a squared lattice of fixed size. In particular, for $M = (M_1, M_2) \in \mathbb{N} \times \mathbb{N}$ we define the finite dimensional sampling space by

$$\mathcal{S}_M^{(\varepsilon)} := \operatorname{span} \left\{ s_\ell^{(\varepsilon)} \,:\, \ell = (\ell_1, \ell_2) \in \mathbb{Z}^2, -M_i \leq \ell_i \leq M_i, i = 1, 2 \right\}.$$

The number of acquired measurements are then determined by the width of the sampling lattice, indeed, asymptotically we have $M_1 \cdot M_2$ many samples taken.

In order to analyse the stable sampling rate we have to put the number of samples $M := M_1 \cdot M_2$ in relation with the number of reconstruction elements N_J in accordance with Definition 2.10. This would yield the existence of stable and convergent shearlet reconstructions which lies in the primal focus of this chapter.

Stable sampling rate for shearlets

The following theorem describes the stable sampling rate for the Fourier sampling space using a shearlet reconstruction space.

Theorem 2.14 ([Ma15a])**.** *Let $\mathcal{SH}(\phi, \psi, \widetilde{\psi})$ be a compactly supported shearlet frame with generators ϕ, ψ, and $\widetilde{\psi}$ and let $N \leq N_J = \mathcal{O}(2^{2J})$. Then for all $\theta > 1$ there exists $S_\theta > 0$ such that*

$$c_{N,M} = \inf_{\substack{f \in \mathcal{R}_N \\ \|f\|=1}} \|P_{\mathcal{S}_M^{(\varepsilon)}} f\| \geq \frac{1}{\theta},$$

where $M = (M_1, M_2) \in \mathbb{N} \times \mathbb{N}$ with $M_i = \lceil S_\theta A_N^{-1/(2r-1)} \cdot 2^{J(1+\delta)}/\varepsilon \rceil$, $\delta \geq \frac{2}{2r-1}$ and $r > 0$ is the regularity parameter from (2.9) and (2.10). Therefore $\Theta(N, \theta) = \mathcal{O}(N^{1+\delta} A_N^{-1/(2r-1)})$. Further, the constant S_θ does not depend on N but on θ, α, and r.

Before we give a proof of Theorem 2.14 we first discuss some important issues. First, this theorem only gives a sufficient condition but not a necessary one. Second, in contrary to the wavelet case Theorem 2.14 shows a dependence on the lower frame bound on the side of the number of measurements. Such a dependence naturally does not occur in the wavelet case, since there the system was assumed to be an orthonormal basis whereas for the shearlet case, the reconstruction systems forms a truly redundant system. However, if one interprets the lower frame bound as a measure for redundancy, then such a dependence seems very plausible. Theorem 2.14 would roughly speaking mean: The more redundant the system, i.e. the smaller the lower frame bound, the more measurements need to be taken in order to guarantee stable and convergent solutions. Third and finally, Theorem 2.14 shows a slightly worse than linear rate as it was obtained in Theorem 2.12 for wavelets.

We will now first justify why Theorem 2.14 is still a useful result.

2.4 Comparison to wavelets

In Theorem 2.12 it is shown that the stable sampling rate for wavelets is linear, i.e. we have $\Theta(N,\theta) = \mathcal{O}(N)$. For shearlets the results appears to be worse since we have to consider an additional oversampling by a factor N^{δ}, where δ is controlled by the regularity of the shearlet atoms. Note that δ can be made arbitrarily small if the regularity parameters increase arbitrarily.

As we will explain now this additional oversampling factor N^{δ} is not so harmful. Our discussion is based on the following principle. We first fix the number of samples, say M, that are allowed to be used for both reconstructions methods. Now based on this number of measurements M and the computed stable sampling rates of Theorem 2.12 and Theorem 2.14, we are allowed to use more wavelets than shearlets to build the wavelet reconstruction space and the shearlet reconstruction space, respectively.

More precisely, let $\sigma : \mathbb{N} \longrightarrow \mathbb{N}$ be the following *oversampling function*

$$\sigma(N) = \left\lceil N^{1+\delta} \frac{1}{A_N^{\frac{2}{2r-1}}} \right\rceil, \quad N \in \mathbb{N}. \tag{2.12}$$

Then the following result can be used to show that shearlet reconstructions are still more appealing than the wavelet reconstructions in this context, at least for the class of cartoon-like functions.

Proposition 2.15 ([Ma15a]). *Let $\mathcal{SH}(\phi, \psi, \widetilde{\psi})$ be a compactly supported shearlet frame with generators ϕ, ψ, and $\widetilde{\psi}$ with sufficiently large regularity r and $\delta \geq 2/(2r-1)$. Further, let f be a cartoon-like function f. For $N \in \mathbb{N}$ denote by f_N^s the best N-term approximation of f using shearlets and $f_{\sigma(N)}^w$ the best $\sigma(N)$-approximation using wavelets, cf. Definition 1.5 and the preluding discussion before that. Further, let $N_J = 2^{2J}$, $J \in \mathbb{N}$ be the smallest number such that $N, \sigma(N) \lesssim N_J$. If $\mathcal{R}_N^s$ denotes the shearlet reconstruction space so that $f_N^s \in \mathcal{R}_N^s$ and $\mathcal{R}_{\sigma(N)}^w$ denotes the wavelet reconstruction space so that $f_{\sigma(N)}^w \in \mathcal{R}_{\sigma(N)}^w$, then*

$$\|f - G_{N,M}^s(f)\| \lesssim N^{-1}(\log N)^{3/2},$$

and

$$\|f - G_{\sigma(N),M'}^w(f)\| \lesssim \sigma(N)^{-1/2},$$

where M and M' are of order $\sigma(N_J)$ and $G_{N,M}^s(f)$ as well as $G_{N,M}^w(f)$ are the GS solutions with respect to the spaces $\mathcal{R}_N^s$ and $\mathcal{R}_{\sigma(N)}^w$, respectively.

We first finish the discussion and then give a proof of Proposition 2.15 in the next section after the proof of Theorem 2.14.

Remark 2.16. *We have $N^{-1}(\log N)^{3/2} \lesssim \sigma(N)^{-1/2}$ if*

$$N^{-(1-\delta)/2}(\log N)^{3/2} \lesssim A_N^{1/(2r-1)}, \tag{2.13}$$

and therefore, if $\|f - f_N^s\| \asymp \|f - G_{N,M}^s(f)\|$ and $\|f - f_N^w\| \asymp \|f - G_{\sigma(N),M}^w(f)\|$, then

$$\|f - G_{N,M}^s(f)\| \lesssim \|f - G_{\sigma(N),M'}^w(f)\|,$$

where "$\asymp$" means equality up to some constant.

In Proposition 2.15 we required a certain behavior on the oversampling function $\sigma(N)$ which again depends on the lower frame bound A_N, see (2.12). The asymptotic behavior of the lower frame bound of a finite shearlets system is in general unknown. It is reasonable to expect, that there is no general results that can guarantee a stable behaviour of these bounds as this is also the case for wavelet frames [CL]. However, we will numerically demonstrate that for compactly supported shearlets used in applications the lower frame bound decreases in a controlable manner, more precisely, in Figure 2.1 we numerically confirm Inequality (2.13).

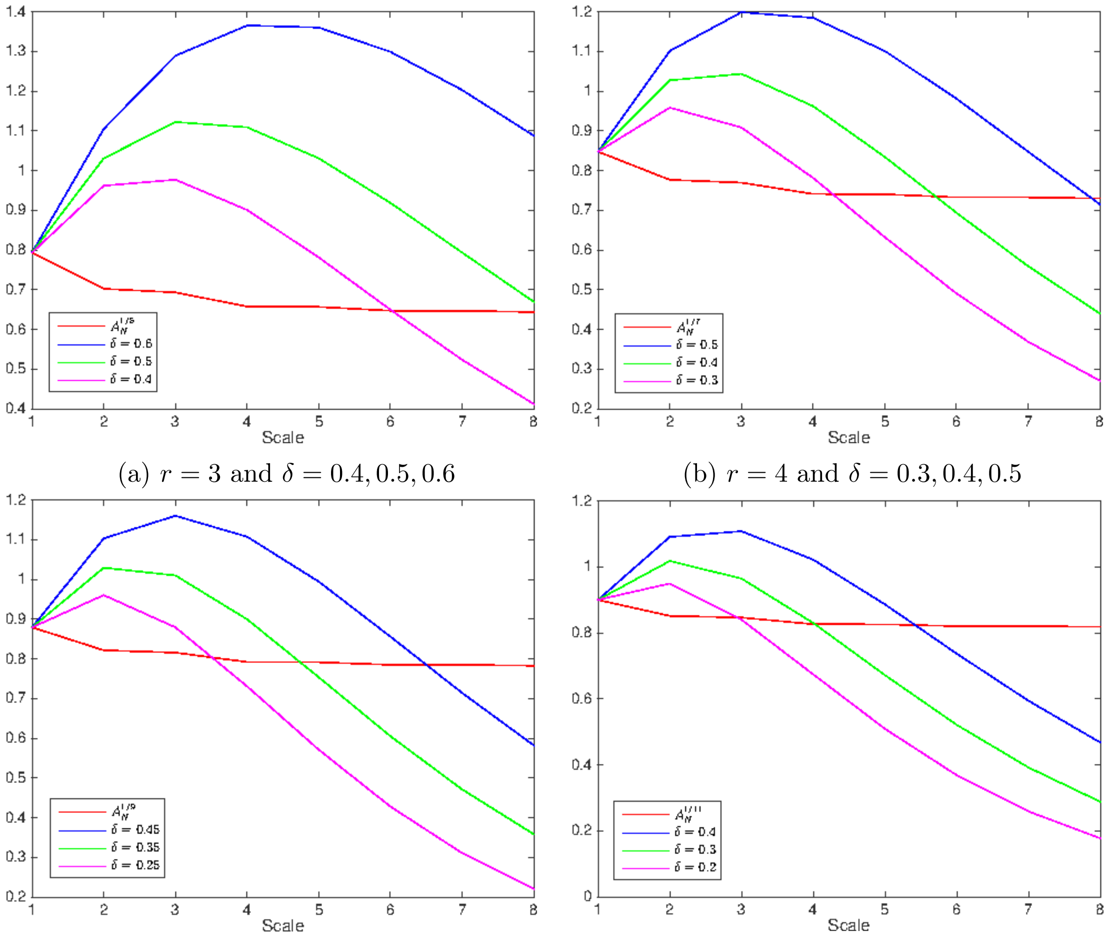

(a) $r = 3$ and $\delta = 0.4, 0.5, 0.6$

(b) $r = 4$ and $\delta = 0.3, 0.4, 0.5$

(c) $r = 5$ and $\delta = 0.25, 0.35, 0.45$

(d) $r = 6$ and $\delta = 0.2, 0.3, 0.4$

Figure 2.1: Plot of the behavior of lower frame bound and the critical function $N^{-(1-\delta)/2}(\log N)^{3/2}$ for different values of r and δ

The statement made in Proposition 2.15 delivers a positive result for shearlet reconstruction for cartoon-like functions in terms of generalized sampling, only if $N^{-1}(\log N)^{3/2}$ grows slower than $\sigma(N)^{-1/2}$. Above we show some numerical examples that compare these two quantities. Note that aiming to verify (2.13) is equivalent to checking the behavior of the lower frame bound. More precisely, it is sufficient to check

$$N^{-(1-\delta)/2}(\log N)^{3/2} \lesssim A_N^{1/(2r-1)}$$

for the lower frame bound A_N. For this we compute the lower frame bound for the scales $J = 1, \ldots, 8$. N is chosen to be exactly 2^{2J}. In Figure 2.1 we plot the functions $N^{-(1-\delta)/2}(\log N)^{3/2}, A_N^{1/(2r-1)}$ in terms of N for different values of r and δ. These plots suggest that (2.13) may hold asymptotically.

We now continue with a proof of Theorem 2.14 which is followed by a proof of Proposition 2.15.

Proof of Theorem 2.14

The main goal of this section is to present a proof of Theorem 2.14. This will be done by first presenting some preliminary considerations and auxiliary results.

Effective frequency support

The main idea of the proof of Theorem 2.14 is to connect the Fourier sampling with the behavior of the shearlets in the frequency domain. Although compactly supported shearlets are everywhere supported in the frequency domain, the shearlets are strongly localized in the frequency plane. This is due to the decay assumption of the scaling function (2.9) and the decay assumptions on the shearlets (2.10), respectively. Such decay properties remain unchanged if the function is scaled or translated, however, it is not hard to imagine that shearing does affect the localization property.

The next result gives a more quantitative statement about the controllability of the essential supports of the shearlet atoms $(\psi_\lambda)_\lambda$ in the frequency domain, see also Figure 2.2.

Figure 2.2: Effective frequency support of shearlets and tiling of the frequency plane, light regions correspond to large values, therefore regions with large energy and dark regions to small values, i.e. regions with small energy. Images are computed using the ShearLab package downloaded from `http://www.shearlab.org/`

Proposition 2.17 ([Ma15a]). *Let $J \in \mathbb{N}$ and $(\psi_\lambda)_{\lambda \le N_J}$ be all shearlets up to scale $J-1$ according to the selection procedure explained in the previous sections. Then, for $\omega > 0$ there exists a constant $S := S(\omega, r, \varepsilon)$ such that for $I_M := \{(\ell_1, \ell_2) \in \mathbb{Z}^2 : -M_i \le \ell_i \le M_i, i = 1, 2\}$ with $M_i = S2^{J(1+\delta)}, i = 1, 2$ and $\delta \ge \frac{2}{2r-1}$ we have*

$$\sum_{\ell \in (I_M)^c} \sum_{\lambda \le N_J} |(\psi_\lambda)^\wedge(\varepsilon \ell)|^2 \le \omega.$$

For the proof of Proposition 2.15 we will use the following auxiliary lemma.

Lemma 2.18 ([Gra08]). *For $y \in \mathbb{R}, r > 1$, and $a, b > 0$ we have*

$$\int_0^\infty \frac{1}{(1+a|x|)^r} \frac{1}{(1+b|x-y|)^r}\, dx \lesssim \frac{1}{\max(a,b)} \frac{1}{(1+\min(a,b)|y|)^r}.$$

Proof of Proposition 2.17. Let $\omega > 0$. Then we have to show the existence of an $M = (M_1, M_2) \in \mathbb{N} \times \mathbb{N}$, so that

$$\left(\sum_{|l_2| > M_2} \sum_{|l_1| > M_1} + \sum_{|l_2| < M_2} \sum_{|l_1| > M_1} + \sum_{|l_2| > M_2} \sum_{|l_1| < M_1} \right) \sum_{\lambda \le N_J} |(\psi_\lambda)^\wedge(\varepsilon \ell)|^2 \le \omega, \tag{2.14}$$

where M_1, M_2 scales like $S2^{J(1+\delta)}$ with a constant S independent of J. By direct computations we obtain

$$\begin{aligned}
&\sum_{\lambda \le N_J} |(\psi_\lambda)^\wedge(\varepsilon \ell)|^2 \\
&= \sum_{m' \in \Omega} \left| \varepsilon e^{-2\pi i \varepsilon \langle l, m' \rangle} \widehat{\phi}(\varepsilon l) \right|^2 + \sum_{(j,k,m) \in \Lambda_J} \left| \frac{\varepsilon}{2^{3j/4}} e^{-2\pi i \varepsilon \langle (S_k A_{2^j})^{-T} l, m \rangle} \widehat{\psi}\left(\varepsilon \left(S_k A_{2^j} \right)^{-T} l \right) \right|^2 + \\
&\quad + \sum_{(\tilde{j}, \tilde{k}, \tilde{m}) \in \tilde{\Lambda}_J} \left| \frac{\varepsilon}{2^{3\tilde{j}/4}} e^{-2\pi i \varepsilon \langle \left(S_{\tilde{k}} \widetilde{A}_{2^{\tilde{j}}} \right)^{-T} l, \tilde{m} \rangle} \widehat{\tilde{\psi}}\left(\varepsilon \left(S_{\tilde{k}} \widetilde{A}_{2^{\tilde{j}}} \right)^{-T} l \right) \right|^2, \\
&\le C \left| \varepsilon \widehat{\phi}(\varepsilon l) \right|^2 + \sum_{j=0}^{J-1} \sum_{k=-2^{j/2}}^{2^{j/2}} \left| \widehat{\psi}\left(\varepsilon \left(S_k A_{2^j} \right)^{-T} l \right) \right|^2 + \sum_{\tilde{j}=0}^{J-1} \sum_{\tilde{k}=-2^{\tilde{j}/2}}^{2^{\tilde{j}/2}} \left| \widehat{\tilde{\psi}}\left(\varepsilon \left(S_{\tilde{k}} \widetilde{A}_{2^{\tilde{j}}} \right)^{-T} l \right) \right|^2,
\end{aligned} \tag{2.15}$$

since the cardinality of $\Omega_{j,k}$ and $\widetilde{\Omega}_{\tilde{j},\tilde{k}}$ is of order $2^{3/2j}$. Further, we have used the fact that the cardinality of Ω is independent of J and solely depends on the size of the region of interest and the support size of the scaling function ϕ.

For the rest of the proof we denote by $\mathrm{I}, \mathrm{II}, \mathrm{III}$ the following terms

$$\mathrm{I} := \left(\sum_{|l_2| > M_2} \sum_{|l_1| > M_1} + \sum_{|l_2| < M_2} \sum_{|l_1| > M_1} + \sum_{|l_2| > M_2} \sum_{|l_1| < M_1} \right) \left| \varepsilon \widehat{\phi}(\varepsilon l) \right|^2,$$

$$\text{II} := \left(\sum_{|l_2|>M_2} \sum_{|l_1|>M_1} + \sum_{|l_2|<M_2} \sum_{|l_1|>M_1} + \sum_{|l_2|>M_2} \sum_{|l_1|<M_1} \right) \sum_{j=0}^{J-1} \sum_{k=-2^{j/2}}^{2^{j/2}} \left| \widehat{\psi} \left(\varepsilon \left(S_k A_{2^j} \right)^{-T} l \right) \right|^2,$$

$$\text{III} := \left(\sum_{|l_2|>M_2} \sum_{|l_1|>M_1} + \sum_{|l_2|<M_2} \sum_{|l_1|>M_1} + \sum_{|l_2|>M_2} \sum_{|l_1|<M_1} \right) \sum_{\tilde{j}=0}^{J-1} \sum_{\tilde{k}=-2^{\tilde{j}/2}}^{2^{\tilde{j}/2}} \left| \widehat{\widetilde{\psi}} \left(\varepsilon \left(S_{\tilde{k}} \widetilde{A}_{2^{\tilde{j}}} \right)^{-T} l \right) \right|^2.$$

In order to obtain (2.14) for sufficiently large S independent on J with $M_i = \frac{2^{J(1+\delta)}}{\varepsilon} S, i = 1, 2$ we will now estimate each of these sums by using the decay conditions (2.9) and (2.10), respectively. By assumption (2.9) we have

$$\left| \varepsilon \widehat{\phi}(\varepsilon l) \right|^2 \leq C_1^2 \varepsilon^2 \left| \frac{1}{(1+|\varepsilon l_1|)^r} \frac{1}{(1+|\varepsilon l_2|)^r} \right|^2. \tag{2.16}$$

and thus

$$\begin{aligned} \sum_{|l_2|>M_2} \sum_{|l_1|<M_1} \left| \widehat{\phi}(\varepsilon l) \right|^2 &\leq \sum_{|l_2|>M_2} \sum_{|l_1|<M_1} C_1^2 \frac{1}{(1+|\varepsilon l_1|)^{2r}} \frac{1}{(1+|\varepsilon l_2|)^{2r}} \\ &\leq C_1^2 \sum_{|l_1|>M_1} \frac{1}{(1+|\varepsilon l_1|)^{2r}} \\ &\leq C_1^2 \frac{1}{(1+S^{J(1+\delta)})^{2r-1}}, \end{aligned} \tag{2.17}$$

where the constant C_1 changed in each step. Along the same lines one obtains

$$\sum_{|l_2|<M_2} \sum_{|l_1|>M_1} \left| \widehat{\phi}(\varepsilon l) \right|^2 \leq C_1^2 \frac{1}{(1+S2^{J(1+\delta)})^{2r-1}} \tag{2.18}$$

and

$$\sum_{|l_2|>M_2} \sum_{|l_1|>M_1} \left| \widehat{\phi}(\varepsilon l) \right|^2 \leq C_1^2 \frac{1}{(1+S2^{J(1+\delta)})^{2r-1}}. \tag{2.19}$$

Hence, combinging (2.17), (2.18) and (2.19) gives

$$\text{I} \leq C_1^2 \frac{1}{(1+S2^{J'(1+\delta)})^{2r-1}} \tag{2.20}$$

Concerning the second sum II we obtain by a use of assumption (2.10) the estimate

$$\begin{aligned} &\sum_{j=0}^{J-1} \sum_{k=-2^{j/2}}^{2^{j/2}} \left| \widehat{\psi} \left(\varepsilon \left(S_k A_{2^j} \right)^{-T} l \right) \right|^2 \\ &\qquad \leq \sum_{j=0}^{J-1} \sum_{k=-2^{j/2}}^{2^{j/2}} \frac{C_2^2}{(1+|\varepsilon 2^{-j} l_1|)^{2r} (1+|-\varepsilon k 2^{-j} l_1 + \varepsilon 2^{-j/2} l_2|)^{2r}}, \end{aligned} \tag{2.21}$$

and, likewise for III,

$$\sum_{\widetilde{j}=0}^{J-1} \sum_{\widetilde{k}=-2^{\widetilde{j}/2}}^{2^{\widetilde{j}/2}} \left| \widehat{\widetilde{\psi}} \left(\varepsilon \left(S_{\widetilde{k}}^T A_{2^{\widetilde{j}}} \right)^{-T} l \right) \right|^2$$

$$\leq \sum_{\widetilde{j}=0}^{J-1} \sum_{\widetilde{k}=-2^{\widetilde{j}/2}}^{2^{\widetilde{j}/2}} \frac{C_3^2}{(1 + |\varepsilon 2^{-\widetilde{j}} l_2|)^{2r} (1 + |\varepsilon 2^{-\widetilde{j}/2} l_1 - \varepsilon \widetilde{k} 2^{-\widetilde{j}} l_2|)^{2r}}. \tag{2.22}$$

We continue with (2.21) and leave out the computations for (2.22) since the arguments will apply in the same manner.

In order to further bound (2.21) we distinguish between two cases. The first case concerns shearlets, that are *wavelet-like*, these are those shearlets part of the full shearlet system, that are not sheared. These are can be seen as parabolically scaled wavelets.

Case I: Let $0 \leq j \leq J-1, k = 0$. By direct computations similar to (2.17) we have

$$\begin{aligned}
&\sum_{|l_2|>M_2} \sum_{|l_1|<M_1} \sum_{j=0}^{J-1} C_2^2 \frac{1}{(1 + |\varepsilon 2^{-j} l_1|)^{2r}} \frac{1}{(1 + |\varepsilon 2^{-j/2} l_2|)^{2r}} \\
&\leq \sum_{j=0}^{J-1} C_2^2 \sum_{|l_2|>M_2} \frac{1}{(1 + |\varepsilon 2^{-j/2} l_2|)^{2r}} \sum_{|l_1|<M_1} \frac{1}{(1 + |\varepsilon 2^{-j} l_1|)^{2r}} \\
&\leq \sum_{j=0}^{J-1} C_2^2 \frac{2^j}{\varepsilon} \sum_{|l_2|>M_2} \frac{1}{(1 + |\varepsilon 2^{-j/2} l_2|)^{2r}} \\
&\leq \sum_{j=0}^{J-1} C_2^2 \frac{2^{3/2j}}{\varepsilon^2} \frac{1}{(1 + S 2^{J'(1+\delta) - j/2})^{2r-1}} \\
&\leq C_2^2 \frac{2^{3/2J}}{\varepsilon^2} \frac{1}{(1 + S 2^{J(1/2+\delta)})^{2r-1}}.
\end{aligned} \tag{2.23}$$

where C_2 changed over time. By similar computations we obtain

$$\sum_{|l_2|<M_2} \sum_{|l_1|>M_1} \sum_{j=0}^{J-1} C_2^2 \frac{1}{(1 + |\varepsilon 2^{-j} l_1|)^{2r}} \frac{1}{(1 + |\varepsilon 2^{-j/2} l_2|)^{2r}} \leq C_2^2 \frac{2^{3/2J}}{\varepsilon^2} \frac{1}{(1 + S 2^{J\delta})^{2r-1}}, \tag{2.24}$$

and

$$\sum_{|l_1|>M_1} \sum_{|l_2|>M_2} \sum_{j=0}^{J-1} C_2^2 \frac{1}{(1 + |\varepsilon 2^{-j} l_1|)^{2r}} \frac{1}{(1 + |\varepsilon 2^{-j/2} l_2|)^{2r}}$$

$$\leq C_2^2 \frac{2^{3/2J}}{\varepsilon^2} \frac{1}{\big((1 + S 2^{J\delta})(1 + S 2^{J(1/2+\delta)})\big)^{2r-1}}. \tag{2.25}$$

We now turn to the second case of sheared elements.

Case 2: Let $0 \leq j \leq J-1, k \neq 0$. By a use of Lemma 2.18 we have

$$
\begin{aligned}
&\sum_{|l_2|>M_2} \sum_{|l_1|<M_1} \sum_{j=0}^{J-1} \sum_{\substack{k=-2^{j/2} \\ k\neq 0}}^{2^{j/2}} C_2^2 \frac{1}{(1+|\varepsilon 2^{-j} l_1|)^{2r}} \frac{1}{(1+|-\varepsilon k 2^{-j} l_1 + \varepsilon 2^{-j/2} l_2|)^{2r}} \\
&\leq \sum_{j=0}^{J-1} \sum_{\substack{k=-2^{j/2} \\ k\neq 0}}^{2^{j/2}} \sum_{|l_2|>M_2} C_2^2 \frac{1}{\varepsilon |k 2^{-j}|} \frac{1}{(1+|\varepsilon 2^{-j}||2^{j/2} l_2/k|)^{2r}} \\
&\leq \sum_{j=0}^{J-1} \sum_{\substack{k=-2^{j/2} \\ k\neq 0}}^{2^{j/2}} C_2^2 \frac{2^j}{\varepsilon |k|} \frac{|k| 2^{j/2}}{\varepsilon} \frac{1}{(1+|\frac{S}{\varepsilon} 2^{J'(1+\delta)-j/2}/k|)^{2r-1}} \\
&= \sum_{j=0}^{J-1} \sum_{\substack{k=-2^{j/2} \\ k\neq 0}}^{2^{j/2}} C_2^2 \frac{2^{3/2j}}{\varepsilon^2} \frac{1}{(1+|\frac{S}{\varepsilon} 2^{J(1+\delta)-j/2}/k|)^{2r-1}} \\
&\leq C_2^2 \frac{2^{2J}}{\varepsilon^2} \frac{1}{(1+|\frac{S}{\varepsilon} 2^{J\delta}|)^{2r-1}}. \qquad (2.26)
\end{aligned}
$$

Since

$$
\sum_{|l_2|<M_2} \frac{1}{(1+|-\varepsilon k 2^{-j} l_1 + \varepsilon 2^{-j/2} l_2|)^{2r}} \lesssim \int_{\mathbb{R}} \frac{1}{(1+|-\varepsilon k 2^{-j} l_1 + \varepsilon 2^{-j/2} x|)^{2r}} \, dx \lesssim \frac{2^{j/2}}{\varepsilon}
$$

we have

$$
\begin{aligned}
&\sum_{|l_2|<M_2} \sum_{|l_1|>M_1} \sum_{j=0}^{J-1} \sum_{\substack{k=-2^{j/2} \\ k\neq 0}}^{2^{j/2}} C_2^2 \frac{1}{(1+|\varepsilon 2^{-j} l_1|)^{2r}} \frac{1}{(1+|-\varepsilon k 2^{-j} l_1 + \varepsilon 2^{-j/2} l_2|)^{2r}} \\
&\leq \sum_{j=0}^{J-1} \sum_{\substack{k=-2^{j/2} \\ k\neq 0}}^{2^{j/2}} C_2^2 \frac{2^{3/2j}}{\varepsilon^2} \frac{1}{(1+|\frac{S}{\varepsilon} 2^{J(1+\delta)-j}|)^{2r-1}} \\
&\leq C_2^2 \frac{2^{2J}}{\varepsilon^2} \frac{1}{(1+|\frac{S}{\varepsilon} 2^{J\delta}|)^{2r-1}}. \qquad (2.27)
\end{aligned}
$$

Lastly, the final sum in II can be bounded as in (2.26). In fact, invoking Lemma 2.18 yields

$$
\begin{aligned}
&\sum_{|l_2|>M_2} \sum_{|l_1|>M_1} \sum_{j=0}^{J-1} \sum_{\substack{k=-2^{j/2} \\ k\neq 0}}^{2^{j/2}} C_2^2 \frac{1}{(1+|\varepsilon 2^{-j} l_1|)^{2r}} \frac{1}{(1+|-\varepsilon k 2^{-j} l_1 + \varepsilon 2^{-j/2} l_2|)^{2r}} \\
&\leq \sum_{j=0}^{J-1} \sum_{\substack{k=-2^{j/2} \\ k\neq 0}}^{2^{j/2}} C_2^2 \frac{2^{3/2j}}{\varepsilon^2} \frac{1}{(1+|S_\theta 2^{J(1+\delta)-j}|)^{2r-1}}
\end{aligned}
$$

$$\leq C_2^2 \frac{2^{2J}}{\varepsilon^2} \frac{1}{(1+|\frac{S}{\varepsilon}2^{J\delta}|)^{2r-1}}. \tag{2.28}$$

Therefore, combining (2.23), (2.24), (2.25), (2.26) (2.27), (2.28) yields

$$\mathrm{II} \leq C_2^2 \frac{2^{2J}}{\varepsilon^2} \frac{1}{(1+|\frac{S}{\varepsilon}2^{J\delta}|)^{2r-1}}. \tag{2.29}$$

As already mentioned above, we can bound III by performing the same computations as we did for II, therefore we conclude

$$\mathrm{III} \leq C_2^2 \frac{2^{2J}}{\varepsilon^2} \frac{1}{(1+|\frac{S}{\varepsilon}2^{J\delta}|)^{2r-1}}. \tag{2.30}$$

The estimates (2.20), (2.29), and (2.30) yields

$$\mathrm{I}+\mathrm{II}+\mathrm{III} \leq C \frac{\varepsilon^{2r-3}}{(S2^{J(\delta-2/(2r-1))})^{2r-1}},$$

with a constant that does not depend on J. Therefore, if $\delta \geq \frac{2}{2r-1}$ the result follows for S greater than $C^{-1}(\frac{\varepsilon^{2r-3}}{\omega})^{1/(2r-1)}$ which is independent of J. □

Proof of Theorem 2.14

The proof of Theorem 2.14 is a consequence of Proposition 2.17.

Proof of Theorem 2.14. Let $\theta > 1$. Then we want to show

$$\inf_{\substack{f\in\mathcal{R}_N \\ \|f\|=1}} \|P_{\mathcal{S}_M^{(\varepsilon)}} f\| \geq \frac{1}{\theta} \tag{2.31}$$

for an appropriate M stated in the theorem. For this, let $f \in \mathcal{R}_N$ with $\|f\| = 1$. Instead of showing (2.31) we equivalently show

$$\|P^{\perp}_{\mathcal{S}_M^{(\varepsilon)}} f\|^2 \leq \frac{\theta^2-1}{\theta^2}, \tag{2.32}$$

for the claimed M. Since $(s_\ell^{(\varepsilon)})_\ell$ is an orthonormal system, we have

$$\|P^{\perp}_{\mathcal{S}_M^{(\varepsilon)}} f\|^2 = \sum_{l\in(I_M)^c} |\langle f, s_l^{(\varepsilon)}\rangle|^2,$$

where $(I_M)^c$ denotes the set complement of I_M in $\mathbb{Z}^2$, in particular

$$\sum_{l\in(I_M)^c} |\langle f, s_l^{(\varepsilon)}\rangle|^2$$
$$= \sum_{|l_2|>M_2} \sum_{|l_1|>M_1} |\langle f, s_l^{(\varepsilon)}\rangle|^2 + \sum_{|l_2|<M_2} \sum_{|l_1|>M_1} |\langle f, s_l^{(\varepsilon)}\rangle|^2 + \sum_{|l_2|>M_2} \sum_{|l_1|<M_1} |\langle f, s_l^{(\varepsilon)}\rangle|^2.$$

Since the frame operator

$$S_N : \mathcal{R}_N \longrightarrow \mathcal{R}_N, \quad f \mapsto \sum_{\lambda \leq \mathbb{N}} \langle f, \psi_\lambda \rangle \psi_\lambda$$

is an bijection we have for any $f \in \mathcal{R}_N$

$$f = \sum_{\lambda \leq N_J} \langle f, S_N^{-1} \psi_\lambda \rangle \psi_\lambda = \sum_{m' \in \Omega} \alpha_{m'} \phi_{m'} + \sum_{(j,k,m) \in \Lambda_J} \beta_{j,k,m} \psi_{j,k,m} + \sum_{(\widetilde{j},\widetilde{k},\widetilde{m}) \in \widetilde{\Lambda}_J} \gamma_{\widetilde{j},\widetilde{k},\widetilde{m}} \widetilde{\psi}_{\widetilde{j},\widetilde{k},\widetilde{m}}$$

with

$$\alpha_{m'} = \langle \phi_{m'}, s_l \rangle, \quad \beta_{j,k,m} = \langle \psi_{j,k,m}, s_l \rangle, \quad \gamma_{j,k,m} = \langle \widetilde{\psi}_{\widetilde{j},\widetilde{k},\widetilde{m}}, s_l \rangle.$$

Furthermore,

$$\sum_{m' \in \Omega} |\alpha_{m'}|^2 + \sum_{(j,k,m) \in \Lambda_J} |\beta_{j,k,m}|^2 + \sum_{(\widetilde{j},\widetilde{k},\widetilde{m}) \in \widetilde{\Lambda}_J} \left| \gamma_{\widetilde{j},\widetilde{k},\widetilde{m}} \right|^2 = \sum_{\lambda \leq N_J} |\langle S_N^{-1} f, \psi_\lambda \rangle|^2 \leq \frac{1}{A_N} \|f\|^2.$$

Therefore by Cauchy-Schwarz

$$\begin{aligned}
&\sum_{l \in (I_M)^c} |\langle f, s_l \rangle|^2 \\
&= \sum_{l \in (I_M)^c} \left| \langle \sum_{m' \in \Omega} \alpha_{m'} \phi_{m'} + \sum_{(j,k,m) \in \Lambda_J} \beta_{j,k,m} \psi_{j,k,m} + \sum_{(\widetilde{j},\widetilde{k},\widetilde{m}) \in \widetilde{\Lambda}_J} \gamma_{\widetilde{j},\widetilde{k},\widetilde{m}} \widetilde{\psi}_{\widetilde{j},\widetilde{k},\widetilde{m}}, s_l \rangle \right|^2 \\
&= \sum_{l \in (I_M)^c} \left| \sum_{m' \in \Omega} \alpha_{m'} \widehat{\phi_{m'}}(\varepsilon l) + \sum_{(j,k,m) \in \Lambda_J} \beta_{j,k,m} \widehat{\psi_{j,k,m}}(\varepsilon l) + \sum_{(\widetilde{j},\widetilde{k},\widetilde{m}) \in \widetilde{\Lambda}_J} \gamma_{\widetilde{j},\widetilde{k},\widetilde{m}} \widehat{\widetilde{\psi}_{\widetilde{j},\widetilde{k},\widetilde{m}}}(\varepsilon l) \right|^2 \\
&\leq \sum_{l \in (I_M)^c} \left[\left(\sum_{m' \in \Omega} |\alpha_{m'}|^2 + \sum_{(j,k,m) \in \Lambda_J} |\beta_{j,k,m}|^2 + \sum_{(\widetilde{j},\widetilde{k},\widetilde{m}) \in \widetilde{\Lambda}_J} |\gamma_{\widetilde{j},\widetilde{k},\widetilde{m}}|^2 \right) \right. \\
&\qquad \left. \left(\sum_{m' \in \Omega} |\widehat{\phi}_{m'}(\varepsilon l)|^2 + \sum_{(j,k,m) \in \Lambda_J} |\widehat{\psi_{j,k,m}}(\varepsilon l)|^2 + \sum_{(\widetilde{j},\widetilde{k},\widetilde{m}) \in \widetilde{\Lambda}_J} |\widehat{\widetilde{\psi}_{\widetilde{j},\widetilde{k},\widetilde{m}}}(\varepsilon l)|^2 \right) \right] \\
&\leq \frac{1}{A_N} \sum_{l \in (I_M)^c} \left[\sum_{m' \in \Omega} \left| \widehat{\phi_{m'}}(\varepsilon l) \right|^2 + \sum_{(j,k,m) \in \Lambda_J} \left| \varepsilon \widehat{\psi_{j,k,m}}(\varepsilon l) \right|^2 + \sum_{(\widetilde{j},\widetilde{k},\widetilde{m}) \in \widetilde{\Lambda}_J} \left| \varepsilon \widehat{\phi_{m'}}(\varepsilon l) \right|^2 \right].
\end{aligned}$$

Now by Proposition 2.17 there exists a constant $S(\theta, r, \varepsilon)$ independent of J such that for

$$M_i = \left\lceil S(\theta, r, \varepsilon) 2^{J(1+\delta)} A_N^{\frac{1}{2r-1}} \right\rceil \in \mathbb{N}, \quad i = 1, 2$$

we can conclude

$$\sum_{l \in (I_M)^c} |\langle f, s_l \rangle|^2 \leq \frac{\theta^2 - 1}{\theta^2}$$

which shows (2.32) and thus finishes the proof. □

Proof of Proposition 2.15

For the proof of Proposition 2.15 we recall some characteristic approximation properties of shearlets and wavelets. Indeed, by Theorem 1.6 the best N-term approximation f_N^s of shearlets for cartoon-like functions obeys

$$\|f - f_N^s\| \lesssim N^{-1}(\log N)^{3/2},$$

and for wavelets the best N-term approximation f_N^w obeys

$$\|f - f_N^w\| \lesssim N^{-1/2},$$

see [KL12a]. Furthermore, these bounds are sharp, i.e. there exist cartoon-like functions such that the above inequalities hold with equality up to some constant.

Proof of Proposition 2.15. Let $N \in \mathbb{N}, f_N^s, f_{\sigma(N)}^w, \mathcal{R}_N^s, \mathcal{R}_{\sigma(N)}^w$ be as in the proposition. For a fixed $\theta > 1$ there exist by Theorem 2.14 an $M = (M_1, M_2)$ such that

$$c_{N,M} = \inf_{\substack{f \in \mathcal{R}_N^s \\ \|f\|=1}} \|P_{\mathcal{S}_M^{(\varepsilon)}} f\| \geq \frac{1}{\theta}$$

and similarly, by Theorem2.12 there exists an $M' = (M_1', M_2')$ in $\mathbb{N} \times \mathbb{N}$ so that

$$c_{\sigma(N),M'} = \inf_{\substack{f \in \mathcal{R}_{\sigma(N)}^w \\ \|f\|=1}} \|P_{\mathcal{S}_{M'}^{(\varepsilon)}} f\| \geq \frac{1}{\theta}.$$

More precisely, we can choose $M_1 \cdot M_2$ and $M_1' \cdot M_2'$ to be of order $\sigma(N_J)$ due to the stable sampling rate for shearlets and wavelets, respectively.

By Theorem 2.3 and the approximation rate for cartoon-like functions we can bound the error of the generalized sampling reconstruction by

$$\|f - G_{\sigma(N),M'}^w(f)\| \lesssim \|f - P_{\mathcal{R}_{\sigma(N)}^w}(f)\| \lesssim \|f - f_{\sigma(N)}^w\| \lesssim \sigma(N)^{-1/2}.$$

Analogously, for shearlets we obtain

$$\|f - G_{N,M}^s(f)\|^2 \lesssim \|f - P_{\mathcal{R}_N^s}(f)\|^2 \lesssim \left\| f - \sum_{\lambda \in I_N} \langle f, \psi_\lambda^d \rangle \psi_\lambda \right\|^2 \lesssim \sum_{\lambda \notin I_N} |\langle f, \psi_\lambda^d \rangle|^2,$$

where $(\psi_\lambda^d)_\lambda$ is the dual shearlet system of $(\psi_\lambda)_\lambda$ and I_N denotes the index set of the N largest coefficients $(\langle f, \psi_\lambda \rangle_\lambda)$ with respect to the best N-term approximation f_N^s.

Furthermore, if the regularity is sufficiently large, it was shown in [Gro13] that we can relate the analysis coefficients of the primal frame with those of the dual frame by the relation

$$(\langle f, \psi_\lambda \rangle)_\lambda = G(\langle f, \psi_\lambda^d \rangle)_\lambda,$$

where G is the Gramian operator associated to the shearlet system (ψ_λ). Therefore the claimed rate follows from the decay rate of the shearlet coefficients. Hence,

$$\|f - G^s_{N,M}(f)\|^2 \lesssim \sum_{\lambda \notin I_N} |\langle f, \psi_\lambda \rangle|^2 \lesssim N^{-2}(\log N)^3$$

which yields the result. $\square$

So far we have considered the reconstruction of Fourier measurements using compactly supported shearlets within the framework of GS. Further, our main result showed that an almost linear stable sampling rate provides successful reconstructions. However, in practice it would not be efficient to sample with such a rate. In fact, using the concept of *compressed sensing* one can reduce the number of measurements dramatically. We will discuss this in the next section.

Chapter 3

Structured compressed sensing

In this chapter we study the reconstruction problem under the presence of *sparsity*. Loosely speaking, a signal is *sparse in a system* $(\psi_\lambda)_\lambda$ if it can be represented in the span of $(\psi_\lambda)_\lambda$ using only very few non-zero coefficients. We shall give a precise definition further below. The concept of sparsity leads us to a situation that falls into the field of *compressed sensing*. In particular, compressed sensing is a theory that was developed by Donoho in [Don06] and Candès, Romberg and Tao in [CRT06] that allows one to recover a sparse signal from far less measurements than classical sampling theorems such as the Nyquist sampling theorem suggests.

In this chapter we will be in particular interested in applying compressed sensing to multiscale dictionaries such as shearlets. In particular, we will present our results for *α-shearlets* which are a special instance of *α-molecules* [GKKS]. These systems are again a generalization of so-called *parabolic molecules* [GK14] which is a concept that unifies the concepts of wavelets, curvelets and shearlets. We will give some details about the concept and the notations later in this chapter. First, we proceed with a brief introduction into compressed sensing.

Compressed sensing

The reconstruction problem considered in compressed sensing can be considered as solving a linear system of equations

$$Ax = y, \tag{3.1}$$

where x takes the role of the signal in $\mathbb{R}^n$, $y \in \mathbb{R}^m$ represents the acquired measurements and A is the $m \times n$ sampling matrix which is usually fixed and given by the application. As the matrix A represents the acquisition device it would be of great desire to keep m, the number of measurements, small. Ideally, one wants m to be much smaller than n, however, in this event the system (3.1) does not admit a unique solution anymore. In particular, without any further assumptions we cannot hope to recover the signal x exactly.

The fundamental property that changes the non-unique solvability of the linear system of equations is the concept of *sparsity*.

Definition 3.1. *Let $x \in \mathbb{R}^n$ or $\mathbb{C}^n$. Then x is called* s-sparse *if the number of non-zero entries does not exceed $s \in \mathbb{N}$. In other words, the $\|.\|_0$-map*

$$\|x\|_0 := \#\{i \leq n \,:\, x_i \neq 0\}$$

of x is bounded by s.

In order to find the *sparsest solution* fulfilling the constraint (3.1) one could consider the constraint minimization problem

$$\min_x \|x\|_0 \quad \text{subject to} \quad Ax = y. \tag{3.2}$$

However, this minimization problem (3.2) is unfortunately in general NP-hard [FR13] to solve wherefore the following convex relaxation has been commonly used in compressed sensing [CT06, Can08, CT05, CRT05, CRT06]:

$$\min_x \|x\|_1 \quad \text{subject to} \quad Ax = y. \tag{3.3}$$

Furthermore, in order to allow *noisy measurements* one usually considers the following minimization problem

$$\min_x \|x\|_1 \quad \text{subject to} \quad \|y - Ax\|_2 \leq \varepsilon,$$

where we call ε the *fidelity parameter*.

Assuming certain properties such as the *null space property* for the measurement matrix A the ℓ^1-minimization problem (3.3) is capable of recovering the exact solution, see, for instance, [FR13].

Now, both minimization problems (3.2) and (3.3) require sparsity of the signal x directly. This is, however, not always the case. In particular it is not the case for the type of images that one is interested in applications such as MRI. In fact, it is much more frequent that the signal is sparse in some specific domain, meaning it is sparse after an application of some transform Ψ.

For example, natural images are rarely sparse in a pixel basis, but the shearlet transform of the image admits a sparse signal. For instance, in Figure 3.1 we depicted the distribution of the 5%-largest shearlets coefficients of all available shearlet coefficients up to a fixed maximum number of scales. It can be observed that most of the largest coefficients are located at the low frequencies and then with increasing scales, the number of non-zero coefficients decrease very fast.

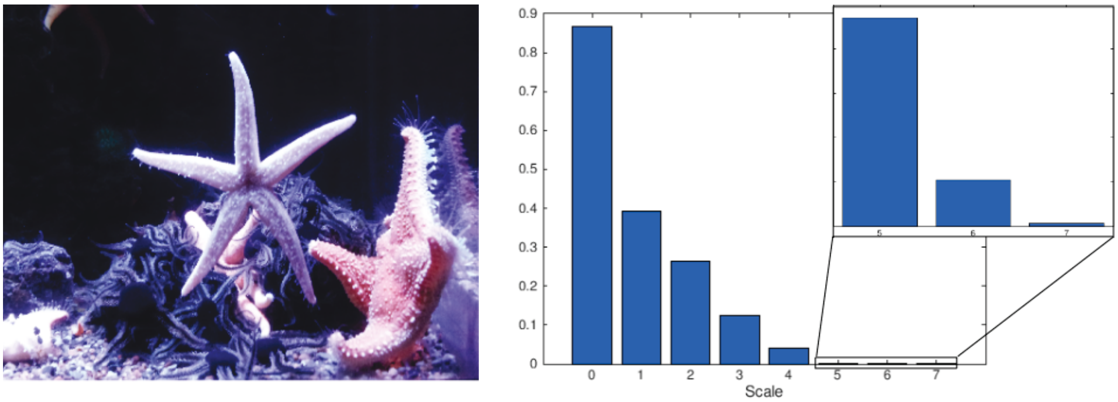

Figure 3.1: **Left:** A natural image of size 2048 × 2048. **Right:** Distribution of the shearlet coefficients of the best N-term approximation using 5% of the largest coefficients in modulus.

The reconstruction problem from Fourier measurements using compactly supported shearlets studied in the previous Chapter 2 does perfectly fit into the regime of compressed sensing. In fact, for this specific problem the sensing matrix A is simply the subsampled Fourier transform and Ψ is the analysis operator of the shearlet frame. This then leads to a reconstruction that is sparse in the shearlet frame or more precisely, its dual. However, note that the above introduction considered the finite dimensional scenario whereas the problem studied in Chapter 2 is an infinite dimensional one. However, the theory of compressed sensing was generalized by Adcock and Hansen to the infinite dimensional setting in [AH] which was then later further developed in [AHPR15, Poo15] by, among other things, taking into account the multilevel structure of sparsifying transforms such as wavelets and shearlets. The infinite dimensional reconstruction problem reads as

$$\inf_{f \in \mathcal{H}, \widetilde{\Psi} f \in \ell^1} \|\widetilde{\Psi} f\|_1 \quad \text{subject to} \quad \|P_\Omega A f - y\| \leq \varepsilon, \tag{3.4}$$

where P_Ω is the projection onto the span of the unit vector $e_j \in \ell^2$ with $j \in \Omega$ and Ω determines the subsampling pattern and $\widetilde{\Psi}$ denotes the analysis operator associated to the canonical dual frame. Canonically we will denote by $\widetilde{\Psi}^*$ the synthesis operator associated to the canonical dual frame of $(\psi_\lambda)_\lambda$.

Our main contribution in this chapter is to provide a more detailed analysis on how the sampling pattern can be designed if structured systems such as shearlets are used. Before we can present our main results, we first have to generalize the main quantities and concepts that were introduced in [Poo15]. More precisely, in [Poo15] the author has investigated the above infinite dimensional minimization problem for Ψ corresponding to a tight frame. Unfortunately, the compactly supported shearlets that we have investigated in the previous chapter do not form a tight frame and thus these generalizations are needed. We therefore first extend the recovery results of [Poo15] to arbitrary frames and then we discuss the application of the stability result to systems which have a localized Gramian such as shearlet frames.

3.1 Structured sampling and structured sparsity

Several main concepts introduced in [AHPR15] and further developed in [Poo15] are *multilevel sampling schemes*, *structured sparsity*, and *local incoherence*. We now recall these definitions.

Multilevel sampling scheme

The multilevel sampling scheme is perfectly suited for the reconstruction problem that deals with sampling Fourier coefficients of a signal and recovering it in a sparse domain such as those generated by wavelets or shearlets. The general definition is as follows.

Definition 3.2 ([AHPR15, Poo15]). *Let* $r \in \mathbb{N}, \mathbf{M} = (M_1, \dots, M_r) \in \mathbb{N}^r$ *with* $0 = M_0 < M_1 < \dots < M_r$, $\mathbf{m} = (m_1, \dots, m_r) \in \mathbb{N}^r$ *with* $m_k < M_k - M_{k-1}, k = 1, \dots, r$. *Further, suppose*

$$\Omega_k \subset \{M_{k-1} + 1, \dots, M_k\},$$

with $|\Omega_k| = m_k$ *for* $k = 1, \dots, r$ *are chosen uniformly at random. The set* $\Omega = \Omega_{\mathbf{M},\mathbf{m}} = \Omega_1 \cup \dots \cup \Omega_r$ *is called* $(\mathbf{M}, \mathbf{m})$-sampling scheme.

Sparsity in levels

As we already showed in Figure 3.1 natural images are sparse in wavelet domains. However, this type of sparsity can be characterized more precisely and can generally be observed for other systems such as shearlets and curvelets. We proceed with the definition of signals that are *sparse in levels* which is a structure that is inherited in natural signals.

Definition 3.3 ([Poo15]). *Let* x *be in* $\mathbb{C}^N$ *or* $\ell^2(\mathbb{N})$. *For* $r \in \mathbb{N}$ *let* $\mathbf{N} = (N_1, \dots, N_r) \in \mathbb{N}^r$ *with* $0 = N_0 < N_1 < \dots < N_r$ *and* $\mathbf{s} = (s_1, \dots, s_r) \in \mathbb{N}^r$ *with* $s_k \leq N_k - N_{k-1}$ *and* $k = 1, \dots, r$. *We say that* x *is* $(\mathbf{s}, \mathbf{N})$-sparse *if for each* $k = 1, \dots, r$ *the* level support $\Delta_k := \operatorname{supp}(x) \cap \{N_{k-1} + 1, \dots, N_k\}$, *satisfies* $|\Delta_k| \leq s_k$. *The set of* $(\mathbf{s}, \mathbf{N})$*-sparse signals is denoted by* $\Sigma_{\mathbf{s},\mathbf{N}}$.

The next definition concerns the minimal error approximation of an arbitrary signal by (s, N)-sparse signals.

Definition 3.4 ([Poo15]). *Let* x *be in* $\mathbb{C}^N$ *or* $\ell^2(\mathbb{N})$. *The* $(\mathbf{s}, \mathbf{N})$-term approximation *is defined as*

$$\sigma_{\mathbf{s},\mathbf{N}}(x) = \min_{z \in \Sigma_{\mathbf{s},\mathbf{N}}} \|x - z\|_1.$$

If one is given a frame $(\psi_\lambda)_\lambda \subseteq \mathcal{H}$ together with its canonical dual $(\widetilde{\psi}_\lambda)_\lambda$ and Ψ^* denotes the synthesis operator with respect to the primal frame and $\widetilde{\Psi}$ denote the analysis operator of the dual frame, then by definition we have for any $f \in \mathcal{H}$

$$\Psi^* \widetilde{\Psi} f = f.$$

However, in general $\widetilde{\Psi}\Psi^* : \ell^2 \longrightarrow \ell^2$ is not the identity operator. But since we are minimizing over the dual coefficients $\widetilde{\Psi}f$ for $f \in \mathcal{H}$, it is a natural question how $\widetilde{\Psi}\Psi^*$ distorts the sparsity of a signal $\Psi^* x$ for $x \in \Sigma_{\mathbf{s},\mathbf{N}}$. This will be measured by the next definition which is a straightforward generalization of the analogue given in [Poo15].

Definition 3.5. *Let $r \in \mathbb{N}$ and $\mathbf{N} = (N_1, \ldots, N_r) \in \mathbb{N}^r$ with $0 = N_0 < N_1 < \ldots < N_r$ and $\mathbf{s} = (s_1, \ldots, s_r) \in \mathbb{N}^r$. Let $\Lambda_j = \{N_{j-1}+1, \ldots, N_j\}$ for $j = 1, \ldots, r-1$ and $\Lambda_r = \{N_{r-1}+1, N_{r-1}+2, \ldots\}$. Further, let $p = 2^{-J}$ for some $J \in \mathbb{N} \cup \{0\}$ and $\kappa > 0$ the smallest number such that*

$$\kappa^{1-p/q} \geq \sup\left\{ \|\widetilde{\Psi}g\|_p^p \,:\, g = \Psi^* x, \|\widetilde{\Psi}g\|_q = 1, x \in \Sigma_{\mathbf{s},\mathbf{N}} \right\}, \quad q \in \{2, \infty\},$$

where we set $p/\infty = 0$. Then $\kappa(\mathbf{N}, \mathbf{s}, p) = \kappa$ is said to be the localized sparsity with respect to $\mathbf{N}, \mathbf{s}$ and p. *For each $j = 1, \ldots, r$ let $\kappa_j > 0$ be the smallest number such that*

$$\kappa_j^{1-p/q} \geq \sup\left\{ \|P_{\Lambda_j}\widetilde{\Psi}g\|_p^p \,:\, g = \Psi^* x, \|P_{\Lambda_j}\widetilde{\Psi}g\|_q = 1, x \in \Sigma_{\mathbf{s},\mathbf{N}} \right\}, \quad q \in \{2, \infty\}.$$

Then $\kappa_j(\mathbf{N}, \mathbf{s}, p) = \kappa_j$ is said to be the j^{th} localized level sparsity with respect to N, s, and p.

While Definition 3.5 essentially concerns the localization properties of the cross Gramian between the primal frame and its canonical dual, the next definition involves the sampling operator. It is again a straightforward generalization of the definition given in [Poo15] to the scenario where the frame is not necessarily tight.

Definition 3.6. *Let $A, \Psi : \mathcal{H} \longrightarrow \mathcal{H}'$ be linear bounded operators where $\mathcal{H}$ is a Hilbert space and $\mathcal{H}'$ is either $\mathbb{C}^N$ or ℓ^2. Further, let $\kappa = (\kappa_1, \ldots, \kappa_r), \mathbf{N} = (N_1, \ldots, N_r), \mathbf{M} = (M_1, \ldots, M_r) \in \mathbb{N}^r$ with $0 = N_0 < N_1 < \ldots < N_r$ and $0 = M_0 < M_1 < \ldots < M_r$. For $1 \leq k \leq r$, the k^{th}* relative sparsity *is given by*

$$\widehat{\kappa}_k = \widehat{\kappa}_k(\mathbf{N}, \mathbf{M}, \kappa) = \max_{g \in \Theta} \|P_{\Gamma_k} A g\|^2,$$

where $\Gamma_k = \{M_{k-1}+1, \ldots, M_k\}$ and Θ is the set

$$\Theta = \{g \in \mathcal{H} \,:\, g \in \operatorname{ran}\Psi^*, \|P_{\Lambda_l}\widetilde{\Psi}g\|_2^2 \leq \kappa_l, l = 1, \ldots, r\},$$

where $\Lambda_l = \{N_{k-1}+1, \ldots, N_k\}$.

Local incoherence

The final ingredient that we use in order to analyze the recovery problem for level sparse signals and multilevel sampling schemes is the definition of *local incoherence.*

Definition 3.7 ([Poo15])**.** *Let $A, \Psi : \mathcal{H} \longrightarrow \mathcal{H}'$ where $\mathcal{H}$ is a Hilbert space and $\mathcal{H}'$ is either $\mathbb{C}^N$ or ℓ^2. For $r \in \mathbb{N}$ let $\mathbf{M} = (M_1, \ldots, M_r) \in \mathbb{N}^r$ with $0 = M_0 < M_1 < \ldots < M_r$ and $\mathbf{N} = (N_1, \ldots, N_r) \in \mathbb{N}^r$ with $0 = N_0 < N_1 < \ldots < N_r$. Furthermore, let $\Gamma_k = \{M_{k-1}+1, \ldots, M_k\}, k \leq r$ and $\Lambda_k = \{N_{k-1}+1, \ldots, N_k\}, k \leq r-1$ and let $\Lambda_r = \{n \in \mathbb{N} \,:\, n > N_r\}$. The (k,l)-*local incoherence between A and Ψ with respect to $\mathbf{N}$ and $\mathbf{M}$ *is given by*

$$\mu_{\mathbf{N},\mathbf{M}}(k,l) = \sqrt{\mu(P_{\Gamma_k}A\Psi^* P_{\Lambda_l})\mu(P_{\Gamma_k}A\Psi^*)}, k, l = 1, \ldots, r.$$

We now turn to the stability theorem and its assumptions.

3.2 Stability guarantee for general frames

The stability result for solutions of the problem (3.4) relies on the *balancing property* that was first introduced by Adcock and Hansen in [AH] which was then customized for the analysis case in [Poo15]. We shall introduce the balancing property similar as in [Poo15] for the general frame case, i.e. not necessarily tight-frame case.

Balancing property

The balancing property is a helpful tool that allows one to exploit more structure of the reconstruction system and essentially predicts in which measurements should be acquired.

Definition 3.8. *Let $A, \Psi : \mathcal{H} \longrightarrow \ell^2$ be linear bounded operators. Then $M \in \mathbb{N}$ and $K \geq 1$ satisfy the balancing property with respect to $A, \Psi, N, s \in \mathbb{N}$ and $\kappa_2 \geq \kappa_1 > 0$ if for all $\mathcal{R} = \operatorname{span}\{\{\Psi^* e_i : i \in \Delta\} \cup \{\widetilde{\Psi}^* e_j : j \in \Delta\}\}$ where $\Delta \subset [N]$ is such that $|\Delta| = s$,*

$$\|\Psi P_{\mathcal{R}} A^* P_{[M]}^{\perp} A P_{\mathcal{R}} \Psi^*\|_{2\to 2} \leq \frac{\sqrt{\kappa_1/\kappa_2}}{8} \left(\log_2^{1/2}(4\sqrt{\kappa_2} K M)\right)^{-1}$$

and

$$\|\Psi P_{\mathcal{R}}^{\perp} A^* P_{[M]} A P_{\mathcal{R}} \Psi^*\|_{2\to\infty} \leq 1/(8\sqrt{\kappa_2})$$

holds.

Now, let $r \in \mathbb{N}$ and $\mathbf{N} = (N_1, \dots, N_r)$, $\mathbf{M} = (M_1, \dots, M_r)$, $\mathbf{s} = (s_1, \dots, s_r) \in \mathbb{N}^r$ with $0 = N_0 < N_1 < \dots < N_r$. For $p \in (0, 1]$ let $\kappa = (\kappa_1, \dots, \kappa_r)$ be $\kappa_j = \kappa_j(\mathbf{N}, \mathbf{s}, p)$ and $\widehat{\kappa}_j = \widehat{\kappa}_j(\mathbf{N}, \mathbf{M}, \kappa)$. Further, let

$$\begin{aligned}\widetilde{M} = {} & \|\widetilde{\Psi}\Psi^*\|_{\infty\to\infty} \\ & \cdot \min\left\{ i \in \mathbb{N} : \max_{j \geq i} \|P_{[M]} A \Psi^* e_j\|_2 \leq q/(8\sqrt{\kappa_{\max}}), \max_{j\geq i} \|P_{\operatorname{ran}\Psi^* P_{[N]}} \Psi^* e_j\| \leq \sqrt{5q}/4 \right\},\end{aligned}$$

and

$$B(\mathbf{s}, \mathbf{N}) = \sup\{\widetilde{B}(\Delta) : \Delta \text{ is } (\mathbf{s}, \mathbf{N})\text{-sparse}\},$$

where $\Delta \subset \mathbb{N}$ and

$$\widetilde{B}(\Delta) = \max\left\{ \|\widetilde{\Psi} P_{\mathcal{R}}^{\perp} \Psi^*\|_{\infty\to\infty}, \sqrt{\|\Psi P_{\mathcal{R}} \widetilde{\Psi}^*\|_{\infty\to\infty} \max_{l=1,\dots,r} \sum_{t=1}^{r} \|P_{\Lambda_l} \Psi P_{\mathcal{R}} \widetilde{\Psi}^* P_{\Lambda_t}\|_{\infty\to\infty}} \right\}.$$

Then the stability result is formulated as follows.

Theorem 3.9. *Let $\mathcal{H}$ be a Hilbert space, $A : \mathcal{H} \longrightarrow \ell^2$ a linear, bounded operator and Ψ the analysis operator of a frame. Let $f \in \mathcal{H}$ and suppose $\Omega = \Omega_{\mathbf{M},\mathbf{m}}$ is a multilevel sampling scheme. Further, let $(\mathbf{s}, \mathbf{N})$ be such that the following holds:*

i) The parameters $M = M_r, q^{-1} = \max_{k=1,\dots,r}\{(M_k - M_{k-1})/m_k\}$ satisfy the balancing property with respect to $A, \Psi, N := N_r, \kappa_{min} = r\min\{\kappa_j\}$ and $\kappa_{max} = r\max\{\kappa_j\}$.

ii) For $\gamma \in (0, e^{-1}]$ and $k = 1, \dots, r$

$$\sqrt{r}\log(\gamma)\log(q^{-1}\widetilde{M}\sqrt{\kappa_{max}})B(s,N)\frac{M_k - M_{k-1}}{m_k}\left(\sum_{l=1}^{r}\mu^2_{\mathbf{N},\mathbf{M}}(k,l)\kappa_l\right) \lesssim 1,$$

and $r\widehat{m}_k B(\mathbf{s},\mathbf{N})^2\log(\gamma^{-1})\log(q^{-1}\widetilde{M}\sqrt{\kappa_{max}}) \lesssim m_k$ where $\widehat{m}_k$ is such that

$$\sum_{k=1}^{r}\left(\frac{M_k - M_{k-1}}{\widehat{m}_k} - 1\right)\mu_{\mathbf{N},\mathbf{M}}(k,l)\widehat{\kappa}_k \lesssim 1, \quad l = 1, \dots, r.$$

Suppose that $\widehat{f}$ is a minimizer of (3.4) with $y = P_\Omega V f + \eta$ and $\|\eta\|_2 \le \varepsilon$. Then with probability exceeding $1 - \gamma$ we have

$$\|f - \widehat{f}\| \le C_1\varepsilon + C_2\sigma_{\mathbf{s},\mathbf{N}}(\widetilde{\Psi}f)$$

for some constants C_1 and C_2 that depend on q, γ, κ_{max} and the frame bounds of the frame corresponding to Ψ. If $m_k = M_k - M_{k-1}$ for $k = 1, \dots, r$ then this holds with probability 1.

Proof. See Appendix C.8 □

The proof of Theorem 3.9 is build on the next result which is Proposition 6.1 in [Poo15] adapted to the non-tight frame case. We include it here for completeness as its proof also visualizes why we had to enlarge the reconstruction space

$$\mathcal{R} = \operatorname{span}\{\{\Psi^* e_i \,:\, i \in \Delta\} \cup \{\widetilde{\Psi}^* e_j \,:\, j \in \Delta\}\}$$

by the dual elements in the balancing property.

Proposition 3.10. *Let $f \in \mathcal{H}$, $\Delta \subset \mathbb{N}$ and $\mathcal{R} = \operatorname{span}\{\{\Psi^* e_i \,:\, i \in \Delta\} \cup \{\widetilde{\Psi}^* e_j \,:\, j \in \Delta\}\}$. Further, let $r \in \mathbb{N}$ and $q = (q_1, \dots, q_r) \in (0,1]^r$ and let $\Omega = \Omega_1 \cup \ldots \cup \Omega_r$ where $\Omega_1, \dots, \Omega_r$ are disjoint subsets of $\mathbb{N}$. Suppose*

i) $\left\|P_\mathcal{R} A^* \left(\bigoplus_{i=1}^r q_i^{-1} P_{\Omega_i}\right) A P_\mathcal{R} - P_\mathcal{R}\right\| < 1/4$,

ii) $\sup_{i\in\mathbb{N}} \left\|P_i \Psi P_\mathcal{R}^\perp A^* \left(\bigoplus_{i=1}^r q_i^{-1} P_{\Omega_i}\right) A P_\mathcal{R}^\perp \Psi^* P_i\right\| < 5/4$,

iii) there exists $\rho = A^* P_\Omega w$ and $L > 0$ such that

- *a)* $\left\|\widetilde{\Psi}^* P_\Delta \operatorname{sgn}(P_\Delta \widetilde{\Psi} f) - P_\mathcal{R}\rho\right\| \le \sqrt{q}/8$,
- *b)* $\left\|P_\Delta^\perp \Psi P_\mathcal{R}^\perp \rho\right\|_\infty \le 1/4$,
- *c)* $\|w\|_2 \le L\sqrt{\kappa}$.

Let $y \in \ell^2$ be a feasible vector, i.e. $\|P_\Omega A f - y\| \le \varepsilon$. Then any minimizer $\widehat{f} \in \mathcal{H}$ of (3.4) satisfies

$$\|f - \widehat{f}\| \le C_1\varepsilon + C_2\|P_\Delta^\perp \widetilde{\Psi} f\|_1,$$

for some constants C_1, C_2 that depend on B and q. The constant C_1 further depends on L and κ.

Proof. Let $P_{\mathcal{R}}$ denote the orthogonal projection onto $\mathcal{R}$. Then by construction of the reconstruction space $\mathcal{R}$ we have

$$P_{\mathcal{R}}^{\perp} g = P_{\mathcal{R}}^{\perp} \Psi^* P_{\Delta}^{\perp} \widetilde{\Psi} g + P_{\mathcal{R}}^{\perp} \Psi^* P_{\Delta} \widetilde{\Psi} g = P_{\mathcal{R}}^{\perp} \Psi^* P_{\Delta}^{\perp} \widetilde{\Psi} g$$

for all $g \in \mathcal{H}$. Therefore

$$\|g\| \leq \|P_{\mathcal{R}} g\| + \|P_{\mathcal{R}}^{\perp} \Psi^* P_{\Delta}^{\perp} \widetilde{\Psi} g\| \leq \|P_{\mathcal{R}} g\| + B^{1/4} \|P_{\Delta}^{\perp} \widetilde{\Psi} g\|_1 \tag{3.5}$$

for all $g \in \mathcal{H}$. Now, let $\widehat{f}$ be a minimizer of (3.4) and set $h = \widehat{f} - f$. Further, we denote $A_{\Omega,q} = P_{\mathcal{R}} A^* \left(\bigoplus_{i=1}^r q_i^{-1} P_{\Omega_i} \right) A P_{\mathcal{R}}$. Then, by $i)$ and Neumann series we have

- ▷ $\|A_{\Omega,q} - \mathrm{Id}_{P_{\mathcal{R}}(\mathcal{H})}\| < 1/4$,
- ▷ $A_{\Omega,q}$ is invertible on $P_{\mathcal{R}}(\mathcal{H})$ with $\|A_{\Omega,q}^{-1}\| \leq 4/3$,
- ▷ $\left\| \left(\bigoplus_{i=1}^r q_i^{-1/2} P_{\Omega_i} \right) A P_{\mathcal{R}} \right\| \leq \sqrt{5/4}$.

By feasibility we have $\|P_{\Omega} A h\|_2 \leq 2\varepsilon$, hence

$$\begin{aligned}
\|P_{\mathcal{R}} h\| &= \|A_{\Omega,q}^{-1} A_{\Omega,q} P_{\mathcal{R}} h\| \\
&\leq \|A_{\Omega,q}^{-1}\| \left\| P_{\mathcal{R}} A^* \left(\bigoplus_{i=1}^r q_i^{-1} P_{\Omega_i} \right) A (\mathrm{Id} - P_{\mathcal{R}}^{\perp}) h \right\| \\
&\leq 4/3 \left[\sqrt{5/4} \left(q^{-1/2} 2\varepsilon + \left\| \left(\bigoplus_{i=1}^r q_i^{-1/2} P_{\Omega_i} \right) A P_{\mathcal{R}}^{\perp} h \right\| \right) \right].
\end{aligned} \tag{3.6}$$

Using $ii)$ we obtain

$$\begin{aligned}
\left\| \left(\bigoplus_{i=1}^r q_i^{-1/2} P_{\Omega_i} \right) A P_{\mathcal{R}}^{\perp} h \right\| &= \left\| \left(\bigoplus_{i=1}^r q_i^{-1/2} P_{\Omega_i} \right) A P_{\mathcal{R}}^{\perp} \Psi^* P_{\Delta}^{\perp} \widetilde{\Psi} h \right\| \\
&= \sup_{i \in \Delta^c} \left\| \left(\bigoplus_{i=1}^r q_i^{-1/2} P_{\Omega_i} \right) A P_{\mathcal{R}}^{\perp} \Psi^* e_i \right\| \left\| P_{\Delta}^{\perp} \widetilde{\Psi} h \right\| \\
&\leq \sqrt{5/4} \left\| P_{\Delta}^{\perp} \widetilde{\Psi} h \right\|_1 .
\end{aligned} \tag{3.7}$$

Using (3.7) in (3.6) yields

$$\|P_{\mathcal{R}} h\| \leq 4\sqrt{5}/3 q^{-1/2} \varepsilon + 5/3 \|P_{\Delta}^{\perp} \widetilde{\Psi} h\|_1. \tag{3.8}$$

We proceed by bounding $\|P_{\Delta}^{\perp} \widetilde{\Psi} h\|_1$. By direct estimation we obtain

$$\begin{aligned}
\|\widetilde{\Psi} \widehat{f}\|_1 &= \|P_{\Delta}^{\perp} \widetilde{\Psi}(f + h)\|_1 + \|P_{\Delta} \widetilde{\Psi}(f + h)\|_1 \\
&\geq \|P_{\Delta}^{\perp} \widetilde{\Psi} h\|_1 - \|P_{\Delta}^{\perp} \widetilde{\Psi} f\|_1 + \|P_{\Delta} \widetilde{\Psi} f\|_1 + \mathrm{Re}\langle P_{\Delta} \widetilde{\Psi} h, \mathrm{sgn}(P_{\Delta} \widetilde{\Psi} f)\rangle \\
&= \|P_{\Delta}^{\perp} \widetilde{\Psi} h\|_1 - 2\|P_{\Delta}^{\perp} \widetilde{\Psi} f\|_1 + \|\widetilde{\Psi} f\|_1 + \mathrm{Re}\langle P_{\Delta} \widetilde{\Psi} h, \mathrm{sgn}(P_{\Delta} \widetilde{\Psi} f)\rangle \\
&\geq \|P_{\Delta}^{\perp} \widetilde{\Psi} h\|_1 - 2\|P_{\Delta}^{\perp} \widetilde{\Psi} f\|_1 + \|\widetilde{\Psi} \widehat{f}\|_1 + \mathrm{Re}\langle P_{\Delta} \widetilde{\Psi} h, \mathrm{sgn}(P_{\Delta} \widetilde{\Psi} f)\rangle
\end{aligned}$$

where we have used that $\widehat{f}$ is a minimizer in the last estimate. By rearranging the terms above we have

$$\|P_\Delta^\perp \widetilde{\Psi} h\|_1 \leq 2\|P_\Delta^\perp \widetilde{\Psi} f\|_1 + |\langle P_\Delta \widetilde{\Psi} h, \operatorname{sgn}(P_\Delta \widetilde{\Psi} f)\rangle|. \tag{3.9}$$

By *iii)* we have

$$\begin{aligned}
|\langle P_\Delta \widetilde{\Psi} h, \operatorname{sgn}(P_\Delta \widetilde{\Psi} f)\rangle| &= |\langle h, \widetilde{\Psi}^* P_\Delta \operatorname{sgn}(P_\Delta \widetilde{\Psi} f)\rangle| \\
&\leq |\langle h, \widetilde{\Psi}^* P_\Delta \operatorname{sgn}(P_\Delta \widetilde{\Psi} f) - P_{\mathcal{R}}\rho\rangle| + |\langle h, \rho\rangle| + |\langle h, P_{\mathcal{R}}^\perp \rho\rangle| \\
&\leq \sqrt{q}/8\|h\| + \|P_\Omega A h\|_2 \|w\|_2 + |\langle \Psi^* P_\Delta^\perp \widetilde{\Psi} h, P_{\mathcal{R}}^\perp \rho\rangle| \\
&\leq \sqrt{5}/6\varepsilon + 5\sqrt{q}/24\|P_\Delta^\perp \widetilde{\Psi} h\|_1 + \sqrt{q}/8\|P_{\mathcal{R}}^\perp h\| + 2\varepsilon L\sqrt{\kappa} + \\
&\quad + 1/4\|P_\Delta^\perp \widetilde{\Psi} h\|_1 \\
&\leq \sqrt{5}/6\varepsilon + 2\varepsilon L\sqrt{\kappa} + (5\sqrt{q}/3 + \sqrt{q}B^{1/4} + 2)/8\|P_\Delta^\perp \widetilde{\Psi} h\|_1.
\end{aligned}$$

Hence, (3.9) can further be estimated as

$$\|P_\Delta^\perp \widetilde{\Psi} h\|_1 \leq \sqrt{5}/6\varepsilon + 2\varepsilon L\sqrt{\kappa} + (5\sqrt{q}/3 + \sqrt{q}B^{1/4} + 2)/8\|P_\Delta^\perp \widetilde{\Psi} h\|_1 + 2\|P_\Delta^\perp \widetilde{\Psi} f\|_1$$

which is equivalent to

$$\|P_\Delta^\perp \widetilde{\Psi} h\|_1 \leq \frac{\sqrt{5}/6\varepsilon + 2\varepsilon L\sqrt{\kappa} + 2\|P_\Delta^\perp \widetilde{\Psi} f\|_1}{3/4 - \sqrt{q}(5/3 + B^{1/4})/8} \tag{3.10}$$

By using (3.10) and (3.8) we can conclude

$$\|h\| \leq \|P_{\mathcal{R}} h\| + \|P_{\mathcal{R}}^\perp h\| \leq C_1\varepsilon + C_2\|P_\Delta^\perp \widetilde{\Psi} f\|_1$$

with

$$C_1 = \frac{4\sqrt{5}/3q^{-1/2} + (5/3 + B^{1/4})(\sqrt{5}/6 + 2L\sqrt{\kappa})}{3/4 - \sqrt{q}(5/3 + B^{1/4})/8}, \quad C_2 = \frac{2(5/3 + B^{1/4})}{3/4 - \sqrt{q}(5/3 + B^{1/4})/8}.$$

□

Remark 3.11. *Note that the noise free case is also covered in the proof of Proposition 3.10 as ε can simply be set to zero.*

In order to prove Theorem 3.9 one has to check that the assumptions of Proposition 3.10 can be fulfilled with high probability. A contruction of a dual certificate such that this is the case can be done in the same way as it has been done in [Poo15] for tight frames with corresponding adaptions of the arguments to the non-tight case. We therefore present this construction in Appendix C.8, see also [Poo15].

In order to make Theorem 3.9 more applicable we discuss its assumption in the next section in more detail.

3.3 Sufficient condition for the balancing property

In this section we want to discuss the assumptions of Theorem 3.9 in more detail. More precisely, we discuss the assumption of the balancing property and present an approach how to verify it for for systems that are (cross-)localized, i.e. whose Gramians $\Psi\Psi^*$ and $\Psi\widetilde{\Psi}^*$ have a strong off diagonal decay and have good incoherence properties, i.e. essentially ΨA^* has strong off-diagonal decay. Note that the second assumption *ii*) of Theorem 3.9 solely depends on the incoherence properties and the relative sparsities of the underlying system.

Recall that the balancing property requires to bound the following two terms, first

$$\|\Psi P_{\mathcal{R}} A^* P_{[M]}^{\perp} A P_{\mathcal{R}} \Psi^*\|_{2\to 2} \leq \frac{\sqrt{\kappa_{\min}/\kappa_{\max}}}{8} \left(\log_2^{1/2}(4\sqrt{\kappa_{\max}}KM)\right)^{-1} \tag{3.11}$$

and second

$$\|\Psi P_{\mathcal{R}}^{\perp} A^* P_{[M]} A P_{\mathcal{R}} \Psi^*\|_{2\to\infty} \leq 1/(8\sqrt{\kappa_{\max}}). \tag{3.12}$$

Also recall that

$$\mathcal{R} = \operatorname{span}\{\{\Psi^* e_i \,:\, i \in \Delta\} \cup \{\widetilde{\Psi}^* e_j \,:\, j \in \Delta\}\}.$$

which is twice as large as in the case when the frame is tight.

We now give separate bounds for (3.11) and (3.12) starting with (3.11).

Lemma 3.12. *There exists a constant $C > 0$, such that for any $\Delta' \subset \mathbb{N}$ we have*

$$\begin{aligned}\|\Psi P_{\mathcal{R}} A^* P_{[M]}^{\perp} A P_{\mathcal{R}} \Psi^*\|_{2\to 2} \leq{}& \|P_{\Delta'} \Psi \widetilde{\Psi}^* P_{\Delta}^{\perp} \Psi A^* P_{[M]}^{\perp}\|_{2\to 2}^2 + \|P_{\Delta'} \Psi P_{\mathcal{R}} \widetilde{\Psi}^* P_{\Delta} \Psi A^* P_{[M]}^{\perp}\|_{2\to 2}^2 \\ &+ C\left(\|P_{\Delta'}^{\perp} \Psi \Psi^* P_{\Delta}\|_{2\to 2}^2 + \|P_{\Delta'}^{\perp} \Psi \widetilde{\Psi}^* P_{\Delta}\|_{2\to 2}^2\right).\end{aligned}$$

Proof. Note that

$$\begin{aligned}\|\Psi P_{\mathcal{R}} A^* P_{[M]}^{\perp} A P_{\mathcal{R}} \Psi^*\|_{2\to 2} &= \|\Psi P_{\mathcal{R}} A^* P_{[M]}^{\perp}\|_{2\to 2}^2 \\ &= \|P_{\Delta'} \Psi P_{\mathcal{R}} A^* P_{[M]}^{\perp}\|_{2\to 2}^2 + \|P_{\Delta'}^{\perp} \Psi P_{\mathcal{R}} A^* P_{[M]}^{\perp}\|_{2\to 2}^2.\end{aligned} \tag{3.13}$$

Let Υ be the following linear bounded

$$\begin{aligned}\Upsilon : \ell^2 \times \ell^2 &\longrightarrow \mathcal{H} \\ ((c_\lambda)_\lambda, (d_\lambda)_\lambda) &\mapsto \sum_\lambda c_\lambda \psi_\lambda + \sum_\lambda d_\lambda \widetilde{\psi}_\lambda\end{aligned}$$

and $P_{\Delta\times\Delta} : \ell^2 \times \ell^2 \longrightarrow \ell^2 \times \ell^2$ be the orthogonal projection onto the index set $\Delta \times \Delta \subset \ell^2 \times \ell^2$. Then we have

- ▷ $\Upsilon P_{\Delta\times\Delta}$ is a linear and bounded operator,
- ▷ $\mathcal{R} = \operatorname{ran}(\Upsilon P_{\Delta\times\Delta})$, and
- ▷ $P_{\mathcal{R}} = \Upsilon P_{\Delta\times\Delta} \left(\Upsilon P_{\Delta\times\Delta}\right)^{\dagger}$.

Therefore, we have

$$
\begin{aligned}
&\|P_{\Delta'}\Psi P_{\mathcal{R}} A^* P_{[M]}^{\perp}\|_{2\to 2}\\
&\quad = \|P_{\Delta'}\Psi(\mathrm{Id} - P_{\mathcal{R}}^{\perp}\widetilde{\Psi}^* P_{\Delta}^{\perp}\Psi)A^* P_{[M]}^{\perp}\|_{2\to 2}\\
&\quad = \|P_{\Delta'}\Psi(\widetilde{\Psi}^* P_{\Delta}\Psi + \widetilde{\Psi}^* P_{\Delta}^{\perp}\Psi - P_{\mathcal{R}}^{\perp}\widetilde{\Psi}^* P_{\Delta}^{\perp}\Psi)A^* P_{[M]}^{\perp}\|_{2\to 2}\\
&\quad \le \|P_{\Delta'}\Psi\widetilde{\Psi}^* P_{\Delta}\Psi A^* P_{[M]}^{\perp}\|_{2\to 2} + \|P_{\Delta'}\Psi P_{\mathcal{R}}\widetilde{\Psi}^* P_{\Delta}^{\perp}\Psi A^* P_{[M]}^{\perp}\|_{2\to 2}\\
&\quad \le \|P_{\Delta'}\Psi\widetilde{\Psi}^* P_{\Delta}\Psi A^* P_{[M]}^{\perp}\|_{2\to 2} + \|P_{\Delta'}^{\perp}\Psi\Upsilon P_{\Delta\times\Delta}\left(\Upsilon P_{\Delta\times\Delta}\right)^{\dagger} A^* P_{[M]}^{\perp}\|_{2\to 2} \qquad (3.14)
\end{aligned}
$$

Furthermore,

$$
\begin{aligned}
&\|P_{\Delta'}^{\perp}\Psi\Upsilon P_{\Delta\times\Delta}\left(\Upsilon P_{\Delta\times\Delta}\right)^{\dagger} A^* P_{[M]}^{\perp}\|_{2\to 2}\\
&\quad \le \left(\|P_{\Delta'}^{\perp}\Psi\Psi^* P_{\Delta}\| + \|P_{\Delta'}^{\perp}\Psi\widetilde{\Psi}^* P_{\Delta}\|\right)\|\left(\Upsilon P_{\Delta\times\Delta}\right)^{\dagger} A^* P_{[M]}^{\perp}\|_{(2,2)\to 2} \qquad (3.15)
\end{aligned}
$$

Using (3.14) and (3.15) in (3.13) gives the result. □

The next result is trivial to prove and we therefore omit it.

Lemma 3.13. *We have*

$$\|\Psi P_{\mathcal{R}}^{\perp} A^* P_{[M]} A P_{\mathcal{R}}\Psi^*\|_{2\to\infty} = \|\Psi P_{\mathcal{R}}^{\perp}\widetilde{\Psi}^* P_{\Delta}^{\perp}\Psi A^* P_{[M]} A P_{\mathcal{R}}\Psi^*\|_{2\to\infty}.$$

Using Lemma 3.12 and Lemma 3.13 we can obtain bounds for (3.11) and (3.12) by designing $\Delta' \subset \mathbb{N}$ such that

$$\|P_{\Delta'}^{\perp}\Psi\Psi^* P_{\Delta}\|_{2\to 2} \quad \text{and} \quad \|P_{\Delta'}^{\perp}\Psi\widetilde{\Psi}^* P_{\Delta}\|_{2\to 2} \qquad (3.16)$$

can be nicely controlled if the system is *intrinsically localized.* Furthermore, it should also be designed in such a way, so that

$$\|P_{\Delta'}\Psi\widetilde{\Psi}^* P_{\Delta}^{\perp}\Psi A^* P_{[M]}^{\perp}\|_{2\to 2} \qquad (3.17)$$

can be controlled by using either intrinsic localization arguments for

$$\|P_{\Delta'}\Psi\widetilde{\Psi}^* P_{\Delta}^{\perp}\|_{2\to 2}$$

or incoherence arguments for

$$\|P_{\Delta}\Psi A^* P_{[M]}^{\perp}\|_{2\to 2}.$$

Note that this has to be done in a balanced way, since $\Delta' \cap \Delta^c$ might not be empty and hence produces some energy in the norm of $P_{\Delta'}\Psi\widetilde{\Psi}^* P_{\Delta}^{\perp}$. More precisely, on the one hand one wants to choose Δ' far away from Δ in order to gain most from the intrinsic localization which will keep (3.16) small. On the other hand it must not be too far away from Δ otherwise there is too much overlap of the index sets Δ' and Δ^c which would mean that M has to be larger than maybe necessary in order to apply some incoherence argument.

Further, by Lemma 3.13

$$\|\Psi P_{\mathcal{R}}^{\perp} A^* P_{[M]} A P_{\mathcal{R}} \Psi^*\|_{2\to\infty}$$

can be controlled by incoherence arguments. In fact it is sufficient to bound

$$\|P_{\Delta}^{\perp} \Psi A^* P_{[M]}\|_{2\to 2}$$

by incoherence arguments.

In the next sections we will present the precise arguments for the intrinsic localization that is used in this intuitive discussion and explain how such Δ' can be designed. We will thereby focus on *α-shearlets* although the arguments can be carried over to more general *α-molecules*.

3.4 Balancing property for α-shearlets

For the sake of completeness and notation, we first give a short introduction into the basics of α-molecules. We thereby only focus on the basic definitions and properties that we will use for α-molecules. For a more detailed presentation of these systems we refer to [GKKS].

Basics of α-molecules

The systems of α-molecules were introduced by Grohs et al. in [GKKS] as a generalization of parabolic molecules to arbitray degrees of anisotropy. Indeed for $\alpha = 1/2$ both systems agree. We now define a *parametrization* which will be used to define a system of α-molecules.

Definition 3.14 ([GKKS]). *A* parametrization *consists of a pair* (Λ, Φ_λ) *where* Λ *is an index set and* Φ_Λ *is a mapping*

$$\begin{aligned} \Phi : \Lambda &\longrightarrow \mathbb{R}^+ \times \mathbb{T} \times \mathbb{R}^2 \\ \lambda &\mapsto (s_\lambda, \theta_\lambda, x_\lambda) \end{aligned}$$

which associates with each $\lambda \in \Lambda$ *a* scale $s_\lambda \in \mathbb{R}^+$, *a* direction $\theta_\lambda \in \mathbb{T}$ *and a* location $x_\lambda \in \mathbb{R}^2$ *where* $\mathbb{T}$ *denotes the one dimensional torus with opposite sites identified.*

A family of α-molecules is defined using an anisotropic scaling matrix and a rotation matrix. Indeed, for $s > 0$, $\alpha \in [0,1]$ and $\theta \in [0, 2\pi)$ we let

$$A_s = \begin{pmatrix} s & 0 \\ 0 & s^\alpha \end{pmatrix}, \quad R_\theta = \begin{pmatrix} \cos(\theta) & -\sin(\theta) \\ \sin(\theta) & \cos(\theta) \end{pmatrix},$$

be the *scaling matrix* and *rotation matrix*, respectively. Then a system of α-molecules is defined as follows.

Definition 3.15. *Let* (Λ, Φ_Λ) *be a parametrization and* $R, M, N_1, N_2 > 0$. *A family* $(\psi_\lambda)_{\lambda\in\Lambda} \subset L^2(\mathbb{R}^2)$ *is called* a family of α-molecules with respect to the parametrization (Λ, Φ_Λ) of order (R, M, N_1, N_2) *if it can be written as*

$$\psi_\lambda = s_\lambda^{(1+\alpha)/2} f^{(\lambda)}(A_{s_\lambda} R_{\theta_\lambda}(\cdot - x_\lambda))$$

such that for all $|\beta| \leq R$,

$$|\partial^\beta f^{(\lambda)}(\xi)| \lesssim \frac{\min(1, s_\lambda^{-1} + |\xi_1| + s_\lambda^{-(1-\alpha)}|\xi_2|)^M}{(1+\|\xi\|^2)^{N_1}(1+\xi_2^2)^{N_2}}, \tag{3.18}$$

for all $\xi = (\xi_1, \xi_2) \in \mathbb{R}^2$, *where the constant in* (3.18) *is uniform over* $\lambda \in \Lambda$.

The shearlet systems that we have considered in Chapter 2 are a special instance of α-molecules, indeed, they can be classified as so-called *α-shearlet molecules.*

Definition 3.16 ([GKKS]). *Let* $\alpha \in [0,1], c > 0$ *and* $g > 1$ *be fixed parameters. Further, let* $(\eta_j)_{j\in\mathbb{N}_0}$ *and* $(L_j)_{j\in\mathbb{N}_0}$ *be sequences of positive real numbers with* $\eta_j \asymp g^{-(1-\alpha)}, \eta_{-1} = 0$ *and* $L_j \lesssim g^{(1-\alpha)j}$. *Let*

$$\begin{aligned}\Lambda^s := &\{(0,-1,0,k) \,:\, k \in \mathbb{Z}^2\} \\ &\cup \{(\varepsilon, j, l, k) \,:\, \varepsilon \in \{0,1\}, j \in \mathbb{N}_0, l \in \mathbb{Z} \text{ with } |l| \leq L_j, k \in \mathbb{Z}^2\}\end{aligned}$$

and

$$\Phi^s : \Lambda^s \longrightarrow P, \quad (\varepsilon, j, l, k) \mapsto \left(g^j, \varepsilon\pi/2 + \arctan(-l\eta_j), (S^\varepsilon_{l\eta_j})^{-1} A^\varepsilon_{g^{-j}} k\right)$$

where

$$A^0_{g^j} = \begin{pmatrix} g^j & 0 \\ 0 & g^{\alpha j}\end{pmatrix}, \quad A^1_{g^j} = \begin{pmatrix} g^{\alpha j} & 0 \\ 0 & g^j\end{pmatrix}$$

and $S^0_{l\eta_j} = S_{l\eta_j}, S^1_{l\eta_j} = S^T_{l\eta_j}$. *Then we call the pair* (Λ^s, Φ^s) *an* α-shearlet parametrization. *Furthermore, a system* $(\psi_\lambda)_{\lambda\in\Lambda^s}$ *defined by*

$$\psi_{(\varepsilon,j,l,k)} := g^{(1+\alpha)/2} f^\varepsilon_{j,l,k}(A^\varepsilon_{g^j} S^\varepsilon_{l\eta_j} \cdot - \tau k) \quad \textit{for some} \quad f^\varepsilon_{j,l,k} \in L^2(\mathbb{R}^2)$$

is a system of α-shearlet molecules of order (L, M, N_1, N_2) *if for every* $|\beta| \leq L$

$$|\partial^\beta f^{(\lambda)}(\xi)| \lesssim \frac{\min(1, g^{-j} + |\xi_{1+\varepsilon}| + g^{-(1-\alpha)j}|\xi_{2-\varepsilon}|)^M}{(1+\|\xi\|^2)^{N_1}(1+\xi^2_{2-\varepsilon})^{N_2}},$$

with an implicit constant independent of $(\varepsilon, j, l, k) \in \Lambda^s$.

It was shown in [GKKS] that an α-shearlet molecule as it is defined above is indeed a system of α-molecules. In particular, an α-shearlet system with compactly supported generators is a system of α-molecules. More precisely, the following result summarizes the properties that we require in the next section.

Proposition 3.17. *Let $h = (c, \alpha, L, M, N_1, N_2)$ where $c > 0$, $\alpha \in (0,1)$, $M, N_1, N_2 \in \mathbb{N}$ and $L \in \{0, \dots, M\}$. Further, let $\phi \in C_0^{N_1+N_2}(\mathbb{R}^2)$, $\psi_1 \in C_0^{N_1}$, $\psi_2 \in C_0^{N_2}$ and assume that ψ_1 has M vanishing moments. Define*

$$\psi(x_1, x_2) := \psi_1(x_1)\psi_(x_2) \quad \text{and} \quad \widetilde{\psi}(x_1, x_2) = \psi(x_2, x_1).$$

Then

$$\begin{aligned}\Sigma(h) = &\left\{\phi(\cdot - cm) \,:\, m \in \mathbb{Z}^2\right\} \\ &\cup \left\{g^{(1+\alpha)j/2}\psi\left((A^0_{g^j} S^0_{l\eta_j} \cdot - cm\right) \,:\, j \in \mathbb{N}_0, |l| \le \eta_j, m \in \mathbb{Z}^2\right\} \\ &\cup \left\{g^{(1+\alpha)j/2}\widetilde{\psi}\left((A^1_{g^j} S^1_{l\eta_j} \cdot - cm\right) \,:\, j \in \mathbb{N}_0, |l| \le \eta_j, m \in \mathbb{Z}^2\right\}\end{aligned} \tag{3.19}$$

is a system of α-molecules of order $(L, M-L, N_1, N_2)$ with respect to the shearlet parametrization (Λ^s, Φ^s), where $g = 2^{\alpha^{-1}/2}$, $\eta_j = g^{-(1-\alpha)j}$ and $L_j = \lceil g^{(1-\alpha)j} \rceil$. Moreover, we have

$$|\partial^\beta \psi(\xi)| \lesssim \frac{\min(1, |\xi_1|)^M}{(1 + \|\xi\|_2^2)^{N_1}(1 + |\xi_2|^2)^{N_2}} \quad \text{and} \quad |\partial^\beta \widetilde{\psi}(\xi)| \lesssim \frac{\min(1, |\xi_2|)^M}{(1 + \|\xi\|_2^2)^{N_1}(1 + |\xi_1|^2)^{N_2}}.$$

In particular, there exists an h such that $\Sigma(h)$ forms a frame for $L^2(\mathbb{R}^2)$.

Proof. The first statement of Proposition 3.17 follows from Proposition 2.11 in [GKKS]. The moreover-part is simply a concatenation of Lemma 3.10 in [GK14] and the fact that the 1D generators are assumed to be in $C_0^{N_1}$ and $C_0^{N_2}$, respectively. The in particular-part follows from Theorem 1.2. □

Remark 3.18. *In Proposition 3.17 it is stated that there exists a configuration h such that the corresponding system of compactly supported α-shearlets forms a frame for $L^2(\mathbb{R}^2)$. This result already follows from Theorem 1.2 as the cone-adapted shearlet system can be written in the form of* (3.19).

In [GV15, Gro13] the authors have shown that if a system $(\psi_\lambda)_\lambda$ of α-molecules forms a frame and is N-localized, i.e. for $N > 0$ it holds

$$|\langle \psi_\lambda, \psi_\mu \rangle| \lesssim \omega(\lambda, \mu)^{-N}, \tag{3.20}$$

where

$$\begin{aligned}\omega(\lambda, \lambda') = 1 &+ g^j |\langle (S^{\varepsilon'}_{l'\eta_{j'}})^{-1} A^{\varepsilon'}_{g^{-j'}} k' - (S^{\varepsilon}_{l\eta_j})^{-1} A^{\varepsilon}_{g^{-j}} k, \left(\mathrm{ca}(\varepsilon'\pi/2, l'\eta_{j'}), -\mathrm{sa}(\varepsilon\pi/2, l\eta_j)\right)\rangle|^2 + \\ &+ g^{2(1-\alpha)j} |\varepsilon'\pi/2 + \arctan(l'\eta_{j'}) - \varepsilon\pi/2 - \arctan(l\eta_j)|^2 + \\ &+ g^{2\alpha j} \|(S^{\varepsilon'}_{l'\eta_{j'}})^{-1} A^{\varepsilon'}_{g^{-j'}} k' - (S^{\varepsilon}_{l\eta_j})^{-1} A^{\varepsilon}_{g^{-j}} k\|^2,\end{aligned}$$

and $\mathrm{ca}(x, y) = \cos(x) + \arctan(y)$ and $\mathrm{sa}(x, y) = \sin(x) + \arctan(y)$, then there exists an N' such that

$$|\langle \widetilde{\psi}_\lambda, \psi_\mu \rangle| \lesssim \omega(\lambda, \mu)^{-N'}. \tag{3.21}$$

In other words, if the Gramian is localized then the cross-Gramian between the system and its canonical dual is localized as well.

Remark 3.19. *The localization the Gramian is one of the key tools in the recent developments of α-molecules or its predecessor parabolic molecules. Using the localization of the Gramian and the cross Gramian between different systems the authors of [GK14] were able to show the sparsity equivalence of two different systems sets of parabolic molecules at hand which in turn implies the same sparse approximation rate. That again is one of the characteristics of parabolic molecules themselves such as curvelets and shearlets.*

Balancing property for α-shearlets

We now return to the balancing property, i.e. we first ought to bound

$$\|P_{\Delta'}^{\perp}\Psi(\Psi^* + \widetilde{\Psi}^*)P_{\Delta}\|_{2\to 2}$$

for some appropriately chosen $\Delta' \supset \Delta$. Hence, for such Δ' it would be sufficient to bound

$$\sum_{\lambda'\notin\Delta'}\sum_{\lambda\in\Delta}\frac{1}{\omega(\lambda',\lambda)^N}, \tag{3.22}$$

provided that the α-molecule used for the reconstruction forms a frame and is N-localized. Clearly, one can make Δ' sufficiently large, i.e. the indices belonging to δ and those not belonging to Δ' sufficiently wide separated, so that (3.22) becomes sufficiently small. However, for the balancing property we also have to bound

$$\|P_{\Delta'}\Psi\widetilde{\Psi}^* P_{\Delta}^{\perp}\Psi A^* P_{[M]}^{\perp}\|_{2\to 2}$$

which means if Δ' is too large, then its intersection with Δ^c will be large which makes it unlikely that this second term is small. So we must construct Δ' so that

(B1) $\sum_{\lambda'\notin\Delta'}\sum_{\lambda\in\Delta}\frac{1}{\omega(\lambda',\lambda)^N}$ is small: This directly bounds (3.16).

(B2) $\Delta'\cap\Delta^c$ is small enough so that $\|P_{\Delta'}\Psi\widetilde{\Psi}^* P_{\Delta}^{\perp}\Psi A^* P_{[M]}^{\perp}\|_{2\to 2}$ can partly be controlled by intrinsic localization arguments from (3.21) and the rest -that is close to Δ - by standard incoherence arguments.

We will now construct such Δ'. To this end, let Δ denote the index set of all α-shearlets up to some fixed scale J whose support intersect a fixed region so that the number of translates at a scale $j \le J$ is of the order g^{2j}. By assumption there exist positive number $K_{1,\varepsilon}^j \asymp g^j, K_{2,\varepsilon}^j \asymp g^{\alpha j}$ such that these give upper bounds for the number of translations contained in our parameter set, i.e.

$$\Delta \subseteq \left\{(\varepsilon,j,l,k)\in\mathbb{N}\times\mathbb{Z}\times\mathbb{Z}^2 \,:\, \varepsilon\in\{0,1\}, j\le J, |l|\le L_j, |k_1|\le K_{1,\varepsilon}^j, |k_2|\le K_{2,\varepsilon}^j\right\}.$$

As it is typical for α-molecules we identified λ with $(\varepsilon,j,l,(k_1,k_2))$. In order to determine $\Delta'\supset\Delta$ such that

$$\sum_{\lambda'\notin\Lambda'}\sum_{\lambda\in\Lambda}\frac{1}{\omega(\lambda,\lambda')^N}$$

is small we choose to find $T > 0$ such that

$$\sum_{\varepsilon'\in\{0,1\}} \sum_{j'>J+T} \sum_{|l'|\le L_{j'}} \sum_{\substack{|k_1'|\le K_{1,\varepsilon'}^{j'} \\ |k_2'|\le K_{2,\varepsilon'}^{j'}}} \sum_{\varepsilon\in\{0,1\}} \sum_{j\le J} \sum_{|l|\le L_j} \sum_{\substack{|k_1|\le K_{1,\varepsilon}^{j} \\ |k_2|\le K_{2,\varepsilon}^{j}}} \omega\left((\varepsilon',j',l',k'),(\varepsilon,j,l,k)\right)^{-N}$$

is small. Then we could set

$$\Delta' := \left\{(\varepsilon,j,l,k) \,:\, \varepsilon\in\{0,1\}, j\le J+T, |l|\le L_j, |k_1|\le K_{1,\varepsilon}^j, |k_2|\le K_{2,\varepsilon}^j\right\}.$$

The separation parameter T should ideally be independent of J yielding a linear behaviour of the intrinsic localization of the frame $(\psi_\lambda)_\lambda$ which in turn implies a linear intrinsic localization rate between the primal frame and its canoncial dual. The linearity is important so that we can really use incoherence arguments for the remaining terms in (3.17).

The next theorem secures that (B1) can be accomplished with an arbitrary small bound.

Theorem 3.20. *Let $\alpha \in (0,1)$ and $(\psi_\lambda)_\lambda$ be a compactly supported α-shearlet frame that satisfies*

$$|\langle\psi_\lambda,\psi_\mu\rangle| \lesssim \omega(\lambda,\mu)^{-N}$$

with $N > (1+\alpha)/(1-\alpha)$. Then for any $\delta > 0$ there exists a $T > 0$ that further depends on the regularity of the α-shearlet system, such that

$$\sum_{\substack{(\varepsilon,j',l',(k_1',k_2'))\notin\Delta' \\ (\varepsilon,j,l,(k_1,k_2))\in\Delta}} \omega((\varepsilon,j',l',(k_1',k_2')),(\varepsilon,j,l,(k_1,k_2)))^{-N} < \delta,$$

where

$$\Delta' := \left\{(\varepsilon,j,l,k) \,:\, \varepsilon\in\{0,1\}, j\le J+T, |l|\le L_j, |k_1|\le K_{1,\varepsilon}^j, |k_2|\le K_{2,\varepsilon}^j\right\} \tag{3.23}$$

Proof. Clearly, we have

$$\begin{aligned}&\sum_{\substack{(\varepsilon,j',l',(k_1',k_2'))\notin\Delta' \\ (\varepsilon,j,l,(k_1,k_2))\in\Delta}} \frac{1}{\omega\left((\varepsilon',j',l',k'),(\varepsilon,j,l,k)\right)^N} \\ &\lesssim \sum_{\substack{(\varepsilon',j',l',(k_1',k_2'))\notin\Delta' \\ (\varepsilon,j,l,(k_1,k_2))\in\Delta}} \Big(g^{j'-j}\big(1+g^{2(1-\alpha)j}|\varepsilon'\pi/2+\arctan(l'\eta_{j'})-\varepsilon\pi/2-\arctan(l\eta_j)|^2+ \\ &\quad + g^{2\alpha j}\|(S^{\varepsilon'}_{l'\eta_{j'}})^{-1}A_j^{\varepsilon'}k' - (S^{\varepsilon}_{l\eta_j})^{-1}A_j^{\varepsilon}k\|^2\big)\Big)^{-N}.\end{aligned}$$

We will now proceed the proof by assuming

Case I: $\varepsilon' = \varepsilon$ and ${}'\eta_{j'} \neq l\eta_j$.

Let

$$A_{j',j} = g^{2(1-\alpha)j}\left(\frac{1+L_{j'}\eta_{j'}}{l'\eta_{j'}-l\eta_j}\right)^2, B_{j',l',k',j,l} = k_1'g^{-j'} - l'\eta_{j'}k_2' - l\eta_j k_2, C_{j',k'} = g^{-\alpha j'}k_2'.$$

Then by direct computations we obtain

$$\begin{aligned}
&\sum_{\substack{(\varepsilon,j',l',(k_1',k_2'))\notin\Delta' \\ (\varepsilon,j,l,(k_1,k_2))\in\Delta \\ '\eta_{j'}\neq l\eta_j}} \frac{1}{\omega\left((\varepsilon',j',l',k'),(\varepsilon,j,l,k)\right)^N} \\
&\lesssim \sum_{\substack{(\varepsilon,j',l',(k_1',k_2'))\notin\Delta' \\ (\varepsilon,j,l,(k_1,k_2))\in\Delta \\ '\eta_{j'}\neq l\eta_j}} \left(g^{j'-j}\left(1+A_{j',j}+g^{2\alpha j}\left(\left(k_1'g^{-j'}-l'\eta_{j'}k_2'-l\eta_j k_2-g^{-j}k_1\right)^2+\right.\right.\right. \\
&\qquad \left.\left.\left.+\left(g^{-\alpha j'}k_2'-g^{-\alpha j}k_2\right)^2\right)\right)\right)^{-N} \\
&\lesssim \sum_{\substack{(\varepsilon,j',l',(k_1',k_2'))\notin\Delta' \\ (\varepsilon,j,l,(k_1,k_2))\in\Delta \\ '\eta_{j'}\neq l\eta_j}} \left(\frac{g^{j-j'}/A_{j',j}}{\left(1+g^{2\alpha j}A_{j',j}^{-1}\left(\left(B_{j',l',k',j,l}-g^{-j}k_1\right)^2+\left(C_{j',k'}-g^{-\alpha j}k_2\right)^2\right)\right)}\right)^N \\
&\lesssim \sum_{\substack{(\varepsilon,j',l',(k_1',k_2'))\notin\Delta' \\ j\leq J,|l|\leq L_j,'\eta_{j'}\neq l\eta_j}} \int_{K_{1,\varepsilon}^j}^{K_{1,\varepsilon}^j}\int_{-K_{2,\varepsilon}^j}^{K_{2,\varepsilon}^j} \frac{(g^{(j-j')}/A_{j',j})^N}{\left(1+g^{2\alpha j}\frac{\left(B_{j',l',k',j,l}-g^{-j}k_1\right)^2+\left(C_{j',k'}-g^{-\alpha j}k_2\right)^2}{A_{j',j}}\right)^N}\,dk_2dk_1 \\
&\lesssim \sum_{\substack{(\varepsilon,j',l',(k_1',k_2'))\notin\Delta' \\ j\leq J,|l|\leq L_j,'\eta_{j'}\neq l\eta_j}} \int_{-g^{-j}K_{1,\varepsilon}^j-B_{j',l',k',j,l}}^{g^{-j}K_{1,\varepsilon}^j-B_{j',l',k',j,l}}\int_{-g^{-\alpha j}K_{2,\varepsilon}^j-C_{j',k'}}^{g^{-\alpha j}K_{2,\varepsilon}^j-C_{j',k'}} \frac{g^{(\alpha+1)j}g^{N(j-j')}A_{j',j}^{-N}}{\left(1+g^{2\alpha j}A_{j',j}^{-1}\left(k_1^2+k_2^2\right)\right)^N}\,dk_2dk_1 \\
&\lesssim \sum_{\substack{(\varepsilon,j',l',(k_1',k_2'))\notin\Delta' \\ j\leq J,|l|\leq L_j,'\eta_{j'}\neq l\eta_j}} g^{N(j-j')}A_{j',j}^{-N}g^{(\alpha+1)j}\int_0^\infty\int_0^\infty \frac{1}{\left(1+g^{2\alpha j}A_{j',j}^{-1}\left(k_1^2+k_2^2\right)\right)^N}\,dk_2dk_1 \\
&\lesssim \sum_{j'>J+T}\sum_{|l'|\leq L_{j'}}\sum_{|k_1'|\leq K_{1,\varepsilon'}^{j'}}\sum_{|k_2'|\leq K_{2,\varepsilon'}^{j'}}\sum_{j\leq J}\sum_{|l|\leq L_j} g^{N(j-j')}g^{(1-\alpha)j}A_{j',j}^{-N+1} \\
&\lesssim \sum_{j'>J+t}\sum_{j\leq J} L_{j'}K_{1,\varepsilon'}^{j'}K_{2,\varepsilon'}^{j'}L_j g^{N(j-j')}g^{(1-\alpha)j}A_{j',j}^{-N+1},
\end{aligned} \tag{3.24}$$

where we have used

$$|\arctan(l'\eta_{j'})-\arctan(l\eta_j)| \geq |l'\eta_{j'}-l\eta_j|/(1+L_j'\eta_j')$$

in the first estimate. By assumption $L_j \lesssim g^{j(1-\alpha)}, K_{1,\varepsilon}^j \asymp g^j$ and $K_{2,\varepsilon}^j \asymp g^{\alpha j}$. Furthermore, note that

$$A_{j',j}^{-1} \leq g^{2(\alpha-1)j}.$$

Therefore (3.24) can further be bounded to obtain

$$\begin{aligned}\sum_{\substack{(\varepsilon,j',l',(k_1',k_2'))\notin\Delta'\\(\varepsilon,j,l,(k_1,k_2))\in\Delta}} \frac{1}{\omega\left((\varepsilon',j',l',k'),(\varepsilon,j,l,k)\right)^N} &\lesssim \sum_{j'>J+t}\sum_{j\leq J} g^{(2(1-\alpha)+2(\alpha-1)(N-1)+N)j} g^{(2-N)j'}\\ &= \sum_{j'>J+t}\sum_{j\leq J} g^{(2(\alpha-1)(N-2)+N)j} g^{(2-N)j'}\\ &\lesssim \sum_{j'>t} g^{(2(\alpha-1)(N-2)-2)J} g^{(2-N)j'}\\ &= \sum_{j'>t} g^{(2(\alpha-1)(N-2)-2)J} g^{-(N-2)j'}.\end{aligned}$$

Using the same arguments as above one can verify the claim for

Case II: $\varepsilon' \neq \varepsilon$ and $l'\eta_{j'} \neq \eta_j$.

We next turn to

Case III: $\varepsilon' \neq \varepsilon$ and $l'\eta_{j'} = \eta_j$.

In this case the computations are again the same as in **Case I**, indeed one can choose $A_{j',j}$ to be $g^{2(1-\alpha)j}$. Then the computations go through.

The claim follows from the following estimate for this case

$$\begin{aligned}&\sum_{\substack{(\varepsilon,j',l',(k_1',k_2'))\notin\Delta'\\(\varepsilon,j,l,(k_1,k_2))\in\Delta}} \omega((\varepsilon,j',l',(k_1',k_2')),(\varepsilon,j,l,(k_1,k_2)))^{-N}\\ &\lesssim \sum_{\substack{(\varepsilon,j',l',(k_1',k_2'))\notin\Delta'\\(\varepsilon,j,l,(k_1,k_2))\in\Delta}} \frac{1}{\left(g^{j'-j}(1+g^{2(1-\alpha)j}\right)^N}\\ &\lesssim \sum_{j'>J+t}\sum_{j\leq J} g^{(1+\alpha)j'} g^{(1+\alpha)j} \frac{1}{\left(g^{j'-j}(1+g^{2(1-\alpha)j}\right)^N}\\ &= \sum_{j'>J+t}\sum_{j\leq J} g^{(1+\alpha)j'} g^{(1+\alpha)j} g^{(j-j')N} g^{2(\alpha-1)Nj}\\ &= \sum_{j'>J+t}\sum_{j\leq J} g^{((1+\alpha)-N)j'} g^{((1+\alpha)+N-2(1-\alpha)N)j}\\ &\lesssim \sum_{j'>t} g^{((1+\alpha)-N)j'} g^{((1+\alpha)+N-2(1-\alpha)N-N+(1+\alpha))J}\\ &= \sum_{j'>t} g^{((1+\alpha)-N)j'} g^{(2(1+\alpha)-2(1-\alpha)N)J}.\end{aligned}$$

As long as α is not equal to 1 this sum becomes small for increasing N. The final case that needs to be addressed is

Case IV: $\varepsilon' = \varepsilon$ and $l'\eta_{j'} = \eta_j$.

First, note that

$$\widehat{\psi}((A_j S_{l\eta_j})^{-T}\xi) = \widehat{\psi}\left(\left(\begin{pmatrix} g^{-j} & -l\eta_j g^{-\alpha j}\\ 0 & g^{-\alpha j}\end{pmatrix}\right)^T \xi\right)$$

$$\begin{aligned}
&\lesssim \frac{\min\{1,|g^{-j}\xi_1|\}^M}{\left(1+\|(A_jS_{l\eta_j})^{-T}\xi\|_2^2\right)^{N_1}\left(1+|l\eta_j g^{-\alpha j}\xi_1+g^{-\alpha j}\xi_2|^2\right)^{N_2}}\\
&\lesssim \frac{\min\{1,|g^{-j}\xi_1|\}^M}{\left(1+\|A_{-j}\xi\|_2^2\right)^{N_1}\left(1+|l\eta_j g^{-\alpha j}\xi_1+g^{-\alpha j}\xi_2|^2\right)^{N_2}}.
\end{aligned}$$

Therefore, we have

$$\begin{aligned}
&\sum_{\substack{|k_1'|\le K_{1,\varepsilon'}^{j'}\\|k_2'|\le K_{2,\varepsilon'}^{j'}}}\sum_{|l'|\le\eta_{j'}}\sum_{\substack{|k_1|\le K_{1,\varepsilon}^{j}\\|k_2|\le K_{2,\varepsilon}^{j}}}|\langle\psi_{\lambda'},\psi_\lambda\rangle|\\
&\lesssim \sum_{\substack{|k_1'|\le K_{1,\varepsilon'}^{j'}\\|k_2'|\le K_{2,\varepsilon'}^{j'}}}\sum_{|l'|\le\eta_{j'}}\sum_{\substack{|k_1|\le K_{1,\varepsilon}^{j}\\|k_2|\le K_{2,\varepsilon}^{j}}}\int_{\mathbb{R}^2}\left|g^{-(1+\alpha)(j'+j)/2}\widehat{\psi}\left((A_{j'}S_{l'\eta_{j'}})^{-T}\xi\right)\widehat{\psi}\left((A_jS_{l\eta_j})^{-T}\xi\right)\right|d\xi\\
&\lesssim \sum_{\substack{|k_1'|\le K_{1,\varepsilon'}^{j'}\\|k_2'|\le K_{2,\varepsilon'}^{j'}}}\sum_{|l'|\le\eta_{j'}}\sum_{\substack{|k_1|\le K_{1,\varepsilon}^{j}\\|k_2|\le K_{2,\varepsilon}^{j}}}\int_{\mathbb{R}^2}\frac{g^{-(1+\alpha)(j'+j)/2}\min\{1,|g^{-j'}\xi_1|\}^M}{\left(1+\|A_{-j'}\xi\|_2^2\right)^{N_1}\left(1+|l\eta_{j'}g^{-\alpha j'}\xi_1+g^{-\alpha j'}\xi_2|^2\right)^{N_2}}\cdot\\
&\qquad\qquad\cdot\frac{\min\{1,|g^{-j}\xi_1|\}^M}{\left(1+\|A_{-j}\xi\|_2^2\right)^{N_1}\left(1+|l\eta_j g^{-\alpha j}\xi_1+g^{-\alpha j}\xi_2|^2\right)^{N_2}}\,d\xi\\
&\lesssim \sum_{\substack{|k_1'|\le K_{1,\varepsilon'}^{j'}\\|k_2'|\le K_{2,\varepsilon'}^{j'}}}\sum_{\substack{|k_1|\le K_{1,\varepsilon}^{j}\\|k_2|\le K_{2,\varepsilon}^{j}}}g^{-(1+\alpha)(j'+j)/2}\int_{\mathbb{R}^2}\frac{\min\{1,|g^{-j'}\xi_1|\}^{M-1}\min\{1,|g^{-j}\xi_1|\}^M}{\left(1+\|A_{-j'}\xi\|_2^2\right)^{N_1}\left(1+\|A_{-j}\xi\|_2^2\right)^{N_1}}\,d\xi\\
&=\int_{\mathbb{R}^2}\frac{g^{(1+\alpha)(j'+j)/2}g^{-2(M-1)(j'+j)}|\xi_1|^{2(M-1)}}{\left(1+|g^{-j'}\xi_1|^2+|g^{-\alpha j'}\xi_2|^2\right)^{N_1}\left(1+|g^{-j}\xi_1|^2+|g^{-\alpha j}\xi_2|^2\right)^{N_1}}\,d\xi\\
&=\int_{\mathbb{R}^2}\frac{g^{(1+\alpha)(j'+j)/2}g^{-2(M-1)(j'+j)}}{\left(|\xi_1|^{-2}+|g^{-j}|^2+|g^{-\alpha j}\xi_2/\xi_1|^2\right)^{M-1}}\cdot\\
&\qquad\qquad\cdot\frac{1}{\left(1+|g^{-j}\xi_1|^2+|g^{-\alpha j}\xi_2|^2\right)^{N_1-M_1+1}\left(1+|g^{-j'}\xi_1|^2+|g^{-\alpha j'}\xi_2|^2\right)^{N_1}}\,d\xi\\
&\lesssim \int_{\mathbb{R}^2}\frac{g^{(1+\alpha)(j'+j)/2-2(M-1)j'}}{\left(1+|g^{-j}\xi_1|^2+|g^{-\alpha j}\xi_2|^2\right)^{N_1-M_1+1}\left(1+|g^{-j'}\xi_1|^2+|g^{-\alpha j'}\xi_2|^2\right)^{N_1}}\,d\xi\\
&\lesssim \int_{\mathbb{R}^2}\frac{g^{(1+\alpha)(j'+j)/2-2(M-1)j'+(1+\alpha)j}}{\left(1+|\xi_1|^2+|\xi_2|^2\right)^{N_1-M_1+1}\left(1+|g^{j-j'}\xi_1|^2+|g^{\alpha(j-j')}\xi_2|^2\right)^{N_1}}\,d\xi.
\end{aligned}$$

Since the integral is finite with a bound independent of j and j' we can conclude

$$\begin{aligned}
&\sum_{\substack{(\varepsilon,j',l',(k_1',k_2'))\notin\Delta'\\(\varepsilon,j,l,(k_1,k_2))\in\Delta}}\omega((\varepsilon,j',l',(k_1',k_2')),(\varepsilon,j,l,(k_1,k_2)))^{-N}\\
&\qquad\lesssim\sum_{j'>J+t}\sum_{j\le J}g^{((1+\alpha)/2-2(M-1))j'+3(1+\alpha)j/2}\lesssim\sum_{j'>J+t}g^{2((1+\alpha)-(M-1))j'}.
\end{aligned}$$

Hence, for any $\delta > 0$ there exists $T > 0$ and $N_1, N_2, M > 0$ such that

$$\sum_{\substack{(\varepsilon,j',l',(k_1',k_2'))\notin\Delta' \\ (\varepsilon,j,l,(k_1,k_2))\in\Delta}} \omega((\varepsilon, j', l', (k_1', k_2')), (\varepsilon, j, l, (k_1, k_2)))^{-N} < \delta.$$

□

Using Theorem 3.20 we can obtain a small bound for (3.11).

Corollary 3.21. *For any $\delta > 0$ there exists Δ' of the form* (3.23) *such that*

$$\|P_{\Delta'}^{\perp}\Psi(\Psi^* + \widetilde{\Psi}^*)P_\Delta\|_{2\to2} \leq \delta.$$

Proof. Clearly,

$$\|P_{\Delta'}^{\perp}\Psi(\Psi^* + \widetilde{\Psi}^*)P_\Delta\|_{2\to2} \leq \sum_{\lambda'\in\Delta'}\sum_{\lambda\in\Delta} |\langle\psi_{\lambda'}, \psi_\lambda\rangle|^2 + \sum_{\lambda'\in\Delta'}\sum_{\lambda\in\Delta} |\langle\psi_{\lambda'}, \widetilde{\psi}_\lambda\rangle|^2.$$

For $N'' := \min\{N, N'\}/2$, where N' is as in (3.21) we conclude

$$\|P_{\Delta'}^{\perp}\Psi(\Psi^* + \widetilde{\Psi}^*)P_\Delta\|_{2\to2} \lesssim \sum_{\lambda'\in\Delta'}\sum_{\lambda\in\Delta} \omega(\lambda', \lambda)^{-N''}.$$

By Theorem 3.20 we find for fixed $\delta > 0$ some Δ' of the form (3.23) such that

$$\|P_{\Delta'}^{\perp}\Psi(\Psi^* + \widetilde{\Psi}^*)P_\Delta\|_{2\to2} \leq \delta.$$

□

Corollary 3.21 shows that the intrinsic localization of α-shearlets is sufficient for the balancing property to hold. A similar conclusion can be drawn for other α-molecules that satisfy a similar intrinsic localization property.

As for (B2) we must comment on the notation first. The number M refers to the number measurements that must be drawn. Since we are now in the 2D Fourier domain, we again consider the same setup as in Chapter 2, in particular Section 2.3. So M specifies the width of a grid where we draw the samples from. Then the following holds.

Theorem 3.22. *Retaining the notations from Theorem 3.20 we have: For any $\delta > 0$ there exists an $M \lesssim g^{J(1+\rho)}$ such that*

$$\|P_{\Delta'}\Psi\widetilde{\Psi}^* P_\Delta^{\perp}\Psi A^* P_{[M]}^{\perp}\|_{2\to2} \leq \delta$$

where $\rho \geq 2/(2\min N_1, N_2 - 1)$.

Proof. For $T > 0$ we define

$$\Delta_T'' := \{(\varepsilon, j, l, k) \in \Delta^c \cap \Delta' \,:\, j \leq J + T\} \quad \text{and} \quad \Delta''' = (\Delta_T'')^c \cap \Delta^c.$$

Then

$$\|P_{\Delta'}\Psi\widetilde{\Psi}^* P_\Delta^{\perp}\Psi A^* P_{[M]}^{\perp}\|_{2\to2}$$

$$\leq \|P_{\Delta'}\Psi\widetilde{\Psi}^* P_{\Delta^c\cap\Delta''_T}\Psi A^* P_{[M]}^\perp\|_{2\to 2} + \|P_{\Delta'}\Psi\widetilde{\Psi}^* P_{\Delta^c\cap\Delta'''}\Psi A^* P_{[M]}^\perp\|_{2\to 2}.$$

By Theorem 3.20 for every $\sigma > 0$ we can choose T sufficiently large, but independent of J such that

$$\sum_{\substack{(\varepsilon,j',l',(k_1',k_2'))\in\Delta''' \\ (\varepsilon,j,l,(k_1,k_2))\in\Delta'}} \omega((\varepsilon,j',l',(k_1',k_2')),(\varepsilon,j,l,(k_1,k_2)))^{-N'} \leq \sigma$$

with N' from (3.21). In particular, for any $\delta > 0$ we can obtain

$$\|P_{\Delta'}\Psi\widetilde{\Psi}^* P_{\Delta}^\perp\Psi A^* P_{[M]}^\perp\|_{2\to 2} \leq \delta/2 + \|P_{\Delta'}\Psi\widetilde{\Psi}^* P_{\Delta^c\cap\Delta'''}\Psi A^* P_{[M]}^\perp\|_{2\to 2}.$$

Now since

$$\begin{aligned}\|P_{\Delta'}\Psi\widetilde{\Psi}^* P_{\Delta^c\cap\Delta'''}\Psi A^* P_{[M]}^\perp\|_{2\to 2} &\leq \|P_{\Delta'}\Psi\widetilde{\Psi}^*\|_{2\to 2}\|P_{\Delta^c\cap\Delta'''}\Psi A^* P_{[M]}^\perp\|_{2\to 2} \\ &\leq \|P_{\Delta'}\Psi\widetilde{\Psi}^*\|_{2\to 2}\sum_{\substack{\lambda\in\Delta' \\ \ell\in(I_M)^c}} |\widehat{\psi_\lambda}(\ell)|^2\end{aligned}$$

the rest of the proof follows the same argumentation as in Proposition (2.17) which following from the effective frequency behaviour of compactly supported shearlets with sufficient regularity. The degree of anisotropy which is regulated by α does not effect the argumentation but only the estimates. However, following the estimates of the proof of Proposition (2.17) line by line gives the result. □

Remark 3.23. *In the proof of Theorem 3.22 we mentioned that the same argumentation as in the proof of Proposition* (2.17) *can be applied, in particular, we have assumed that* Δ *contains all shearlets up to a certain scale. This again corresponds to the worst possible sparsity case if* Δ *was that large. However, if this is not the case and* Δ *was much smaller, then the estimates for the incoherence can be significantly improved as we only need to employ the frequency decay of those elements that are indexed by* Δ*. Note that the arguments for the intrinsic localization would not change.*

Chapter 4

Non-convex compressed sensing

As we have seen in the previous chapter one of the promising methods to retrieve sparse signals from highly undersampled data is to solve an ℓ^1-minimization problem. However, this ℓ^1-minimization program has been considered as a substitution of the ℓ^0-minimization problem. In this chaper we want to study the scenario of ℓ^p-minimization with $p \in (0,1)$. The results presented in this chapter are based on [Ma15b] and we follow the presentation of these results closely as in [Ma15b].

ℓ^p-minimization

Using the ℓ^p-quasi norm as a sparsity prior in (3.3) is a prominent approach that has been widely studied in the literature [Cha07, SCY08, FL09, ACP12, LLSZ13] in order to strengthen the emphasize of sparse solutions. In fact, the ℓ^p-quasi norms are closer to the ℓ^0-function $\|\cdot\|_0$ than $\|\cdot\|_1$ is, see Figure 4.1.

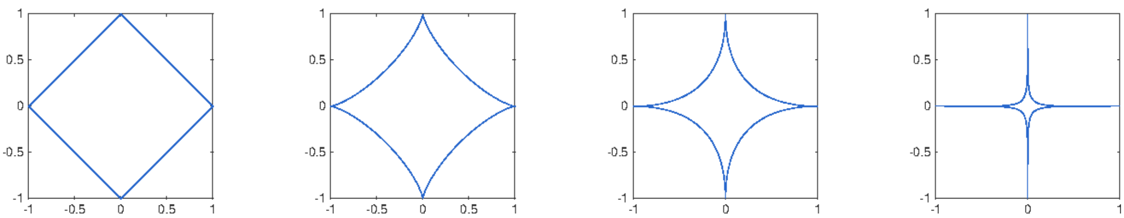

Figure 4.1: From ℓ^1 to ℓ^0: Unit balls with respect to the ℓ^p-quasi norm for decreasing p.

Therefore in this chapter we consider the ℓ^p-minimization in analysis formulation, that is

$$\min_x \|\Psi x\|_p^p \quad \text{subject to} \quad \|y - Ax\|_2 \le \varepsilon \tag{4.1}$$

for arbitrary redundant transforms that arise from a general frame. More precisely, we will focus on the stability of the minimization problem (4.1) for arbitrary redundant frames and sensing matrices that fulfill a *restricted isometry property* that is adapted to the analysis minimization problem. The obtained result can be seen as a generalization of the work by Candès et al. in [CENR11]. We will make the relation more precise in the following.

For the convenience of the reader we continue with an overview of known stability results for the *synthesis* formulation as well as the *analysis formulation*. This will then make the contribution more clear.

Overview of related work

The following minimization problems are well studied in the literature and the stability results that are obtained for these problems are the ones that we also want to prove for (4.1). We will now only discuss the case where the model covers noisy measurements, i.e. in the equality constrained minimization problem (3.3) the constrained $y = Ax$ is replaced by a relaxation $\|y - Ax\|_2 \leq \varepsilon$.

Synthesis approach for ℓ^1

The following minimization problem is generally called the *synthesis formulation* for the ℓ^1-minimization problem

$$\min_x \|x\|_1 \quad \text{subject to} \quad \|y - Ax\|_2 \leq \varepsilon. \tag{ℓ^1-$\mathrm{P}_\mathrm{S}^\varepsilon$}$$

It also known as *basis pursuit* and has been studied a lot since the early days of compressed sensing. Furthermore, stability results are known under the presence of the so-called *restricted isometry property* ([CRT05, Fou10, FR13]).

Definition 4.1. *An $m \times n$ matrix A satisfies the* restricted isometry property *(RIP) of order s with* RIP constant δ_s, *if there exists $\delta_s > 0$ such that*

$$(1 - \delta_s)\|x\|_2^2 \leq \|Ax\|_2^2 \leq (1 + \delta_s)\|x\|_2^2,$$

for all s-sparse vectors $x \in \mathbb{R}^n$.

A stability estimate is guaranteed by the following theorem.

Theorem 4.2 ([CRT05])**.** *For any vector $x \in \mathbb{R}^n$ and noisy measurement vector $y = Ax + e$ with $A \in \mathbb{R}^{m \times n}$ and $\|e\| \leq \varepsilon$ we have if A satisfies the RIP with $\delta_{3s} + 3\delta 4s < 2$, there exists constants C_1 and C_2 such that the solution x^* of (ℓ^1-$\mathrm{P}_\mathrm{S}^\varepsilon$) satisfies*

$$\|x - x^*\|_2 \leq C_1 \varepsilon + C_2 \frac{\|x - x_s\|_1}{\sqrt{s}}$$

where x_s is the vector that consists only of the s largest entries of x in magnitude.

Synthesis approach for ℓ^p

As we already mentioned in the introduction of this chapter, the ℓ^p-quasi norm approximates the ℓ^0-map better than the ℓ^1 norm. Hence, the ℓ^1-minimization problem above has been generalized in the works [SCY08, Cha07, FL09] and the resulting ℓ^p-minimization problem reads as follows:

$$\min_x \|x\|_p^p \quad \text{subject to} \quad \|y - Ax\|_2 \leq \varepsilon \tag{ℓ^p-$\mathrm{P}_\mathrm{S}^\varepsilon$}$$

Similar as for the standard ℓ^1-minimization problem a stability result is of major interest. The following theorem delivers such a result

Theorem 4.3 ([SCY08]). *For arbitrary signals $x \in \mathbb{R}^n$ and noisy measurements $y = Ax + e$ with $A \in \mathbb{R}^{m\times n}$ and $\|e\| \leq \varepsilon$ we can guarantee stability provided that for $s \in \mathbb{N}$ there exists $k > 1$ such that $ks \in \mathbb{N}$ and*

$$\delta_{ks} = k^{2/p-1}\delta_{(k+1)s} < k^{2/p-1} - 1. \tag{4.2}$$

More precisely, if (4.2) *holds, then there exists constants $C_1(s,k,p) > 0$ and $C_2(s,k,p) > 0$ such that*

$$\|x - x^*\|_2^p \leq C_1(s,k,p)\varepsilon^p + C_2(s,k,p)\frac{\|x - x_s\|_p^p}{s^{1-p/2}}$$

holds, where x^* denotes the solution of (ℓ^p-$\mathrm{P}_\mathrm{S}^\varepsilon$).

The constants $C_1(s,k,p), C_2(s,k,p)$ in Theorem 4.3 are given explicitly in [SCY08]. Moreover, these constants agree with the constants C_1 and C_2 in Theorem 4.2 if $p = 1$.

Analysis approach for ℓ^1

For the case that the signal is sparse after some transformation Ψ it is more convenient to consider the following *analysis formulation*:

$$\min_x \|\Psi x\|_1 \quad \text{subject to} \quad \|y - Ax\|_2 \leq \varepsilon, \tag{ℓ^1-$\mathrm{P}_\Psi^\varepsilon$}$$

where Ψ is the sparsifying transform, e.g. the analysis operator associated to a frame that is used as the reconstruction system. A stability result for the case that Ψ is the analysis operator associated to a tight frame can be proven based on the so-called *Ψ-RIP*, see Definition 4.4 below.

Definition 4.4 ([CENR11, KNW15]). *Let $\Psi \in \mathbb{R}^{N\times n}$ be a matrix whose rows span $\mathbb{R}^n$ and $A \in \mathbb{R}^{m\times n}$. If there exists $\delta_s > 0$ such that*

$$(1 - \delta_s)\|\Psi^* x\|_2^2 \leq \|A\Psi^* x\|_2^2 \leq (1 + \delta_s)\|\Psi^* x\|_2^2, \tag{4.3}$$

for all s-sparse vectors x, then we say A satisfies the Ψ-RIP *of order s with* Ψ-RIP constant *δ_s.*

The Ψ-RIP can therefore be interpreted as an isometry property of the measurement matrix A for all vectors that are sparse in the row space of Ψ. The stability result for this case reads as follows.

Theorem 4.5 ([CENR11, KNW15]). *If $\Psi \in \mathbb{R}^{N\times n}$ is a Parseval frame and $A \in \mathbb{R}^{m\times n}$ satisfies the Ψ-RIP with $\delta_{2s} < 0.08$. Then the solution x^* of the minimization problem* (ℓ^1-$\mathrm{P}_\Psi^\varepsilon$) *satisfies the stability estimate*

$$\|x^* - x\|_2 \leq C_1\varepsilon + C_2\frac{\|\Psi x - (\Psi x)_s\|_1}{\sqrt{s}} \tag{4.4}$$

for some constants C_1 and C_2.

A generalization of Theorem 4.5 to the ℓ^p-quasi norm has been studied by Aldroubi et al. in [ACP12] if the frame is a Parseval frame. For general frames a stability result can be obtained based on the so-called Ψ-*null space property* as it was introduced in [ACP12]. We will prove stability of the minimization problem for general frames that are not assumed to be a Parseval frame and thus close this gap. Furthermore, if the frame is not assumed to be Parseval, then, as we will outline, the restricted isometry property does not completely fit to the minimization problem (4.1).

Our stability result will also be based on the Ψ-RIP. Therefore we first discuss this property in more detail first.

4.1 Restricted isometry property

As we have shown in the overview the restricted isometry property can be used to secure the stability of solutions obtained by ℓ^1-minimization, let it be the synthesis or the analysis problem. Therefore, one is very much interested in RIP guarantees. In [KNW15] Krahmer et al. presented a result for matrices to satisfy the Ψ-RIP provided the frame Ψ is a Parseval frame. The proof of their result can be generalized to arbitrary frames in a straightforward manner. Indeed, the analogous result reads as follows

Theorem 4.6 ([Ma15b, KNW15]). *Fix a probability measure ν on $\{1,\dots,N\}$, sparsity level $s < N$, and constant $0 < \delta < 1$. Let $\Psi = (\psi_\lambda)_{\lambda \le N}$ be a frame for $\mathbb{R}^n$ with frame bounds c_1 and c_2 and let A be an $n \times n$ matrix whose rows $(r_i)_{i \le n}$ satisfy*

$$\sum_i r_k(i) r_j(i) \nu_i = \delta_{j,k}.$$

Furthermore, let K be a number such that $\|\psi_\lambda\| \le K$ for all $\lambda \le N$ and

$$L = \sup_{\substack{\|\Psi^* c\|=1 \\ \|c\|_0 \le s}} \frac{\|(\Psi\Psi^* c)_\lambda\|_1}{\sqrt{s}}. \tag{4.5}$$

If $\widetilde{A}$ is an $m \times n$ submatrix whose rows are subsampled from A according to ν, then there exists $C > 0$ independent of all relevant parameters such that for

$$m \ge Cs \left(\frac{KL}{\delta c_1}\right)^2 \max\left\{ \log^3\left(s\left(\frac{KL}{c_1}\right)^2\right)\log(N), \log(1/\gamma)\right\}.$$

the normalized submatrix $\sqrt{\frac{1}{m}}\widetilde{A}$ satisfies the Ψ-RIP of order s with Ψ-RIP constant δ with probability $1-\gamma$.

Remark 4.7. *Note that the factor L that appears in Theorem 4.6 is again a localization factor similar to* (3.5) *which determines the number of measurements in the case where analysis minimization is considered.*

The proof of this theorem follows very closely the arguments of Theorem 3.1 in [KNW15] and will be presented in Appendix C.9.

Remark 4.8. *In Theorem 4.6 the localization factor L and the reciprocal of the lower frame bound c_1 determine the number of measurements that are needed. In fact, similar as in Chapter 3 the use of localized frames can overcome both issues. Indeed, by Greshgorin's Circle Theorem there exists a $\lambda \in \{1, \dots, N\}$ such that*

$$\left| \frac{1}{c_1} - \|\psi_\lambda\|^2 \right| \leq \sum_{\mu \neq \lambda} |\langle \widetilde{\psi}_\lambda, \widetilde{\psi}_\mu \rangle|$$

and therefore

$$\frac{1}{c_1} \leq \sum_{\mu \leq N} |\langle \widetilde{\psi}_\lambda, \widetilde{\psi}_\mu \rangle|.$$

Therefore good localization properties help to control the lower frame bound and therefore also the number of measurements.

4.2 Stability of analysis-based ℓ^p-minimization solutions

We will show a similar stability result to Theorem 4.5 for the minimization problem (4.1) while assuming the Ψ-RIP. Recall that this means that we are assuming the measurement matrix A to behave like an isometry for all signals that are sparse in the primal frame $(\psi_\lambda)_\lambda$. However, at the same time we are also minimizing over the primal frame coefficients $(\langle f, \psi_\lambda \rangle)_\lambda$. This causes a sparsity mismatch since the primal frame coefficients, however, do not lead to a representation of a signal f in general. More precisely, we do not have

$$f \neq \sum_\lambda \langle f, \psi_\lambda \rangle \psi_\lambda,$$

unless $(\psi_\lambda)_\lambda$ happens to be a Parseval frame. In fact minimizing over the primal coefficients assumes sparsity with respect to some dual system. Due to this mismatch in the sparsity we propose two different approaches to proceed.

(A1) We introduce a novel concept – the one of *identifiable duals*, cf. Definition 4.9 – that can be used to overcome this sparsity mismatch. For frames that have an identifiable dual, we will be able to prove a desired stability estimate that extends Theorem 4.5.

(A2) We study the minimization problem with the 'correct' transform, namely the analysis operator with respect to some dual system of the primal frame.

While the second approach seems more natural in the context of compressed sensing, the first approach also has a merit in its own. In fact, the concept of identifiable duals extends the class of *scalable frames* ([KOPT13]) which has arisen in the literature from a completely different perspective. We give a short introduction into this concept in Appendix A.2.

Identifiable duals

As we already explained, we propose the following definition to circumvent the sparsity mismatch of the the primal frame and the primal frame coefficients.

Definition 4.9 ([Ma15b]). *We say a frame $\Psi = (\psi_\lambda)_{\lambda\in I}$ for $\mathcal{H}$ has an* identifiable dual *if there exists a dual frame $\widetilde{\Psi}$ such that for all $f \in \mathcal{H}$ and any $\lambda \in I$ the coefficient in modulus $|\langle f, \widetilde{\psi}_\lambda\rangle|$ can be bounded from above and below by $|\langle f, \psi_\lambda\rangle|$, i.e. there exist constants $d_1, d_2 > 0$ such that*

$$d_1|\langle f, \psi_\lambda\rangle| \le |\langle f, \widetilde{\psi}_\lambda\rangle| \le d_2|\langle f, \psi_\lambda\rangle| \tag{4.6}$$

for all $f \in \mathcal{H}$ and all $\lambda \in I$.

If Ψ is a frame that has an identifiable dual, then this assures that there exists a dual such that the sparsity of the primal frame coefficients leads to a sparse representation in this dual system. We now make a couple of comments about the class of frames that have an identifiable dual.

Remark 4.10.

(A) Clearly, every tight frame has an identifiable dual.

(B) From the identifiability condition (4.6) *we can deduce that*

$$(\operatorname{span}\psi_\lambda)^\perp = (\operatorname{span}\widetilde{\psi}_\lambda)^\perp \quad \forall\, \lambda \le N.$$

which implies that there exists $c_\lambda \in \mathbb{C}$ such that $\psi_\lambda = c_\lambda \widetilde{\psi}_\lambda$. In particular, all scalable frames[(v)] *have an identifiable dual, cf. Proposition A.10. Therefore, the class frame that have an identifiable duals is a generalization of the class of scalable frames.*

(C) The set of vectors

$$\Psi = \left\{ \begin{pmatrix} 2 \\ 1 \end{pmatrix}, \begin{pmatrix} 2 \\ 2 \end{pmatrix}, \begin{pmatrix} 1 \\ 2 \end{pmatrix} \right\}$$

is frame for $\mathbb{R}^2$ that has an identifiable dual, e.g.

$$\widetilde{\Psi} = \left\{ \begin{pmatrix} 2 \\ 1 \end{pmatrix}, \begin{pmatrix} -2 \\ -2 \end{pmatrix}, \begin{pmatrix} 1 \\ 2 \end{pmatrix} \right\}$$

with $d_1 = d_2 = 1$ but is neither a tight nor a scalable frame.

(D) More generally, the identifiability condition could be studied by considering localization properties of the Gramian $G := \Psi\Psi^*$ for the system Ψ. Indeed, for all $f \in \mathcal{H}$ we have

$$(\langle x, \psi_\lambda\rangle)_{\lambda\le N} = \Psi x = G\Psi(\Psi^*\Psi)^{-1}x = G(\langle x, \widetilde{\psi}_\lambda\rangle)_\lambda.$$

Hence, if G is close to a diagonal matrix, then using the pseudo inverse is also close to a diagonal matrix [Gro13] and the identifiability can be analyzed.

(v) A frame $(\psi_\Lambda)_\lambda \subseteq \mathcal{H}$ is called *scalable* if there exists $c_\lambda \in \mathbb{R}^+ \cup \{0\}$ such that $(c_\lambda\psi_\lambda)_\lambda$, is a Parseval frame for $\mathcal{H}$, cf. Appendix A.2.

(E) *With a view to compressed sensing it seems plausible to restrict the set identifiability condition* (4.6) *in Definition 4.9 onto a certain set of elements that we expect to be sparse in the primal frame as one is only interested in these case. This would make the definition more general.*

The second assumption is of technical nature. It will only be used to make the constants in the proof feasible. In fact, as we are not dealing with tight frames, the frame bound ratio c_1/c_2 might be uncontrollable. Hence, we define *q-controllable frame bounds.*

Stable frame bounds

In order to have stronger control on the frame bound ratio and to exclude pathological constants we make the following definition.

Definition 4.11 ([Ma15b]). *We say a frame Ψ has q-*controllable frame bounds *if there exists a $q \in \{1, \dots, N\}$ such that*

$$\frac{c_1^{p/(2-p)}}{c_2^{p/(2-p)}} \geq \frac{q}{N}, \tag{4.7}$$

where c_1 denotes the lower frame bound and c_2 the upper frame bound of Ψ, respectively.

Note that both, the identifiability condition as well as the controllability of the frame bound ratio is not needed for tight frames.

As we already mentioned, the q-controllability will be of great use to bound several parameters that yield feasible constants. Beyond that, it is also important to have q not too small for numerical reasons since a very small frame bound ratio yields a bad conditioning of the frame. Note that the optimal frame bounds equal the boundaries of the spectrum of the frame operator.

Stability for analysis formulation

Using the concept of identifiable duals and the controllability of frame bounds we can guarantee the stability of solutions that are obtained from the minimization problem (4.1).

Theorem 4.12 ([Ma15b]). *Let Ψ be a frame for $\mathbb{R}^n$ that has q-controllable frame bounds and has an identifiable dual. Moreover, let A be an $m \times n$ measurement matrix satisfying the Ψ-RIP with $\delta_\nu < 0.5$, where $\nu = s\frac{2\cdot(1+2^{-p})^{1/(p-2)}c_2^{p/(p-2)}d_2^{p/(p-2)}}{c_1^{p/(p-2)}}$ and $s < \frac{q}{2d_2^2(1+2^{-p})^{1/(p-2)}}$ and $d_2 > 0$ is the upper constant in the identifiability conditions. Then the solution x^* of* (4.1) *satisfies*

$$\|x - x^*\|_2^p \leq C_1(p)\varepsilon^p + C_2(p)\frac{\|\Psi x - (\Psi x)_s\|_p^p}{s^{1-p/2}}$$

for some positive constants $C_1(p)$ and $C_2(p)$ that depend on p, the frame bounds c_1, c_2, the Ψ-constant δ_ν, the sparsity s, the controllability parameter q, and the constants from the identifiability condition.

Before we continue with a proof of Theorem 4.12 we mention that for $p = 1$ Theorem 4.12 generalizes the findings of [CENR11] to the case of non-Parseval frames. Thus our result can be seen as a generalization of the stability result for the analysis formulation of ℓ^1-minimization (ℓ^1-$\mathrm{P}^{\varepsilon}_{\Psi}$). Moreover, if Ψ is a Parseval frame, then the constants $C_1(p), C_2(p)$ agree for $p = 1$ with those obtained in [CENR11]. Furthermore, Theorem 4.20 generalizes Theorem 4.3 to the analysis formulation.

In particular we have the following corollary.

Corollary 4.13 ([Ma15b]). *Let Ψ be a Parseval frame for $\mathbb{R}^n$ and let A be an $m \times n$ measurement matrix satisfying the Ψ-RIP with $\delta_{7s} < 0.6$ and $s < \frac{q}{2\cdot(1+2^{-p})^{1/(p-2)}}$. Then the solution x^* of* (4.1) *satisfies*

$$\|x - x^*\|_2^p \leq C_1(p)\varepsilon^p + C_2(p)\frac{\|\Psi x - (\Psi x)_s\|_p^p}{s^{1-p/2}}$$

for some positive constants $C_1(p)$ and $C_2(p)$ that depend on p. Moreover, the constants can be chosen to be monotonically decreasing for decreasing p with maximal constants agreeing with those obtained in [CENR11] for $p = 1$.

We now present a proof Theorem 4.12 and after that a proof of Corollary 4.13. Moreover, the proof shows that it is sufficient to have the identifiability condition to be valid for signals x that we want to recover, which are usually assumed to be sparse.

Proof of Theorem 4.12

The proof of Theorem 4.12 uses a nowadays standard strategy in compressed sensing that is mainly communicated by the works of Candès et al. in [CENR11] as well Saab et al. in [SCY08] for adaptations to ℓ^p-quasi norms, see also [CRT05] where this strategy was first developed.

Let x, x^* be as in Theorem 4.12 and define $z = x - x^*$. Further, set T_0 as the set consisting of the s largest coefficients of Ψx in p-th modulus. For any set T, Ψ_T should denote the matrix restricted to its columns indexed by T. Then we divide T_0^c into sets $T_1, T_2, \ldots$ of size M in order of decreasing magnitude of $\Psi_{T_0^c} h$. The explicit value of M will be determined later. We will now invoke a sequence of results.

The first one, Lemma 4.14 below, is a trivial modification of the *cone constraint* which is Lemma 2.1 in [CENR11]. For completeness we provide a proof.

Lemma 4.14 ([Ma15b, CENR11]). *The vector Ψz obeys the following cone constraint*

$$\|\Psi_{T_0^c} z\|_p^p \leq 2\|\Psi_{T_0^c} x\|_p^p + \|\Psi_{T_0} z\|_p^p.$$

Proof. Since x and x^* are both feasible and x^* is the minizer of (4.1) we have

$$\begin{aligned}
\|\Psi_{T_0} x\|_p^p + \|\Psi_{T_0^c} x\|_p^p &\geq \|\Psi x\|_p^p \\
&\geq \|\Psi x^*\|_p^p \\
&= \|\Psi x - \Psi h\|_p^p \\
&\geq \|\Psi_{T_0} x\|_p^p - \|\Psi_{T_0^c} x\|_p^p - \|\Psi_{T_0} h\|_p^p + \|\Psi_{T_0^c} x\|_p^p.
\end{aligned}$$

□

The following lemma generalizes Lemma 2.2 in [CENR11] to the case $p \in (0,1)$. For $p = 1$ the two results coincide.

Lemma 4.15 ([Ma15b]). *For $\rho = s/M$ and $\eta = 2\|\Psi_{T_0^c} x\|_p^p / s^{1-p/2}$, we have*

$$\sum_{j\geq 2} \|\Psi_{T_j} z\|_2^p \leq \rho^{1-p/2}(\|\Psi_{T_0} z\|_2^p + \eta).$$

Proof. By construction we have that every entry in $|(\Psi_{T_{j+1}} z)|^p$ which will be denoted by $|(\Psi_{T_{j+1}} z)|_{(k)}^p$ is bounded by

$$|(\Psi_{T_{j+1}} z)|_{(k)}^p \leq \frac{\|\Psi_{T_j} z\|_p^p}{M}.$$

Therefore

$$\|\Psi_{T_{j+1}} z\|_2^2 = \sum_{k=1}^{M} |(\Psi_{T_{j+1}} z)|_{(k)}^2 \leq M^{1-2/p} \|\Psi_{T_j} z\|_p^2$$

and thus

$$\sum_{j\geq 2} \|\Psi_{T_j} z\|_2^p \leq \sum_{j\geq 1} \frac{\|\Psi_{T_j} z\|_p^p}{M^{1-p/2}} = \frac{\|\Psi_{T_0^c} z\|_p^p}{M^{1-p/2}}.$$

Applying Lemma 4.14 and the generalized mean inequality gives

$$\sum_{j\geq 2} \|\Psi_{T_j} z\|_2^p \leq \left(\frac{s}{M}\right)^{1-p/2} \left(\|\Psi_{T_0} z\|_2^p + \frac{2\|\Psi_{T_0^c} x\|_p^p}{s^{1-p/2}}\right).$$

□

The next lemma is trivial to prove and we will use it without further modifications.

Lemma 4.16 ([CENR11], Lemma 2.3). *The vector Az satisfies*

$$\|Az\|_2 \leq 2\varepsilon.$$

Lemma 4.17 ([Ma15b]). *Let c_2 be the upper frame bound for the frame Ψ. Then we have*

$$(1-\delta_{s+M})^{p/2} \|(\Psi_{T_{01}})^* \Psi_{T_{01}} \widetilde{z}\|_2^p - (c_2(1+\delta_M))^{p/2} \rho^{1-p/2} \left(c_2^{p/2} d_2^p \|z\|_2^p + \eta\right) \leq (2\varepsilon)^p$$

where $T_{01} := T_0 \cup T_1$.

Proof. Without loss of generality we assume the identifiable dual is the canonical dual and define $\widetilde{z} := (\Psi^*\Psi)^{-1} z$. Note that $\Psi^*\Psi$ is invertible as it is the frame operator. Then by using Lemma 4.16 we have

$$(2\varepsilon)^p \geq \|Az\|_2^p = \|A\Psi^*\Psi\widetilde{z}\|_2^p \geq \|A(\Psi_{T_{01}})^*\Psi_{T_{01}}\widetilde{z}\|_2^p - \sum_{j\geq 2} \|A(\Psi_{T_j})^*\Psi_{T_j}\widetilde{z}\|_2^p, \tag{4.8}$$

and by the Ψ-RIP we have

$$(1-\delta_{s+M})^{p/2}\|(\Psi_{T_{01}})^*\Psi_{T_{01}}\widetilde{z}\|_2^p \leq \|A(\Psi_{T_{01}})^*\Psi_{T_{01}}\widetilde{z}\|_2^p \tag{4.9}$$

and

$$\sum_{j\geq 2}\|A(\Psi_{T_j})^*\Psi_{T_j}\widetilde{z}\|_2^p \leq (1+\delta_M)^{p/2}\sum_{j\geq 2}\|(\Psi_{T_j})^*\Psi_{T_j}\widetilde{z}\|_2^p. \tag{4.10}$$

Recall that by the identifiability there exist d_1, d_2 be such that

$$d_1|\langle z,\psi_\lambda\rangle| \leq |\langle z,\widetilde{\psi}_\lambda\rangle| \leq d_2|\langle z,\psi_\lambda\rangle| \quad \forall\, \lambda \leq N. \tag{4.11}$$

Using the frame property, the identifiability and Lemma 4.15 yields

$$\begin{aligned}
\sum_{j\geq 2}\|(\Psi_{T_j})^*\Psi_{T_j}\widetilde{z}\|_2^p &\leq \sum_{j\geq 2} c_2^{p/2}d_2^p\|\Psi_{T_j}z\|_2^p && (4.12)\\
&\leq c_2^{p/2}d_2^p\rho^{1-p/2}(\|\Psi_{T_0}z\|_p^p+\eta) && (4.13)\\
&\leq c_2^{p/2}d_2^p\rho^{1-p/2}(c_2^{p/2}\|z\|_p^p+\eta). && (4.14)
\end{aligned}$$

Combing (4.8), (4.9), (4.10) and (4.14) yields the claim. □

Lemma 4.18 ([Ma15b]). *The following inequality is true:*

$$\|z\|_2^{2p} \leq \frac{1}{c_1^p d_1^{2p}}\left(\frac{1}{c_1^{p/2}}\|z\|_2^p\|(\Psi_{T_{01}})^*\Psi_{T_{01}}\widetilde{z}\|_2^p + \rho^{2-p}(c_2^{p/2}\|z\|_2^p+\eta)^2\right),$$

Proof. With $T_{01} := T_0 \cup T_1$ we have by using the frame property and the identifiability of a dual

$$\begin{aligned}
\|h\|_2^{2p} &\leq \frac{1}{c_1^p}\|\Psi z\|_2^{2p}\\
&\leq \frac{1}{c_1^p d_1^{2p}}\left(\|\Psi_{T_{01}}\widetilde{z}\|_2^{2p} + \|\Psi_{T_{01}^c}z\|_2^{2p}\right)\\
&= \frac{1}{c_1^p d_1^{2p}}\left((\langle\widetilde{z},(\Psi_{T_{01}})^*\Psi_{T_{01}}\widetilde{z}\rangle)^p + \|\Psi_{T_{01}^c}z\|_2^{2p}\right)\\
&\leq \frac{1}{c_1^p d_1^{2p}}\left(\|\widetilde{z}\|_2^p\|(\Psi_{T_{01}})^*\Psi_{T_{01}}\widetilde{z}\|_2^p + \|\Psi_{T_{01}^c}z\|_2^{2p}\right)\\
&\leq \frac{1}{c_1^p d_1^{2p}}\left(\frac{1}{c_1^{p/2}}\|z\|_2^p\|(\Psi_{T_{01}})^*\Psi_{T_{01}}\widetilde{z}\|_2^p + \rho^{2-p}(\|\Psi_{T_0}z\|_2^p+\eta)^2\right),
\end{aligned}$$

where the last inequality follows from Lemma 4.15. □

The proof of the main result can now be derived from the previous lemmas.

Proof of Theorem 4.12. By Lemma 4.18, we have

$$
\begin{aligned}
\|z\|_2^{2p} &\leq \frac{1}{c_1^p d_1^{2p}} \left(\frac{1}{c_1^{p/2}} \left(\frac{\gamma_1 \|z\|^{2p}}{2} + \frac{\|(\Psi_{T_{01}})^* \Psi_{T_{01}} \widetilde{z}\|^{2p}}{2\gamma_1} \right) + \rho^{2-p} (c_2^{p/2} d_2^p \|z\|_2^p + \eta)^2 \right) \\
&= \frac{1}{c_1^p d_1^{2p}} \left(\frac{1}{c_1^{p/2}} \left(\frac{\gamma_1 \|z\|^{2p}}{2} + \frac{\|(\Psi_{T_{01}})^* \Psi_{T_{01}} \widetilde{z}\|^{2p}}{2\gamma_1} \right) + \right. \\
&\qquad \left. + \rho^{2-p} \left(c_2^p d_2^{2p} \|z\|_2^{2p} + 2 c_2^{p/2} d_2^p \|z\|_2^p \eta + \eta^2 \right) \right) \\
&\leq \frac{1}{c_1^p d_1^{2p}} \left(\frac{1}{c_1^{p/2}} \left(\frac{\gamma_1 \|z\|^{2p}}{2} + \frac{\|(\Psi_{T_{01}})^* \Psi_{T_{01}} \widetilde{z}\|^{2p}}{2\gamma_1} \right) + \right. \\
&\qquad \left. + \rho^{2-p} \left(c_2^p d_2^{2p} \|z\|_2^{2p} + \left(c_2^p d_2^{2p} \gamma_2 \|z\|_2^{2p} + \frac{\eta^2}{\gamma_2} \right) + \eta^2 \right) \right) \\
&= \frac{1}{c_1^p d_1^{2p}} \left(\frac{1}{c_1^{p/2}} \left(\frac{\gamma_1 \|z\|^{2p}}{2} + \frac{\|(\Psi_{T_{01}})^* \Psi_{T_{01}} \widetilde{z}\|^{2p}}{2\gamma_1} \right) + \right. \\
&\qquad \left. + \rho^{2-p} \left(c_2^p d_2^{2p} (1+\gamma_2) \|z\|_2^{2p} + \left(\frac{1}{\gamma_2} + 1 \right) \eta^2 \right) \right).
\end{aligned}
$$

Therefore

$$
\begin{aligned}
&\left(1 - \frac{1}{c_1^p d_1^{2p}} \left(\frac{\gamma_1}{2 c_1^{p/2}} + \rho^{2-p} c_2^p d_2^{2p} (1+\gamma_2) \right) \right) \|z\|_2^{2p} \\
&\qquad \leq \frac{1}{c_1^p d_1^{2p}} \left(\frac{\|(\Psi_{T_{01}})^* \Psi_{T_{01}} \widetilde{z}\|^{2p}}{2\gamma_1 c_1^{p/2}} + \rho^{2-p} \left(\frac{1}{\gamma_2} + 1 \right) \eta^2 \right).
\end{aligned}
$$

and in particular

$$
\begin{aligned}
&\left(c_1^p d_1^{2p} - \left(\frac{\gamma_1}{2 c_1^{p/2}} + \rho^{2-p} c_2^p d_2^{2p} (1+\gamma_2) \right) \right)^{1/2} \|z\|_2^p \\
&\qquad \leq \frac{\|(\Psi_{T_{01}})^* \Psi_{T_{01}} \widetilde{z}\|^p}{\sqrt{2\gamma_1 c_1^{p/2}}} + \rho^{1-p/2} \left(\frac{1}{\gamma_2} + 1 \right)^{1/2} \eta.
\end{aligned}
$$

Hence, by using Lemma 4.17 we obtain

$$
\Gamma_1(p) \|z\|_2^p - \Gamma_2(p) \eta \leq (2\varepsilon)^p
$$

with

$$
\begin{aligned}
\Gamma_1(p) = &\sqrt{2\gamma_1 c_1^{p/2} (1-\delta_{s+M})^p \left(c_1^p d_1^{2p} - \left(\frac{\gamma_1}{2 c_1^{p/2}} + \rho^{2-p} c_2^p d_2^{2p} (1+\gamma_2) \right) \right)} - \\
&- \sqrt{(c_2 d_2^2 (1+\delta_M))^p \rho^{2-p}}
\end{aligned}
$$

and

$$\Gamma_2(p) = \sqrt{2\gamma_1 c_1^{p/2}(1-\delta_{s+M})^p \rho^{2-p}\left(\frac{1}{\gamma_2}+1\right)} - \sqrt{(c_2 d_2^2(1+\delta_M))^p \rho^{2-p}}.$$

It is left to choose γ_1, γ_2, and ρ so that $\Gamma_1(p)$ and $\Gamma_2(p)$ are non-negative. W.l.o.g. we can assume $c_1 \geq 1$; otherwise a rescaling can be performed. We now choose $\gamma_1 = c_1^{3p/2} d_1^{2p}$ and $M = s\frac{2\cdot(1+2^{-p})^{1/(p-2)} c_2^{p/(p-2)} d_2^{2p/(p-2)}}{c_1^{p/(p-2)}}$. Then $\Gamma_1(p)$ is larger than zero and for γ_2 sufficiently small $\Gamma_2(p)$ is also larger than zero. This completes the proof.

□

Proof of Corollary 4.13

Large parts of corollary 4.13 follow immediately from Theorem 4.12 and we only have to verify that the statements that appear naturally in the proof are not increasing with respect to p.

Proof. For $c_1 = c_2 = 1$ the computations in the proof of Theorem 4.12 yield

$$\Gamma_1(p)\|z\|_2^p - \Gamma_2(p)\eta \leq (2\varepsilon)^p$$

with the constants

$$\Gamma_1(p) = \sqrt{2\gamma_1(1-\delta_{s+M})^p\left(1-\left(\frac{\gamma_1}{2}+\rho^{2-p}(1+\gamma_2)\right)\right)} - \sqrt{((1+\delta_M))^p\rho^{2-p}},$$

$$\Gamma_2(p) = \sqrt{2\gamma_1(1-\delta_{s+M})^p\rho^{2-p}\left(\frac{1}{\gamma_2}+1\right)} - \sqrt{((1+\delta_M))^p\rho^{2-p}}.$$

One possibility to guarantee $\Gamma_1(p)$ and $\Gamma_2(p)$ to be positive is to choose $\gamma_1 = 1$ and $M = 6s$. Then $\Gamma_1(p)$ is positive and for γ_2 sufficiently small $\Gamma_2(p)$ is positive. Moreover, note that

$$\Gamma_1'(p) < 0 \quad \text{and} \quad \Gamma_2'(p) > 0$$

for γ_2 small enough. □

We end this section with a comment on the identifiability condition.

On the identifiability condition

The identifiability condition was introduced in order to compensate the mismatch between the sparsity that is required by the RIP and the sparsity of the dual system due to the minimization of the primal frame coefficients. However, condition (4.6) does not have to be assumed for the complete Hilbert space $\mathcal{H}$. In fact, as we already stated, assuming the identifiability condition (4.6) to hold for all signals $f \in \mathcal{H}$ is equivalent to have a dual frame whose elements are multiples of the corresponding elements in the primal frame. For some frames used in practice, this seems to be a strong assumption. However, in the proof of Theorem 4.12 we also saw that we only apply the identifiability condition to the vector $x - x^*$ so the identifiability condition need not to hold for all signals but can actually be reduced.

Remark 4.19. *Generally speaking, in practice one can very often observe the identifiability condition for wavelet and also shearlet systems for images that are sparse in either of these dictionaries. One of the reasons is because, the dual system can be implemented in the Fourier domain and the explicit dual functions are obtained by a stable Fourier multiplier of the primal frame elements, i.e. if* $(\psi_\lambda)_\lambda$ *is a frame then a dual system can often be constructed to be of the form*

$$\widehat{\widetilde{\psi}}_\lambda = \widehat{\psi}/\widehat{a}. \tag{4.15}$$

where $\widehat{a}$ *is a function that is uniformly bounded from above and below which means, it essentially does not change the Fourier behaviour and thus not the sparsity structure in frequency. In fact, having a dual that is of the form* (4.15) *yields*

$$|\langle f, \widetilde{\psi}_\lambda\rangle| \lesssim |\langle |\widehat{f}|, |\psi_\lambda|\rangle|,$$

which preserves the multiscale sparsity, see also Figure 4.2. The digital shearlet system *is for instance a system for which duals of the form* (4.15) *can be constructed, [Lim13].*

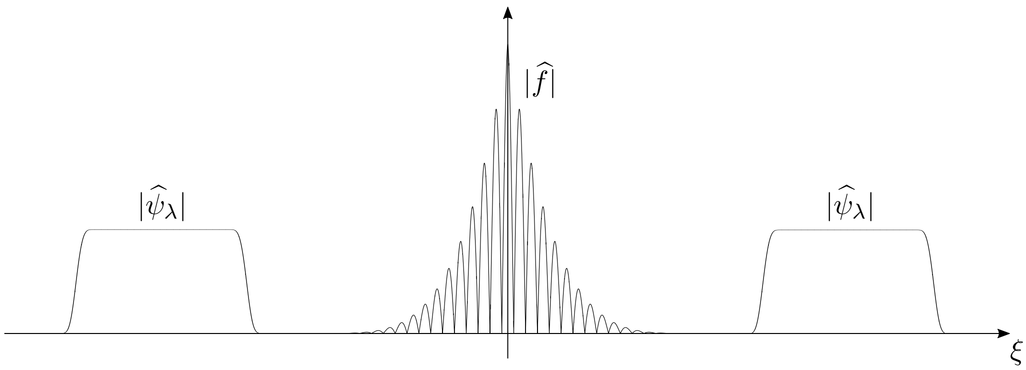

Figure 4.2: Simplified presentation (in 1D) of the identifiability condition for functions f that are well behaved. Stable Fourier multipliers do not change the global sparsity pattern.

We now return to the discussion that we started with at the beginning of Section 4.2. Theorem 4.12 and Corollary 4.13 are the desired resulting statements that we aimed to achieve when formulating the approach (A1). In the next section we discuss approach (A2) which was to change the minimization problem (4.1) by minimizing over dual coefficients instead of primal coefficients.

4.3 Stability for the dual analysis formulation

Since the concept of identifiable duals was used to cope with the mismatch in the sparsity scheme, it is very much expected that when minimizing over dual coefficients, such a property is not necessary. Indeed, for the minimization problem

$$\min_x \|\widetilde{\Psi}x\|_p^p \quad \text{subject to} \quad \|y - Ax\|_2 \leq \varepsilon \qquad (\ell^1\text{-P}^{\varepsilon}_{\widetilde{\Psi}})$$

one can show the following theorem.

Theorem 4.20 ([Ma15b]). *For an $m \times n$ measurement matrix A that satisfies the Ψ-RIP with $\delta_\nu < 0.5$ where $\nu = s\left(\frac{3}{c_1^{2p}}\right)^{1/(2-p)}$ and $s < N\left(\frac{c_1^{2p}}{3}\right)^{1/(2-p)}$ the solution x^* of $(\ell^1\text{-P}^{\varepsilon}_{\widetilde{\Psi}})$ satisfies*

$$\|x - x^*\|_2^p \leq C_1(p)\varepsilon^p + C_2(p)\frac{\|\widetilde{\Psi}x - (\widetilde{\Psi}x)_s\|_p^p}{s^{1-p/2}}$$

for some positive constants $C_1(p)$ and $C_2(p)$ that depend on p, the frame bounds c_1, c_2, the Ψ-RIP constant δ_ν, and the sparsity s.

The assumptions in Theorem 4.20 are less restrictive than those of Theorem 4.12 which is to be expected as the sparsity setup appears in the correct form. This means we assume sparsity in the primal frame, hence, we minimize over the dual frame coefficients. However, this in particular means, we need to know how to compute $\widetilde{\Psi}x$ for any $x \in \mathbb{R}^n$ which sometimes can be a numerical difficulty.

The proof of Theorem 4.20 is very similar to the proof of the previous Theorem 4.12. We therefore shorten it a little bit by summarizing the key steps in the following proposition.

Proposition 4.21 ([Ma15b]). *Retaining the notations and definition of Theorem 4.12 and its proof, the following estimates hold*

i) $\|\widetilde{\Psi}_{T_0^c} z\|_p^p \leq 2\|\widetilde{\Psi}_{T_0^c} x\|_p^p + \|\widetilde{\Psi}_{T_0} z\|_p^p$.

ii) $\sum_{j\geq 2} \|\widetilde{\Psi}_{T_j} z\|_2^p \leq \rho^{1-p/2}(\|\widetilde{\Psi}_{T_0} z\|_2^p + \eta)$.

iii) $(1-\delta_{s+M})^{p/2}\|(\Psi_{T_{01}})^*\Psi_{T_{01}}\widetilde{z}\|_2^p - (c_2(1+\delta_M))^{p/2}\rho^{1-p/2}\left(c_1^{-p/2}\|z\|_2^p + \eta\right) \leq (2\varepsilon)^p$

iv) $\|z\|_2^{2p} \leq c_2^p\left(\|z\|_2^p\|(\widetilde{\Psi}_{T_{01}})^*\widetilde{\Psi}_{T_{01}}\widetilde{z}\|_2^p + \rho^{2-p}(\|\widetilde{\Psi}_{T_0} z\|_2^p + \eta)^2\right)$.

Proof. Item *i)*, *ii)*, and *iv)* are trivial adaptions of the proof of Theorem 4.12 and will be skipped. As for item *iii)*, note that

$$\begin{aligned}
(2\varepsilon)^p &\geq \|Az\|_2^p \\
&\geq \|A(\Psi_{T_{01}})^*\Psi_{T_{01}}\widetilde{z}\|_2^p - \sum_{j\geq 2}\|A(\Psi_{T_j})^*\Psi_{T_j}\widetilde{z}\|_2^p \\
&\geq (1-\delta_{s+M})^{p/2}\|(\Psi_{T_{01}})^*\Psi_{T_{01}}\widetilde{z}\|_2^p - (1+\delta_M)^{p/2}\sum_{j\geq 2}\|(\Psi_{T_j})^*\Psi_{T_j}\widetilde{z}\|_2^p.
\end{aligned}$$

By *ii)* we have

$$\sum_{j\geq 2}\|(\Psi_{T_j})^*\Psi_{T_j}\widetilde{z}\|_2^p \leq c_2^{p/2}\sum_{j\geq 2}\|\Psi_{T_j}\widetilde{z}\|_2^p$$

$$
\begin{aligned}
&= c_2^{p/2} \sum_{j \geq 2} \|\widetilde{\Psi}_{T_j} z\|_2^p \\
&\leq c_2^{p/2} \rho^{1-p/2} (\|\widetilde{\Psi}_{T_0} z\|_2^p + \eta).
\end{aligned}
$$

Thus the claim follows. □

Proof of Theorem 4.20. By Proposition 4.21 *iv)* we have

$$
\begin{aligned}
\|z\|_2^{2p} &\leq c_2^p \left[\left(\frac{\gamma_1 \|z\|_2^{2p}}{2} + \frac{\|(\widetilde{\Psi}_{T_{01}})^* \widetilde{\Psi}_{T_{01}} z\|_2^p}{2\gamma_1} \right) + \rho^{2-p} (\|\widetilde{\Psi}_{T_{01}} z\|_2^{2p} + 2 \|\widetilde{\Psi}_{T_0} z\|_2^p \eta + \eta^2 \right] \\
&\leq c_2^p \left[\left(\frac{\gamma_1 \|z\|_2^{2p}}{2} + \frac{\|(\widetilde{\Psi}_{T_{01}})^* \widetilde{\Psi}_{T_{01}} z\|_2^p}{2\gamma_1} \right) + \right. \\
&\qquad \left. + \rho^{2-p} \left(\|\widetilde{\Psi}_{T_{01}} z\|_2^{2p} + \eta^2 + \left(\gamma_2 \|\widetilde{\Psi}_{T_0} z\|_2^{2p} + \frac{\eta^2}{\gamma_2} \right) \right) \right] \\
&\leq c_2^p \left[\left(\frac{\gamma_1 \|z\|_2^{2p}}{2} + \frac{\|(\widetilde{\Psi}_{T_{01}})^* \widetilde{\Psi}_{T_{01}} z\|_2^p}{2\gamma_1} \right) + \rho^{2-p} \left(\frac{1}{c_1^{2p}} (1+\gamma_2) \|z\|_2^{2p} + \left(1 + \frac{1}{\gamma_2} \right) \eta^2 \right) \right].
\end{aligned}
$$

Therefore

$$
\left(1 - \frac{c_2^p \gamma_1}{2} - \frac{\rho^{2-p}(1+\gamma_2)}{c_1^{2p}} \right) \|z\|_2^{2p} \leq \frac{c_2^p}{2\gamma_1} \|(\widetilde{\Psi}_{T_{01}})^* \widetilde{\Psi}_{T_{01}} z\|_2^{2p} + \rho^{2-p} \left(1 + \frac{1}{\gamma_2} \right) \eta^2
$$

which in turn implies

$$
\sqrt{\frac{2\gamma_1}{c_2^p}} \left[\left(1 - \frac{c_2^p \gamma_1}{2} - \frac{\rho^{2-p}(1+\gamma_2)}{c_1^{2p}} \right) \|z\|_2^p - \rho^{1-p/2} \left(1 + \frac{1}{\gamma_2} \right)^{1/2} \eta \right] \leq \|(\widetilde{\Psi}_{T_{01}})^* \widetilde{\Psi}_{T_{01}} z\|_2^p.
$$

Using Proposition 4.21 *iii)* we conclude

$$
\Gamma_1(p) \|z\|_2^p - \Gamma_2(p) \eta \leq (2\varepsilon)^p
$$

where

$$
\begin{aligned}
\Gamma_1(p) &= \sqrt{\frac{2\gamma_1}{c_2^p} \left(1 - \frac{c_2^p \gamma_1}{2} - \frac{\rho^{2-p}(1+\gamma_2)}{c_1^{2p}} \right) (1 - \delta_{s+M})^p} - \sqrt{(1+\delta_M)^p \left(\frac{c_2}{c_1} \right)^p \rho^{2-p}} \\
\Gamma_2(p) &= \sqrt{(1-\delta_{s+M})^p \rho^{2-p} \left(1 + \frac{1}{\gamma_2} \right) \frac{2\gamma_1}{c_1^p}} - \sqrt{\rho^{2-p} \left(\frac{c_2}{c_1} \right)^p (1 + \delta_M)^p}.
\end{aligned}
$$

Thus choosing, for example, $\gamma_1 \leq c_1^{-p}$ and $M = s \left(\frac{2}{c_1^{2p}} \right)^{1/(2-p)}$ yields the result. Note that it is possible to choose to choose the constants such that they obey

$$
\Gamma_1'(p) < 0 \quad \text{and} \quad \Gamma_2'(p) > 0.
$$

□

Optimizing over duals

Of course, when considering the minimization problem (ℓ^1-$\mathrm{P}^{\varepsilon}_{\widetilde{\Psi}}$) the following question arises immediately: Which dual should one choose for the optimization? This question is very delicate, since a dual frame is not always unique, unless Ψ is a basis. One canonical choice is the canonical dual. However, since the frame coefficients with respect to the canonical dual minimizes all possible coefficients that are used for representing the signal in the primal frame, it is fair to believe that these coefficients are not very sparse. In fact, the dual coefficient vector has very likely the structure of lots of small coefficients with its energy spread over all entries, as it is the element with the minimal ℓ^2-norm.

The problem of choosing a good dual – meaning so that the frame coefficients in that dual are sparse with respect to the ℓ^p-quasi norm – is clearly a same problem in the infinite dimensional scenario, cf. (4.17), since then a dual is not computed by inverting a finite matrix, but an operator acting on infinite dimensional spaces.

Remark 4.22. *The compactly supported shearlet frame from Section 1.1 also suffers from the fact that there are no duals known for this system.*

If one were to know a set of duals, then one could minimize over this set as well. This has been done in [LML12]. Consider

$$\min_{\widetilde{\Psi},x} \|\widetilde{\Psi}x\|_p^p \quad \text{subject to} \quad \|y - Ax\|_2 \le \varepsilon, \qquad (\ell^p\text{-}\mathrm{P}^{\varepsilon}_{\text{dual}})$$

where the minimization is to be considered over all $\widetilde{\Psi}$ such that $\Psi^*\widetilde{\Psi} = \mathrm{Id}$ and $x \in \mathbb{C}^{n^2}$. From a theoretical point of view the minimization problem (ℓ^p-$\mathrm{P}^{\varepsilon}_{\text{dual}}$) is equivalent to the standard synthesis formulation (ℓ^p-$\mathrm{P}^{\varepsilon}_{\mathrm{S}}$)

$$\min_{z} \|z\|_p^p \quad \text{subject to} \quad \|y - A\Psi^* z\|_2 \le \varepsilon. \tag{4.16}$$

This has already been noticed in [LML12] for $p = 1$ but the proof can be generalized to $p \in (0, 1)$, see Theorem 4.24 below.

Remark 4.23. *Although the two problems* (ℓ^p-$\mathrm{P}^{\varepsilon}_{\text{dual}}$) *and* ($\ell^p$-$\mathrm{P}^{\varepsilon}_{\mathrm{S}}$) *are equivalent, practical results often differ strongly.*

Theorem 4.24 ([Ma15b, Li11])**.** *The minimization problems* (ℓ^p-$\mathrm{P}^{\varepsilon}_{\text{dual}}$) *and* (4.16) *are equivalent.*

Proof. As shown in [Li11] all duals can be characterized by the formula

$$\widetilde{\Psi}^* = (\Psi^*\Psi)^{-1}\Psi^* + W(\mathrm{Id} - (\Psi^*\Psi)^{-1}\Psi^*), \tag{4.17}$$

where W is an arbitrary $d \times n^2$ matrix. Hence, the minimization problem (ℓ^p-$\mathrm{P}^{\varepsilon}_{\text{dual}}$) is equivalent to

$$\min_{x,x'} \|\widetilde{\Psi}x + Px'\|_p^p \quad \text{subject to} \quad \|y - Ax\|_2 \le \varepsilon. \tag{4.18}$$

The fact that

$$\mathbb{C}^d = \operatorname{ran}\Psi \oplus \ker \Psi^*$$

implies that any $z \in \mathbb{C}^d$ can be expressed as

$$z = \Psi(\Psi^*\Psi)^{-1}x + Px'$$

for some $x \in \mathbb{C}^{n^2}, x' \in \mathbb{C}^d$. Further, $x = \Psi^* z$. Thus (ℓ^p-$\mathrm{P}^\varepsilon_{\mathrm{dual}}$) reads as

$$\min_z \|z\|_p^p \quad \text{subject to} \quad \|y - A\Psi^* z\|_2 \leq \varepsilon.$$

Clearly, the above argumentation holds in reversed order which shows that (4.16) can be written in the form (ℓ^p-$\mathrm{P}^\varepsilon_{\mathrm{dual}}$). □

Theorem 4.24 in particular implies that if the reconstruction system happens to form a basis, then the synthesis minimization problem (4.16) is equivalent to

$$\min_x \|\Psi(\Psi^*\Psi)^{-1}x\|_p^p \quad \text{subject to} \quad \|y - Ax\|_2 \leq \varepsilon.$$

For linearly independent tight frames this reduces to (ℓ^1-$\mathrm{P}^\varepsilon_\Psi$)

$$\min_x \|\Psi x\|_p^p \quad \text{subject to} \quad \|y - Ax\|_2 \leq \varepsilon.$$

Remark 4.25. *Note that the proof of Theorem* (4.24) *can also be done in infinite dimensions since the analysis operator has closed range, hence, the argumentation works equally well by applying the closed range theorem.*

Remark on analysis vs. synthesis based methods

In practice both sparse recovery methods – analysis based and synthesis based – are widely used. From a practical point of view, there is no clear indication which method works better, in fact, the method of choice should depend on the application and the signal class. More precisely, it is sometimes easier to design a transform Ψ such that $(\langle f, \psi_\lambda \rangle)_\lambda$ has fast decay than finding a dictionary Ψ such that f has a compressible representation in. In particular, both approaches are fundamentally different. The analysis based method assumes a sparsifying transform and based on this transform there is only one analysis representation. On the other hand for the synthesis approach one assumes a sparsifying dictionary and for that dictionary there are possibly infinitely many sparse representations.

4.4 Algorithm for the analysis-based ℓ^p-minimization problem

Many different algorithms have been proposed to solve or rather approximate the non-convex ℓ^p-minimization problem and a comparison of some methods can be found, for instance, in [LLSZ13]. Most of these methods are based on *reweighted ℓ^1-minimization* which originally stems from [CWB08] and has been used to strengthen the effect of sparsity. Reweighted ℓ^1-minimization will also be of great interest in the next chapter where we will also properly motivate the ideas behind reweighted ℓ^1-minimization. However, we now present one particular instance of typical methods that are used to heuristically solve (4.1).

Approximating the ℓ^p-problem by reweighting

The algorithm that we use has also been proposed in [FL09] to solve the ℓ^p-minimization problem in the synthesis formulation. We give a short motivation for how this algorithm works and then proceed with some theoretical and numerical results of this algorithm.

Solving the minimization problem (4.1), that is

$$\min_x \|\Psi x\|_p^p \quad \text{subject to } \|y - Ax\|_2 \le \varepsilon,$$

is equivalent to solving

$$\min_x \sum_\lambda \frac{|\Psi x|_\lambda}{|\Psi x|_\lambda^{1-p}} \quad \text{subject to } \|y - Ax\|_2 \le \varepsilon,$$

where we assume for a moment that dividing by $|\Psi x|_\lambda$ is legitimate. This minimization problem can then be tackled by using reweighted ℓ^1-minimization, [CWB08], indeed, the denominator will now be interpreted as a weight that is ideally set in a such way, that the sparsest solution will be computed. More precisely, if we were to use the exact (sparse) signal x_0, then the minimization problem would read as

$$\min_x \sum_\lambda \frac{|\Psi x|_\lambda}{|\Psi x_0|_\lambda^{1-p}} \quad \text{subject to} \quad \|y - Ax\|_2 \le \varepsilon.$$

In case $(\Psi x_0)_\lambda = 0$, the weight will be set as ∞. Clearly, multiplying the denominator by some constant, say $\mu > 0$, does not change the minimizer, hence, we consider

$$\min_x \sum_\lambda \frac{|\Psi x|_\lambda}{(\mu|\Psi x_0|_\lambda)^{1-p}} \quad \text{subject to} \quad \|y - Ax\|_2 \le \varepsilon.$$

The role of μ is simply to have more numerical flexibility. We expect the optimal choice for such μ to be signal dependent.

However, we have used the sparse signal x_0 as a weight in the above discussion and of course, that is the vector that one would like to find in the first place. Hence, we consider an approximative vector x^k that iteratively approached to a *good*, i.e. sparse, weight. Indeed, consider

$$\min_x \sum_\lambda \frac{|\Psi x|_\lambda}{(\mu|\Psi x^k|_\lambda)^{1-p}} \quad \text{subject to} \quad \|y - Ax\|_2 \le \varepsilon.$$

Finally, in order to prevent any instabilities we integrate some $\nu > 0$ and solve

$$\min_x \sum_\lambda \frac{|\Psi x|_\lambda}{(\mu|\Psi x^k|_\lambda + \nu)^{1-p}} \quad \text{subject to} \quad \|y - Ax\|_2 \le \varepsilon. \tag{4.19}$$

The vector x^k will then be updated iteratively and leads to the following final program.

Input : y, μ, ε, M.
Output: x
Initialize $k = 0, W = (w_\lambda)_\lambda = 1$.
while $k \leq M$ **do**
  Find solution of (4.19), i.e. find x^{k+1} such that

$$x^{k+1}k = \text{argmin}_x \|W\Psi x\|_1 \quad \text{subject to} \quad \|y - Ax\|_2 \leq \varepsilon. \tag{4.20}$$

  Update W by setting

$$W_\lambda = \frac{1}{(\mu|\Psi x^k|_\lambda + \nu)^{1-p}}.$$

  Increase $k \to k+1$.
end

Algorithm 1: Algorithm used to solve the minimization problem (4.1)

Next we show some numerical experiments regarding the recovery of objects that are sparse in shearlets from their Fourier measurements.

Reconstruction from Fourier measurements using shearlets

As already mentioned in the introduction, one of the applications of the analysis-based ℓ^p-minimization problem is magnetic resonance imaging where the sampling process is modeled by taking samples of the Fourier transform of the signal. The minimization problem reads as follows:

$$\min_x \|\Psi x\|_p^p \quad \text{subject to} \quad \|y - \mathcal{F}x\|_2 \leq \varepsilon \tag{4.21}$$

where Ψ is the sparsifying transform and $\mathcal{F}$ is the undersampled Fourier transform.

In the following experiment we use the well known GLPU phantom introduced in [GKLPU12] which can be downloaded at

`http://bigwww.epfl.ch/algorithms/mriphantom/#soft`

For the sampling pattern we have used a radial sampling mask consisting of 30 radial lines, see Figure 4.3.

For solving (4.20) there are many different ℓ^1-solvers, however, we have used NESTA in the upcoming experiments which is available at

`http://statweb.stanford.edu/~candes/nesta/`

For *shearlets* we have used the shearlet transform available at

`http://www.shearlab.org/`

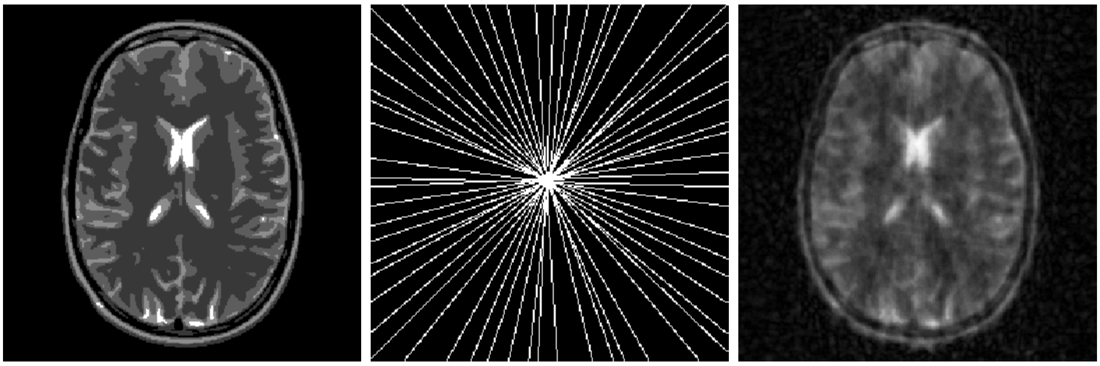

Figure 4.3: **Left:** GLPU Phantom from [GKLPU12]. **Middle:** Radial sampling pattern used in Fourier domain. **Right:** Fourier inversion of data.

We now let Algorithm 1 run for a maximum of 10 iterations, i.e. $M = 10$. Further, note that $p = 1$ indeed corresponds to ℓ^1-minimization and resolving the problem iteratively, i.e. (4.20) does not contribute anything as W is one in every for every k. Hence, the error stays constant over k, see also Figure 4.4.

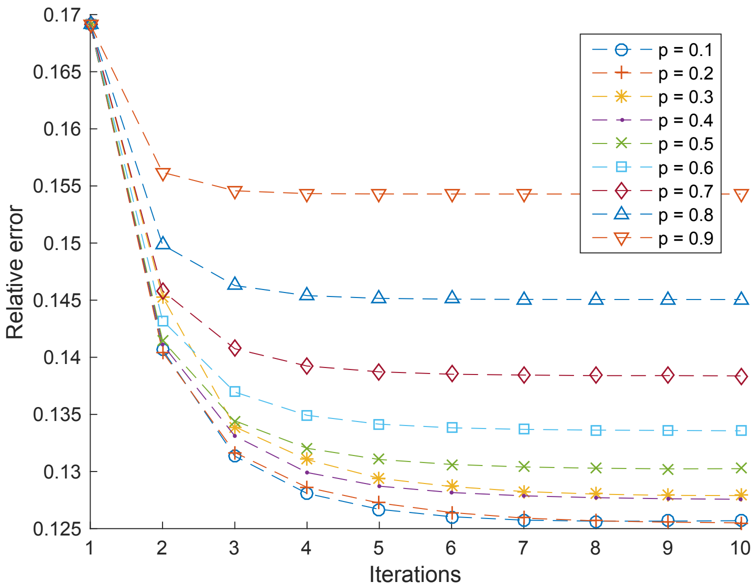

Figure 4.4: Relative error.

Figure 4.4 suggests that there is some merit in ℓ^p-minimization with p much smaller than 1 and we should now make some further analysis of the reconstructions and the algorithm itself.

Reduced artifacts

In Figure 4.5 we display the reconstruction for $p = 0.1$ and $p = 1$. The reconstruction for $p = 1$ itself shows the significant benefit of applying ℓ^1-minimization as opposed to the Fourier inversion of the data which can be seen in Figure 4.3. This corresponds to the standard approach of how sparse solutions are obtained in compressed sensing. Now what the iterative reweighting method does is to return the solution to the algorithm and uses it to compute a new solution. It can be observed that for $p = 0.1$ the solution is significantly better and edges are sharper than for, say, $p = 1$. Also the amount of artifacts is reduced which can becomes strongly visible inside the constant regions.

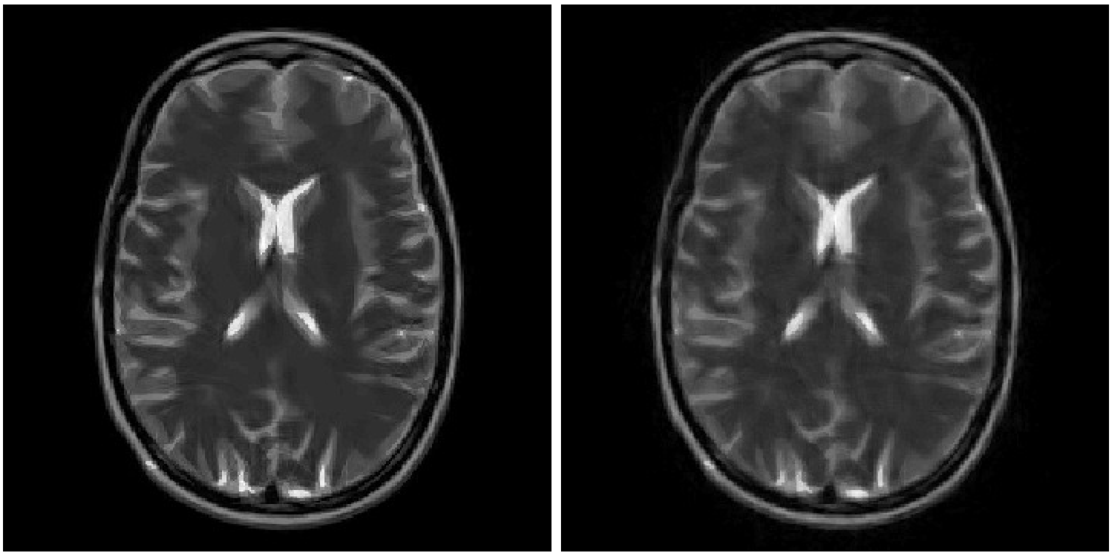

Figure 4.5: **Left:** Reconstruction for $p = 0.1$. **Right:** Reconstruction for $p = 1$.

Relative error and numerical convergence

Of course one immediate question concerning Algorithm 1 is the matter of convergence. However, as the algorithm is a special case of reweighted ℓ^1-minimization for which no general convergence results exist, it is not to be expected that one can derive a convergence result for this algorithm. In fact, the convergence properties strongly depend on the initial vector x_0 as it was outlined in [FL09]. Nevertheless, some weak convergence results that are known and have been shown in [FL09] for the synthesis formulation can easily be extended to the analysis formulation.

Theorem 4.26 ([Ma15b])**.** *Let $\mu \geq 1, \nu > 0$ and $(x^k)_k$ a sequence of minimizers generated from* (4.19)*. Then $(x^k)_k$ and $(\Psi x^k)_k$ contain a convergent subsequence.*

Proof. The proof follows the lines of [FL09] followed by an application of the frame inequality. For any $\nu > 0$ we obtain by Hölder's inequality

$$\sum_{\lambda \leq N} \left(\mu |\Psi x^{k+1}|_\lambda + \nu\right)^p = \sum_{\lambda \leq N} \frac{\left(\mu |\Psi x^{k+1}|_\lambda + \nu\right)^p}{\left(\mu |\Psi x^k|_\lambda + \nu\right)^{p(1-p)}} \left(\mu |\Psi x^k|_\lambda + \nu\right)^{p(1-p)}$$

$$\leq \left(\sum_{\lambda\leq N}\frac{\left(\mu|\Psi x^{k+1}|_\lambda+\nu\right)}{\left(\mu|\Psi x^{k}|_\lambda+\nu\right)^{1-p}}\right)^p\left(\sum_{\lambda\leq N}\left(\mu|\Psi x^{k}|_\lambda+\nu\right)^p\right)^{1-p}$$
$$\leq \left(\sum_{\lambda\leq N}\frac{\left(\mu|\Psi x^{k}|_\lambda+\nu\right)}{\left(\mu|\Psi x^{k}|_\lambda+\nu\right)^{1-p}}\right)^p\left(\sum_{\lambda\leq N}\left(\mu|\Psi x^{k}|_\lambda+\nu\right)^p\right)^{1-p}$$

Therefore

$$\sum_{\lambda\leq N}\left(\mu|\Psi x^{k+1}|_\lambda+\nu\right)^p\leq\sum_{\lambda\leq N}\left(\mu|\Psi x^{k}|_\lambda+\nu\right)^p. \tag{4.22}$$

By (4.22) we can conclude

$$\|\Psi x^k\|_\infty\leq\|\Psi x^k\|_p\leq\|(\mu|\Psi x^k|_\lambda+\nu)_\lambda\|_p\leq\|(\mu|\Psi x^0|_\lambda+\nu)_\lambda\|_p=:C.$$

The boundedness of the sequence $(x^k)_k$ follows from

$$\|x^k\|_\infty\leq\|x^k\|_2\leq\sqrt{\frac{\|\Psi x^k\|_2^2}{a}}\leq\sqrt{\frac{N}{A}}\|\Psi x^k\|_\infty\leq\sqrt{\frac{N}{A}}C.$$

□

In Figure 4.6 we plot the relative error from different number of iterations. Indeed, the first 3×3 block of plots show the nine sequences

$$\left(\frac{\|\Psi x_p^{k+1}-\Psi x_p^k\|}{\|\Psi x_p^{k+1}\|}\right)_{k=1,\ldots,10}\quad\text{for } p=0.1,0.2,\ldots,0.9,$$

where

$$x_p^{k+1}=\operatorname{argmin}_x\|W\Psi x\|_1\quad\text{subject to}\quad\|y-Ax\|_2\leq\varepsilon$$

with

$$W_\lambda=\frac{1}{(\mu|\Psi x^k|_\lambda+\nu)^{1-p}}.$$

The second 3×3 block shows the same sequence but starting from $k=2$

$$\left(\frac{\|\Psi x_p^{k+1}-\Psi x_p^k\|}{\|\Psi x_p^{k+1}\|}\right)_{k=2,\ldots,10}\quad\text{for } p=0.1,0.2,\ldots,0.9,$$

and the last one shows

$$\left(\frac{\|\Psi x_p^{k+1}-\Psi x_p^k\|}{\|\Psi x_p^{k+1}\|}\right)_{k=3,\ldots,10}\quad\text{for } p=0.1,0.2,\ldots,0.9.$$

We plotted the same sequence with $k\geq 2$ and $k\geq 3$ just for better visual assessment of the error curves. It can be observed that the relative error decreases very quickly to zero which suggest fast numerical convergence of the algorithm. However, the method seems to become less stable for very small p which is visible in the third 3×3 block plot for $p=0.1$.

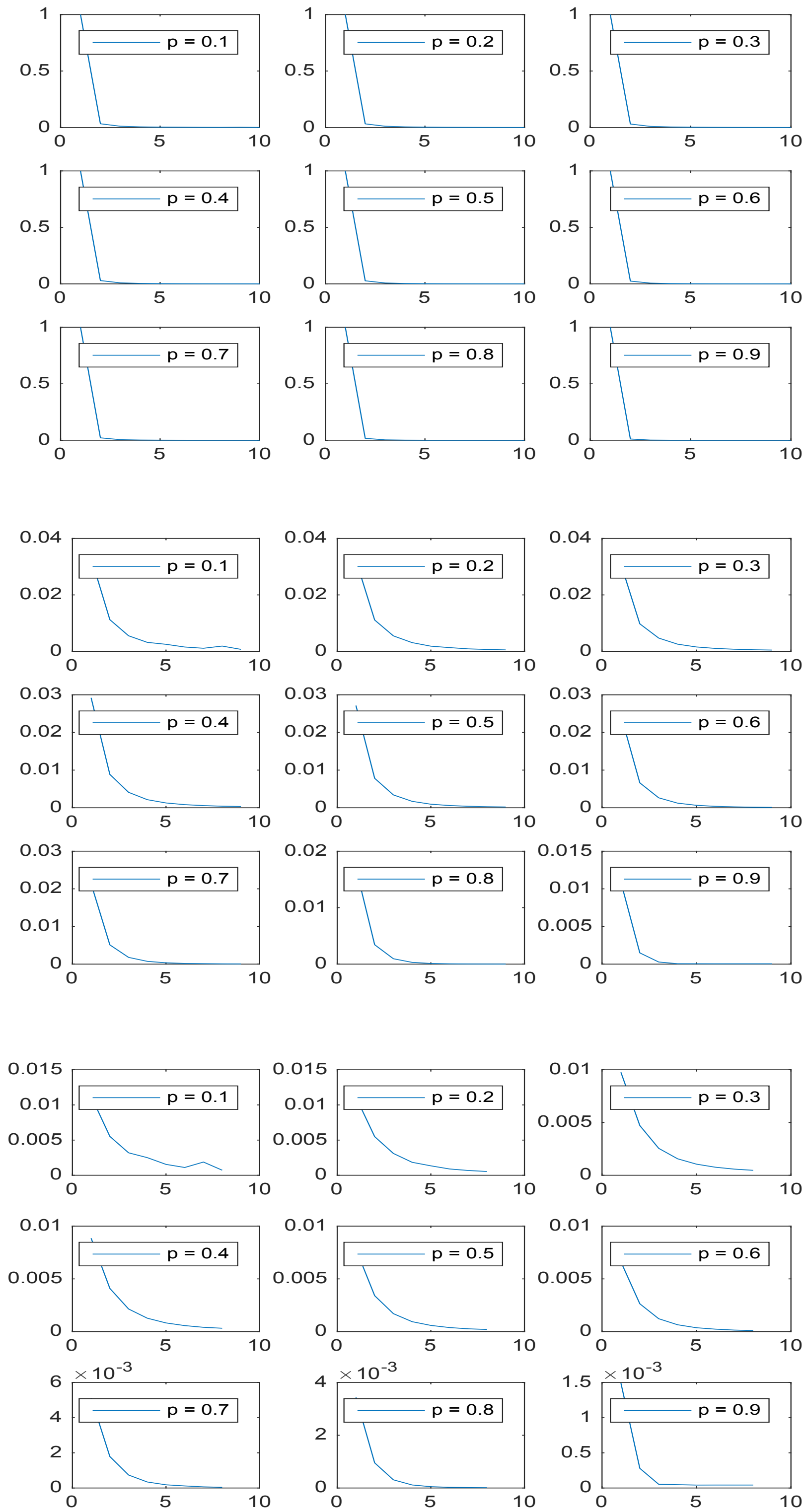

Figure 4.6: Relative error of the sequence of iterations. Starting from $k = 1, 2$, and 3, respectively.

Chapter 5

A multilevel based reweighting algorithm

In this chapter we present an algorithm that was developed by the author of this thesis and his collaborator in [MM16] which combines several ideas from compressed sensing and optimization. Moreover, the algorithm is used to compute the numerical experiments shown in Chapter 6 of this thesis. The upcoming presentation contains large parts of [MM16].

In the next two section we recall some basics that we need in order to formalize our algorithm. First, we recall some basics about *reweighted ℓ^1-minimization* and then, about the *split Bregman algorithm*.

5.1 Reweighted ℓ^1-minimization

Standard ℓ^1-minimization

In this thesis we have considered different types of analyses for the compressed sensing reconstruction problem that is finding x from the equation

$$Ax = y, \tag{5.1}$$

where y is a vector representing the acquired data, A is a sensing matrix, and x is the object of interest or some intermediate object that can be processed to the sought object. For example, x could be a coefficient vector that leads to the sought object of interest by using a synthesis operation. Recall that the common approach to obtain solutions of (5.1) is to solve the convex optimization problem

$$\min_{x \in \mathbb{C}^n} \|x\|_1 \quad \text{subject to} \quad Ax = y. \tag{5.2}$$

However, there is also an additional step that one can do on top of (5.2) which is to solve the problem iteratively again by adding weights, similar as we did in the previous chapter. Before we present our idea and the resulting algorithm, we first recall the basic idea behind *reweighted ℓ^1-minimization* in the next section which was first developed by Candès et al. in [CWB08].

Reweighted ℓ^1-minimization

In order to improve on the recovery model and to strengthen the effect of sparsity in the minimization problem Candès and his collaborators have introduced *reweighted* ℓ^1 in [CWB08].

The idea is as follows. Suppose $x_0 = (x_{0,1}, \ldots, x_{0,n}) \in \mathbb{C}^n$ is s-sparse. Further let $y \in \mathbb{C}^m$ be the measurements of x_0 where the measurement process is represented by a matrix $A \in \mathbb{C}^{m \times n}$ with $m < n$ and consider the optimization problem

$$\operatorname{argmin}_x \|x\|_1 \quad \text{subject to} \quad Ax = y. \tag{5.3}$$

When solving the minimization problem (5.3) iteratively, one would ask for the following effect: large coefficients should be quickly identified, whereas small coefficients should be neglected since they are most likely to be zero in the true signal. Such a behaviour can be obtained by introducing a diagonal $n \times n$ weighting matrix W defined by

$$W_{i,i} = \begin{cases} \frac{1}{|x_{0,i}|}, & x_{0,i} \neq 0 \\ \infty, & x_{0,i} = 0, \end{cases} \tag{5.4}$$

in the minimization problem (5.3), that is to consider

$$\operatorname{argmin}_x \|Wx\|_1 \quad \text{subject to} \quad Ax = y. \tag{5.5}$$

However, since x_0 is usually unknown such weights are infeasible. Therefore in [CWB08] the authors have proposed adaptive weights that change at each iteration depending on the previously computed solution x^k which should serve as an approximation of the weights corresponding to the true signal x_0. This leads to the following iteration of minimization problems

$$x_{k+1} = \operatorname{argmin}_u \|W^k x\|_1 \quad \text{subject to} \quad Ax = y, \tag{5.6}$$

with weighting matrix

$$W^k_{i,i} = \frac{1}{|x_{k,i}| + \varepsilon},$$

where $\varepsilon > 0$ is a stability parameter and the initial weighting matrix W^0 is set to be the identity. In a series of numerical experiments it was shown in [CWB08] that such reweighting methods find sparse solution much faster with significantly reduced errors.

5.2 Split Bregman

Split Bregman (SB) is an algorithm to solve constrained optimization problems by introducing split variables and then solve the resulting decoupled problems with *Bregman Iterations*. SB was by Goldstein and Osher in [GO09] and has since then become a popular algorithm to solve regularized inverse problems [COS10, WT10, PM11, STS10]. We now present the basic SB algorithm for ℓ^1-regularized problems and thereby follow the presentation given in [OBG$^+$05, GO09, YOGD08].

Consider the minimization problem

$$\min_x \|W\Psi x\|_1 \quad \text{subject to} \quad \|y - Ax\|_2 \leq \sigma, \tag{5.7}$$

for a possibly redundant dictionary $\Psi \in \mathbb{R}^{N\times n}$, a measurement matrix $A \in \mathbb{R}^{m\times n}$, a fidelity parameter $\sigma > 0$, and an $N \times N$ diagonal weighting matrix $W = \operatorname{diag}(W(l))$ for $l = 1, \dots, N$. Then instead of using a continuation method for enforcing the constraint, i.e. taking $\beta \to \infty$ in

$$x = \operatorname{argmin}_x \|W\Psi x\|_1 + \frac{\beta}{2}\|y - Ax\|_2^2,$$

problem (5.7) is transformed into a sequence of unconstrained problems using *Bregman iterations*

$$\begin{cases} x_{k+1} = \operatorname{argmin}_x \|W\Psi x\|_1 + \frac{\beta}{2}\|y - Ax + y_k\|_2^2, \\ y_{k+1} = y_k + y - Ax_{k+1}. \end{cases} \tag{5.8}$$

We continue by introducing a split variable $d = \Psi x$ for the ℓ^1-part of the minimization problem (5.8) and executing an additional Bregman iteration step to obtain

$$\begin{cases} (x_{k+1}, d_{k+1}) & = \operatorname{argmin}_{x,d} \|Wd\|_1 + \frac{\beta}{2}\|y - Ax + y_k\|_2^2 + \frac{\mu}{2}\|d - \Psi x - b_k\|_2^2, \\ b_{k+1} & = b_k + \Psi x_{k+1} - d_{k+1}, \\ y_{k+1} & = y_k + y - Ax_{k+1}. \end{cases}$$

To solve the (x, d)-minimization problem one or multiple *nonlinear block Gauss-Seidel* iterations are used, which alternate between minimizing with respect to x and d. This yields the *Split Bregman Algorithm*

for $i = 1 : N$ **do**
  $x_{k+1} = \operatorname{argmin}_u \frac{\beta}{2}\|y - Ax + y_k\|_2^2 + \frac{\mu}{2}\|d^{\text{current}} - \Psi x - b_k\|_2^2$
  $d_{k+1} = \operatorname{argmin}_d \|Wd\|_1 + \frac{\mu}{2}\|d - \Psi c^{\text{current}} - b_k\|_2^2,$
end for
$b_{k+1} = b_k + \Psi c_{k+1} - d_{k+1},$
$y_{k+1} = y_k + y - Ac_{k+1},$

Algorithm 2: Split Bregman algorithm

where x^{current} denotes the latest available variable. Note that the solution of the d-subproblem is explicitly given by *soft-thresholding*

$$d_{k+1}(l) = \operatorname{shrink}\left(\left(\Psi x^{\text{current}}\right)(l) + b_k(l), \frac{1}{\mu}W(l)\right),$$

for $l = 1, \dots, N$ and

$$\operatorname{shrink}(z, \lambda) = \begin{cases} \frac{\max(\|z\| - \lambda, 0)}{\|z\|} z, & z \neq 0, \\ 0, & z = 0. \end{cases}$$

In [GO09] it was furthermore observed that the minimization with respect to x in (2) does not need to be solved to full precision and in many applications only few steps of an iterative method are sufficient.

Total generalized variation

Total variation based methods were initially proposed by Rudin, Osher, and Fatemi in 1992 for image denoising [ROF92] and are now widely used for image reconstruction and in compressed sensing, see, for example, [WYYZ08, NW13]. TV is based on the model assumption that the image of interest is gradient sparse. A TV regularized minimization results in reconstructions where sharp edges are preserved, however, for realistic images, which are usually not piecewise constant and are not truly gradient sparse, this can lead to the so-called *oil painting artifacts* or *staircasing effects* leading to unnatural looking reconstruction. Among others, *Total Generalized Variation* (TGV), has been proposed as a generalization of TV to improve on these issues by involving higher order derivatives [BKP10]. We will now briefly recall the definition and some basics for the second order TGV regularizer in $\mathbb{R}^2$. This is mainly to fix the notation. Its general derivation and more details can be found in [BH14, BH15a, BKP10, BH15b, BH15c].

The so-called *pre-dual* formulation of second order TGV is given by

$$\mathrm{TGV}_\alpha^2(x) = \sup\left\{ \int_\Omega x \operatorname{div}^2 v \, dt : v \in C_c^2(\Omega, \mathcal{S}^{2\times 2}), \|v\|_\infty \le \alpha_0, \|\operatorname{div} v\|_\infty \le \alpha_1 \right\}, \tag{5.9}$$

for $\alpha = (\alpha_0, \alpha_1) \in \mathbb{R}_+^2$, $\Omega \subseteq \mathbb{R}^2$ a bounded domain with a smooth boundary curve, $\mathcal{S}^{2\times 2}$ the space of symmetric 2×2 matrices and $x \in L^1(\Omega)$. Thereby the divergences are defined as

$$(\operatorname{div} v)_i = \sum_{j=1}^{2} \frac{\partial v_{ij}}{\partial t_j}, \qquad i = 1, 2,$$

and

$$\operatorname{div}^2 v = \sum_{i,j=1}^{2} \frac{\partial^2 w_{ij}}{\partial t_i \partial t_j},$$

together with the norms

$$\|v\|_\infty = \sup_{l\in\Omega} \left(\sum_{i,j=1}^{2} |v_{ij}(l)|^2 \right)^{1/2},$$

and

$$\|\operatorname{div} v\|_\infty = \sup_{l\in\Omega} \left(\sum_{i=1}^{2} |(\operatorname{div} v)_i(l)|^2 \right)^{1/2}.$$

Under certain conditions, an equivalent and more convenient form of TGV_α^2 is given by the *minimum representation* as

$$\mathrm{TGV}_\alpha^2(x) = \inf_{v\in \mathrm{BD}(\Omega,\mathbb{C}^2)} \alpha_1 \|\nabla x - v\|_1 + \alpha_0 \|\mathcal{E}(v)\|_1, \tag{5.10}$$

where $\mathrm{BD}(\Omega)$ is the space of symmetric tensor fields of bounded deformation and $\mathcal{E}$ the symmetrized derivative defined as

$$\mathcal{E}(v) = \begin{pmatrix} \partial_{t_1} v_1 & \frac{1}{2}(\partial_{t_2} v_1 + \partial_{t_1} v_2) \\ \frac{1}{2}(\partial_{t_2} v_1 + \partial_{t_1} v_2) & \partial_{t_2} v_2 \end{pmatrix}.$$

In this form TGV_α^2 can be interpreted as balancing the first and second derivatives of x controlled by the ratio of α_0 and α_1. In [BKP10] and [KBPS11] it was observed that the use of TGV as a regularizer indeed leads to reconstructed images with sharp edges but without the staircaising effects of TV.

5.3 Multilevel based reweighting algorithm

In this section we explain how we incorporate the ideas of reweighted ℓ^1-minimization into the split Bregman algorithm for multilevel sparsifying transforms combined with a joint TGV regularizer. We mainly integrate the reweighting process into the split Bregman algorithm by adapting the soft-thresholding procedure accordingly. The additional TGV regularizer is added, in order to reduce artifacts and improve the reconstruction of piecewise constant regions. This idea of combining a multiscale transform such as shearlets with TGV has already been studied in great detail by Guo et al. in [GQY14], although without any reweighting strategy. The algorithm therein is build on an ADMM approach to solve the optimization problem and is therefore due to the natural connection to the split Bregman framework also related to the algorithm that we present.

Let A be a measurement operator, y the measurements of our signal of interest x, and let $\varepsilon > 0$ be a fidelity parameter. The recovery problem can then be stated as

$$\min_x \sum_{j=1}^{\infty} \lambda_j \|W_j \Psi_j x\|_1 + \mathrm{TGV}_\alpha^2(x) \quad \text{subject to} \quad \|y - Ax\|_2 \leq \sigma,$$

where Ψ_j corresponds to the j-th level of the multilevel transform with analysis operator Ψ, λ_j are regularization parameters accounting for the multilevel structure of Ψ and W_j are diagonal weights. For the sake of clearness we assume that there is only one subband per level. Otherwise an additional index has to be attached to Ψ_j to specify the current subband. Note that after we have established a basic split Bregman framework for solving the minimization problem we will aim to update λ_j and W_j iteratively. Using the characterization of TGV_α^2, the objective can be rewritten as

$$\min_{x,v} \sum_{j=1}^{\infty} \lambda_j \|W_j \Psi_j x\|_1 + \alpha_1 \|\nabla x - v\|_1 + \alpha_0 \|\mathcal{E}(v)\|_1. \tag{5.11}$$

For the *discretization* let $x \in \mathbb{R}^{n^2}$ be the vectorized finite-dimensional image of interest which is for simplicity assumed to be of square size. Let $A \in \mathbb{R}^{m \times n^2}$ be the finite dimensional measurement matrix and $y \in \mathbb{R}^m$ the observed data. Let ∇^f and ∇^b denote a discrete gradient operator with periodic boundary conditions using forward and respectively backward differences. Following [BKP10, BH15c] we approximate the derivatives in (5.11) by

$$\nabla x \approx \nabla^f x = \begin{pmatrix} \nabla_1^f x \\ \nabla_2^f x \end{pmatrix}$$

and

$$\mathcal{E}(v) \approx \mathcal{E}^b v = \begin{pmatrix} \nabla_1^b v_1 & \frac{1}{2}(\nabla_2^b v_1 + \nabla_1^b v_2) \\ \frac{1}{2}(\nabla_2^b v_1 + \nabla_1^b v_2) & \nabla_2^b v_2 \end{pmatrix}.$$

A finite dimensional approximation of (5.11) is then given by

$$\min_{x,v} \sum_{j=1}^{J} \lambda_j \|W_j \Psi_j x\|_1 + \alpha_1 \|\nabla^f x - v\|_1 + \alpha_0 \|\mathcal{E}^b v\|_1, \tag{5.12}$$

where J is some fixed a priori chosen maximum scale and Ψ is the discrete transform acting on the vectors. For wavelets and shearlets this is greatly documented in the literature, see Chapter 8 in [Wal02] for wavelets and [KLR16] for shearlets. Note that the ℓ^1-norm in the second summand is thereby defined as

$$\|v\|_1 = \sum_{l=1}^{n^2} \left(|v_1(l)|^2 + |v_2(l)|^2\right)^{1/2},$$

and for the third summand as

$$\|e\|_1 = \sum_{l=1}^{n^2} \|e(l)\|_F = \sum_{l=1}^{n^2} \left\| \begin{pmatrix} e(l)_1 & e(l)_2 \\ e(l)_2 & e(l)_3 \end{pmatrix} \right\|_F,$$

where $\|\cdot\|_F$ is the Frobenius norm of a 2×2 matrix.

Split Bregman framework

The proposed constrained optimization problem can be casted into the form given in (5.7) by introducing the variable $\mathbf{x} = (x, v)^T$ together with the matrix

$$\boldsymbol{\Psi} = \begin{pmatrix} \Psi & 0 \\ \nabla^f & -I \\ 0 & \mathcal{E}^b \end{pmatrix}.$$

In order to come up with the explicit form of the resulting split Bregman algorithm as given in Section 5.2, let us split as follows:

$$\begin{pmatrix} w \\ d \\ t \end{pmatrix} = \begin{pmatrix} \Psi x \\ \nabla^f x - v \\ \mathcal{E}^b v \end{pmatrix}.$$

The (x, v)-subproblem of Algorithm 2 is then given by

$$(u_{k+1}, v_{k+1}) = \operatorname{argmin}_{x,v} \frac{\beta}{2}\|y - Au + y_k\|_2^2 + \frac{\mu_1}{2}\|w^{\text{current}} - \Psi x - b_k^w\|_2^2$$

$$+ \frac{\mu_2}{2}\|d^{\text{current}} - (\nabla^f x - v) - b_k^d\|_2^2 + \frac{\mu_3}{2}\|t^{\text{current}} - \mathcal{E}^b v - b_k^t\|_2^2. \tag{5.13}$$

We furthermore obtain the subproblems

$$w_{k+1}^j = \operatorname{argmin}_{w^j} \lambda_j \|W_j w^j\|_1 + \frac{\mu_1}{2}\|w^j - \Psi_j x^{\text{current}} - b_k^{w,j}\|_2^2, \tag{5.14}$$

for $j = 1, \dots, J$, as well as

$$d_{k+1} = \operatorname{argmin}_d \alpha_1 \|d\|_1 + \frac{\mu_2}{2}\|d - (\nabla^f x^{\text{current}} - v^{\text{current}}) - b_k^d\|_2^2, \tag{5.15}$$

and

$$t_{k+1} = \operatorname{argmin}_t \alpha_0 \|t\|_1 + \frac{\mu_3}{2}\|t - \mathcal{E}^b v^{\text{current}} - b_k^t\|_2^2. \tag{5.16}$$

Note that the regularization parameters λ_j, α_0 and α_1 have thereby been subsumed into a weighting matrix W and that we are allowing some more flexibility by incorporating different values for μ_i for $i = 1, 2, 3$. Furthermore we obtain the following *Bregman updates:*

$$\begin{cases} b_{k+1}^w &= b_k^w + \Psi x_{k+1} - w^{k+1}, \\ b_{k+1}^d &= b_k^d + (\nabla^f x_{k+1} - v_{k+1}) - d_{k+1}, \\ b_{k+1}^t &= b_k^t + \mathcal{E}^b v_{k+1} - t_{k+1}, \end{cases}$$

as well as

$$y_{k+1} = y_k + y - Au_{k+1}.$$

Solutions of the subproblems

The solution of the subproblem (5.13) can be obtained by setting the first derivatives with respect to x, v_1 and v_2 to zero. This results in the following linear system

$$\begin{pmatrix} b_1 & b_4^* & b_5^* \\ b_4 & b_2 & b_6^* \\ b_5 & b_6 & b_3 \end{pmatrix} \begin{pmatrix} u \\ v_1 \\ v_2 \end{pmatrix} = \begin{pmatrix} R_1 \\ R_2 \\ R_3 \end{pmatrix}, \tag{5.17}$$

where b_i are $n^2 \times n^2$ block matrices defined as

$$\begin{aligned} b_1 &= \beta A^* A + \mu_1 \Psi^* \Psi + \mu_2 (\nabla^f)^* \nabla^f, \\ b_2 &= \mu_3 (\nabla_1^b)^* \nabla_1^b + \frac{\mu_3}{2}(\nabla_2^b)^* \nabla_2^b + \mu_2 I, \\ b_3 &= \mu_3 (\nabla_2^b)^* \nabla_2^b + \frac{\mu_3}{2}(\nabla_1^b)^* \nabla_1^b + \mu_2 I, \\ b_4 &= -\mu_2 \nabla_1^f, \\ b_5 &= -\mu_2 \nabla_2^f, \\ b_6 &= \frac{\mu_3}{2}(\nabla_1^b)^* \nabla_2^b, \end{aligned}$$

and the components of the right hand side are given by

$$\begin{aligned}
R_1 &= \beta A^*(y+y_k) + \mu_1 \Psi^*(w^{\text{current}} - b_k^w) + \mu_2(\nabla^f)^*(d^{\text{current}} - b_k^d),\\
R_2 &= \mu_2(b_{k,x}^d - d_x^{\text{current}}) + \mu_3\left((\nabla_1^b)^*(t_1^{\text{current}} - b_{k,1}^t) + (\nabla_2^b)^*(t_2^{\text{current}} - b_{k,2}^t)\right),\\
R_3 &= \mu_2(b_{k,y}^d - d_y^{\text{current}}) + \mu_3\left((\nabla_1^b)^*(t_2^{\text{current}} - b_{k,2}^t) + (\nabla_2^b)^*(t_3^{\text{current}} - b_{k,3}^t)\right).
\end{aligned}$$

Similar to [GO09], it was observed in [GQY14], that in many cases the linear system in (5.17) can be efficiently solved by using the 2D-Fourier transform $\mathcal{F} \in \mathbb{C}^{n^2 \times n^2}$. Note that ∇^f and ∇^b are circulant since they correspond to periodic boundary conditions. Therefore

$$\mathcal{F}^* \nabla^* \nabla \mathcal{F}$$

is a diagonal matrix.

In case of Fourier measurements that are generated using the `fft2` the measurement matrix can be written as

$$A = P\mathcal{F},$$

where $P \in \{0,1\}^{m \times n^2}$ is a binary matrix selecting the measurements. In this case

$$A^*A = \mathcal{F}^* P \mathcal{F}$$

is naturally diagonalized by the 2D Fourier transform.

If all blocks b_i for $i = 1, \ldots, 6$ can be diagonalized in this way, the authors of [GQY14] proposed to multiply with a preconditioner matrix from the left to obtain the system

$$\begin{pmatrix} \widehat{b_1} & \widehat{b_4}^* & \widehat{b_5}^* \\ \widehat{b_4} & \widehat{b_2} & \widehat{b_6}^* \\ \widehat{b_5} & \widehat{b_6} & \widehat{b_3} \end{pmatrix} \begin{pmatrix} \mathcal{F}u \\ \mathcal{F}v_1 \\ \mathcal{F}v_2 \end{pmatrix} = \begin{pmatrix} \mathcal{F}R_1 \\ \mathcal{F}R_2 \\ \mathcal{F}R_3 \end{pmatrix}, \tag{5.18}$$

where each $\widehat{b_j} = \mathcal{F} b_j \mathcal{F}^*$ is a $n^2 \times n^2$ diagonal matrix. A closed form solution can then be obtained by applying Cramer's rule. The solutions of the other subproblems are obtained in closed-form by shrinkage again:

$$w_{k+1}^j(l) = \operatorname{shrink}\left(\left(\Psi_j x^{\text{current}}\right)(l) + b_k^{w,j}(l), \frac{\lambda_j W_j(l)}{\mu_1}\right), \tag{5.19}$$

for $l = 1, \ldots, N_j - N_{j-1} + 1$. For equation (5.15) we obtain

$$d_{k+1}(l) = \operatorname{shrink}_2\left(\nabla^f x^{\text{current}}(l) - v^{\text{current}}(l) + b_k^d(l), \frac{\alpha_1}{\mu_2}\right),$$

for $l = 1, \ldots, n^2$ and the shrinkage rule

$$\operatorname{shrink}_2(x, \lambda) = \begin{cases} \frac{\max(\|x\|_2 - \lambda), 0)}{\|x\|_2} x, & x \neq 0, \\ 0, & x = 0. \end{cases}$$

Similarly, the solution of (5.16) is given by

$$t_{k+1}(l) = \text{shrink}_F\left(\left(\mathcal{E}^b v^{\text{current}}\right)(l) + b_k^t(l), \frac{\alpha_0}{\mu_3}\right),$$

for $l = 1, \dots, n^2$ and

$$\text{shrink}_F(x, \lambda) = \begin{cases} \frac{\max(\|x\|_F - \lambda), 0)}{\|x\|_F} x, & x \neq 0, \\ 0, & x = 0. \end{cases}$$

Combining reweighted ℓ^1 with multiscale transforms

Recall that the guiding principle of reweighted-ℓ^1 is that small coefficients of an iterative solution are likely going to be zero in the true signal. However, this principle is not necessarily valid for multiscale sparse signals, i.e. signals that can be sparsely represented under a multiscale transform. The magnitudes of multiscale coefficients naturally decrease with increasing scales, but the high scale nonzero coefficients of an iterative solution are not necessarily less important or more likely zero in the actual signal, if compared to low scale coefficients which are intrinsically larger. In the following section we are aiming to compensate for this misfit by including additional weighting parameters for each level in the transformation.

Suppose $x \in \mathbb{R}^{n^2}$ is the true signal and

$$\Psi x = (\Psi_j x)_{j=0,\dots,J} = (\langle \psi_{j,l}, x \rangle)_{j=0,\dots,J, l=1,\dots,N_j} \tag{5.20}$$

are the analysis coefficients divided into J subbands with $N_j \in \mathbb{N}$ many elements per level. In [AS15] a multi dictionary reweighting algorithm was proposed which iteratively updates λ_j^k in the objective of

$$x^{k+1} = \text{argmin}_x \sum_{j=0}^{J} \lambda_j^k \|W_j \Psi_j x\|_1, \quad \text{subject to} \quad \|y - Ax\|_2 \leq \sigma, \tag{5.21}$$

by setting

$$\lambda_j^k = \frac{N_j}{\varepsilon + \|\Psi_j x^k\|_1}, \tag{5.22}$$

and $W_j = I$ for all iterations of solving (5.21). It was shown therein that the resulting algorithm can be interpreted as applying a Majorization-Minimization algorithm to the unconstrained formulation of (5.21) with regularizer

$$\sum_{j=0}^{J} N_j \log\left(\varepsilon + \|\Psi_j x\|_1\right).$$

This update rule was proposed in [AS15] for a composition of multiple different dictionaries instead of just one multiscale dictionary divided into its subbands. In the latter case it seems to be less likely to expect that $\log\left(\varepsilon + \|\Psi_j x\|_1\right)$ promotes the sparsity structure

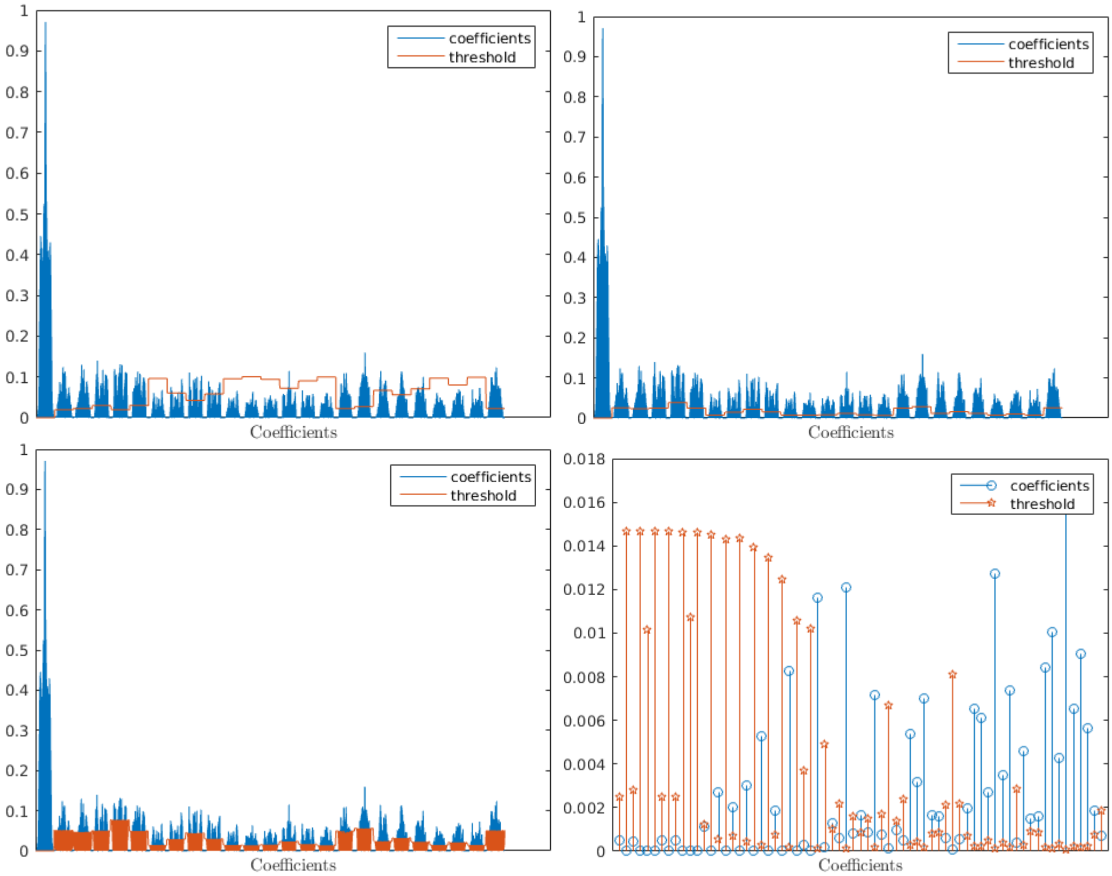

Figure 5.1: **Upper left**: Coefficients of in blue with a multi-level reweighting curve as in (5.22) in orange. **Upper right**: Coefficients in blue with multi-level curve in orange using (5.24) only. **Lower left**: Coefficients with the proposed reweighting strategy in orange. **Lower right**: Zoom of proposed multilevel reweighting strategy.

of x within each of the subbands Ψ_j sufficiently. Indeed, as it was argued in [CWB08], the log-sum penalty is more sparsity enforcing than the ℓ^1-norm by putting a larger penalty on small nonzero coefficients. In the case of the ℓ^1-norm of an entire subband this approach seems to be less effective in promoting the sparsity within each level. It was furthermore proposed in [AS15] to combine the update rule (5.22) with the classical elementwise reweighting update

$$W_j = \operatorname{diag}\left(\frac{1}{\varepsilon + |\langle \psi_{j,l}, x^k\rangle|}\right), \tag{5.23}$$

for $j = 1, \ldots, J$. However, note that this combination is very different to what we are aiming for, since there is even more emphasize put on penalizing the smaller coefficients in higher levels which can happen to delete too many highscale coefficients.

This fact is visualized from a different point of view in Figure 5.1, where we have depicted the shearlet coefficients of a MRI phantom introduced in [GKLPU12] together with the reweighting rule we have just discussed in the top-left of the figure. The shearlet

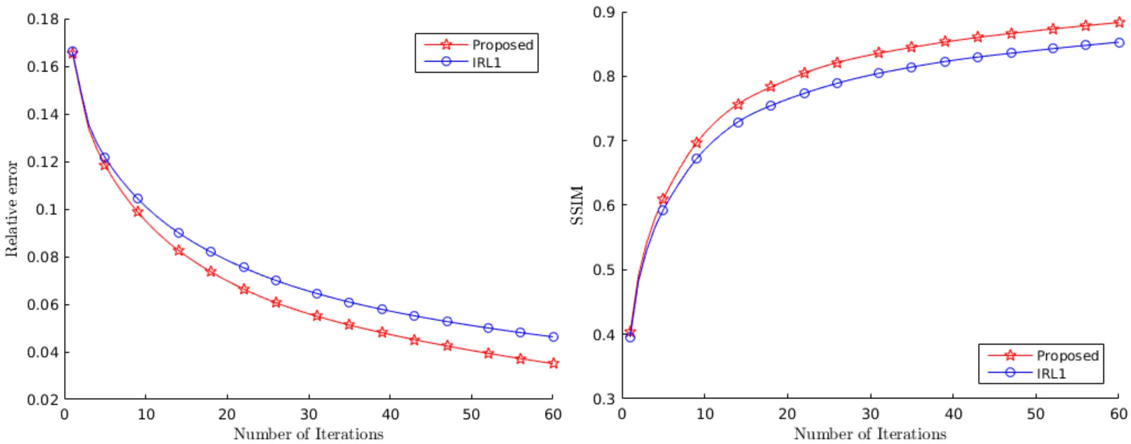

Figure 5.2: Convergence plot: Behavior of the error and structured similarity index for reweighting with true shearlet coefficients with respect to increasing number of iterations. Used signal: phantom from [GKLPU12]. Reconstructed from 6%(!) of Fourier data with proposed algorithm without TGV. In IRL1 we are choosing W_j as in (5.23) and λ_j constant and for the proposed emthod we additionally define λ_j as in (5.24). **Upper figure**: Relative error of in each iteration. **Lower figure**: SSIM of each iteration.

coefficients are depicted in blue and the values of $\frac{\lambda_j}{\mu_1}$ for a realistic value μ_1 are shown in orange. Note that according to the update rule (5.19) of the split Bregman algorithm everything below the orange curve would be thresholded.

Proposed method

Considering the previous discussion one of the disadvantages is that the weights corresponding to higher levels might become too large. This can be prevented, for instance, by choosing the regularization parameters as

$$\lambda_j = \max \left\{ |\langle \psi_{j,l}, x \rangle| : l = 1, \ldots, N_j \right\}, \tag{5.24}$$

for $j = 1, \ldots, J$ and zero otherwise, i.e. if $j = 0$. Note that we exclude the subband for $j = 0$ since for real life signals the low frequency part is usually not sparse. This was also proposed in [SF09], where it was shown that this idea can be accomplished more effectively using an analysis prior. For some exotic signals it might happen that the magnitude of the analysis coefficients are very irregular per level, in particular one could have strong outliers. For such cases it might be better to take a quantile instead of the maximum. However, for our test images this will not happen and thus we have used the maximum. Also note that this is a heuristic rule accounting for the unknown constant in the theoretical decay of the multilevel coefficients. A schematic representation from the thresholding perspective of split Bregman can be found in the second image of Figure 5.1.

Our proposed method combines the classical reweighting of (5.23) with the above choice for λ_j. The idea behind this is that we are still using the power of pointwise iterative reweighting, but since our multiscale coefficients naturally come in levels of different orders of magnitude, we apply it to each level separately weighted with λ_j. That means that within each level we follow the democratic philosophy of reweighting which is that small coefficients of the current iterate $\Psi_j u^{\text{current}}$ are likely to be zero in u. By multiplying with the latter choice of λ_j we also gain more control and account for the multilevel structure of Ψu. An artificial experiment using the (in reality unknown) true analysis coefficients demonstrates that this update rule does seem to perform better than standard reweighting without such a compensation of multilevel weights, see Figure 5.2. For the signal u we are choosing the phantom of [GKLPU12]. Using the usually unknown shearlet coefficients for the construction of λ_j and W_j for $j = 1, \ldots, J$ as explained above we are reconstructing u from only 6% of its Fourier measurements obtained by radial lines through the k-space origin by using the proposed algorithm of the last section, but without the additional TGV regularizer. Note that both reconstructions approximately start with the same error, which indicates that the set of regularization parameters is chosen equally good. However, it can be said that tuning the iterative reweighted shrinking method within the split Bregman framework without the automatic choice of the subband-weights λ_j is rather difficult and highly signal dependent. This example further shows the potential of reweighting as the data is significantly undersampled.

Proposed algorithm

Having explained the idea of our method, we now state the final resulting algorithm that is a composition of the split Bregman framework for solving the constrained optimization problem (5.12) and the previously explained idea of multilevel weighting and iteratively reweighting, respectively. In contrast to the traditional reweighted-$\ell 1$ approaches we do not iterate between solving the ℓ^1-problem up to convergence and updating the weights. We propose to incorporate the multilevel adapted reweighting rule directly into the split Bregman algorithm. This is done in such a way that only the shrinking of the w-subproblem is changed to a *multilevel adapted, iteratively reweighted shrinking rule*. Note that by choosing the level-weights λ_j depending on the magnitude of the signal coefficients the resulting method appears to stable towards the alternation of signals.

Another advantage is that we observe in our numerical experiments that the computational complexity stays almost the same. In comparison to the traditional split Bregman approach we are adding only the updates of W_j and λ_j within each iteration. However, due to the iteratively selected weights this could potentially lead to a much faster algorithm.

We like to comment on two things regarding the algorithm above. First, the weighting matrix W_j depends on the initialization of an $\varepsilon > 0$. The choice of ε is rather empirical and many cases does not effect the solution. This was already noticed in the beginning of reweighted-ℓ^1 in [CWB08]. This is also the case for our algorithm. The role of ε is essentially to bound the maximum threshold that the algorithm will perform. It provides stability by preventing a division by zero, but the magnitude of the coefficient is mostly determined by the respective analysis coefficient. It is also common to decrease ε iteratively as it is assumed that the more iterations one runs, the closer one gets to actual coefficients of the signal. However, this appears unnecessary for us and is not further considered.

Furthermore, we have not incorporated an additional stopping criterion besides a maximum number of iterations. For our algorithm it does not seem to be necessary as

Input:
Measurement operator A, multilevel transform Ψ,
regularization parameters: $\alpha_0, \alpha_1, \mu_1, \mu_2, \mu_3, \beta$,
iteration numbers N and maxIter.
Data:
Measured data y.
Initialization:
$k \leftarrow 0$;
$u_0 \leftarrow A^* y$;
$y_0, v_0, d_0, w_0, t_0, b_0^t, b_0^d, b_0^w \leftarrow 0$;
while $k \leq$ maxIter **do**
  for $i = 1, \ldots, N$ **do**
    $(u_{k+1}, v_{k+1}) \leftarrow$ solve linear system (5.18);
    for $j = 1, \ldots, J$ **do**
      $\lambda_j = \max \{ |\langle \psi_{j,l}, u \rangle| : l = 1, \ldots, N_j \}$;
      $W_j = \operatorname{diag}\left(\frac{1}{\varepsilon + |\langle \psi_{j,l}, u^{\text{current}} \rangle|} \right)$;
      $w_{k+1}^j(l) \leftarrow \operatorname{shrink}\left(\left(\Psi_j u^{\text{current}} \right)(l) + b_k^{w,j}(l), \frac{\lambda_j W_j(l)}{\mu_1} \right), \quad l = 1, \ldots, N_j$;
    end for
    $d_{k+1}(l) \leftarrow \operatorname{shrink}_2 \left(\nabla^f u^{\text{current}}(l) - v^{\text{current}}(l) + b_k^d(l), \frac{\alpha_1}{\mu_2} \right), \quad l = 1, \ldots, N_j$;
    $t_{k+1}(l) \leftarrow \operatorname{shrink}_F \left(\left(\mathcal{E}^b v^{\text{current}} \right)(l) + b_k^t(l), \frac{\alpha_0}{\mu_3} \right), \quad l = 1, \ldots, N_j$;
  end for
  $b_{k+1}^w \leftarrow b_k^w + \Psi u_{k+1} - w_{k+1}$;
  $b_{k+1}^d \leftarrow b_k^d + (\nabla^f u_{k+1} - v_{k+1}) - d_{k+1}$;
  $b_{k+1}^t \leftarrow b_k^t + \mathcal{E}^b v_{k+1} - t_{k+1}$;
  $y_{k+1} \leftarrow y_k + y - A u_{k+1}$;
  $k \leftarrow k + 1$;
end while
return Reconstruction u_{maxIter}.

Algorithm 3: Proposed algorithm

the convergence plots suggest, see Figure 5.2, 5.4 and 5.5.

5.4 Numerics

In this section we will recover several different signals from their Fourier measurements. This is a typical problem in applied mathematics, which has a wide range of applications. One of the most known applications is magnetic resonance imaging (MRI) where data is collected in the so-called *k-space* which is the Fourier domain, i.e. every point in the k-space can be interpreted as a Fourier coefficient of the object of interest. This is also one of the very first areas where compressed sensing has had a great impact, see, for instance [LDP07].

We will now present some extensive numerical testings that verify the performance of the proposed algorithm for the particular setup where Fourier measurements are taken. However, we like to mention that our algorithm is implemented for very general sampling operators. These can, for example, be binary masks as in inpainting or non-uniform Fourier operator for more sophisticated sampling patterns in MRI.

We have chosen the following three criteria that we wish to analyse our algorithm on:

(N1) Quality,

(N2) Convergence,

(N3) Stability.

For (N1) we compare our algorithm with different existing and established methods that are known to perform well in the recovery problem from Fourier measurements these methods are shown in Table 5.1.

For (N2) we use two quality measurements. First, the relative error which is computed by the formula

$$\mathrm{RE} = \frac{\|x^{\mathrm{ref}} - x^{\mathrm{rec}}\|_2}{\|x^{\mathrm{ref}}\|_2}$$

where x^{ref} is the reference image and x^{rec} the reconstructed image. Second, we use the structural similarity index that as introduced in [ZBSS04]. This value can be directly computed in MATLAB.

The stability (N3) is verified by the fact that we have chosen the same parameters for each multiscale transform across all experiments. Although an extensive tuning of all parameters for different images might yield superior results we have chosen not to do so. The reason behind is two-fold: First, our algorithm already performance very well with a fixed choice of parameters for all different images used in this section. Second, iterative reweighting combined with the proposed multilevel weighting strategy already suggests the level of thresholds for all coefficients and should therefore be less sensitive to the choice of additional parameters.

Numerical setup

The sparsifying transforms that we use in the numerical experiments of this section are the wavelet transform and the shearlet transform. We first give some more details about the parameters that are used and then proceed with the results.

As for wavelets we have used the undecimated 2D wavelet transform provided by the `spot` package available at

`http://www.cs.ubc.ca/labs/scl/spot/`

Unless it is stated differently we have used a 4 scale Daubechies-2 wavelet system. The chosen parameters for the proposed algorithm (WIRL1 + TGV) are

- ▷ μ: [6e2 1e1 2e1],
- ▷ α: [1 2],
- ▷ β: 1e4,
- ▷ ε: 1e-4.

For shearlets we have used the shearlet transform from the `ShearLab` package available at

`http://www.shearlab.org/`

The discrete shearlet system is generated by using 4 scales and [1 1 2 2] for the directional parameters. Further parameters for the proposed algorithm (SIRL1 + TGV) are chosen as follows:

- ▷ μ: [5e3 1e1 2e1],
- ▷ α: [1 1],
- ▷ β: 1e5,
- ▷ ε: 1e-5.

The performance of the algorithm certainly depends on the parameter set. However, it is very stable with respect to different type of images once a proper parameter set is chosen. In fact, all experiments of this section are computed with the same parameter set given above. The parameter that is most sensitive is ε. This is to be expected as this is the parameter that controls the maximum magnitude of the thresholding value.

Comparison with other methods

Fourier inverse	Fourier inversion of data
RecPF	Total variation and wavelet regularization from [WYYZ08]
FFST+TGV	Shearlets with TGV from [GQY14]
Co-IRL1	Composite iterative reweighting from [AS15]
PANO	Patch-based nonlocal operator, [QHL+14]
TV	Total variation with our algorithm
TGV	Total generalized variation with our algorithm
WL1	Wavelets without reweighting
WIRL1	Wavelets with proposed reweighting
WIRL1+TGV	Wavelets with proposed reweighting and TGV
SL1	Shearlets without reweighting
SR + TGV	Shearlets with standard reweighting and TGV
SIRL1	Shearlets with proposed reweighting
SIRL1+TGV	Shearlets with proposed reweighting and TGV

Table 5.1: Table for abbreviations

Our first experiment shows the recovery from a 256×256 rose image available from the open source framework

`http://aforgenet.com/framework/`

We used 30 radial lines through the k-space origin ($\approx 12,2\%$ of Fourier data) to represent the subsampling pattern. The data is then obtained by a pointwise multiplication in `MATLAB` by multiplying the mask with the Fourier transformed image. This is then used as the measured subsampled Fourier data.

We then compared our results obtained by the proposed algorithm for wavelets as a sparsifying transform. Our resulting reconstruction, shown in Figure 5.3 is obtained by using the proposed iterative multi-level reweighting strategy as well as an additional generalized total variation regularizer. In the same figure, we compare are results to RecPF by Yang et al. [WYYZ08], Co-IRL1 by Ahmad and Schniter [AS15], PANO by Qu et al. [QHL+14], and FFST+TGV by Guo et al. [GQY14]. In order to make the experiments comparable we have used the same scales and number of directions in [GQY14]. Furthermore, for Co-IRL1 we have used two redundant Daubechies wavelet dictionaries with the same number of scales. More precisely, one dictionary consists of Haar wavelets (Daubechies 2) and the second one of Daubechies 4 wavelets. It can be observed that the recovery obtained by the proposed method shows the least amount of artifacts while still recovering all structures.

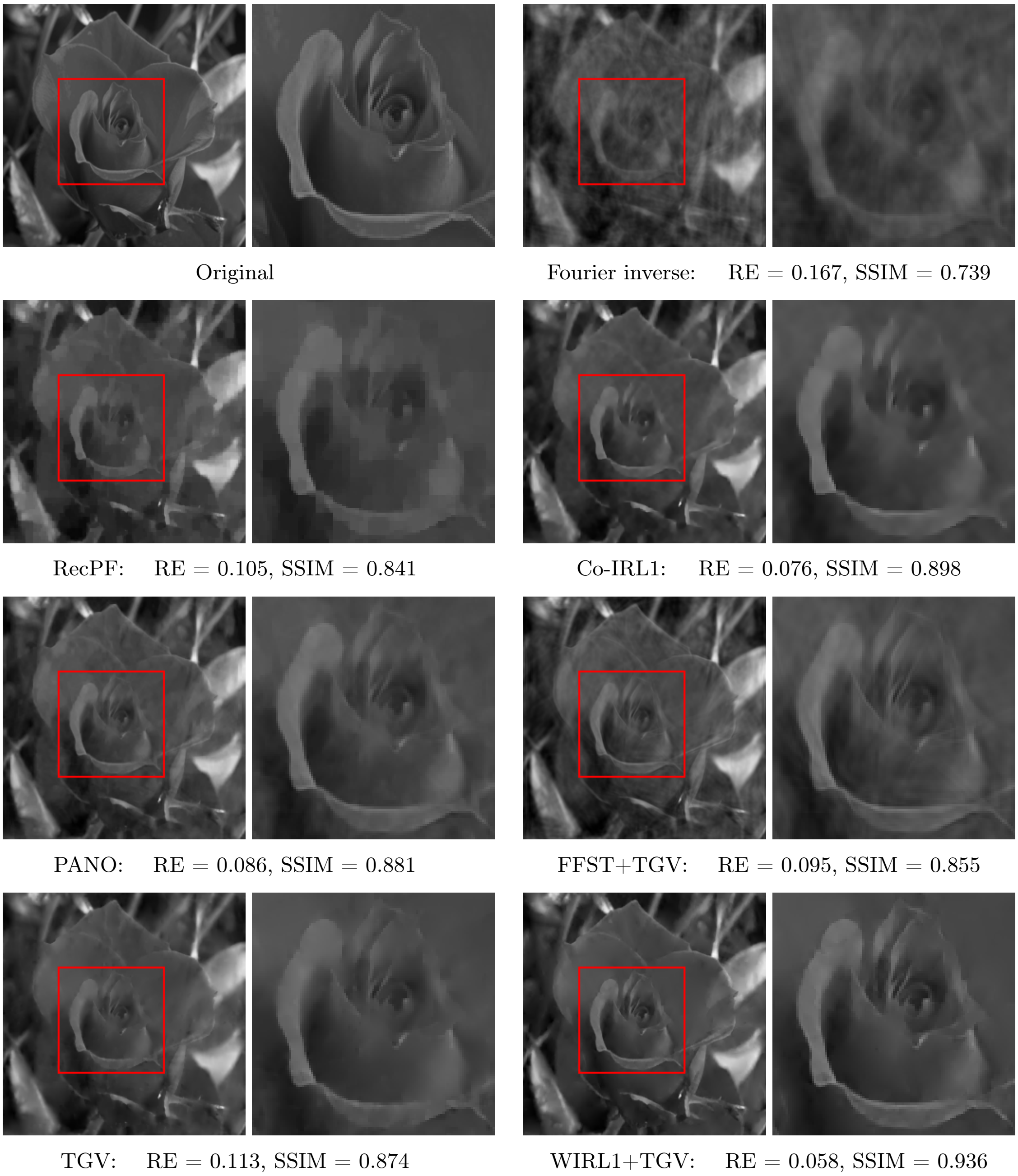

Figure 5.3: Different reconstructions from 30 radial lines ($\approx 12,2\%$) through the k-space origin with relative error and structured similarity index. 50 iterations are used for the reconstruction. See Table 5.1 for used abbreviations.

Convergence, signal independence, and the effect of reweighting

In this section we analyze (N2) for our algorithm. We do this by considering two images, one that is well suited for wavelets and the other one where shearlets perform better. We start with a 256×256 phantom that was designed by Guerquin-Kern et al. in

[GKLPU12] for MRI studies. As this image is piecewise constant we have chosen a 4 scale wavelet transform generated by Haar wavelets. We reconstructed the image using our algorithm for TV only, WL1, WIRL1 and WIRL1+TGV. Moreover, as this image is very compressible in a Haar wavelet basis, the recovery allows a much lower sampling rate. In fact, we have only used 21 radial lines which corresponds to only 8.73%. It is interesting to mention that the exact solution is returned after almost 80 iterations when WIRL1+TGV is used for 21 radial lines. Additionally, for 24 lines (≈ 9.83%) wavelets with the proposed iterative reweighting step (WIRL1) will eventually also return the exact solution, see Figure 5.4.

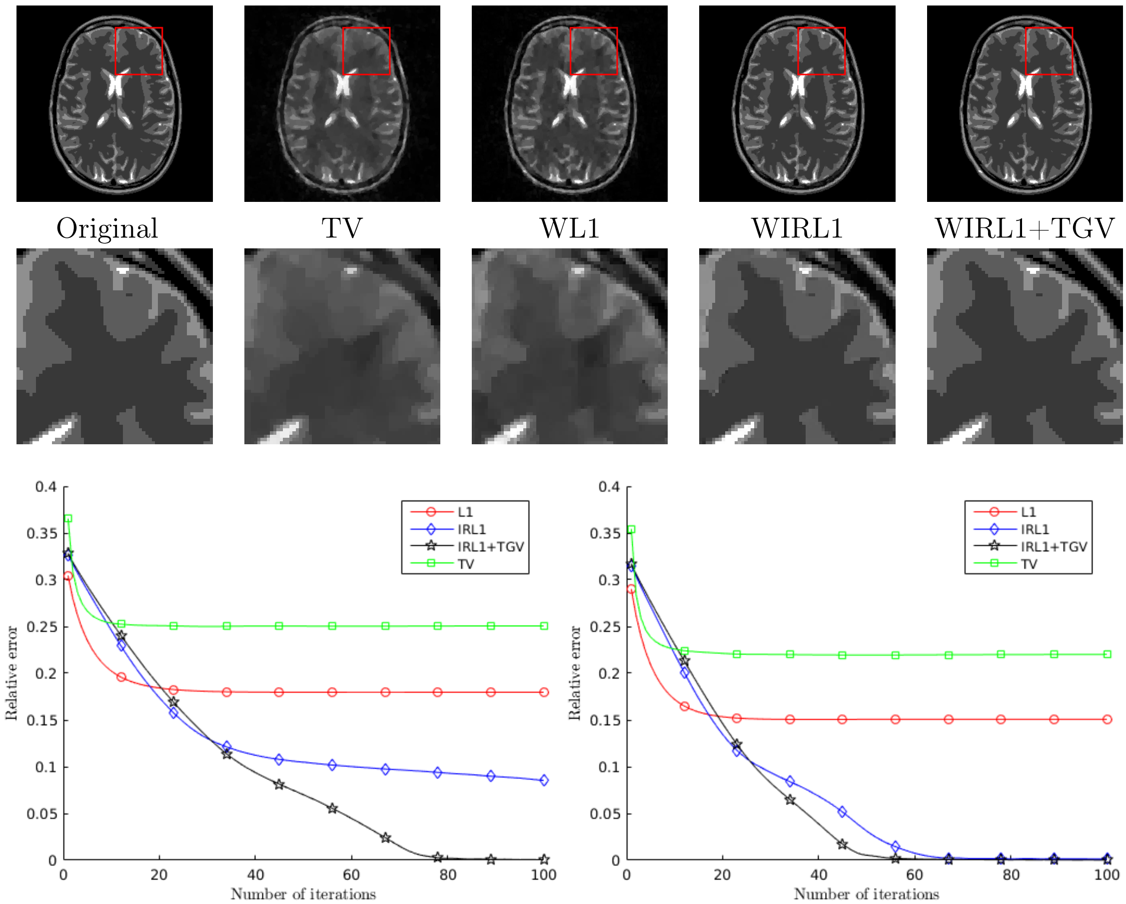

Figure 5.4: Different reconstructions from 24 radial lines through the k-space origin with relative error and structured similarity index. The lower left graphics corresponds to 21 radial lines (≈ 8.73%) and the lower right to 24 radial lines (≈ 9.83%). 100 iterations are used for the reconstruction. See Table 5.1 for used abbreviations.

Our third numerical example concerns the 256 × 256 pepper image, see Figure 5.5. It has many more structures than the previously considered GLPU phantom. More importantly, it does not consist of piecewise constant areas. This image is particularly well suited for shearlets and thus we have chosen the shearlet transform with four scales. We have compared three different scenarios. First, without any reweighting or exploitation of the multilevel structure, in fact, we have used a fixed threshold (SL1). The second image (SR+TGV) uses reweighting with TGV, but not with the proposed multilevel adaption of the weights. The third image shows the proposed method (SIRL+TGV) which, in particular, exploits the multilevel structure of the transform coefficients. It reduces the artefacts, caused by the subsampling, significantly and thus suggests a better treatment of the sparsity structure.

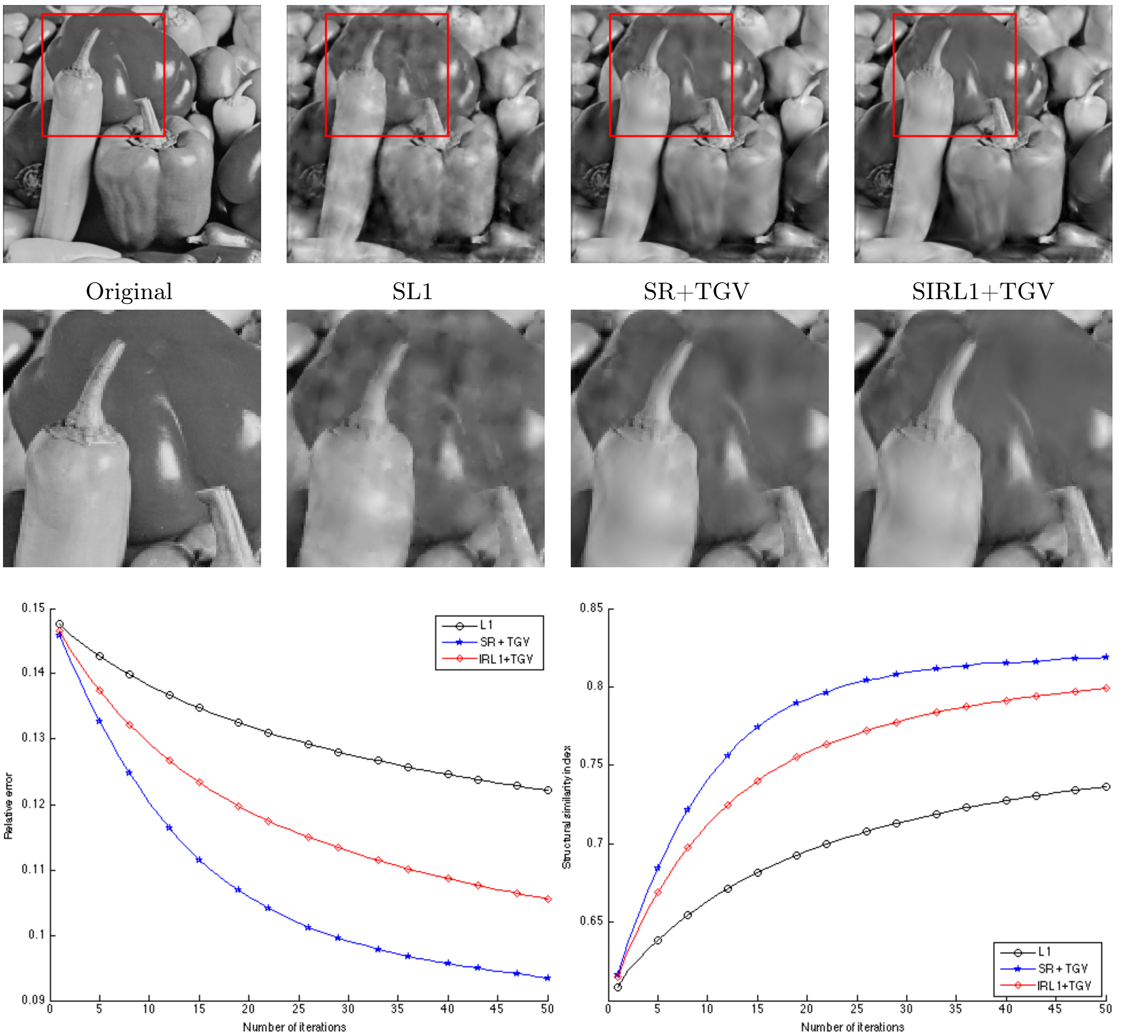

Figure 5.5: Different reconstruction from 30 radial lines ($\approx 12,2\%$) through the k-space origin with relative error and structured similarity index. See Table 5.1 for used abbreviations. 50 iterations are used for the reconstruction. The two graphs at the bottom show the relative error and the structural similarity index with respect to the number of iterations.

Concluding remarks

Our algorithm shows that standard methods – such as the split Bregman algorithm – can be significantly improved by adding a reweighting strategy for the sparsifying coefficients. Furthermore, this reweighting strategy should take into account the multilevel structure, as we have demonstrated in Figure 5.5. Furthermore, due to the reweighting strategy the parameter set becomes relatively stable to an alternation of the image that is to be reconstructed.

As a further step, one could consider a non-convex optimization problem by using the ℓ^p-quasi norm for $p \in (0, 1)$ and then work with a reweighting strategy that depends on p. This has not been tested yet, but could be worth to be considered in more detail in the future, as we have seen in Chapter 4 that ℓ^p-minimization can improve the recovery significantly.

Finally, the algorithm is implemented is a very general manner. In particular, the sampling operator and the sparsifying transform are part of the input arguments and can, thus, be directly changed.

Part II

Applications

Chapter 6

Magnetic resonance imaging

In this chapter we present some results of the application of shearlets using the algorithm from Chapter 5 to real experimental MR data. This results will be discussed more intesively in the upcoming work [MMK$^+$16].

It was mentioned multiple times in this thesis that the measurement process in MRI can be understood as sampling Fourier coefficients of the signal of interest. In the next section we want to make this a little bit more precise and discuss the inverse problem that is considered in MRI. However, our presentation is from a medical and physical perspective rather loose and we refer to [Kol12, BCH$^+$14, WKM09] for more details about the medical and physical backgrounds.

6.1 Reconstruction problem

Magnetic resonance imaging is an imaging technique that relies on the spin angular momentum of hydrogen atoms. In particular, magnetic gradient fields can be applied in order to align all hydrogen atoms into one specified direction. After the magnetic gradient field is switched off the spinning atoms will align back to their initial position thereby inducing a signal that is measured by receiver coils implemented in the MRI machine. This signal y then represents frequency information an image - or volume in the 3D case - x. Indeed, the acquired signal y is called *k-space* information and can be written as the Fourier transform of x with respect to specific frequencies.

Mathematically speaking, the discretized problem can be formalized as follows: In order to obtain the image of interest one has to solve the inverse problem

$$Ax = y, \tag{6.1}$$

where y represents the acquired k-space information, A is the sampling operator that is essentially a partial Fourier matrix and hence, not invertible. However, in practice different modalities can lead to better conditioned sampling matrices A and thus lead to better image reconstructions. We shall next discuss one particular method which is *parallel magnetic resonance imaging*.

Encoding operator A for pMRI

From now on we will call A *encoding operator* instead of sampling operator in order to emphasize that the encoding process consists of several operations other than acquiring partial samples of the Fourier transform as we will explain now. Indeed, in *parallel MRI* (pMRI) additional sensitivity coils are involved where each coil has characterizing sensitivity profiles that are responsible for certain (different) areas of the k-space. This is additional information of the acquired signal and can be used for an enhanced image recovery ([PWSB99]).

The sampling matrix A in the inverse problem (6.1) is now a concatenation of the form

$$A = PFS,$$

where PF is a partial Fourier matrix with possibly non-uniform samples and S is a sensitivity matrix. Depending on the number of sensitivity profiles $N_s \in \mathbb{N}$ we obtain N_s equations of the form

$$A_{n_s} = PFS_{n_s}x = y, \quad n_s = 1, \dots, N_s. \tag{6.2}$$

Each solution x_{n_s} of these equations can then be combined, for instance, by using the sum of squares method [PWSB99]. Therefore the decoding operation A^* of the encoding operator A is considered to be the concatenation of the following operations: First, apply the inverse Fourier transform to each of k-spaces, then a multiplication with the respective sensitivity maps followed by a combination of the single coil images by, for instance, sum of squares. The encoding operator A certainly does the opposite by applying the sensitivity maps first and then the partial Fourier transform.

In particular for the 3D case the encoding operator A, as well as its adjoint operation A^* is even more evolved, since it requires an additional handling of *motion artefacts*.

6.2 Data

The data that we use in the following experiment is k-space data that was acquired using a radial 3D sampling scheme according the golden radial phase encoding (GRPE) as documented in [WSK$^+$07]. The data was acquired and provided by the Physikalisch-Technische Bundesanstalt Braunschweig und Berlin (PTB). In particular, 9216 lines per coil were acquired in total. Furthermore, 8 coils were used for the sensitivity resulting in a k-space of dimension $192 \times 9216 \times 8$ (spatial resolution $\times$ number of lines $\times$ number of coils).

The reconstructed signal has a dimension of the size $192 \times 192 \times 192$ and represents a 3D volume in spatial domain.

6.3 Experiment

We recovered the data in the image domain using the algorithm presented in Chapter 5. In particular, the sparsifying transform is the 3D shearlet transform available from the package ShearLab [KLR16] which can be accessed at `www.shearlab.org/`

However, as the experiments in 3D are computationally very demanding we did not applied the iterative reweighting method, but instead used a fixed threshold in the algorithm presented in Chapter 5. For the shearlet system we have used 2 scales and 3 directions per scale.

The code for the encoding operator was provided by Dr. Christoph Kolbitsch from the PTB. Fruther, the experiments have been conducted in MATLAB on 'cluster16' of the math cluster of TU Berlin.

6.4 Results

In Figure 6.1 we present the result of the signal recovery from MR data using compactly supported shearlets in 3D. In particular, we depicted several different slices along different directions of the whole 3D volume. In the first column of Figure 6.1 we see a reconstruction by applying the inverse operation of the encoding operator. In the second column the reconstruction using shearlets is shown. As the reconstruction is a three dimensional object, say $x \in \mathbb{C}^{192\times192\times192}$ we show a slice along the first dimension, that is $x(n,:,:)$ for some $n \in \{1,\dots,192\}$ in the first row. where we have used the matlab notation ':' to indicate that the full size along the second and third dimension is used. Furthermore, single dimensions are squeezed, i.e. $x(:,:,n) \in \mathbb{C}^{192\times192}$. Similarly, the second row shows a slice through the second dimension and the third row shows the reconstruction along a slice in the third dimension, respectively.

Note that the shearlet reconstruction shows almost no streaking artifacts coming from the sampling pattern opposed also the background noise is reduced significantly. This is an advantage due to the three dimensional setup, as the background noise as well as the streaking artifacts have almost no three dimensional volume. Hence, these will not be picked up in the reconstruction using a 3D shearlet system. The same argument applies to other systems such as wavelets.

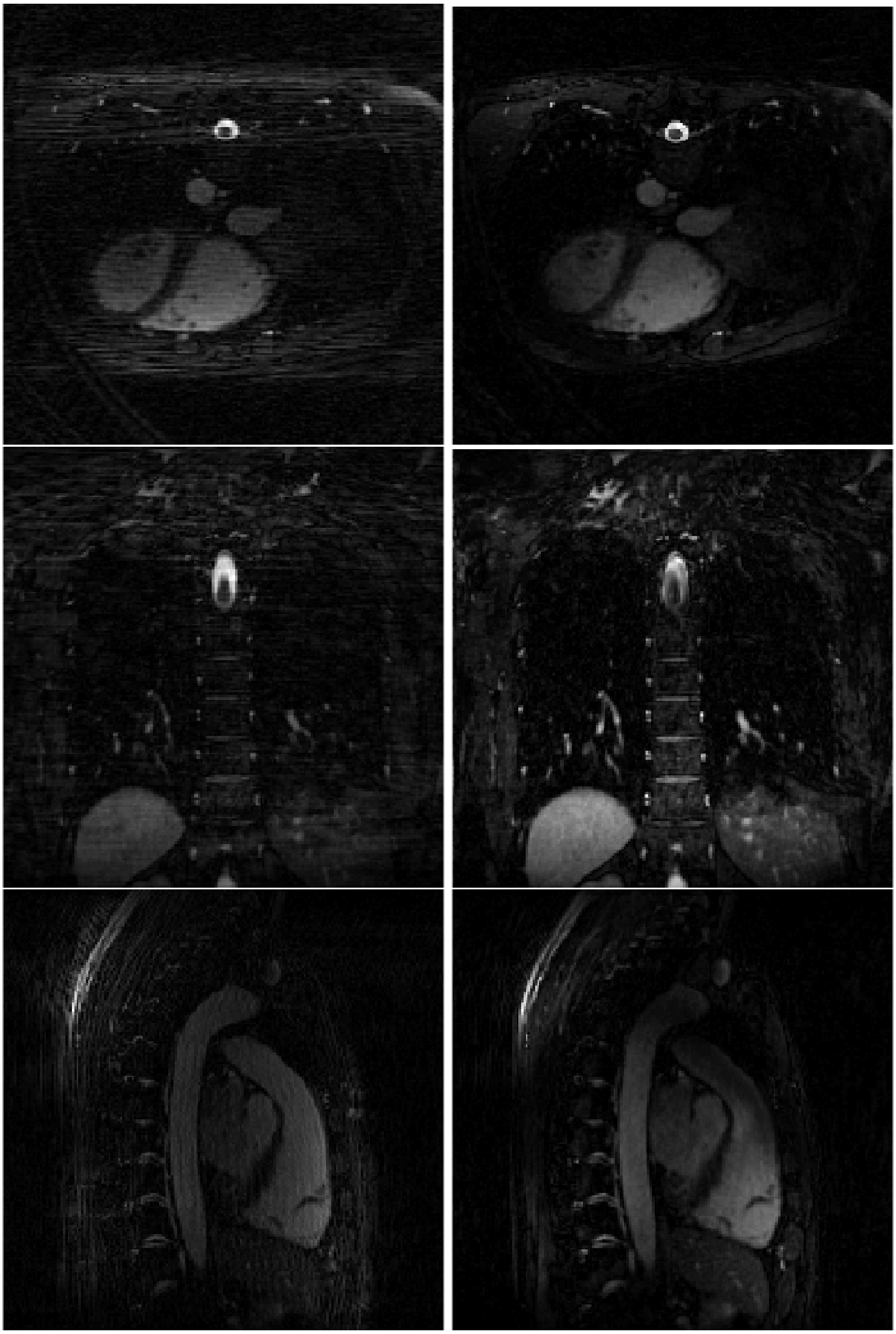

Figure 6.1: Comparison of reconstruction obtained by the inverse operation of the encoding operator (left) and the shearlet reconstruction (right). **First row:** Slice 140 along the first direction. **Second row:** Slice 65 along the second direction. **Third row:** Slice 85 along the third direction.

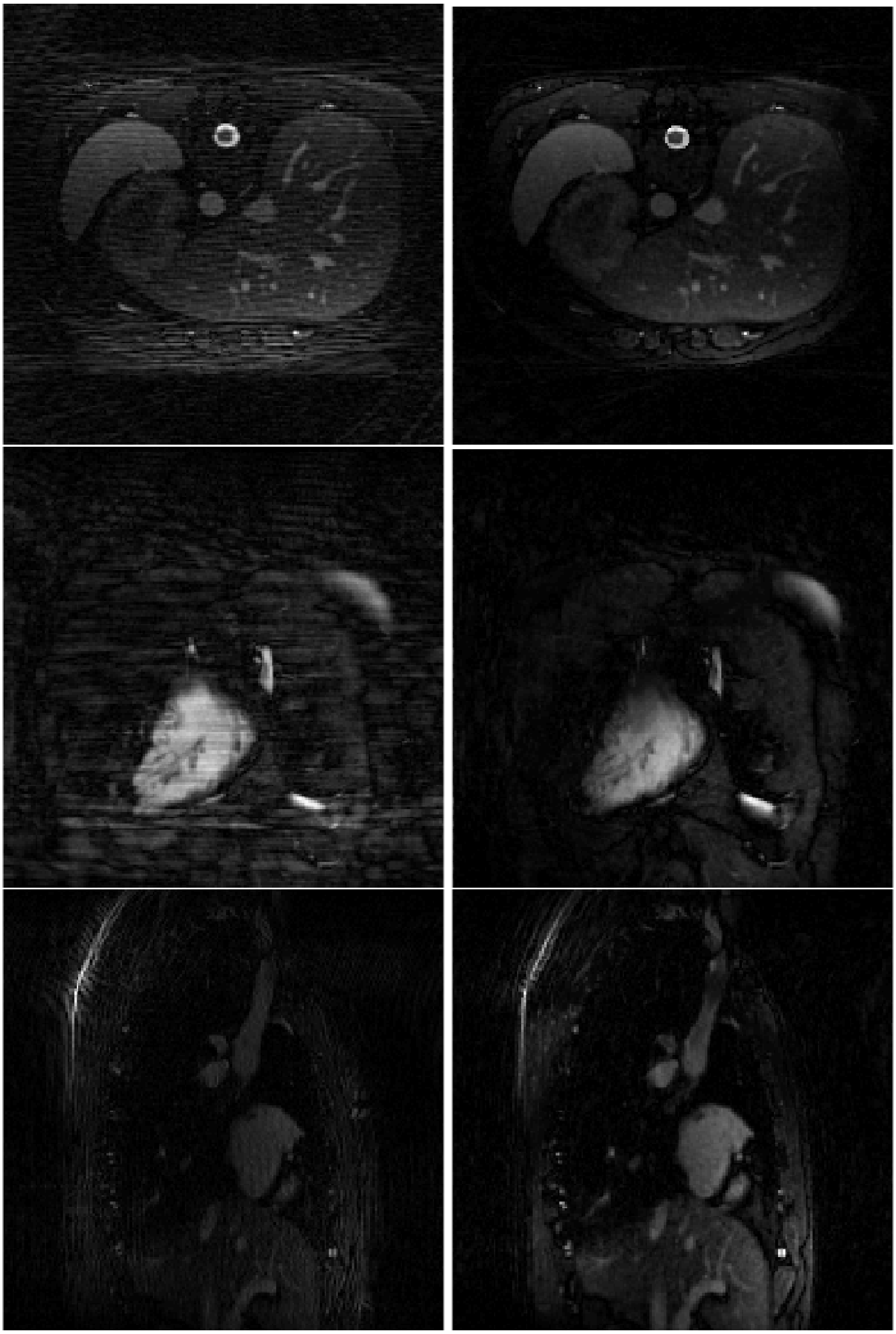

Figure 6.2: Comparison of reconstruction obtained by the inverse operation of the encoding operator (left) and the shearlet reconstruction (right). **First row:** Slice 170 along the first direction. **Second row:** Slice 140 along the second direction. **Third row:** Slice 120 along the third direction.

Chapter 7

Electron microscopy

In this chapter we briefly show a different application of shearlets to *signal transmission electron microscopy* (STEM) a problem that is located in the larger field *electron microscopy* (EM).

The results presented in this paper are obtained in the experimental paper [MBS+16] and we refer the reader to that work for more interest in the experimental setup, interest in the particular data sets or the application behind. Further, applications can also be found in [MHAS+16]. However, we briefly sketch the experiment in form of an inverse problem and wish to present the application of shearlets to this problem.

7.1 Reconstruction problem

In STEM small objects of nanosize can be visualized by scanning the object. The scanning is usually done pixelwise, which results in an inpainting problem. More precisely, suppose $x \in \mathbb{R}^{N \times N}$ is the object of interest and let $A \in \mathbb{R}^{N \times N}$ be a binary mask where 1 represents the measured pixel and 0 corresponds to a not having measured the pixel, see Figure 7.1. However, there is usually also a quite significant amount of noise on the data as we shall see in the data in Section 7.3.

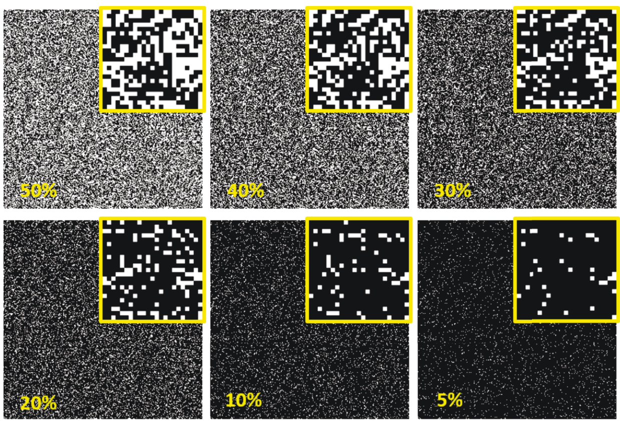

Figure 7.1: Random masks with different subsampling rates.

The reconstruction problem is then again to find x (the full image) from the equation

$$Ax = y, \tag{7.1}$$

where y is the masked data as visualized in Figure 7.2.

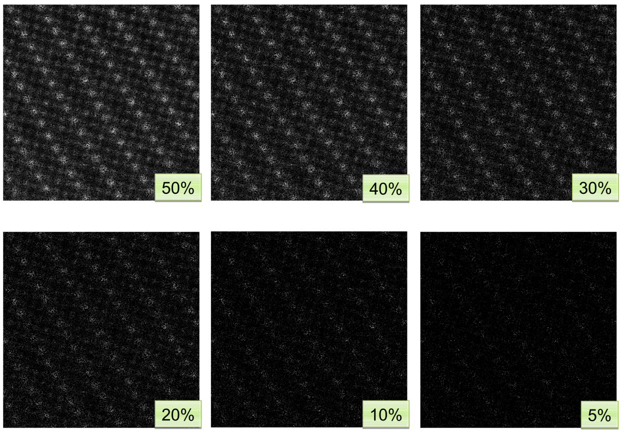

Figure 7.2: Masked data.

As the problem is ill-posed we regularized the inverse problem (7.1) using different methods known to work well in inpainting, indeed, in [MBS+16] we considered

$$\min_x \frac{1}{2}\|Ax - y\|_2^2 + \lambda J(x),$$

where J is a regularizing functional such as the composition of the ℓ^1 norm with a shearlet transform., wavelet transform, or cosine transform. Furthermore, a regularization based on total variation and total generalized variation has been considered as well.

7.2 Algorithm

The algorithm used for the wavelet-, shearlet- and cosine transform is an iterative thresholding algorithm which stems from [SED05, KLR16]. For the sake of completeness we present the algorithm here.

Let y be the masked data, A be the mask itself, $\lambda, \mu > 0$, and maxIter be the maximal number of iterations. Further, let thresh denote the thresholding operator given by

$$\mathrm{thresh}_\varepsilon(c(k)) = \begin{cases} c(k) & |c(k)| \geq \varepsilon, \\ 0 & \text{else.} \end{cases}$$

Further we use the matlab notation '$A.*B$' to denote the entrywise multiplication of the matrices A and B.

Input : $y, A, \lambda, \mu,$ maxIter.
Output: x
Initialize $x := 0, \varepsilon := \lambda, \delta := \mu^{1/(\text{maxIter}-1)}, k := 1$.
while $k \leq$ maxIter **do**
  $\widetilde{x} := A. * (y - x)$;
  $x := \widetilde{\Psi}^* \operatorname{thresh}_\varepsilon \Psi(y - x)$;
  $\varepsilon := \delta\varepsilon$;
  Increase $k \to k + 1$.
end

Algorithm 4: Algorithm used for image inpainting

7.3 Experiment

For the reconstruction we have applied Algorithm 4 to the shearlet transform again from

`www.shearlab.org/`

as well as the wavelet transform from the `spot` toolbox available at

`www.cs.ubc.ca/labs/scl/spot/`

For the cosine transform we have used the one available from MATLAB.

The data from where a reconstruction is to be computed is shown in Figure 7.2. Note that the image shows a very uniform chessboard pattern except for certain vacancies. Furthermore the objects are supposed to be round and smooth which suggest that these three transform should work fairly well. The computed reconstructions are shown in Figure 7.3.

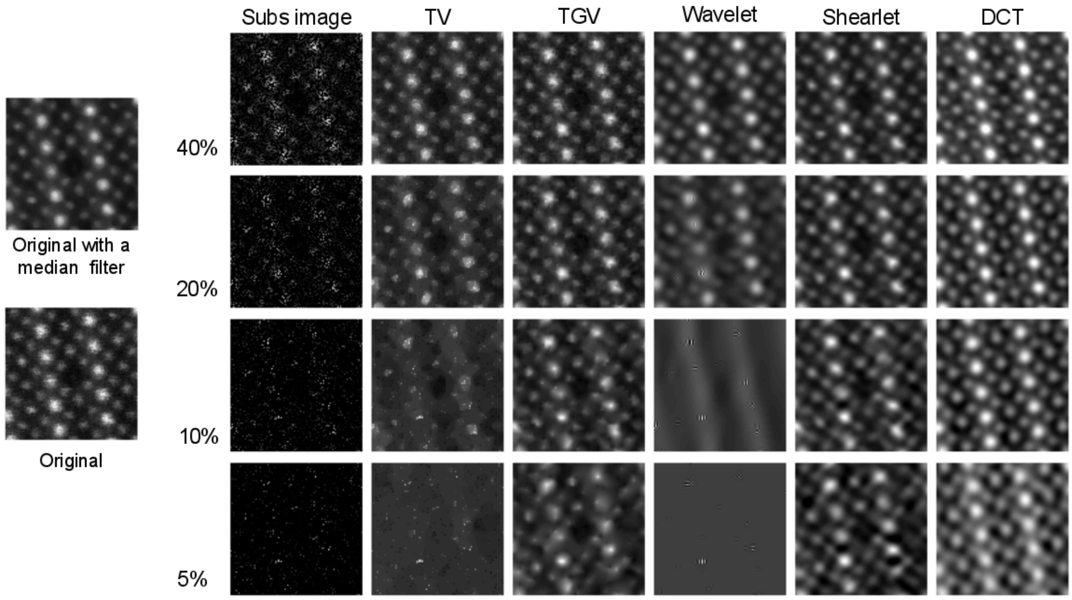

Figure 7.3: Reconstruction of oxides, [MBS+16]

As the original image contains a lot of noise it seems not appropriate to use standard image quality metrics such as relative error or peak-signal to noise ratio as we have chosen the parameters so that the noise is also thresholded. Instead we rely on the visual assessment and present line profiles in Figure 7.4. Indeed the line goes through the vacancy as shown in Figure 7.4. For a better quality assessment we also depicted the original fully sampled region in the same figure as well as a median filtered version that smoothes the data but reduces noise.

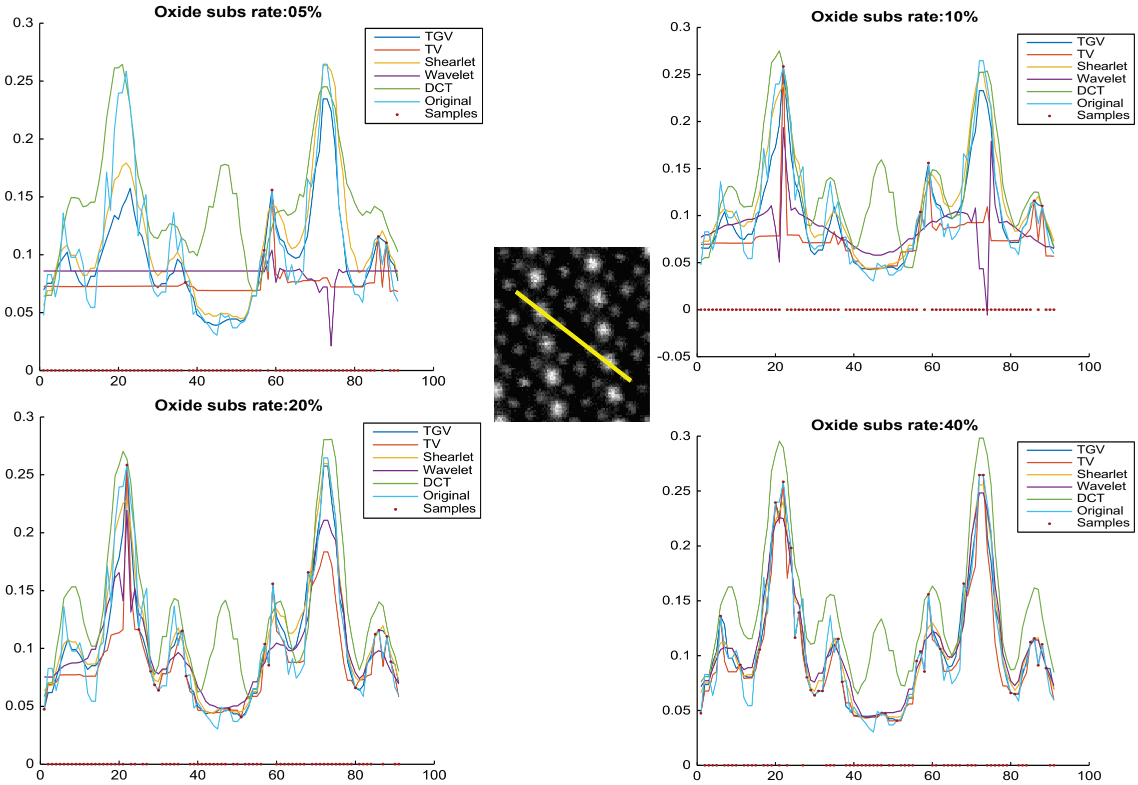

Figure 7.4: Line profiles for the reconstruction shown in Figure 7.3, [MBS+16]

7.4 Discussion

The reconstruction from shearlets, wavelets and cosines are much smoother than the reconstruction obtained from TV and TGV which is mainly the case because of the two different algorithms that have been used. For the TV and TGV reconstruction an interpolation based approach was used, see [MBS+16] and the references therein where Algorithm 4 thresholds transform coefficients and then synthesises the remaining coefficients in the respect system which in all three cases consists of smooth functions.

However, there are visual differences between these three transforms. For instance, using shearlets the elements to not appear perfectly round as the anisotropy destroys as well as the directionality is not capable of reproducing the structure. On the other hand, the cosine transform which uses smooth and periodic functions reconstruct perfectly round objects. However, due to the periodicity it also fills vacancies which where it should not. For wavelets the reconstruction do show a good shape of the atoms, however, as the transform is less redundant the algorithm suffers from stability issues and thus fails to reconstruct the object.

Overall it must be stated, that the optimal transform depends on the data.

Appendix

Appendix A

Frames

More than 60 years ago Duffin and Schaeffer introduced the concept of *frames* in [DS52]. Nowadays, they are widely used in applied harmonic analysis and we next give a short introduction about the basics of frame theory that are needed for the content of this thesis. For a more detailed presentation of frames we refer the reader to the excellent book [Chr03].

A.1 Basic definitions and properties

Recall that $\mathcal{H}$ denotes a (separable) Hilbert space.

Definition A.1 ([Chr03]). *A set of vectors $\Psi = \{\psi_\lambda : \lambda \in \mathbb{N}\} \subset \mathcal{H}$ is called a* frame *for $\mathcal{H}$, if there exist positive but finite constants c_1 and c_2 such that*

$$c_1\|f\|^2 \leq \sum_{\lambda\in\mathbb{N}} |\langle f, \psi_\lambda\rangle|^2 \leq c_2\|f\|^2 \quad \forall\, f \in \mathcal{H}. \tag{A.1}$$

The constants c_1 and c_2 are called lower frame bound *and* upper frame bound*, respectively. If c_1 equals c_2, then we we call the frame Ψ* tight*. Moreover, a tight frame with frame bound equal to one is called a* Parseval frame*.*

The frame bounds c_1 and c_2 in Definition A.1 are certainly not unique. Clearly, a multiplication of c_1 by a positive constant smaller than one and a multiplication of c_2 by a positive, but finite constant, larger than one gives rise to another pair of frame bounds. However, in some cases it is important to have the lower frame bound as large as possible and the upper frame bound as small as possible, respectively. In this case, if c_1 is the largest constants such that (A.1) holds, and c_2 is the smallest constant such that (A.1) holds, then we call these frame bounds *optimal*.

The *frame inequality* (A.1) guarantees the boundedness of the following two operators which we, by a slight abuse of notation, denote by Ψ and Ψ^*, respectively. In fact, the following *synthesis operator*

$$\begin{aligned} \Psi : \ell^2(\mathbb{N}) &\longrightarrow \mathcal{H} \\ (c_\lambda)_\lambda &\mapsto \sum_{\lambda\in\mathbb{N}} c_\lambda\psi_\lambda \end{aligned}$$

is a linear bounded operator. Its adjoint, called the *analysis operator*, is given by

$$\Psi^* : \mathcal{H} \longrightarrow \ell^2(\mathbb{N}),$$
$$f \mapsto (\langle f, \psi_\lambda \rangle)_{\lambda\in\mathbb{N}}.$$

The composition of the synthesis operator and the analysis operator is called the *frame operator* of the frame Ψ.

Theorem A.2 ([Chr03]). *Let Υ be the frame operator of a frame with frame bounds c_1 and c_2. Then Υ is a bounded, self-adjoint, invertible, and positive operator. Moreover, if c_1 and c_2 are the optimal frame bounds, then*

$$\|\Upsilon^{-1}\| = \frac{1}{c_1} \quad \text{and} \quad \|\Upsilon\| = c_2.$$

The inverse of a frame operator can be used to construct another frame in a very canonical way.

Theorem A.3 ([Chr03]). *Under the assumptions of Theorem A.2, with c_1 and c_2 not necessarily being optimal, the set of vectors*

$$\widetilde{\Psi} := \Upsilon^{-1}(\Psi) = \left\{\Upsilon^{-1}\psi_\lambda \,:\, \lambda \in \mathbb{N}\right\} =: \left\{\widetilde{\psi}_\lambda \,:\, \lambda \in \mathbb{N}\right\}$$

is a frame with frame bounds c_2^{-1} and c_1^{-1}. The frame operator associated to $\widetilde{\Psi}$ is Υ^{-1}.

The frame $\widetilde{\Psi}$ in Theorem A.2 is called *canonical dual frame of* Ψ. As already suggested by the name, the canonical dual frame is one among possibly many other *dual frames*, cf. Definition A.4.

Definition A.4 ([Chr03]). *Let $\Phi = \{\varphi_\lambda \,:\, \lambda \in\}$ and $\Psi = \{\psi_\lambda \,:\, \lambda \in\}$ be frames. If $\Psi^*\Phi = \mathrm{Id}$, i.e.*

$$f = \sum_{\lambda\in\mathbb{N}} \langle f, \varphi_\lambda \rangle \psi_\lambda, \quad \forall\, f \in \mathcal{H}$$

then Φ is called a dual frame *of Ψ.*

In general a frame possess more than just one dual. Li characterized in [Li11] the set of all duals. In fact, he proved the following result.

Theorem A.5 ([Li11]). *Let Ψ be a frame. Then all left inverses of the analysis operator Ψ are given by*

$$\widetilde{\widetilde{\Psi}}^* = \Upsilon^{-1}\Psi^* + \Upsilon(\mathrm{Id} - \Psi\Upsilon^{-1}\Psi^*).$$

Moreover, if $(\eta_\lambda)_\lambda$ denotes an orthonormal basis of $\mathcal{H}$, then all dual frames of Ψ are given by

$$\widetilde{\widetilde{\Psi}} = \left\{ \Upsilon^{-1}\psi_\lambda + \varphi_\lambda - \sum_{\mu\in\mathbb{N}} \langle \Upsilon^{-1}\psi_\lambda, \psi_\mu \rangle \varphi_\lambda \,:\, \lambda \in \mathbb{N} \right\},$$

where $\Phi = \{\varphi_\lambda \,:\, \lambda \in \mathbb{N}\}$ is a Bessel sequence in $\mathcal{H}$, i.e. only the second inequality in (A.1) *is assumed for Φ to hold.*

As we outlined in Theorem A.5, a frame might not have a unique dual frame. Among all duals, the canonical dual has a special property as we have the following theorem.

Theorem A.6 ([Chr03]). *Let Ψ be a frame and $\widetilde{\Psi}$ its canonical dual frame, cf Theorem A.3. Let $f \in \mathcal{H}$ and $(c_\lambda)_\lambda \in \ell^2(\mathbb{N})$ such that $f = \sum_{\lambda \in \mathbb{N}} c_\lambda \psi_\lambda$. Then*

$$\|(\langle f, \widetilde{\psi}_\lambda \rangle)_{\lambda \in \mathbb{N}}\|_2 \leq \|(c_\lambda)_\lambda\|_2.$$

Theorem (A.6) shows that the dual coefficients have the smallest ℓ^2-norm. This could be understood as the most uniform spread of energy among all coefficients. This is not always a desired property, for instance in the sparsity regime, hence having the flexibility of alternative duals can be advantageous.

All results presented so far in this section are fairly standard in frame theory and the interested reader may consult [Chr03] for further results in frame theory.

We shall proceed with a rather new branch of frame theory that is called *scalable frames*. This is interesting for us as the new type of frames that we have introduced in Chapter [?] can be seen as a generalization of this class of frames.

A.2 Scalable frames

Without an argue, Parseval frames are a very special class of frames. Recall that for a Parseval frame Ψ it holds by definition

$$\|f\|^2 = \sum_{\lambda \in \mathbb{N}} |\langle f, \psi_\lambda \rangle|^2, \quad \forall\, f \in \mathcal{H} \tag{A.2}$$

which is known as *Parseval's Identity*. Equation (A.2) is very reminiscent of an orthonormal bases and, indeed, a normalized Parseval frame is an orthonormal basis.

The question that one might want to ask is whether every frame can be transformed into a Parseval frame. The authors of [KOPT13] have studied this question and have introduced the class of *scalable frames*.

Definition A.7 ([KOPT13]). *A frame $\Psi = \{\psi_\lambda : \lambda \in \mathbb{N}\}$ for $\mathcal{H}$ is called* scalable *if there exists scalars $c_\lambda \geq 0, \lambda \in \mathbb{N}$ such that*

$$\{c_\lambda \psi_\lambda : \lambda \in \mathbb{N}\}$$

forms a Parseval frame for $\mathcal{H}$. If there exists $\delta > 0$ such that $c_j > \delta$, then we call Ψ strictly scalable.

The following result proven in [KOPT13] gives an equivalent condition of scalable frames using the notion of *diagonal operators*. An operator D is called a *diagonal operator corresponding to* $(c_\lambda)_{\lambda \in \mathbb{N}} \subset \mathbb{C}$ if it is of the form

$$\begin{aligned} D : \ell^2(\mathbb{N}) \supset \operatorname{dom} D &\longrightarrow \ell^2(\mathbb{N}) \\ (d_\lambda)_{\lambda \in \mathbb{N}} &\mapsto (c_\lambda d_\lambda)_{\lambda \in \mathbb{N}}, \end{aligned}$$

where $\operatorname{dom} D = \{(d_\lambda)_{\lambda \in \mathbb{N}} : (c_\lambda d_\lambda)_{\lambda \in \mathbb{N}} \in \ell^2(\mathbb{N})$.

Proposition A.8 ([KOPT13]). *Let Ψ be a frame for $\mathcal{H}$. Then Ψ is scalable if and only if there exists a non-negative operator D such that $\overline{\Psi^* D} D\Psi = \mathrm{Id}$. In particular, if $\liminf_\lambda \|\psi_\lambda\| > 0$, then Ψ is strictly scalable if and only if there exists a strictly positive diagonal operator D such that $D\Psi$ is isometric.*

Remark A.9. *Note that the isometry condition in Proposition A.8 is one of the key steps used in the proof of Theorem 4.12.*

Finally, recall that a frame $(\psi_\lambda)_\lambda \subset \mathcal{H}$ is said to have an identifiable dual if there exists a dual frame $(\psi_\lambda)_\lambda \subset \mathcal{H}$ and some constants $0 < d_1 \leq d_2 < \infty$ such that

$$d_1 |\langle f, \psi_\lambda \rangle| \leq \langle f, \widetilde{\psi}_\lambda \rangle| \leq d_2 |\langle f, \psi_\lambda \rangle|, \quad \forall f \in \mathcal{H}, \tag{A.3}$$

cf. Definition 4.9. Then we have the following

Proposition A.10. *Every scalable frame has an identifiable dual.*

Proof. Let $(\psi_\lambda)_\lambda \subset \mathcal{H}$ be scalable. Then there exists $c_\lambda \in \mathbb{R}^+ \cup \{0\}$ such that

$$f = \sum_\lambda \langle f, c_\lambda \psi_\lambda \rangle c_\lambda \psi_\lambda .$$

Therefore, $(c_\lambda^2 \psi_\lambda)_\lambda$ is an identifiable dual of $(\psi_\lambda)_\lambda$ as (A.3) holds if and only if there exists scalars $a_\lambda \in \mathbb{C}$ such that

$$\widetilde{\psi}_\lambda = a_\lambda \psi_\lambda .$$

□

Appendix B

Wavelets

We give a short overview of some wavelet results that we used in this thesis. For a more detailed presentation of wavelets we refer to the classical book by Daubechies [Dau92], Mallat [Mal09], and Hernández and Weiss [HW96].

In this thesis we mainly used wavelets as an orthonormal basis for $L^2(\mathbb{R}^2)$ and so will this be our main focus. There are plenty of other beautiful mathematical properties of wavelet theory, but this goes beyond the scope of this thesis.

B.1 Multiresolution analysis of 2D wavelets

For a functions $\psi \in L^2(\mathbb{R}^2)$ we denote its *(dyadically) scaled* and *translated* version by

$$\psi_{j,m} := 2^j \psi\left(\begin{pmatrix} 2^j & 0 \\ 0 & 2^j \end{pmatrix} \cdot -m\right), \quad m \in \mathbb{Z}^2.$$

If the function is compactly supported, then one can view these two properties as a zooming into finer resolution and the relocation of the analysing region of interest. This allows one to analyse signals and their behavior very locally.

Of course, there are different type of wavelet systems possible and their analytical properties such as, approximation of a certain type of function, depend strongly on the type of generators that one considers. Typical assumptions on these generators are, for instance, frequency decay.

We will next give the definition of a *multiresolution analysis* which is one of the very famous and desired properties that wavelet systems can achieve.

Let A be the scaling matrix $\begin{pmatrix} 2^j & 0 \\ 0 & 2^j \end{pmatrix}$, for the general case we refer to, for instance, [Maa96].

Definition B.1. *A sequence of closed subspaces* $(V_j)_{j\in\mathbb{Z}}$ *of* $L^2(\mathbb{R}^2)$ *is called a* multiresolution analysis*, if the following properties are satisfied.*

i) $\{0\} \subset \ldots \subset V_j \subset V_{j+1} \subset \ldots \subset L^2(\mathbb{R}^2)$,

ii) $\bigcap_{j\in\mathbb{Z}} V_j = \{0\}$, *iii)* $\overline{\bigcup_{j\in\mathbb{Z}} V_j} = L^2(\mathbb{R}^2)$,

iv) $f \in V_j \Leftrightarrow f(A\cdot) \in V_{j+1}$,

v) *there exists a function* $\phi \in L^2(\mathbb{R}^2)$ *(called* scaling function*), such that*

$$\{\phi_{0,m} := \phi(\cdot - m) \,:\, m \in \mathbb{Z}^2\}$$

constitutes an orthonormal basis for V_0.

The associated *wavelet spaces* $(W_j)_{j\in\mathbb{Z}}$ are then defined by

$$V_{j+1} = V_j \oplus W_j.$$

It is well known that there exist $|\det A| - 1$ corresponding compactly supported wavelets $\psi^1, \dots, \psi^{|\det A|-1}$ such that

$$\left\{\psi^p_{j,m} := |\det A|^{j/2}\psi^p(A^j \cdot -m) : m = (m_1, m_2) \in \mathbb{Z}^2, p = 1, \dots, |\det A| - 1\right\}$$

forms an orthonormal basis for W_j for each j, see, e.g., [Mey87]. We now consider the decomposition

$$L^2(\mathbb{R}^2) = V_0 \oplus \bigoplus_{j=0}^{\infty} W_j,$$

where

$$V_0 := \overline{\operatorname{span}}\{\phi_{0,m} \,:\, m = (m_1, m_2) \in \mathbb{Z}^2\}$$

and

$$W_j := \overline{\operatorname{span}}\{\psi^p_{j,m} \,:\, m = (m_1, m_2) \in \mathbb{Z}^2, p = 1, \dots, |\det A| - 1\}, \quad j = 0, 1, \dots$$

As we motivated in Section 1.4 it is often of great interest to restrict the function system onto a bounded domain. We used *wavelets on the interval* in order to build the shearlet system on bounded domains. Therefore, we briefly recap its construction. However, different approaches are also known, for example by Meyer [Mey92], see also [Mal09].

B.2 1D Wavelets on $[0, 1]$

We start with the 1D construction of wavelets on the interval as introduced in [CDV93]. For this, let ϕ be a compactly supported Daubechies scaling function associated to a wavelet with p vanishing moments. It is well known that ϕ must then have a support of size $2p - 1$. By a shifting argument, we can assume that $\operatorname{supp}(\phi) = [-p + 1, p]$. Now let $j \in \mathbb{N}$ such that $2p \leq 2^j$. Then there exist $2^j - 2p$ *interior scaling functions* scaling functions $\phi^{\text{int}}_{j,n}$ defined by

$$\phi^{\text{int}}_{j,n} = \phi_{j,n} = 2^{j/2}\phi(2^j \cdot -n), \quad \text{for } p \leq n < 2^j - p,$$

which are fully supported in $[0,1]$. Depending on boundary scaling functions $\{\phi_n^{\text{left}}\}_{n=0,\ldots,p-1}$ and $\{\phi_n^{\text{right}}\}_{n=0,\ldots,p-1}$, which we will introduce below, the *p left boundary scaling functions* are defined by

$$\phi_{j,n}^{\text{int}} = 2^{j/2}\phi_n^{\text{left}}(2^j\cdot), \quad \text{for } 0 \leq n < p,$$

and the *p right boundary scaling functions* are

$$\phi_{j,n}^{\text{int}} = 2^{j/2}\phi_{2^j-1-n}^{\text{right}}(2^j(\cdot - 1)), \quad \text{for } 2^j - p \leq n < 2^j.$$

We remark that this leads to 2^j scaling functions in total, which is the number of original scaling functions $(\phi_{j,n})_n$ that intersect $[0,1]$.

We next sketch the idea of the construction of boundary scaling functions $\{\phi_n^{\text{left}}\}_{n=0,\ldots,p-1}$ as well as $\{\phi_n^{\text{right}}\}_{n=0,\ldots,p-1}$ following [CDV93], to the extent to which we require it in our proofs. One starts by defining edge functions $\widetilde{\phi}^k$ on the positive axis $[0,\infty)$ by

$$\widetilde{\phi}^k(x) = \sum_{n=0}^{2p-2} \binom{n}{k} \phi(x + n - p + 1), \quad k = 0, \ldots, p-1,$$

such that these edge functions are orthogonal to the interior scaling functions and such that they together generate all polynomials up to degree $p-1$. After performing a Gram-Schmidt procedure one obtains the left boundary functions $\phi_k^{\text{left}}, k = 0, \ldots, p-1$. The right boundary functions are then – after some minor adjustments – obtained by reflecting the left boundary functions. This construction from [CDV93] allows one to obtain a multiresolution analysis.

Theorem B.2 ([CDV93])**.** *If $2^j \geq 2p$, then $\{\phi_{j,n}^{\text{int}}\}_{n=0,\ldots,2^j-1}$ is an orthonormal basis for a space V_j^{int} that is nested, i.e.*

$$V_j^{\text{int}} \subset V_{j+1}^{\text{int}},$$

and complete, i.e.

$$\overline{\bigcup_{j \geq \log_2 2p} V_j^{\text{int}}} = L^2[0,1].$$

Next, we define an orthonormal basis for the wavelet space W_j^{int}, which is as usual defined as the orthogonal complement of V_j^{int} in V_{j+1}^{int}. For this, let ψ be the corresponding wavelet function to ϕ with p vanishing moments and $\operatorname{supp}\psi = [-p+1, p]$. Similar to the construction of the scaling functions, we will obtain interior wavelets and boundary wavelets, which then constitutes the set of wavelets in the interval. Again based on a careful choice of boundary wavelets $(\psi_n^{\text{left}})_n$ and $(\psi_k^{\text{right}})_k$, for which we refer to [CDV93], we define $2^j - 2p$ *interior wavelets* by

$$\psi_{j,n}^{\text{int}} = \psi_{j,n} = 2^{j/2}\psi(2^j \cdot - n), \quad \text{for } p \leq n < 2^j - p,$$

p left boundary wavelets

$$\psi_{j,n}^{\text{int}} = 2^{j/2}\psi_n^{\text{left}}(2^j\cdot), \quad \text{for } 0 \leq n < p,$$

and p *right boundary wavelets*

$$\psi_{j,n}^{\text{int}} = 2^{j/2}\psi_{2^j-1-n}^{\text{right}}(2^j(\cdot - 1)), \quad \text{for } 2^j - p \leq n < 1^j.$$

Summarizing, the following result hold for these wavelet functions.

Theorem B.3 ([CDV93])**.** *Let $2^J \geq 2p$. Then the following properties hold:*

i) $\{\psi_{J,n}^{\text{int}}\}_{n=0,\ldots,2^J-1}$ *is an orthonormal basis for* W_J^{int}.

ii) $L^2[0,1]$ *can be decomposed as*

$$L^2[0,1] = V_J^{\text{int}} \oplus W_J^{\text{int}} \oplus W_{J+1}^{\text{int}} \oplus W_{J+2}^{\text{int}} \oplus \ldots = V_J^{\text{int}} \bigoplus_{j=J}^{\infty} W_j^{\text{int}}.$$

iii) $\left\{\{\phi_{J,m}^{\text{int}}\}_{m=0,\ldots,2^J-1}, \{\psi_{j,n}^{\text{int}}\}_{j\geq J, n=0,\ldots,2^j-1}\right\}$ *is an orthonormal basis for* $L^2[0,1]$.

iv) If $\phi, \psi \in C^r[0,1]$, *then* $\left\{\{\phi_{j,m}^{\text{int}}\}_{m=0,\ldots,2^J-1}, \{\psi_{j,n}^{\text{int}}\}_{j\geq J, n=0,\ldots,2^j-1}\right\}$ *is an unconditional basis for* $C^s[0,1]$ *for all* $s < r$.

We start with the 1D construction of wavelets on the interval as introduced in [CDV93]. For this, let ϕ be a compactly supported Daubechies scaling function associated to a wavelet with p vanishing moments. It is well known that ϕ must then have a support of size $2p - 1$. By a shifting argument, we can assume that $\operatorname{supp}(\phi) = [-p+1, p]$. Now let $j \in \mathbb{N}$ such that $2p \leq 2^j$. Then there exist $2^j - 2p$ *interior scaling functions* scaling functions $\phi_{j,n}^{\text{int}}$ defined by

$$\phi_{j,n}^{\text{int}} = \phi_{j,n} = 2^{j/2}\phi(2^j \cdot - n), \quad \text{for } p \leq n < 2^j - p,$$

which are fully supported in $[0,1]$. Moreover, there exist *left* and *right boundary scaling functions* $(\phi_m^{\text{left}})_{m=0,\ldots,p-1}$ and $(\phi_m^{\text{right}})_{n=0,\ldots,p-1}$ such that for

$$\phi_{j,m}^{\text{int}} := 2^{j/2}\phi_m^{\text{left}}(2^j \cdot), \quad \text{for } 0 \leq m < p,$$

and

$$\phi_{j,m}^{\text{int}} := 2^{j/2}\phi_{2^j-1-m}^{\text{right}}(2^j(\cdot - 1)), \quad \text{for } 2^j - p \leq m < 2^j,$$

the sequence $(\phi_{j,n}^{\text{int}})_{n=0,\ldots,2^j-1}$ forms a multiresolution analysis ([CDV93], [Mal09]), see also Theorem B.4 below.

Theorem B.4 ([CDV93])**.** *Let* $V_j^{\text{int}} := \overline{\operatorname{span}(\phi_{j,n}^{\text{int}})}_{n=0,\ldots,2^j-1}$. *Then the sequence of spaces* $(V_j^{\text{int}})_{j\in\mathbb{N}_0}$ *is nested, i.e.,*

$$V_0^{\text{int}} \subset \ldots \subset V_j^{\text{int}} \subset V_{j+1}^{\text{int}} \subset \ldots$$

Moreover, for all $j \in \mathbb{N}$ *such that* $2^j \geq 2p$, *the system* $(\phi_{j,m}^{\text{int}})_{m=0,\ldots,2^j-1}$ *constitutes an orthonormal basis for* V_j^{int} *and the respective sequence of spaces* V_j^{int} *is complete, i.e.*

$$\overline{\bigcup_{j>\log_2 p} V_j^{\text{int}}} = L^2([0,1]).$$

Let now W_j^{int} denote the orthogonal complement of V_j^{int} in V_{j+1}^{int}. Then an orthonormal basis of wavelets for each space W_j^{int} can be constructed as follows. Let ϕ^1 be a compactly supported scaling function with supp $\psi^1 = [-p+1, p]$, and let ψ^1 be the corresponding wavelet possessing p vanishing moments. Similar to the construction of the boundary scaling functions previously discussed, we can construct wavelets, which are fully supported in $[0,1]$. Again, there exist boundary adapted wavelets $(\psi_n^{\text{left}})_n$ and $(\psi_n^{\text{right}})_n$ [CDV93, Mal09], leading to $2^j - 2p$ *interior wavelets*

$$\psi_{j,m}^{\text{int}} := \psi_{j,m}^1 := 2^{j/2}\psi^1(2^j \cdot - m), \quad \text{for } p \le m < 2^j - p,$$

p left boundary wavelets

$$\psi_{j,m}^{\text{int}} := 2^{j/2}\psi_m^{\text{left}}(2^j \cdot), \quad \text{for } 0 \le m < p,$$

and *p right boundary wavelets*

$$\psi_{j,m}^{\text{int}} := 2^{j/2}\psi_{2^j-1-m}^{\text{right}}(2^j(\cdot - 1)), \quad \text{for } 2^j - p \le m < 2^j.$$

This set of wavelets satisfies the following properties.

Theorem B.5 ([CDV93]). *Retaining the notations from this subsection, for $J \in \mathbb{N}$ with $2^J \ge 2p$, the following properties hold:*

i) $(\psi_{J,m}^{\text{int}})_{m=0,\ldots,2^J-1}$ *is an orthonormal basis for* W_J^{int}.

ii) $L^2([0,1])$ *can be decomposed as*

$$L^2([0,1]) = V_J^{\text{int}} \oplus W_J^{\text{int}} \oplus W_{J+1}^{\text{int}} \oplus W_{J+2}^{\text{int}} \oplus \ldots = V_J^{\text{int}} \oplus \bigoplus_{j=J}^{\infty} W_j^{\text{int}}.$$

iii) $\left\{(\phi_{J,m}^{\text{int}})_{m=0,\ldots,2^J-1}, (\psi_{j,m}^{\text{int}})_{j\ge J, m=0,\ldots,2^j-1}\right\}$ *is an orthonormal basis for* $L^2([0,1])$.

iv) If $\phi^1, \psi^1 \in C^r([0,1])$, *then* $\left\{(\phi_{j,m}^{\text{int}})_{m=0,\ldots,2^J-1}, (\psi_{j,m}^{\text{int}})_{j\ge J, m=0,\ldots,2^j-1}\right\}$ *is an unconditional basis for* $C^s([0,1])$ *for all* $s < r$.

Appendix C

Supplementary proofs

C.1 Proof of Lemma 1.13

Exploiting the MRA structure and using the assumptions we can conclude

$$f \in V_{J+1}.$$

Furthermore, as $(\phi^1_{J+1,l})_{l\in\mathbb{Z}}$ is an ONB for V_{J+1} we obtain

$$f = \sum_{l\in\mathbb{Z}} \left\langle f, \phi^1_{J+1,l} \right\rangle \phi^1_{J+1,l}. \tag{C.1}$$

Due to the fact that $f \neq 0$ and f and ϕ are compactly supported we obtain from (C.1) that there exist $l_0, l_1 \in \mathbb{Z}$, $l_0 < l_1$ such that

$$\left\langle f, \phi^1_{J+1,l_0} \right\rangle \neq 0 \quad \text{and} \quad \left\langle f, \phi^1_{J+1,l} \right\rangle = 0$$

forall $l \notin \{l_0+1, \ldots, l_1-1\}$. Hence,

$$f = \sum_{l=l_0}^{l_1} \left\langle f, \phi^1_{J+1,l} \right\rangle \phi^1_{J+1,l}.$$

Since the scaling function is continuous, f must also be continuous. Therefore, we can conclude that

$$\min\left(\text{supp } f\right) = \min\left(\text{supp } \phi^1_{J+1,l_0}\right) = 2^{-(J+1)} l_0 \in 2^{-(J+1)}\mathbb{Z}.$$

The in particular part of this lemma is clear.

C.2 Proof of Lemma 1.14

W.l.o.g. let $a_1 < \ldots < a_N$, otherwise we reorder the indices. Let $\lambda_1, \ldots, \lambda_N \in \mathbb{C}$ such that

$$\sum_{i=1}^{N} \lambda_i f_i = 0.$$

Since $a_1 < a_2$ we obtain by continuity of f_1, that f_1 is non-zero on a non-empty interval $I_1 \subset [a_1, a_2)$. Therefore λ_1 must be zero and hence $\sum_{i=2}^{N} \lambda_i f_i = 0$. Repeating this process leads to $\lambda_1 = \ldots = \lambda_N = 0$.

C.3 Proof of Proposition 1.15

W.l.o.g. suppose that $\operatorname{supp} \psi^1 = [0, r]$ for some $r \in \mathbb{R}^+$. Let $f_i \in \operatorname{span} \Omega_n^i$ be non-zero functions for $i = 1, \ldots, n$. Observe, that since the sets Ω_n^i have finite cardinality, the functions $f_1, \ldots, f_n$ are compactly supported as a finite linear combination of compactly supported functions. Also, since the wavelets are continuous the functions $f_1, \ldots, f_n$ are continuous as well.

Claim 1: The functions $f_1, \ldots, f_n$ are linearly independent.

Due to Lemma 1.14, it is sufficient to prove that

$$\min(\operatorname{supp} f_{i_1}) \neq \min(\operatorname{supp} f_{i_2}) \quad \forall\, i_1 \neq i_2.$$

To this end, let $T_y : L^2(\mathbb{R}) \longrightarrow L^2(\mathbb{R})$ be the translation operator that maps f to $T_y(f) = f(\cdot + y)$. Then, for any $f^i \in \operatorname{span} \Omega_n^i$, we clearly have $T_{i/n} f^i \in \bigoplus_{0 \le j \le J} W_j$. By Lemma 1.13 we obtain for $i_1, i_2 \in \{1, \ldots, n\}$ with $i_1 \neq i_2$ that

$$\min(\operatorname{supp} f_{i_1}) \in 2^{-(J+1)}\mathbb{Z} + t_{i_1} \qquad \text{and} \qquad \min(\operatorname{supp} f_{i_2}) \in 2^{-(J+1)}\mathbb{Z} + t_{i_2}.$$

If

$$\min(\operatorname{supp} f_{i_1}) = \min(\operatorname{supp} f_{i_2}),$$

then there exist $k, s \in \mathbb{Z}$ such that

$$2^{-(J+1)}k + t_{i_1} = 2^{-(J+1)}s + t_{i_2}. \tag{C.2}$$

Multiplying (C.2) by 2^{J+1} yields

$$2^{J+1}t_{i_1} + k = 2^{J+1}t_{i_2} + s$$

which is equivalent to

$$2^{J+1}(t_{i_1} - t_{i_2}) = s - k. \tag{C.3}$$

By the assumptions on t_i we obtain that (C.3) cannot be true. Therefore, (C.2) is false. This proves Claim 1.

Claim 2: For fixed $i \in \{1, \ldots, n\}$ the set of functions

$$\Omega_n^i = \left\{\psi^1(2^j(\cdot - t_i) + l) \,:\, l \in L_j^i, j = 0, \ldots, J\right\}$$

is orthogonal.

Since $\{\psi^1(2^j \cdot -l) \,:\, l \in \mathbb{Z}, j = 0, \ldots, J\}$ are orthogonal by the MRA property and orthogonality remains under a fixed shift operation, Ω_n^i are orthogonal for fixed $1 \le i \le n$. This yields Claim 2.

For the sake of brevity of notation, we now denote the elements of Ω_n^i by

$$\Omega_n^i = \left\{ \psi_{j,l}^{(i)} = \psi^1(2^j(\cdot - t_i) + l) \,:\, (j,l) \in P_i \right\}, \text{ with } P_i = \{0, \ldots, J\} \times L_j^i.$$

for $i = 1, \ldots, n$. Note that each set P_i is of finite cardinality. It now remains to prove the following statement:

If

$$\sum_{j,l \in P_1} \lambda_{j,l}^{(1)} \psi_{j,l}^{(1)} + \ldots + \sum_{j \in P_n} \lambda_{j,l}^{(n)} \psi_{j,l}^{(n)} = 0, \quad \lambda_{j,l}^{(i)} \in \mathbb{C} \tag{C.4}$$

then $\lambda_{j,l}^{(i)} = 0$, for all $(j,l) \in P_i,\ i = 1, \ldots, n$. For this, let us shorten the notation by

$$\tilde{f}_i := \sum_{(j,l) \in P_i} \lambda_{j,l}^{(i)} \psi_{j,l}^{(i)}, \qquad \text{for } 1 \leq i \leq n.$$

Towards a contradiction we assume, that for some $m \in \{1, \ldots, n\}$ there exists $(j,l) \in P_m$ such that $\lambda_{j,l}^{(m)} \neq 0$. Consequently, by Claim 2, $\tilde{f}_m \neq 0$. Claim 1 yields linear independence of the $\tilde{f}_i$ and thus

$$\sum_{i=1}^n \tilde{f}_i \neq 0,$$

which contradicts (C.4). This finishes the proof.

C.4 Proof of Theorem 1.16

We only show the linear independence of $\Psi(\psi, c)$. The argument for $\tilde{\Psi}(\tilde{\psi}, c)$ is the same with ψ replaced by $\tilde{\psi}$. Let $\gamma_1, \ldots, \gamma_N \in \Psi(\psi, c)$ with

$$\gamma_i\left(x_1, x_2\right) = 2^{3j_i/4} \psi^1 \left(2^{j_i} x_1 + 2^{\left\lfloor \frac{j_i}{2} \right\rfloor} k_i x_2 + c_1 t_i^{(1)} \right) \cdot \phi^1 \left(2^{\left\lfloor \frac{j_i}{2} \right\rfloor} x_2 + c_2 t_i^{(2)} \right),$$

where $(x_1, x_2) \in \mathbb{R}^2$ and $i = 1, \ldots, N$.A priori for $i, l \in \{1, \ldots, N\}$ with $i \neq l$, it is possible that we have $\left(j_i, k_i, t_i^{(1)}\right) = \left(j_l, k_l, t_l^{(1)}\right)$. By defining an equivalence relation $\sim$ such that $i \sim l$, if $\left(j_i, k_i, t_i^{(1)}\right) = \left(j_l, k_l, t_l^{(1)}\right)$, we can write for $K = \{i \leq N\}/\sim$ and $L_i := \{l : i \sim l\}$,

$$(\gamma_i)_{i=1}^N = \left\{ 2^{3j_i/4} \psi^1 \left(2^{j_i} \cdot + 2^{\left\lfloor \frac{j_i}{2} \right\rfloor} k_i \cdot + c_1 t_i^{(1)} \right) \cdot \phi^1 \left(2^{\left\lfloor \frac{j_i}{2} \right\rfloor} \cdot + c_2 t_{l_i}^{(2)} \right), i \in K, l_i \in L_i \right\}.$$

To obtain linear independence of $(\gamma_i)_{i=1}^N$ we need to show for $\alpha = (\alpha_i)_{i=1}^N \in \mathbb{C}^N$ that

$$0 = \sum_{i \in K} \psi^1 \left(2^{j_i} \cdot + 2^{\left\lfloor \frac{j_i}{2} \right\rfloor} k_i \cdot + c_1 t_i^{(1)} \right) \cdot \left(\sum_{l_i \in L_i} \alpha_{l_i} \phi^1 \left(2^{\left\lfloor \frac{j_i}{2} \right\rfloor} \cdot + c_2 t_{l_i}^{(2)} \right) \right) \implies \alpha = 0.$$

By definition we now have that for any $i, l \in K$, with $i \neq l$

$$\left(j_i, k_i, t_i^{(1)}\right) \neq \left(j_l, k_l, t_l^{(1)}\right). \tag{C.5}$$

Towards a contradiction, we assume $\alpha \in \mathbb{C}^N \setminus \{0\}$ and define the function

$$g_{i,\alpha} := \sum_{l_i \in L_i} \alpha_{l_i} \phi^1 \left(2^{\left\lfloor \frac{j_{l_i}}{2} \right\rfloor} \cdot + c_2 t_{l_i}^{(2)}\right), \qquad \text{for } i \in K.$$

We also set

$$U(\alpha) = \bigcup_{i \in K} \text{supp } g_{i,\alpha}.$$

Case 1: Assume $U(\alpha)$ is non-empty.

Our goal is to show, that

$$\sum_{i \in K} \psi^1 \left(2^{j_i} \cdot + 2^{\left\lfloor \frac{j_i}{2} \right\rfloor} k_i \cdot + c_1 t_i^{(1)}\right) \cdot \left(\sum_{l_i \in L_i} \alpha_{l_i} \phi^1 \left(2^{\left\lfloor \frac{j_i}{2} \right\rfloor} \cdot + c_2 t_i^{(2)}\right)\right) \neq 0. \tag{C.6}$$

We can construct a finite covering of $U(\alpha)$ subordinate to the supports of $g_{i,\alpha}$ in the following sense. We pick $Q \in \mathbb{N}$ closed sets $U_q, q = 1 \ldots, Q$, that cover $U(\alpha)$ and obey

$$\text{int}\{\text{supp } g_{i,\alpha} \cap U_q\} \neq \emptyset \implies \text{supp } g_{i,\alpha} \supseteq U_q.$$

lemma:LinIndNoShear This can be done by taking a disjoint generator of the algebra generated by the sets supp $g_{i,\alpha}$, $i \in K$.

We define corresponding index sets $I_q = \{i \in K : \text{supp } g_{i,\alpha} \cap U_q \neq \emptyset\}$. Now, for all $i \in I_q$ we have that supp $g_{i,\alpha} \supseteq U_q$. For all $i \in K$ we have that $g_{i,\alpha}$ is continuous and hence, the interior of $U(\alpha)$ is non-empty. Since the interior of $U(\alpha)$ is non-empty, there exists a set U_q with non-empty interior. Hence, we can pick a point $\hat{x}_2 \in U_q \setminus \mathbb{Q}$ such that $g_{i,\alpha}(\hat{x}_2) \neq 0$. We define $\tilde{t}_i := 2^{\lceil \frac{j_i}{2} \rceil} k_i \hat{x}_2 + 2^{-j_i}(c_1 t_i - \lfloor c_1 t_i \rfloor)$ and $\tilde{\alpha}_i := g_{i,\alpha}(\hat{x}_2) \neq 0$ for $i \in I_q$ and obtain

$$\begin{aligned} &\sum_{i \in I_q} \psi^1 \left(2^{j_i}(\cdot + \tilde{t}_i) + \lfloor c_1 t_i^{(1)} \rfloor\right) \cdot \left(\sum_{l_i \in L_i} \alpha_{l_i} \phi^1 \left(2^{\left\lfloor \frac{j_i}{2} \right\rfloor} \hat{x}_2 + c_2 t_i^{(2)}\right)\right) \\ &\quad = \sum_{i \in I_q} \tilde{\alpha}_i \psi^1 \left(2^{j_i}(\cdot + \tilde{t}_i) + \lfloor c_1 t_i^{(1)} \rfloor\right). \end{aligned} \tag{C.7}$$

If we have

$$(j_{i_1}, \lfloor c_1 t_{i_1}^1 \rfloor) \neq (j_{i_2}, \lfloor c_1 t_{i_2}^1 \rfloor) \text{ or } \tilde{t}_{i_1} - \tilde{t}_{i_2} \notin 2^{-J-1}\mathbb{Z} \text{ for all } i_1, i_2 \in I_q, i_1 \neq i_2, \tag{C.8}$$

then, since $\tilde{\alpha} \neq 0$, an application of Proposition 1.15 to equation (C.7) yields equation (C.6). In order to show that (C.8) can be achieved, we observe that we can restrict ourselves to subsets I'_q of I_q, such that $j = j_s = j_r$, for $s, r \in I'_q$. By construction we have that $\tilde{t}_{i_1} - \tilde{t}_{i_2} \in 2^{-J-1}\mathbb{Z}$ is only possible if $c_1 t^1_{i_1} - \lfloor c_1 t^1_{i_1} \rfloor = c_1 t^1_{i_2} - \lfloor c_1 t^1_{i_2} \rfloor$. In this case we have by assumption that $k_i = k_j$ and hence with (C.5) we have that $\lfloor c_1 t^1_{i_1} \rfloor \neq \lfloor c_1 t^1_{i_2} \rfloor$.

Case 2: $U(\alpha) = \emptyset$.

In this case we have that $g_{i,\alpha} = 0$ for all $i \in K$. Recall that for $i \in K$

$$g_{i,\alpha} = \sum_{l_i \in L_i} \alpha_{l_i} \phi^1 \left(2^{\left\lfloor \frac{j_i}{2} \right\rfloor} \cdot + c_2 t^{(2)}_{l_i} \right),$$

and observe that $t^{(2)}_{l_i} \neq t^{(2)}_{k_i}$ for all $l_i, k_i \in L_i, l_i \neq k_i$. Thus the functions

$$\left(\phi^1 \left(2^{\left\lfloor \frac{j_i}{2} \right\rfloor} \cdot + c_2 t^{(2)}_{l_i} \right) \right)_{l_i \in L_i}$$

are linearly independent by Lemma 1.14. This implies $\alpha_{l_i} = 0$ for all $l_i \in L_i$ and all $i \in K$. Finally this contradicts the fact that $\alpha \neq 0$ and consequently we will never be in the event of Case 2.

C.5 Proof of Lemma 1.17

The proof uses the linear independence of the one dimensional generator functions. By assumption we have that for a finite set $L \in \mathbb{Z}$ and $J \in \mathbb{N}$ the set

$$\{\phi^1_m, \psi^1_{j,m} \, : \, m \in L, 0 \leq j \leq J\}$$

is linearly independent. Furthermore by rescaling we obtain that

$$\{\phi^1_{j_0,m}, \psi^1_{j,m} \, : \, m \in L, j_0 \leq j \leq J\} \tag{C.9}$$

is linearly independent.

Let $I_1 \subseteq \{0\}$ and $I_2, I_3 \subset \mathbb{N}$ be finite and assume that for every $j \in I_i$ we have finite sets L_1 and $L^j_i \subset \mathbb{Z}^2$, $i = 2, 3$, such that with $\alpha^1_m \neq 0$ for all $m \in L_1$ and $\alpha^i_{j,m} \neq 0$ for all $j \in I_i, m \in L^j_i$ $i = 1, 2, 3$ we have

$$\sum_{m \in L_1} \alpha^1_m \phi_m + \sum_{j \in I_2, m \in L^j_2} \alpha^2_{j,m} \psi_{j,m} + \sum_{j \in I_3, m \in L^j_3} \alpha^3_{j,m} \widetilde{\psi}_{j,m} = 0. \tag{C.10}$$

If we can show that (C.10) implies $L_1 \cup \bigcup_{j \in I_2} L^j_2 \cup \bigcup_{j \in I_3} L^j_3 = \emptyset$, then we obtain linear independence.

Let $j_{max} = \max(I_1 \cup I_2 \cup I_3)$ and assume that $j_{max} > 0$. It will be clear, that the case $j_{max} = 0$ follows similarly. Then (C.10) is equivalent to

$$\sum_{m \in L_1} \alpha^1_m \phi_m + \sum_{j \in I_2 \setminus \{j_{max}\}, m \in L^j_2} \alpha^2_{j,m} \psi_{j,m} + \sum_{j \in I_3 \setminus \{j_{max}\}, m \in L^j_3} \alpha^3_{j,m} \widetilde{\psi}_{j,m}$$

$$= -\sum_{m\in L_2^{j_{max}}} \alpha^2_{j_{max},m}\psi_{j_{max},m} - \sum_{m\in L_3^{j_{max}}} \alpha^3_{j_{max},m}\widetilde{\psi}_{j_{max},m}. \tag{C.11}$$

Let us distinguish two cases. The first case is that one of the two terms in (C.11) does not vanish everywhere. We assume w.l.o.g. that $\sum_{m\in L_2^{j_{max}}} \alpha^2_{j_{max},m}\psi_{j_{max},m} \neq 0$. Then, there exists $\hat{x}_2 \in \mathbb{R}^2$:

$$0 \neq \sum_{m\in L_2^{j_{max}}} \alpha^2_{j_{max},m}\psi_{j_{max},m}(\cdot,\hat{x}_2) = \sum_{m\in L_2^{j_{max}}} \tilde{\alpha}^2_{j_{max},m}\psi^1_{j_{max},m_1} =: f,$$

where $\tilde{\alpha}^2_{j_{max},m} := \alpha^2_{j_{max},m}\phi^1_{\lfloor \frac{j_{max}}{2}\rfloor,m_2}(\hat{x}_2)$. Note that the second term in (C.11) is a sum of scaling functions $\phi^1_{\lfloor \frac{j_{max}}{2}\rfloor,m_1}$, when sampled in x_2. Furthermore, by the linear independence of the one dimensional functions (C.9) it is impossible to represent f with functions on lower levels $j < j_{max}$. This contradicts (C.11).

The second possibility we need to examine is that both terms of (C.11) vanish everywhere. Then, for at least one of the terms we have that $L_i^{j_{max}} \neq \emptyset$, $i = 2,3$. W.l.o.g. we assume that $L_2^{j_{max}} \neq \emptyset$. Then we have that

$$\sum_{m\in L_2^{j_{max}}} \alpha^2_{j_{max},m}\psi_{j_{max},m} = 0. \tag{C.12}$$

Using the linear independence of (C.9), it is straightforward to see that the functions

$$\{\psi_{j_{max},m} \,:\, m \in L_2^{j_{max}}\}$$

are linearly independent. This implies, that (C.12) cannot hold. Hence we obtain that $L_i^{j_{max}} = \emptyset$, $i = 2,3$ and thus the assumption $j_{max} \geq 0$ cannot hold. Consequently, we obtain that $I_1 \cup I_2 \cup I_3 = \emptyset$. This gives the result.

C.6 Proof of Theorem 1.12

By Theorem 1.16 and Lemma 1.17 we obtain that finite subsets of Γ_1, Γ_2, and Γ_3 are linearly independent.

Thus, we first show

$$\operatorname{span}\Gamma_1 \cap \operatorname{span}\Gamma_2 = \{0\}. \tag{C.13}$$

Let $n = b_1 \cdot b_2$ where $c_i = \frac{a_i}{b_i}, i = 1,2$ satisfy the assumptions of the theorem. Furthermore, let, without loss of generality, $\operatorname{supp}\psi^1 = [0,s_1]$ and $\operatorname{supp}\phi^1 = [0,s_2]$ for some $s_1, s_2 \in \mathbb{R}^+$.

We use the following observation that is due to the fact that $W_j \subset V_J$ for all $j < J$. For any $0 \leq j \leq J-1$ and $t \in \mathbb{Z}$ there exists an index set $R_t^j \subset \mathbb{Z}^2$ and scalars $0 \neq \lambda_r \in \mathbb{C}$ with $r \in R_t^j$, such that

$$\psi^1(2^j \cdot -c_1 t) = \sum_{r\in R_t^j} \lambda_r \phi^1\left(2^J \cdot -r/n\right). \tag{C.14}$$

We obtain that for every $x_2 \in \mathbb{R}, k \in \mathbb{Z}$

$$\psi^1(2^j \cdot +2^{\lfloor \frac{j}{2} \rfloor} k x_2 - c_1 t) = \sum_{r \in R_t^j} \alpha_r \phi^1 \left(2^J \cdot +2^{J - \lceil \frac{j}{2} \rceil} k x_2 - r/n \right).$$

Now, let $f \in (\operatorname{span} \Gamma_1) \setminus \{0\}$. We assume that the minimal support bound of f in the second variable is 0, i.e. $f(\cdot, z) = 0$ for all $z < 0$. Otherwise this can be achieved by a suitable global shift of f. Then we have

$$f(x_1, x_2) = \sum_{i=1}^{N} \alpha_i \psi^1 \left(2^{j_i} x_1 + 2^{\frac{j_i}{2}} k_i x_2 + c_1 t_i^{(1)} \right) \phi^1 \left(2^{\frac{j_i}{2}} x_2 + c_2 t_i^{(2)} \right),$$

with $\alpha_i \in \mathbb{C} \setminus \{0\}, N \in \mathbb{N}$. By reordering the indices and a use of equation (C.14), we can expand any $f \in \operatorname{span} \Gamma_1$ by

$$f(x_1, x_2) = \sum_{i \in I} \sum_{r_i \in R_i} \alpha_{i, r_i} \phi^1 \left(2^J x_1 + 2^{J - \left\lceil \frac{j_i}{2} \right\rceil} k_i x_2 - r_i/n \right) \phi^1 \left(2^{\frac{j_i}{2}} x_2 + c_2 t_i^{(2)} \right) \quad \text{(C.15)}$$

with $\alpha_{i,r} \neq 0$, $k_i \neq 0$ and $R_i = R^{j_i}_{t_i^{(1)}}$.

For this, we group the indices into the following sets

$$\tilde{R}_\rho := \bigcup_{\left\{ i \in I:\ 2^{J - \left\lceil \frac{j_i}{2} \right\rceil} k_i = \rho \right\}} R_i, \quad \rho \in \mathbb{Z} \setminus \{0\}, |\rho| \leq 2^J. \quad \text{(C.16)}$$

Then with

$$\alpha'_\rho(x_2) := \sum_{i \in I:\ 2^{J - \left\lceil \frac{j_i}{2} \right\rceil} k_i = \rho} \phi^1 \left(2^{\frac{j_i}{2}} x_2 + c_2 t_i^{(2)} \right), \quad \text{(C.17)}$$

(C.15) becomes

$$\sum_{|\rho| \leq 2^J} \sum_{r_\rho \in R_\rho} {\alpha'}_\rho(x_2) \hat{\alpha}_{\rho, r_\rho} \phi^1 \left(2^J x_1 + \rho x_2 - r_\rho/n \right),$$

with $\hat{\alpha}_{\rho, r_\rho} \neq 0$.

If $f \neq 0$ there exists $x_2 \in \mathbb{R}$ such that $f(\cdot, x_2) \neq 0$. Furthermore since ϕ^1 is continuous we have that for every x_2 there exists $\epsilon > 0$ such that for all $|\rho| \leq 2^J$ either $\alpha'_\rho \neq 0$ for all $\tilde{x}_2 \in B_\epsilon(x_2)$ or $\alpha'_\rho = 0$ for all $x_2 \in B_\epsilon(x_2) \setminus \{x_2\}$. Hence we know that there exists $\emptyset \neq P \subseteq \{-2^J + 1, \ldots, 2^J - 1\}$ and $\epsilon > 0$ such that $\alpha'_\rho(\tilde{x}_2) \neq 0$ for $\rho \in P$ and $0 < \tilde{x}_2 < \epsilon$ and $\alpha'_\rho = 0$ for $\rho \notin P$ and $0 < \tilde{x}_2 < \epsilon$.

By (C.15) for fixed $0 < \tilde{x}_2 < \epsilon$ we obtain coefficients $\alpha'_{\rho, r_\rho} \neq 0$ for $r_\rho \in R_\rho, \rho \in P$ such that

$$f(x_1, x_2) = \sum_{\rho \in P} \sum_{r_\rho \in R_\rho} {\alpha'}_{\rho, r_\rho} \phi^1 \left(2^J x_1 + \rho \tilde{x}_2 - r_\rho/n \right). \quad \text{(C.18)}$$

We now aim to compute the behavior of the lower support bound of f in x_1 with the help of the representation obtained in (C.18). Since ${\alpha'}_{\rho,r_\rho} \neq 0$, we can deduce the lower support bound of $f(\cdot, x_2)$ from (C.18).

First of all, we observe that there is a minimum r_{min}/n of the numbers r_ρ/n, $r \in R_\rho$, $\rho \in P$. So the lower support bound of the above sum as a function in x_1 is given by

$$\min \left(\operatorname{supp} \sum_{|\rho| \leq 2^J} {\alpha'}_{\rho, r_{min}} \phi^1 \left(2^J \cdot + \rho x_2 - r_{min}/n \right) \right). \tag{C.19}$$

Since $x_2 > 0$ the lower support bound of (C.19) can be found by looking at the unique smallest lower support bound of the respective terms. In fact, if we denote the largest $0 < |\rho| \leq 2^J$ such that $\hat{\alpha}_{\rho, r_{min}} \neq 0$ by ρ_{max} we observe, that the lower support bound of $f(\cdot, x_2)$ is given by

$$\left(2^{-J} \left(\frac{r_{min}}{n} - \rho_{max} x_2 \right), x_2 \right) \text{ for } 0 < x_2 < \epsilon. \tag{C.20}$$

Let $\hat{x}_1 = 2^{-J} \frac{r_{min}}{n}$. Assume first, that $\rho_{max} > 0$. Then for some $\epsilon > 0$ the lower support bound of $f(x_1, \cdot)$ is given by

$$\left(x_1, \left(\frac{r_{min}}{n} - 2^J x_1 \right) / \rho_{max} \right) \text{ for } \hat{x}_1 - \epsilon < x_1 < \hat{x}_1.$$

However, if $\rho_{max} < 0$ then locally $\max(\operatorname{supp} f(x_1, \cdot))$ is given by

$$\left(x_1, \left(\frac{r_{min}}{n} - 2^J x_1 \right) / \rho_{max} \right) \text{ for } \hat{x}_1 < x_1 < \hat{x}_1 + \epsilon. \tag{C.21}$$

Now we will see that this behavior of the support bounds is not possible whenever $f \in \Gamma_2$. By the same arguments presented above, we can write f as

$$f(x_1, \cdot) = \sum_{i \in I} \sum_{r_i \in R_i} \beta_{i, r_i} \phi^1 \left(2^J \cdot + 2^{J - \lceil \frac{j_i}{2} \rceil} k_i x_1 - r_i/n \right) \phi^1 \left(2^{\lfloor \frac{j_i}{2} \rfloor} x_1 - c_1 t_i^2 \right)$$

Using the same grouping as in (C.16) and (C.17) we obtain for $|\mu| \leq 2^J - 1$ the index set R_λ and the function β'_μ. Here μ is smaller than 2^J because of the assumption on the parameter set for the second shearlet cone, see Definition 1.1.

Again there exists $\emptyset \neq M \subset \{-2^J + 1, \ldots, 2^J - 1\}$ such that for some $\epsilon > 0$ have that $\beta'_\mu(\tilde{x}_1) \neq 0$ for all $\mu \in M$ and $\hat{x}_1 - \epsilon < \tilde{x}_1 < \hat{x}_1$ and for $\mu \notin M$ we have $\beta'_\mu(\tilde{x}_1) = 0$ for all $\hat{x}_1 - \epsilon < \tilde{x}_1 < \hat{x}_1$ Then we obtain that

$$f(\tilde{x}_1, \cdot) = \sum_{\mu \in M} \sum_{r_\mu \in R_\mu} {\beta'}_{\mu, r_\mu} \phi^1 \left(2^J \cdot + \mu x_1 - r_\mu/n \right).$$

with ${\beta'}_{\mu, r_\mu} \neq 0$

If $\rho_{max} > 0$, then by (C.21)

$$\sum_{\mu \in M} \sum_{r_\mu \in R_\mu} {\beta'}_{\mu, r_\mu} \phi^1 \left(2^J \cdot + \mu x_1 - r_\mu/n \right) \neq 0$$

for all $\hat{x}_1 - \epsilon < x_1 < \hat{x}_1$.

Again, there exists $r'_{min} \in \bigcup_{\mu \in \tilde{M}} \tilde{R}_\mu$ and a corresponding μ_{max} as in the first case. Furthermore, we obtain from Lemma 1.14 that the minimum support bound in a neighborhood of $\tilde{x}_1$ of $\tilde{f}(z, \cdot)$ is given by

$$\left\{(z, 2^{-J}(r'_{min}/n - \mu_{max} z) \,:\, z \in B_\epsilon(\tilde{x}_1)\right\}.$$

Since $|2^{-J}\mu_{max}| < 1$ and $|2^J/\rho_{max}| \geq 1$, we see that the slope of the lower support bound is different to the previous case. Which implies, that f cannot be in the first and the second cone at the same time.

If $\rho_{max} < 0$ then the same arguments yield for an $\tilde{x}_1$ such that $\hat{x}_1 \leq \tilde{x}_1 \leq \hat{x}_1 + \epsilon$ that the lower support bound of $\tilde{f}(\tilde{x}_1, \cdot)$ is given by

$$\left\{(z, 2^{-J}(r'_{min}/n - \mu_{max} z)) \,:\, z \in B_\epsilon(\tilde{x}_1)\right\}.$$

If furthermore $\mu_{max} > 0$ we obtain that the lower support bound of $\tilde{f}(\cdot, \hat{x}_2)$ for $\hat{x}_2 = 2^{-J}(r'_{min}/n - \mu_{max}\tilde{x}_1)$ is locally given as

$$((r'_{min}/n - 2^J \tilde{x}_2)/\mu_{max}, \tilde{x}_2), \text{ for } \tilde{x}_2 \text{ in a neighborhood of } B_\epsilon(\hat{x}_2),$$

which contradicts (C.20)

Lastly, if $\rho_{max} < 0$ and $\mu_{max} < 0$, then $2^{-J}(r'_{min}/n - \mu_{max}\tilde{x}_1) < 0$ which cannot happen since we assumed, that the smallest x_2 such that $f(\cdot, x_2) \neq 0$ is 0.

Hence $\operatorname{span}\Gamma_1 \cap \operatorname{span}\Gamma_2 = 0$. Furthermore, $\operatorname{span}\Gamma_1 \cap \operatorname{span}\Gamma_3 = 0$, since for functions from Γ_3 the lower support bounds along slices remain constant on small intervals in contrast to functions from Γ_1 or Γ_2, see Figure 1.2.

Finally, the behavior of lower supports in (C.19) remain unchanged if we assume $f \in \operatorname{span}(\Gamma_1 \cup \Gamma_3)$ with the exception, that ρ_{min} can now be 0. In that case the lower support bound can also remain constant, which, as we have seen, does not happen for functions in $\operatorname{span}\Gamma_2$.

C.7 Proof of Theorem 1.23

Let $f = P_\Omega(f_1 + \chi_D f_2) \in \mathcal{E}^2(\nu, \Omega)$ and $\theta_n^\omega(f)$ denote the non-increasing rearrangement of $|\langle f, \varphi_n \rangle_{L^2(\Omega)}|^2_{\varphi_n \in \mathcal{W}_{t,\tau}(\phi^1)}$. Further, let $\theta_n^\psi(f)$ denote the non-increasing rearrangement of $|\langle f, \varphi_n \rangle_{L^2(\Omega)}|^2_{\varphi_n \in \mathcal{S}_0}$ where $\mathcal{S}_0 = \{\psi_{j,k,m,\varepsilon} \,:\, (j,k,m,\varepsilon) \in \Lambda_0\}$. Then

$$\|f - f_N^*\|^2_{L^2(\Omega)} \leq \sum_{n \geq N} \theta_n(f) \leq \sum_{n \geq \frac{2N}{3}} \theta_n^\omega(f) + \sum_{n \geq \frac{N}{3}} \theta_n^\psi(f) =: \mathrm{I} + \mathrm{II}. \tag{C.22}$$

By Theorem 1.6 we can bound II as

$$\mathrm{II} \lesssim N^{-2} \log(N)^3. \tag{C.23}$$

As for I we can split the coefficients as follows

$$\theta_n^\omega(f) = |\langle \varphi_m, f \rangle_{L^2(\Omega)}|^2 = \begin{cases} \theta_n^\omega(f)^{(s)}, & \operatorname{supp} \varphi_m \cap \partial D \neq \emptyset \\ \theta_n^\omega(f)^{(s)}, & \text{otherwise.} \end{cases}$$

Then,

$$\mathrm{I} \leq \sum_{n \geq \frac{N}{3}} \theta_n^{\omega}(f)^{(s)} + \sum_{n \geq \frac{N}{3}} \theta_n^{\omega}(f)^{(ns)}. \tag{C.24}$$

It follows from [Coh00] that the coefficients corresponding to the smooth part can be bounded as

$$\sum_{n \geq \frac{N}{3}} \theta_n^{\omega}(f)^{(s)} \lesssim N^{-2} \quad \text{as } N \to \infty. \tag{C.25}$$

The wavelet coefficients corresponding to the non-smooth part of f can be estimated by observing that, since the boundary curve of D intersects $\partial\Omega$ only finitely often, due to the construction of the wavelet system $\mathcal{W}_{t,\tau}(\phi^1)$ for a small enough resolution we obtain that only $\sim 2^{(1-\tau)j} < 2^{(2/3-\mu)j}$ wavelets intersect the boundary of D where $0 < \mu < \tau - 1/3$.

Furthermore, due to the boundedness of f, we have $| \langle \omega_{j,m,\upsilon}, f \rangle_{L^2(\Omega)}|^2 \lesssim 2^{-2j}$. Hence, we obtain

$$\sum_{n} (\theta_n^{\omega}(f)^{(ns)})^{\frac{1}{3}} \lesssim \sum_{j \in \mathbb{N}} 2^{(2/3-\mu)j} (2^{-2j})^{\frac{1}{3}} < \infty.$$

Consequently, $(\theta_n^{\omega}(f)^{(ns)})_{n \in \mathbb{N}} \in \ell^{\frac{1}{3}}$ which, by the Stechkin Lemma, yields

$$\sum_{n \geq N} (\theta_n^{\omega}(f)^{(ns)}) \lesssim N^{-2} \text{ for } N \to \infty. \tag{C.26}$$

Applying (C.23)–(C.26) to (C.22) proves the claim.

C.8 Proof of Theorem 3.9

In order to prove Theorem 3.9 we have to construct a dual certificate and verity the assumptions of Proposition 3.10 $i)-iv)$. This is done precisely as in [Poo15] with canonical adaptions to the general frame case.

Assumptions and preliminary results

Following the notation in [Poo15], let $A : \mathcal{H} \longrightarrow \ell^2$ be a linear bounded operator and $\Psi : \mathcal{H} \longrightarrow \ell^2$ be the analysis operator associated to a frame with upper frame bound equal to 1 and lower frame bound denoted by c_1. For $r \in \mathbb{N}$, $M \in \mathbb{N}$, and $N \in \mathbb{N}$, let $\mathbf{N} = (N_k)_{k=1,\dots,r}$, $\mathbf{M} = (M_k)_{k=1,\dots,r}$, $\mathbf{s} = (s_k)_{k=1,\dots,r} \in \mathbb{N}^r$ and $(m_k)_{k=1,\dots,r} \in \mathbb{N}^r$ with

- ▷ $0 = M_0 < M_1 < \ldots < M_r =: M$ and let $\Gamma_k = (M_{k-1}, M_k] \cap \mathbb{N}$.
- ▷ $0 = N_0 < N_1 < \ldots < N_r =: N$ and let $\Lambda_k = (N_{k-1}, N_k] \cap \mathbb{N}$ for $k < r$ and $\Lambda_r = (N_{r-1}, \infty) \cap \mathbb{N}$.
- ▷ $m_k \leq M_k - M_{k-1}$, $q_j = m_j/(M_j - M_{j-1})$, and $\Omega_k \sim Ber(q_k, \Gamma_k)$.
- ▷ $s_k \leq N_k - N_{k-1}$ and let $\Delta \subset [N]$ be such that $|\Delta| = s_1 + \ldots + s_r =: s$ and $\Delta_k = \Lambda_k \cap \Delta$ with $|\Delta_k| = s_k$.

For some $p \in (0,1]$ we write $\kappa = (\kappa_l)_{l=1,\dots,r}$ let $\kappa_l = \kappa_l(\mathbf{N}, \mathbf{s}, p)$ and $\widehat{\kappa}_k = \widehat{\kappa}_l(\mathbf{N}, \mathbf{M}, \kappa)$ for $l = 1, \dots, r$. Further, let $\kappa_{\min} = r \min_{l=1,\dots r} \kappa_l$ and $\kappa_{\max} = r \max_{l=1,\dots r} \kappa_l$. Finally, define the linear bounded operator

$$\begin{aligned} T : \ell^2 &\longrightarrow \ell^2, \\ x &\mapsto \left(\left(\frac{1}{\max\{1, \sqrt{r\kappa_k}\}} x_j \right)_{j \in \Lambda_k} \right)_{k=1,\dots,r}. \end{aligned}$$

We start by a sequence of propositions that are proved analogously to the ones presented in [Poo15].

Proposition C.1 ([Poo15])**.** *Let $g \in \mathcal{R}$ and let $\alpha > 0$ and $\eta \in (0,1]$. Suppose that*

$$\|T\Psi(P_{\mathcal{R}} A^* P_{[M]} A P_{\mathcal{R}} - P_{\mathcal{R}})\Psi^* T^{-1}\|_{2\to 2} \le \alpha/(2c_1).$$

Then

$$\mathbb{P}\left(\left\| T\Psi \left(P_{\mathcal{R}} A^* \left(\bigoplus_{i=1}^{r} q_i^{-1} P_{\Omega_i} \right) A P_{\mathcal{R}} - P_{\mathcal{R}} \right) g \right\|_2 \ge \alpha \|T\widetilde{\Psi} g\|_2 \right) \le \eta$$

provided that

$$\sqrt{r}\widetilde{B} \log\left(\frac{3}{\eta}\right) \sum_{l=1}^{r} \mu^2_{\mathbf{N},\mathbf{M}}(k,l)\kappa_l \lesssim \alpha, \quad k = 1, \dots, r$$

and

$$r\widetilde{B}^2 \log\left(\frac{3}{\eta}\right) \sum_{k=1}^{r} (q_i^{-1} - 1)\mu^2_{\mathbf{N},\mathbf{M}}(k,l)\widehat{\kappa}_k \lesssim \alpha^2, \quad l = 1, \dots, r$$

where

$$\widetilde{B} = \|\Psi P_{\mathcal{R}} \widetilde{\Psi}^*\|_{\infty\to\infty} \max_{l=1,\dots,r} \sum_{l=1}^{r} \|P_{\Lambda_t} \Psi P_{\mathcal{R}} \Psi^* P_{\Lambda_t}\|_{\infty\to\infty}$$

Proof. Without loss of generality we assume $\|T\widetilde{\Psi} g\|_2 = 1$. Let $(\delta_j)_{j=1,\dots,M}$ be random Bernoulli variables such that $\mathbb{P}(\delta_j = 1) = \widetilde{q}_j$ where $\widetilde{q}_j = q_k$ for $j = M_{k-1}+1, \dots, M_k$. THen

$$\begin{aligned} &T\Psi \left(P_{\mathcal{R}} A^* \left(\bigoplus_{i=1}^{r} q_i^{-1} P_{\Omega_i} \right) A P_{\mathcal{R}} - P_{\mathcal{R}} \right) g \\ &= \sum_{j=1}^{M} (\widetilde{q}_j^{-1}\delta_j - 1) T\Psi P_{\mathcal{R}} A^* (e_j \otimes \overline{e_j}) A P_{\mathcal{R}} g + T\Psi(P_{\mathcal{R}} A^* P_{[M]} A P_{\mathcal{R}} - P_{\mathcal{R}}) g \end{aligned}$$

By assumption we have

$$\|T\Psi(P_{\mathcal{R}} A^* P_{[M]} A P_{\mathcal{R}} - P_{\mathcal{R}}) g\|_{2\to 2} \le \frac{1}{c_1} \|T\Psi(P_{\mathcal{R}} A^* P_{[M]} A P_{\mathcal{R}} - P_{\mathcal{R}})\Psi^* T^{-1} T\widetilde{\Psi} g\|_{2\to 2} \le \alpha/2.$$

Therefore it is sufficient to show that the probability that $\sum_{j=1}^{M}(\widetilde{q_j}^{-1}\delta_j - 1)T\Psi P_{\mathcal{R}}A^*(e_j \otimes \overline{e_j})AP_{\mathcal{R}}g$ is small is large, in particular, we show

$$\mathbb{P}\left(\left\|\sum_{j=1}^{M}\underbrace{(\widetilde{q_j}^{-1}\delta_j - 1)T\Psi P_{\mathcal{R}}A^*(e_j \otimes \overline{e_j})AP_{\mathcal{R}}g}_{=:Y_j}\right\|_2 \geq \alpha/2\right) \leq \eta.$$

We first bound $\max_j \|Y_j\|_2$. Indeed,

$$\begin{aligned}\|Y_j\|_2 &\leq \widetilde{q_j}^{-1}\|T\Psi P_{\mathcal{R}}A^*(e_j \otimes \overline{e}_j)Ag\|_2\\ &= \widetilde{q_j}^{-1}\sup_{\|x\|_2=1}|\langle T\Psi P_{\mathcal{R}}A^*(e_j \otimes \overline{e}_j)Ag, x\rangle\|\\ &= \widetilde{q_j}^{-1}\sup_{\|x\|_2=1}|\langle Ag, e_j\rangle\langle T\Psi P_{\mathcal{R}}A^*e_j, x\rangle|.\end{aligned}$$

Furthermore, for each $j \in \Gamma_k$

$$|\langle Ag, e_j\rangle| = |\langle A\Psi^*\widetilde{\Psi}g, e_j\rangle| \leq \sum_{l=1}^{r}|\langle A\Psi^*P_{\Lambda_l}\widetilde{\Psi}g, e_j\rangle| \leq \sum_{l=1}^{r}\mu(P_{\Gamma_k}A\Psi^*P_{\Lambda_l})\|P_{\Lambda_l}\widetilde{\Psi}g\|_1.$$

By Corollary 5.4 of [Poo15] we obtain

$$|\langle Ag, e_j\rangle| \leq \sqrt{r}\sum_{l=1}^{r}\mu(P_{\Gamma_k}A\Psi^*P_{\Lambda_l})\kappa_l.$$

Furthermore, for $\|x\|_2 = 1$ we obtain

$$\begin{aligned}|\langle T\Psi P_{\mathcal{R}}A^*e_j, x\rangle|^2 &\leq \sum_{l=1}^{r}\|P_{\Lambda_l}T\Psi P_{\mathcal{R}}A^*e_j\|_2^2\\ &= \sum_{l=1}^{r}\|P_{\Lambda_l}T\Psi P_{\mathcal{R}}\widetilde{\Psi}^*\Psi A^*e_j\|_2^2\\ &\leq \sum_{l=1}^{r}\frac{1}{r\kappa_l}\|P_{\Lambda_l}\Psi P_{\mathcal{R}}\widetilde{\Psi}^*\|_{\infty\to 2}^2\|\Psi A^*e_j\|_\infty^2\\ &\|\Psi P_{\mathcal{R}}\widetilde{\Psi}^*\|_{\infty\to 2}^2\mu^2(P_{\Gamma_k}A\Psi).\end{aligned}$$

Therefore

$$\max_j \|Y_j\|_2 \leq \|\Psi p_{\mathcal{R}}\widetilde{\Psi}^*\|_{\infty\to\infty}\sqrt{r}\max_{k=1,\ldots,r}\sum_{l=1}^{r}\mu_{\mathbf{N},\mathbf{M}}^2(k,l)\kappa_l.$$

Furthermore, let $F \subset \ell^2(\mathbb{N})$ be a countable subsets and suppose $\|f\| \leq 1$ for all $f \in F$. Then

$$\sup_{f\in F}\mathbb{E}\sum_{j=1}^{M}|\langle f, Y_j\rangle|^2 \leq \sup_{f\in F}\sum_{j=1}^{M}(\widetilde{q_j}^{-1} - 1)|\langle e_j, Ag\rangle|^2|\langle A^*e_j, P_{\mathcal{R}}\Psi^*Tf\rangle|^2$$

$$\leq \sup_{f\in F}\sum_{k=1}^{r}(\widetilde{q}_k^{-1}-1)\|P_{\Gamma_k}Ag\|_2^2\max_{j\in\Gamma_k}|\langle A^*e_j, P_{\mathcal{R}}\Psi^*Tf\rangle|^2$$
$$\leq \sup_{f\in F}\sum_{k=1}^{r}(\widetilde{q}_k^{-1}-1)\|P_{\Gamma_k}Ag\|_2^2\max_{j\in\Gamma_k}\|T\Psi P_{\mathcal{R}}A^*e_j\|_2^2.$$

By definition of $\widehat{\kappa}_k$ we obtain $\|P_{\Gamma_k}Ag\|_2^2 \leq r\widehat{\kappa}_k$ and for each $j\in\Gamma_k$

$$\begin{aligned}
\|T\Psi P_{\mathcal{R}}A^*e_j\|_2^2 &= \sum_{t=1}^{r}\frac{1}{r\kappa_t}\|P_{\Lambda_t}\Psi P_{\mathcal{R}}A^*e_j\|_2^2\\
&= \sum_{t=1}^{r}\frac{1}{r\kappa_t}\|P_{\Lambda_t}\Psi P_{\mathcal{R}}A^*\widetilde{\Psi}^*\|_{\infty\to 2}\|\Psi A^*e_j\|_\infty\|P_{\Lambda_t}\Psi P_{\mathcal{R}}A^*e_j\|_2\\
&\leq \sum_{t=1}^{r}\frac{1}{r\sqrt{\kappa_t}}\|\Psi P_{\mathcal{R}}\widetilde{\Psi}^*\|_{\infty\to\infty}\|\Psi A^*e_j\|_\infty\|P_{\Lambda_t}\Psi P_{\mathcal{R}}\widetilde{\Psi}^*P_{\Lambda_l}\|_{\infty\to\infty}\|P_{\Lambda_l}\Psi A^*e_j\|_\infty\\
&\leq \sum_{t=1}^{r}\frac{1}{r}\|\Psi P_{\mathcal{R}}\widetilde{\Psi}^*\|_{\infty\to\infty}\sum_{l=1}^{r}\|P_{\Lambda_t}\Psi P_{\mathcal{R}}\widetilde{\Psi}^*P_{\Lambda_l}\|_{\infty\to\infty}\mu_{\mathbf{N},\mathbf{M}}(k,l).
\end{aligned}$$

Therefore

$$\begin{aligned}
&\sup_{f\in F}\mathbb{E}\sum_{j=1}^{M}|\langle f, Y_j\rangle|^2\\
&\quad\leq r\|\Psi P_{\mathcal{R}}\widetilde{\Psi}^*\|_{\infty\to\infty}\sum_{l=1}^{r}\sum_{k=1}^{r}(q_k^{-1}-1)\widehat{\kappa}_k\mu_{\mathbf{N},\mathbf{M}}^2(k,l)\sum_{l=1}^{r}\frac{1}{r}\|P_{\Lambda_t}\Psi P_{\mathcal{R}}\widetilde{\Psi}^*P_{\Lambda_l}\|_{\infty\to\infty}\\
&\quad\leq r\widetilde{B}^2\max_{l=1,\dots,r}\sum_{k=1}^{r}(q_k^{-1}-1)\mu_{\mathbf{N},\mathbf{M}}^2(k,l)\widehat{\kappa}_k,
\end{aligned}$$

with

$$\widetilde{B} = \|\Psi P_{\mathcal{R}}\widetilde{\Psi}^*\|_{\infty\to\infty}\max_{l=1,\dots,r}\sum_{l=1}^{r}\|P_{\Lambda_l}\Psi P_{\mathcal{R}}\widetilde{\Psi}^*P_{\Lambda_l}\|_{\infty\to\infty}.$$

Furthermore, we have

$$\begin{aligned}
\mathbb{E}\left(\left\|\sum_{j=1}^{M}Y_j\right\|_2^2\right) &= \sum_{j=1}^{M}\mathbb{E}\,\|Y_j\|_2^2\\
&\leq \sum_{k=1} r(q_k{-}1-1)\|P_{\Gamma_k}Ag\|_2^2\max_{j\in\Gamma_k}\|T\Psi P_{\mathcal{R}}A^*e_j\|_2^2\\
&\leq \widetilde{B}^2\max_{l=1,\dots,r}\sum_{k=1}^{r}(q_k^{-1}-1)\mu_{\mathbf{N},\mathbf{M}}^2(k,l)\widehat{\kappa}_k.
\end{aligned}$$

This yields

$$\mathbb{E}\left\|\sum_{j=1}^{M}Y_j\right\|_2 \leq \widetilde{B}\sqrt{\max_{l=1,\dots,r}\sum_{k=1}^{r}(q_k^{-1}-1)\mu_{\mathbf{N},\mathbf{M}}^2(k,l)\widehat{\kappa}_k}.$$

Let now

$$C_1 = \|\Psi p_{\mathcal{R}} \widetilde{\Psi}^*\|_{\infty\to\infty} \sqrt{r} \max_{k=1,\dots,r} \sum_{l=1}^{r} \mu^2_{\mathbf{N},\mathbf{M}}(k,l)\kappa_l$$

and

$$C_2 = r\widetilde{B}^2 \max_{l=1,\dots,r} \sum_{k=1}^{r} (q_k^{-1} - 1)\mu^2_{\mathbf{N},\mathbf{M}}(k,l)\widehat{\kappa}_k.$$

Then, for $C := \max\{C_1, 4C_2/\alpha\}$ we have by the above estimates:

$$\max_j \|Y_j\|_2 \le C \quad \text{and} \quad \sup_{f\in F} \mathbb{E} \sum_{j=1}^{M} |\langle f, Y_j\rangle|^2 \le \alpha C/4.$$

Now suppose that $C_2 \le (\alpha/4)^2$. Then

$$\mathbb{E}\left\|\sum_{j=1}^{M} Y_j\right\| \le \alpha/4.$$

Moreover, by Talagrand's inequality ([Led01]), see also Proposition 8.1 in [Poo15], there exists $K > 0$ such that

$$\begin{aligned}
\mathbb{P}\left(\left\|\sum_{j=1}^{M} Y_j\right\| \ge \alpha/2\right) &\le \mathbb{P}\left(\left\|\sum_{j=1}^{M} Y_j\right\| \ge \alpha/4 + \mathbb{E}\left\|\sum_{j=1}^{M} Y_j\right\|\right) \\
&\le \mathbb{P}\left(\left|\left\|\sum_{j=1}^{M} Y_j\right\| - \mathbb{E}\left\|\sum_{j=1}^{M} Y_j\right\|\right| \ge \alpha/4\right) \\
&\le 3\exp\left(-\frac{\alpha}{4KC}\log\left(1 + \frac{\alpha C/4}{\sup_{f\in F}\mathbb{E}\sum_{j=1}^{M}|\langle f, Y_j\rangle|^2 + \alpha C/4}\right)\right) \\
&\le 3\exp\left(-\frac{\alpha}{4KC}\log\left(\frac{3}{2}\right)\right).
\end{aligned}$$

Thus, for any $\eta \in (0,1]$ we have

$$\mathbb{P}\left(\left\|\sum_{j=1}^{M} Y_j\right\| \ge \alpha/2\right) \le \gamma$$

provided

$$C\log(3/\eta) \le \frac{\alpha}{4K}\log(3/2) \quad \text{and} \quad C_2 \le (\alpha/4)^2.$$

In order to let the statement hold it therefore suffices to have

$$\sqrt{r}\widetilde{B}\log\left(\frac{3}{\eta}\right)\sum_{l=1}^{r} \mu^2_{\mathbf{N},\mathbf{M}}(k,l)\kappa_l \le \alpha\frac{\log(3/4)}{4K}, \quad k = 1,\dots,r$$

and

$$r\widetilde{B}^2 \log\left(\frac{3}{\eta}\right)\sum_{k=1}^{r}(q_i^{-1}-1)\mu^2_{\mathbf{N},\mathbf{M}}(k,l)\widehat{\kappa}_k \leq \alpha^2 \min\left\{1/16, \frac{\log(3/2)}{16K}\right\}, \quad l=1,\dots,r.$$

□

The next three proposition will be given here without a proof as they use, similar as the first one, line by line the same arguments with corresponding adaptions to the non-tight frame case.

Proposition C.2 ([Poo15])**.** *Let $g \in \mathcal{H}$ be fixed, $\alpha > 0$ and $\eta \in (0,1]$. If*

$$\|\Psi P_{\mathcal{R}}^{\perp} A^* P_{[M]} A P_{\mathcal{R}} \Psi^* T^{-1}\|_{2\to\infty} \leq \alpha/2$$

then

$$\widetilde{M} := \min\left\{i \in \mathbb{N} : \max_{j\geq i} 2\sqrt{r \max_{j=1,\dots,r}\kappa_j}\max_{j=1,\dots,r} q_k^{-1}\|P_{[M]}A\Psi^* e_j\|_2 \leq \alpha\right\}$$

is finite and

$$\mathbb{P}\left(\left\|P_{\Delta}^{\perp}\Psi P_{\mathcal{R}}^{\perp}A^*\left(\bigoplus_{j=1}^{r} q_j^{-1}P_{\Omega_j}\right)AP_{\mathcal{R}}g\right\|_{\infty} \geq \alpha\|T\Psi g\|_2\right) \leq \eta$$

provided that

$$\sqrt{r}\|\widetilde{\Psi}P_{\mathcal{R}}^{\perp}\Psi^*\|_{\infty\to\infty}\log\left(\frac{4\widetilde{M}}{\eta}\right)q_k^{-1}\sum_{l=1}^{r}\mu^2_{\mathbf{N},\mathbf{M}}(k,l)\kappa_l \lesssim \alpha, \quad k=1,\dots,r$$

and

$$r\|\widetilde{\Psi}P_{\mathcal{R}}^{\perp}\Psi^*\|^2_{\infty\to\infty}\log\left(\frac{4\widetilde{M}}{\eta}\right)\sum_{k=1}^{r}(q_k^{-1}-1)\mu^2_{\mathbf{N},\mathbf{M}}(k,j)\widehat{\kappa}_k \lesssim \alpha^2, \quad j=1,\dots,r.$$

Proposition C.3 ([Poo15])**.** *Let $\alpha > 0$ and $\eta \in (0,1]$. Suppose that*

$$\|P_{\mathcal{R}}A^*P_{[M]}^{\perp}AP_{\mathcal{R}}\|_{\mathcal{H}\to\mathcal{H}} \leq \alpha/2.$$

Then

$$\mathbb{P}\left(\left\|P_{\mathcal{R}}A^*\left(\bigoplus_{j=1}^{r} q_j^{-1}P_{\Omega_j}\right)AP_{\mathcal{R}} - P_{\mathcal{R}}A^*AP_{\mathcal{R}}\right\|_{\mathcal{H}\to\mathcal{H}} \geq \alpha\right) \leq \eta$$

provided that

$$\alpha^{-2}\log\left(\frac{4\widetilde{M}}{\eta}\right)\sum_{l=1}^{r}\mu^2_{N,M}(k,l)\kappa_l \lesssim q_k, \quad k=1,\dots,r.$$

Proposition C.4 ([Poo15]). *Let $\alpha > 0$ and $\gamma \in (0,1]$. Then*

$$\widetilde{M} := \min\left\{ i \in \mathbb{N} \,:\, \max j \geq i \|P_{[M]} A\Psi^* e_j\|_2 + \|P_{\mathrm{ran}(\Psi^* P_{[N]})} \Psi^+ e_j\|_2 < \sqrt{\frac{5q}{4}} \right\}$$

is finite and

$$\mathbb{P}\left(\sup_{j\in\mathbb{N}} \left\| P_{\{j\}} \Psi P_{\mathcal{R}}^{\perp} A^* \left(\bigoplus_{j=1}^{r} q_j^{-1} P_{\Omega_j} \right) A P_{\mathcal{R}} \Psi^* P_{\{j\}} \right\| \geq 5/4 \right) \leq \eta$$

provided that for each $k = 1, \dots, r$ and each $j \in \mathbb{N}$

$$\|\widetilde{\Psi} P_{\mathcal{R}}^{\perp} \Psi^*\|^2 \max_{j=1,\dots,r} (q_k^{-1} - 1) \mu_{\mathbf{N},\mathbf{M}}^2(k,j) \log\left(\frac{2\widetilde{M}}{\eta}\right) \lesssim 1.$$

Construction of the dual certificate

In this section we want to give a construction of a dual certificate such that the condition *iii*) of Proposition 3.10 is satisfied. Properties *i*) and *ii*) are verified in [Poo15]. Note that in [Poo15] the assumption $\|\Psi\| = 1$ is used multiple times so the involved estimates need to be adapted but they work out similarly. The construction of the dual certificate follows the construction given in [Poo15]. However, we have to make some adaptions in the construction.

Let $\widetilde{\gamma} = \gamma/6$ and $\mathcal{L} = \log(4q^{-1}\kappa^{1/2}\widetilde{M}\|\Psi\Psi^*\|_{\infty\to\infty})$ where

$$\widetilde{M} = \min\left\{ i \in \mathbb{N} \,:\, \max_{j\geq i} \left\{ \|P_{[M]} A\Psi^* e_j\|_2 \leq q/(8\kappa_{\max}^{1/2} \right\} \max_{j\geq i} \|P_{\mathrm{ran}\,\Psi^* P_{[N]}} \Psi^* e_j\| \leq \sqrt{5q}/4 \right\}.$$

Further, let

$$\begin{aligned}
&\nu = \log\left(8q^{-1}\kappa_{\max}^{1/2}\widetilde{M}\|\Psi\Psi^*\|_{\infty\to\infty}\right), \\
&\mu = 8\lceil 3\nu + \log(\widetilde{\gamma}^{-1/2}) \rceil, \\
&q_k^1 = q_k^2 = q_k/4, \quad , \widetilde{q}_k = q_k^3 = \ldots = q_k^{\mu}, \quad k = 1, \dots, r, \\
&\alpha_1 = \alpha_2 = \frac{1}{2\sqrt{\mathcal{L}}}, \quad \alpha_i)1/2, \quad i = 3, \dots, \mu, \\
&\beta_1 = \beta_2 = 1/4, \quad \beta_i = \mathcal{L}/4, \quad i = 3, \dots, \mu.
\end{aligned}$$

For $j = 1, \dots, \mu$ define

$$U_j : \ell^2 \longrightarrow \ell^2, \quad U_j := \frac{1}{q_1^j} P_{\Omega_1^j} \oplus \ldots \oplus \frac{1}{q_r^j} P_{\Omega_r^j}.$$

Let $Z_0 := \widetilde{\Psi}^* \operatorname{sgn}(P_\Delta \widetilde{\Psi} f)$ and for $i = 1, 2$ define

$$Z_i = Z_0 - P_{\mathcal{R}} Y_i, \quad Y_i = \sum_{j=i}^{i} A^* U_j A Z_{j-1}.$$

Let $\Theta_1 = \{1\}, \Theta_2 = \{1,2\}$ and for $i \geq 3$, define

$$\Theta_i = \begin{cases} \Theta_{i-1} \cup \{i\}, & \|T\widetilde{\Psi}(Z_{i-1} - A^*U_iAZ_{i-1})\|_2 \leq \alpha_i \|T\widetilde{\Psi}Z_{i-1}\|_2, \\ & \|P_\delta^\perp \Psi P_\mathcal{R}^\perp A^*U_iAZ_{i-1}\|_\infty \leq \beta_i \|T\widetilde{\Psi}Z_{i-1}\|_2, \\ \Theta_{i-1}, & \text{otherwise.} \end{cases}$$

$$Y_i = \begin{cases} \sum_{j\in\Theta_i} A^*U_jAZ_{j-1}, & i \in \Theta_i, \\ Y_{i-1}, & \text{otherwise.} \end{cases}$$

$$Z_i = \begin{cases} Z_0 - P_\mathcal{R} Y_i, & i \in \Theta_i, \\ Z_{i-1}, & \text{otherwise.} \end{cases}$$

Note that $Z_i \in \mathcal{R}$ for each $i = 1, \ldots, \mu$. Using the Proposition C.1-C.4 we can verify the assumptions of Proposition 3.10 for the dual certificate above. This is examined precisely as in [Poo15] and will be left out.

C.9 Proof of Theorem 4.6

The optimal δ_s for which $\widetilde{A} = \begin{pmatrix} r_1 \\ \vdots \\ r_m \end{pmatrix} \in \mathbb{R}^{m\times n}$ satisfies the Ψ-RIP is given by

$$\delta_s = \|\widetilde{A}^*\widetilde{A} - \operatorname{Id}_n\|_\Delta := \sup_{f\in\Delta} \langle (\widetilde{A}^*\widetilde{A} - \operatorname{Id}_n)x, x\rangle$$

where

$$\Delta = \{x \in \operatorname{ran}\Psi^* \,:\, x = \Psi^*c, \|c\|_0 \leq s, \|x\| \leq 1\} \subseteq \mathbb{R}^n.$$

Since $\mathbb{E} r_i^* r_i = \operatorname{Id}_n$ we have

$$\delta_s = \|\widetilde{A}^*\widetilde{A} - \operatorname{Id}_n\|_\Delta = \left\| \frac{1}{m}\sum_{i=1}^m \frac{1}{m}{}_i^* r_i - \operatorname{Id}_N \right\|_\Delta = \frac{1}{m}\left\| \sum_{i=1}^m (r_i^* r_i - \mathbb{E} r_i^* r_i) \right\|_\Delta .$$

For a Rademacher sequence $\varepsilon = (\varepsilon_i)_i$ independent of $(r_i)_i$ we have by Lemma 6.7 in [Rau10]

$$\mathbb{E}\delta_s = \frac{1}{m}\mathbb{E}\left\| \sum_{i=1}^m (r_i^* r_i - \mathbb{E} r_i^* r_i) \right\|_\Delta \leq \frac{2}{m}\mathbb{E}\left\| \sum_{i=1}^m \varepsilon_i r_i^* r_i \right\|_\Delta ,$$

hence,

$$\mathbb{E}\delta_s \leq \frac{2}{m}\mathbb{E}_r\mathbb{E}_\varepsilon \sup_{x\in\Delta} \left| \langle \sum_{i=1}^m \varepsilon_i r_i^* r_i x, x\rangle \right| = \frac{2}{m}\mathbb{E}_r\mathbb{E}_\varepsilon \sup_{x\in\Delta} \left| \sum_{i=1}^m \varepsilon_i |\langle r_i, x\rangle|^2 \right| .$$

Define the pseudo-metric

$$d(x,y) = \left(\sum_{i=1}^m \left(|\langle r_i, x\rangle|^2 - |\langle r_i, y\rangle|^2 \right)^2 \right)^{1/2} .$$

Then, as shown in [KNW15] we have for $x, y \in \Delta$

$$d(x,y) \leq 2 \sup_{z\in\Delta} \left(\sum_{i=1}^{m} |\langle r_i, z\rangle|^{2p} \right)^{1/(2p)} \left(\sum_{i=1}^{m} |\langle r_i, x-y\rangle|^{2p} \right)^{1/(2p)},$$

where $p, q \geq 1$ such that $p^{-1} + q^{-1} = 1$.

Now, for any $h \in \Delta$ of the form $z = \Psi^* c$ with $\|c\|_0 \leq s$ and any realization of $(r_i)_i$ we have

$$\begin{aligned} |\langle r_i, z\rangle| &= |\langle \Psi(\Psi^*\Psi)^{-1} r_i, \Psi\Psi^* c\rangle| \\ &\leq \sum_{\lambda \leq N} |\langle r_i, \widetilde{\psi}_\lambda\rangle| |(\Psi\Psi^* c)_\lambda| \\ &\leq \sum_{\lambda \leq N} \frac{K}{c_1} |(\Psi\Psi^* c)_\lambda|, \end{aligned}$$

where $K > 0$ is so that $\|\psi_\lambda\| \leq K$ for all $\lambda \leq N$ and c_1 denotes the lower frame bound. Therefore

$$|\langle r_i, h\rangle| \leq \frac{K}{c_1} L\sqrt{s}$$

with

$$L = \sup_{\substack{\|\Psi^* c\|=1 \\ \|c\|_0 \leq s}} \frac{\|(\Psi\Psi^* c)_\lambda\|_1}{\sqrt{s}}.$$

Therefore we obtain

$$\begin{aligned} \sup_{z\in\Delta} \left(\sum_{i=1}^{m} |\langle r_i, z\rangle|^{2p} \right)^{1/(2p)} &= \sup_{z\in\Delta} \left(\sum_{i=1}^{m} |\langle r_i, z\rangle|^{2} |\langle r_i, z\rangle|^{2p-2} \right)^{1/(2p)} \\ &\leq \left(s \left(\frac{KL}{c_1} \right)^2 \right)^{(p-1)/(2p)} \left(\sup_{z\in\Delta} \sum_{i=1}^{m} |\langle r_i, z\rangle|^{2p} \right)^{1/(2p)}. \end{aligned}$$

The rest of the proof follows the argumentation given in [KNW15].

For a set Σ, a metric d and a given $t > 0$ the *covering number* $\mathcal{N}(\Sigma, d, t)$ is defined as the smallest number of balls of radius t centered at points of Σ necessary to cover Σ with respect to d. By Dudley's inequality we have

$$\mathbb{E}_\varepsilon \sup_{x\in\Delta} \left| \langle \sum_{i=1}^{m} \varepsilon_i r_i^* r_i x, x\rangle \right| \leq 4\sqrt{2} \int_0^\infty \sqrt{\log(\mathcal{N}(\Delta, d, t)}\, dt. \tag{C.27}$$

Using the semi-norm

$$\|x\|_{X,q} := \left(\sum_{i=1}^{m} |\langle r_i, x\rangle|^{2q} \right)^{1/(2q)}$$

we obtain using covering arguments and (C.27)

$$\mathbb{E}_\varepsilon \sup_{x\in\Delta} \left| \langle \sum_{i=1}^m \varepsilon_i r_i^* r_i x, x\rangle \right|$$
$$\leq C \left(s \left(\frac{KL}{c_1}\right)^2 \right)^{(p-1)/(2p)} \left(\sum_{i=1}^m |\langle r_i, x\rangle|^{2q} \right)^{1/(2q)} \int_0^\infty \sqrt{\log(\mathcal{N}(\Delta, \|\cdot\|_{X,q}, t)}\, dt.$$

Now, following the arguments in [KNW15] we have

$$\int_0^\infty \sqrt{\log(\mathcal{N}(\Delta, \|\cdot\|_{X,q}, t)}\, dt \leq C\sqrt{q(sL^2)m^{1/q}\log(n)\log^2(sL^2)}.$$

Thus in (C.27) we obtain

$$\mathbb{E}\delta_s \leq \frac{C\left(s \left(\frac{KL}{c_1}\right)^2 \right)^{(p-1)/(2p)} \sqrt{qm^{1/q}sL^2\log(n)\log^2(sL^2)}}{m} \mathbb{E}\sup_{x\in\Delta} \left(\sum_{i=1}^m |\langle r_i, x\rangle|^2 \right)^{1/(2p)}$$
$$\leq \frac{C\left(s \left(\frac{KL}{c_1}\right)^2 \right)^{(p-1)/(2p)} \sqrt{q\log(n)\log^2(sL^2)}}{m^{1-1/(2q)-1/(2p)}} \mathbb{E}\left(\frac{1}{m} \| \sum_{i=1}^m r_i^* r_i - \mathrm{Id}_n \|_\Delta + \| \mathrm{Id}_n \|_\Delta \right)^{1/(2p)}$$
$$\leq \frac{C\left(s \left(\frac{KL}{c_1}\right)^2 \right)^{(p-1)/(2p)} \sqrt{q\log(n)\log^2(sL^2)}}{m^{1/2}} \sqrt{\mathbb{E}\delta_s + 1}.$$

We can assume K/c_1 to greater than one, hence

$$\mathbb{E}\delta_s \leq \frac{C\left(s \left(\frac{KL}{c_1}\right)^2 \right)^{(p-1)/(2p)} \sqrt{q\log(n)\log^2(s\left(\frac{KL}{c_1}\right)^2)}}{m^{1/2}} \sqrt{\mathbb{E}\delta_s + 1}.$$

Choosing $p = 1 + (\log(s(KL)^2 c_1^{-2}))^{-1}$ and $q = 1 + \log(s(KL)^2 c_1^{-2})$ yields

$$(s(KL)^2 c_1^{-2})^{1/2+(p-1)/(2p)} \leq \sqrt{e},$$

hence,

$$\mathbb{E}\delta_s \leq C\sqrt{2\log(n)\log^2(s(KL)^2 c_1^{-2})/m}\sqrt{\mathbb{E}\delta_s + 1}.$$

Finally,

$$\mathbb{E}\delta_s \leq C\sqrt{\frac{s(KL)^2 c_1^{-2}\log(n)\log^3(sL^2)}{m}}$$

provided $\frac{s(KL)^2 c_1^{-2}\log(n)\log^3(s(KL)^2 c_1^{-2})}{m} \leq 1$. Therefore, $\mathbb{E}\delta_s \leq \delta/2$ for some $\delta \in (0,1)$ if

$$m \geq C\delta^{-2} s(KL)^2 c_1^{-2} \log^3(s(KL)^2 c_1^{-2}) \log N. \tag{C.28}$$

Let $f_{x,y}(r) = \mathrm{Re}(\langle (r_i^* r_i - \mathrm{Id}_n)z, w\rangle)$ so that

$$m\delta_s = \left\| \sum_{i=1}^{m} (r_i^* r_i - \mathbb{E} r_i^* r_i) \right\|_{\Delta} = \sup_{x,y\in\Delta} \sum_{i=1}^{M} f_{x,y}(r_i).$$

Note that we have

- ▹ $\mathbb{E} f_{x,y}(r_i) = 0$,
- ▹ $|f_{x,y}(r)| \leq s(KL)^2 c_1^{-2} + 1$,
- ▹ $\mathbb{E}|f_{x,y}(r)|^2 = \mathbb{E}\|(r_i^* r_i - \mathrm{Id})x\|_2^2 \leq (s(KL)^2 c_1^{-2} + 1)^2$.

Now, fix some $\delta \in (0,1)$ and choose m in accordance with (C.28). Then by Theorem 6.25 of [Rau10] we haven

$$\begin{aligned}
\mathbb{P}(\delta_s \geq \delta) &\leq \mathbb{P}(\delta_s \geq \mathbb{E}\delta_s + \delta/9) \\
&= \mathbb{P}\left(\left\| \sum_{i=1}^{m} (r_i^* r_i - \mathbb{E} r_i^* r_i) \right\|_{\Delta} \geq \mathbb{E} \left\| \sum_{i=1}^{m} (r_i^* r_i - \mathbb{E} r_i^* r_i) \right\|_{\Delta} + \delta m/9 \right) \\
&\leq \exp\left(- \frac{\left(\frac{\delta m}{9(s(KL)^2 c_1^{-2}+1)} \right)^2}{2m\left(1 + \frac{\delta}{s(KL)^2 c_1^{-2}+1}\right) + \frac{2}{3}\left(\frac{\delta m}{9(s\eta^2+1)} \right)} \right) \\
&\leq \exp\left(- \frac{\delta^2 m}{Cs(KL)^2 c_1^{-2}} \right),
\end{aligned} \tag{C.29}$$

where the constant C might changed in the last estimate. Further, if

$$m \geq C\delta^{-2} s(KL)^2 c_1^{-2} \log(1/\gamma),$$

then (C.29) is bounded by γ. Thus, $\delta_s \leq \delta$ with probability $1-\gamma$ if

$$m \geq C\delta^{-2} s(KL)^2 c_1^{-2} \max\{\log^3(s(KL)^2 c_1^{-2}) \log(N), \log(1/\gamma)\}.$$

The proof is complete.

Bibliography

[ACP12] A. Aldroubi, X. Chen, and A. M. Powell. Perturbations of measurement matrices and dictionaries in compressed sensing. *Appl. Comput. Harmon. Anal.*, 33(2):282–291, 2012.

[AH] B. Adcock and A. C. Hansen. Generalized sampling and infinite-dimensional compressed sensing. *Found. Comp. Math.* (to appear).

[AH12a] B. Adcock and A. C. Hansen. A generalized sampling theorem for stable reconstructions in arbitrary bases. *J. Fourier Anal. Appl.*, 18(4):685–716, 2012.

[AH12b] B. Adcock and A. C. Hansen. Stable reconstructions in Hilbert spaces and the resolution of the Gibbs phenomenon. *Appl. Comput. Harmon. Anal.*, 32(3):357–388, 2012.

[AHKM15] B. Adcock, A. C. Hansen, G. Kutyniok, and J. Ma. Linear Stable Sampling Rate: Optimality of 2D Wavelet Reconstructions from Fourier Measurements. *SIAM J. Math. Anal.*, 47(2):1196–1233, 2015.

[AHP13] B. Adcock, A. C. Hansen, and C. Poon. Beyond consistent reconstructions: optimality and sharp bounds for generalized sampling, and application to the uniform resampling problem. *SIAM J. Math. Anal.*, 45(5):3132–3167, 2013.

[AHP14] B. Adcock, A. C. Hansen, and C. Poon. On optimal wavelet reconstructions from Fourier samples: Linearity and universality of the stable sampling rate. *Appl. Comput. Harmon. Anal.*, 36(3):387–415, 2014.

[AHPR15] B. Adcock, A. C. Hansen, C. Poon, and B. Roman. Breaking the coherence barrier: A new theory for compressed sensing. *submitted*, 2015.

[AS15] R. Ahmad and P. Schniter. Iteratively reweighted ℓ_1 approaches to sparse composite regularization. *IEEE Trans. Comput. Imaging*, 1(4):220–235, 2015.

[BCH$^+$14] R. W. Brown, Y.-C. N. Cheng, E. M. Haacke, M. R. Thompson, and R. Venkatesan. *Magnetic Resonance Imaging: Physical Principles and Sequence Design, Second Edition.* John Wiley & Sons, Inc, 2014.

[BH14] K. Bredies and M. Holler. Regularization of linear inverse problems with total generalized variation. *J. Inverse Ill-Posed Probl.*, 22(6):871–913, 2014.

[BH15a] K. Bredies and M. Holler. *Scale Space and Variational Methods in Computer Vision: 5th International Conference, SSVM 2015, Lège-Cap Ferret, France, May 31 - June 4, 2015, Proceedings*, chapter Artifact-Free Variational MPEG Decompression. Springer International Publishing, 2015.

[BH15b] K. Bredies and M. Holler. A TGV-Based Framework for Variational Image Decompression, Zooming, and Reconstruction. Part I: Analytics. *SIAM J. Imag. Sci.*, 8(4):2814–2850, 2015.

[BH15c] K. Bredies and M. Holler. A TGV-Based Framework for Variational Image Decompression, Zooming, and Reconstruction. Part II: Numerics. *SIAM J. Imag. Sci.*, 8(4):2851–2886, 2015.

[BKP10] K. Bredies, K. Kunisch, and T. Pock. Total generalized variation. *SIAM J. Img. Sci.*, 3(3):492–526, 2010.

[BS06] M. Bownik and D. Speegle. The Feichtinger conjecture for wavelet frames, Gabor frames and frames of translates. *Canad. J. Math.*, 58(6):1121–1143, 2006.

[BS10] M. Bownik and D. Speegle. Linear independence of Parseval wavelets. *Illinois J. Math.*, 54(2):771–785, 2010.

[Can08] E. J. Candès. The restricted isometry property and its implications for compressed sensing. *C. R. Math. Acad. Sci. Paris*, 346(9-10):589–592, 2008.

[CD02] E. J. Candès and D. L. Donoho. New tight frames of curvelets and optimal representations of objects with piecewise C^2-singularities. *Comm. Pure Appl. Math*, (57):219–266, 2002.

[CDD00] A. Cohen, W. Dahmen, and R. DeVore. Multiscale decompositions on bounded domains. *Trans. Amer. Math. Soc.*, 352(8):3651–3685, 2000.

[CDV93] A. Cohen, I. Daubechies, and P. Vial. Wavelet bases on the interval and fast algorithms. *Appl. Comput. Harmon. Anal*, (1):54–81, 1993.

[CENR11] E. J. Candès, Y. C. Eldar, D. Needell, and P. Randall. Compressed sensing with coherent and redundant dictionaries. *Appl. Comput. Harmon. Anal*, 31(1):59–73, 2011.

[Cha07] R. Chartrand. Exact reconstruction of sparse signals via nonconvex minization. *IEEE Signal Process. Lett.*, 14:707–710, 2007.

[Chr03] O. Christensen. *An Introduction to Frames and Riesz Bases*. Applied and Numerical Harmonic Analysis. Birkhäuser Boston, Inc., Boston, MA, 2003.

[CL] O. Christensen and A. M. Lindner. Lower Bounds for Finite Wavelet and Gabor Systems. *Approx. Theory Appl.*, 17(1):18–29.

[CL02] O. Christensen and A. M. Lindner. Decomposition of Riesz frames and wavelets into a finite union of linearly independent sets. *Linear Algebra Appl.*, 355:147–159, 2002.

[Coh00] A. Cohen. Wavelet methods in numerical analysis. In *Handbook of numerical analysis, Vol. VII*, Handb. Numer. Anal., VII, pages 417–711. North-Holland, Amsterdam, 2000.

[COS10] J.-F. Cai, S. Osher, and Z. Shen. Split Bregman Methods and Frame Based Image Restoration. *Multiscale Model. Simul.*, 8(2):337–369, 2010.

[CRT05] E. J. Candès, J. K. Romberg, and T. Tao. Stable signal recovery from incomplete and inaccurate measurements. *Comm. Pure Appl. Math.*, 59:1207–1223, 2005.

[CRT06] E. J. Candès, J. K. Romberg, and T. Tao. Robust uncertainty principles: exact signal reconstruction from highly incomplete frequency information. *IEEE Trans. Inform. Theory*, 52(2):489–509, 2006.

[CT05] E. J. Candès and T. Tao. Decoding by linear programming. *IEEE Trans. Inform. Theory*, 21(12):4203–4215, 2005.

[CT06] E. J. Candès and T. Tao. Near-optimal signal recovery from random projections: universal encoding strategies? *IEEE Trans. Inform. Theory*, 52(12):5406–5425, 2006.

[CWB08] E. J. Candès, M. B. Wakin, and S. P. Boyd. Enhancing sparsity by reweighted ℓ_1 minimization. *J. Fourier Anal. Appl.*, 14(5–6):877–905, 2008.

[Dau92] I. Daubechies. *Ten Lectures on Wavelets*, volume 61 of *CBMS-NSF Regional Conference Series in Applied Mathematics*. Society for Industrial and Applied Mathematics (SIAM), Philadelphia, PA, 1992.

[Don99] D. L. Donoho. Wedgelets: nearly-minimax estimation of edges. *Ann. Statist*, pages 859–897, 1999.

[Don01] D. L. Donoho. Sparse Components of Images and Optimal Atomic Decomposition. *Constr. Approx.*, 17(3):353–382, 2001.

[Don06] D. L. Donoho. Compressed sensing. *IEEE Trans. Inform. Theory*, 52:1289–1306, 2006.

[DS52] R. J. Duffin and A. C. Schaeffer. A class of nonharmonic Fourier series. *Trans. Amer. Math. Soc.*, 72:341–366, 1952.

[Eld03] Y. C. Eldar. Sampling with Arbitrary Sampling and Reconstruction Spaces and Oblique Dual Frame Vectors. *J. Fourier Anal. Appl.*, 9(1):77–96, 2003.

[EW05] Y. C. Eldar and T. Werther. General framework for consistent sampling in Hilbert spaces. *Int. J. Wavelets Multiresolut. Inf. Process.*, 3(4):497–509, 2005.

[FL09] S. Foucart and M.-J. Lai. Sparsest solutions of underdetermined linear systems via l_q-minimization for $0 < q \leq 1$. *Appl. Comput. Harmon. Anal.*, 26(3):395–407, 2009.

[FM15] H. Führ and Y. Maus. Wavelet riesz bases associated to nonisotropic dilations. 2015. preprint.

[Fou10] S. Foucart. A note on guaranteed sparse recovery via ℓ_1-minimization. *Appl. Comput. Harmon. Anal.*, 29(1):97–103, 2010.

[FR13] S. Foucart and H. Rauhut. *A Mathematical Introduction to Compressive Sensing*. Birkhäuser Basel, 2013.

[GK14] P. Grohs and G. Kutyniok. Parabolic molecules. *Foundations of Computational Mathematics*, 14(2):299–337, 2014.

[GKKS] P. Grohs, S. Keiper, G. Kutyniok, and M. Schäfer. α-molecules. *Appl. Comput. Harm. Anal.* to appear.

[GKL06] K. Guo, G. Kutyniok, and D. Labate. Sparse Multidimensional Representations using Anisotropic Dilation and Shear Operators. *Wavelets and Splines: Athens 2005*, 1:189–201, 2006.

[GKLPU12] M. Guerquin-Kern, L. Lejeune, K. Pruessmann, and M. Unser. Realistic analytical phantoms for parallel magnetic resonance imaging. *IEEE Trans. Med. Imag.*, 31(3):626–636, 2012.

[GKMP15] P. Grohs, G. Kutyniok, J. Ma, and P. Petersen. Multiscale anisotropic directional systems on bounded domains. 2015. submitted.

[GL09] K. Guo and D. Labate. Characterization and analysis of edges using the continuous shearlet transform. *SIAM J. Imaging Sci.*, 2(3):959–986, 2009.

[GO09] T. Goldstein and S. Osher. The Split Bregman Method for L1-Regularized Problems. *SIAM J. Imag. Sci.*, 2(2):323–343, 2009.

[GQY14] W. Guo, J. Qin, and W. Yin. A new detail-preserving regularity scheme. *SIAM J. Imag. Sci.*, 7(2), 2014.

[Gra08] L. Grafakos. *Classical Fourier analysis. 2nd ed.* Graduate Texts in Mathematics 249. New York, NY: Springer. xvis, 2008.

[Grö03] K. Gröchenig. Localized frames are finite unions of riesz sequences. *Adv. Comput. Math.*, 18(2-4):149–157, 2003.

[Gro13] P. Grohs. Intrinsic Localization of Anisotropic Frames. *Appl. Comput. Harmon. Anal.*, 35(2):264–283, 2013.

[GV15] P. Grohs and S. Vigogna. Intrinsic localization of anisotropic frames ii: α-molecules. *J. Fourier Anal. Appl.*, 21(1):182–205, 2015.

[HW96] E. Hernández and G. Weiss. *A first course on wavelets.* Studies in Advanced Mathematics. CRC Press, Boca Raton, FL, 1996. With a foreword by Yves Meyer.

[KBPS11] F. Knoll, K. Bredies, T. Pock, and R. Stollberger. Second order total generalized variation (TGV) for MRI. *Magn. Reson. Med.*, 65(2):480–491, 2011.

[KKL12] P. Kittipoom, G. Kutyniok, and W.-Q. Lim. Construction of Compactly Supported Shearlet Frames. *Constr. Approx.*, 35(1):21–72, 2012.

[KL11] G. Kutyniok and W.-Q Lim. Compactly Supported Shearlets are Optimally Sparse. *J. Approx. Theory*, 163(11):1564–1589, 2011.

[KL12a] G. Kutyniok and D. Labate. *Shearlets: Multiscale Analysis for Multivariate Data.* Birkhäuser Basel, 2012.

[KL12b] G. Kutyniok and W.-Q Lim. Image separation using wavelets and shearlets. *Curves and Surfaces (Avignon, France, 2010), Lecture Notes in Computer Science*, 6920,:416–430, 2012.

[KLL12] G. Kutyniok, J. Lemvig, and W.-Q Lim. Optimally sparse approximations of 3D functions by compactly supported shearlet frames. *SIAM J. Math. Anal.*, 44:2962–3017, 2012.

[KLR16] G. Kutyniok, W.-Q Lim, and R. Reisenhofer. ShearLab 3D: Faithful digital shearlet transforms based on compactly supported shearlets. *ACM Trans. Math. Software*, 42(1), 2016.

[KNW15] F. Krahmer, D. Needell, and R. Ward. Compressive sensing with redundant dictionaries and structured measurements. *SIAM J. Math. Anal.*, 2015. to appear.

[Kol12] C. P. Kolbitsch. *Advanced Techniques for Cardiovascular Magnetic Resonance Imaging in Cases of Irregular Motion.* PhD thesis, King's College London (University of London), 2012.

[KOPT13] G. Kutyniok, K. A. Okoudjou, F. Philipp, and E. K. Tuley. Scalable frames. *Linear Algebra and its Applications*, 438(5):2225–2238, 2013.

[KP15] G. Kutyniok and P. Petersen. Classification of edges using compactly supported shearlets. *Appl. Comput. Harmon. Anal.*, pages –, 2015.

[LDP07] M. Lustig, D. Donoho, and J. Pauly. Sparse MRI: The application of compressed sensing for rapid MR imaging. *Magn. Reson. Med.*, 58(6):1182–1195, 2007.

[Led01] M. Ledoux. *The Concentration of Measure Phenomenon*, volume 89 of *Mathematical Surveys and Monographs.* American Mathematical Society, 2001.

[Li11] S. Li. On general frame decompositions. *Numer. Funct. Anal. Optim.*, 16:1269–1281, 2011.

[Lim13] W.-Q Lim. Nonseparable shearlet transform. *IEEE Trans. Image Process.*, 22(5):2056–2065, 2013.

[LLKW05] D. Labate, W.-Q Lim, G. Kutyniok, and G. Weiss. Sparse multidimensional representation using shearlets. *Wavelets XI., Proceedings of the SPIE*, 5914:254–262, 2005.

[LLSZ13] Q. Lyu, Z. Lin, Y. She, and C. Zhang. A comparison of typical ℓ_p minimization algorithms. *Neurocomputing*, 119(0):413 – 424, 2013.

[LML12] Y. Liu, T. Mi, and S. Li. Compressed sensing with general frames via optimal-dual-based ℓ^1-analysis. *IEEE Trans. Inform. Theory*, 58(7):4201–4214, 2012.

[Ma15a] J. Ma. Generalized sampling reconstruction from Fourier measurements using compactly supported shearlets. *Appl. Comput. Harmon. Anal.*, 2015.

[Ma15b] J. Ma. Stable reconstruction for the analysis formulation of ℓ^p-minimization using redundant systems. 2015. submitted.

[Maa96] P. Maass. Families of orthogonal 2d wavelets. *SIAM J. Math. Anal.*, pages 1454–1481, 1996.

[Mal09] S. Mallat. *A Wavelet Tour of Signal Processing.* Elsevier/Academic Press, Amsterdam, third edition, 2009. The sparse way, With contributions from Gabriel Peyré.

[MBS+16] J. Ma, M. Benning, Z. Saghi, R. Leary, P. Abellan, D. Mücke-Herzberg, Q. Ramasse, P. Midgley, and G. Kutyniok. Image restoration techniques for sparse acquisitions in the scanning transmission electron microscope. 2016. In preparation.

[Mey87] Y. Meyer. Ondelettes, fonctions splines et analyses graduées. (Wavelets, spline functions and multiresolution analysis). *Rend. Sem. Mat. Univ. Politec. Torino*, 45(1):1–42, 1987.

[Mey92] Y. Meyer. Ondelettes due l´intervalle. *Rev. Mat. Iberoamericana*, 7:115–133, 1992.

[MHAS+16] D. Mucke-Herzberg, P. Abellan, M. C. Sarahan, I. S. Godfrey, Z. Saghi, R. K. Leary, A. Stevens, J. Ma, G. Kutyniok, F. Azough, R. Freer, P. A. Midgley, N. D. Browning, and Q. M. Ramasse. Practical Implementation of Compressive Sensing for High Resolution STEM. *Microscopy and Microanalysis*, 22:558–559, 2016.

[MM16] J. Ma and M. März. A multilevel based reweighting algorithm with joint regularizers for sparse recovery. 2016. submitted.

[MMK+16] J. Ma, M. März, G. Kutyniok, T. Schäffter, and C. Kolbitsch. Shearlet-based compressed sensing for fast 3D MR imaging using iterative reweighting. 2016. In preparation.

[MP15] J. Ma and P. Petersen. Linear independence of compactly supported separable shearlet systems. *J. Math. Anal. Appl.*, 428(1):238–257, 2015.

[NW13] D. Needell and R. Ward. Stable Image Reconstruction Using Total Variation Minimization. *SIAM J. Imag. Sci.*, 6(2):1035–1058, 2013.

[OBG+05] S. Osher, M. Burger, D. Goldfarb, J. Xu, , and W. Yin. An iterative regularization method for total variation-based image restoration. *Multiscale Model. Simul.*, (4):460–489, 2005.

[Pet16] P. Petersen. *Shearlets on Bounded Domains and Analysis of Singularities using Compactly Supported Shearlets.* PhD thesis, Technische Universität Berlin, 2016.

[PM11] G. Plonka and J. Ma. Curvelet-wavelet regularized split Bregman iteration for compressed sensing. *Int. J. Wavelets Multiresolut. Inf. Process.*, 09(01):79–110, 2011.

[Poo15] C. Poon. Structure dependent sampling in compressed sensing: Theoretical guarantees for tight frames. *Appl. Comput. Harmon. Anal*, 2015.

[PWSB99] K. P. Pruessmann, M. Weiger, M. B. Scheidegger, and P. Boesiger. SENSE: Sensitivity encoding for fast MRI. *Magn. Reson. Med.*, 42(5):952–62, 1999.

[QHL+14] X. Qu, Y. Hou, F. Lam, D. Guo, J. Zhong, and Z. Chen. Magnetic resonance image reconstruction from undersampled measurements using a patch-based nonlocal operator. *Med. Image Anal.*, 18(6):843–856, 2014.

[Rau10] H. Rauhut. Compressive sensing and structured random matrices. In *Theoretical foundations and numerical methods for sparse recovery*, volume 9 of *Radon Ser. Comput. Appl. Math.*, pages 1–92. Walter de Gruyter, Berlin, 2010.

[ROF92] L. I. Rudin, S. Osher, and E. Fatemi. Nonlinear total variation based noise removal algorithms. *Physica D*, 60(1-4):259–268, 1992.

[SCY08] R. Saab, R. Chartrand, and Ö. Yilmaz. Stable sparse approximations via nonconvex optimization. In *Proceedings of the IEEE International Conference on Acoustics, Speech, and Signal Processing, ICASSP 2008*, pages 3885–3888, 2008.

[SED05] J.-L. Starck, M. Elad, and D. L. Donoho. Image decomposition via the combination of sparse representation and a variational approach. *IEEE Trans. Image Process.*, 14(10):1570–82, 2005.

[SF09] I. W. Selesnick and M. A. T. Figueiredo. Signal restoration with overcomplete wavelet transforms: comparison of analysis and synthesis priors, 2009.

[STS10] G. Steidl, T. Teubner, and S. Setzer. Deblurring Poissonian images by split Bregman techniques. *J. Vis. Commun. Image Represent.*, 21(3):193–199, 2010.

[Tan00] W.-S. Tang. Oblique projections, biorthogonal Riesz bases and multiwavelets in Hilbert spaces. *Proc. Amer. Math. Soc.*, 128(2):463–473, 2000.

[UA94] M. Unser and A. Aldroubi. A general sampling theory for nonideal acquisition devices. *IEEE Trans. Signal Process.*, 42(11):2915–2925, 1994.

[Wal02] D. F. Walnut. *An introduction to wavelet analysis.* Applied and Numerical Harmonic Analysis. Birkhäuser, Boston, MA, 2002.

[WKM09] D. Weishaupt, V. Köchli, and B. Marincek. *Wie funktioniert MRI?* Springer-Verlag, 2009.

[WSK$^+$07] S. Winkelmann, T. Schaeffter, T. Koehler, H. Eggers, and O. Doessel. An optimal radial profile order based on the golden ratio for time-resolved MRI. *IEEE Trans. Med. Imag*, 26(1), 2007.

[WT10] C. Wu and X.-C. Tai. Augmented Lagrangian Method, Dual Methods, and Split Bregman Iteration for ROF, Vectorial TV, and High Order Models. *SIAM J. Imag. Sci.*, 3(3):300–339, 2010.

[WYYZ08] Y. Wang, J. Yang, W. Yin, and Y. Zhang. A New Alternating Minimization Algorithm for Total Variation Image Reconstruction. *SIAM J. Imag. Sci.*, 1(3):248–272, 2008.

[YOGD08] W. Yin, S. Osher, D. Goldfarb, and J. Darbon. Bregman iterative algorithms for ℓ_1-minimization with applications to compressed sensing. *SIAM J. Imag. Sci.*, 1(1):143–168, 2008.

[ZBSS04] W. Zhou, A. C. Bovik, H. R. Sheikh, and E. P. Simoncelli. Image qualifty assessment: From error visibility to structural similarity. *IEEE Trans. Image Proces.*, 13(4):600–612, 2004.